NOTE TO USERS

The original manuscript received by UMI contains pages with slanted print. Pages were microfilmed as received.

This reproduction is the best copy available

UMI

INTERACTION OF DEXRAZOXANE WITH ANTICANCER DRUGS

by

Hanna Kozlowska

A thesis submitted to the Faculty of Graduate Studies in Partial Fulfillment of the Requirements for the Degree of

Master of Science

Faculty of Pharmacy
University of Manitoba
Winnipeg, Manitoba, Canada

National Library of Canada
Acquisitions and Bibliographic Services
395 Wellington Street
Ottawa ON K1A 0N4
Canada

Bibliothèque nationale du Canada
Acquisitions et services bibliographiques
395, rue Wellington
Ottawa ON K1A 0N4
Canada

Your file Votre référence

Our file Notre référence

The author has granted a non-exclusive licence allowing the National Library of Canada to reproduce, loan, distribute or sell copies of this thesis in microform, paper or electronic formats.

The author retains ownership of the copyright in this thesis. Neither the thesis nor substantial extracts from it may be printed or otherwise reproduced without the author's permission.

L'auteur a accordé une licence non exclusive permettant à la Bibliothèque nationale du Canada de reproduire, prêter, distribuer ou vendre des copies de cette thèse sous la forme de microfiche/film, de reproduction sur papier ou sur format électronique.

L'auteur conserve la propriété du droit d'auteur qui protège cette thèse. Ni la thèse ni des extraits substantiels de celle-ci ne doivent être imprimés ou autrement reproduits sans son autorisation.

0-612-32158-4

Canada

THE UNIVERSITY OF MANITOBA

FACULTY OF GRADUATE STUDIES

*****

COPYRIGHT PERMISSION PAGE

INTERACTION OF DEXRAZOXANE WITH ANTICANCER DRUGS

BY

HANNA KOZLOWSKA

A Thesis/Practicum submitted to the Faculty of Graduate Studies of The University of Manitoba in partial fulfillment of the requirements of the degree of

MASTER OF SCIENCE

Hanna Kozlowska 1997 (c)

Permission has been granted to the Library of The University of Manitoba to lend or sell copies of this thesis/practicum, to the National Library of Canada to microfilm this thesis and to lend or sell copies of the film, and to Dissertations Abstracts International to publish an abstract of this thesis/practicum.

The author reserves other publication rights, and neither this thesis/practicum nor extensive extracts from it may be printed or otherwise reproduced without the author's written permission.

Abstract. This thesis work consists of two major projects. In the first project the effects of combination of the cardioprotective agent, dexrazoxane, with the anticancer drugs mafosfamide, 5-fluorouracil, vinblastine, doxorubicin, daunorubicin, mitoxantrone and bleomycin were tested on Chinese hamster ovary cells. Four different methods were chosen for drug interaction analysis: the combination index, envelope of additivity, response surface and comparison of slopes. In the second project the cytotoxic mechanism of the anticancer drug mitindomide was evaluated in comparative studies with dexrazoxane. The combined 72 h and 48 h effects of dexrazoxane and mafosfamide was proven to be antagonistic by the combination index, response surface and slope comparison methods; although, the envelope of additivity showed additive effect of the drugs. The antagonistic effect of dexrazoxane and 5-fluorouracil was indicated by four methods used. The analysis of 48 h dexrazoxane-vinblastine data with the slope method showed antagonism. It was indicated by the slope comparison method, that the 48 h combined effects of dexrazoxane with doxorubicin, daunorubicin and mitoxantrone were antagonistic. When dexrazoxane was preincubated for 18 h with the cells before bleomycin was added the combination index, envelope of additivity and response surface methods showed synergy. The anticancer drug mitindomide was shown to inhibit topoisomerase II and not to be cytotoxic towards a dexrazoxane-resistant cell line. It was shown that mitindomide did not stabilize DNA-topoisomerase II cleavable complexes. The similarities between mitindomide and dexrazoxane functions toward cells and topoisomerase II classify mitindomide as topoisomerase II catalytic inhibitor.

Acknowledgments. I would like to thank my supervisor, Professor Brian Hasinoff, for accepting me into the master program at the Faculty of Pharmacy and for all the scientific and financial support I have received from him. I would also like to thank the Faculty of Graduate Studies, University of Manitoba, for awarding me a Graduate Fellowship.

Table of Contents

List of Figures

List of Tables

1. Review of drugs and methods

1.1. Introduction

This thesis work consists of two major projects. The first project involved the testing of four different methods of drug interaction analysis: combination index, envelope of additivity, response surface, and comparison of slopes. The effects of combining the cardioprotective agent dexrazoxane with the anticancer drugs mafosfamide, 5-fluorouracil, vinblastine (Chapter III), doxorubicin, daunorubicin, mitoxantrone (Chapter IV) or bleomycin (Chapter V) were tested on Chinese hamster ovary cells. In the second project (Chapter II) the mechanism of cytotoxicity of mitindomide was studied. Topoisomerase II decatenation and cytotoxicity experiments on Chinese hamster ovary cells were used in a comparative study of mitindomide with dexrazoxane.

1.1.1. Protective effect of dexrazoxane

Dexrazoxane is a cardioprotective drug which may be given to patients receiving anticancer drugs, such as anthracyclines [1-3]. It has been demonstrated that dexrazoxane can lower the pulmonary toxicity of bleomycin [4]. Free radical formation is the most likely mechanism of cardiac toxicity of the anthracyclines and pulmonary toxicity of bleomycin [4-9]. It has been shown that doxorubicin, daunorubicin, and mitoxantrone are able to induce free radical formation in cardiac mitochondria [5, 7]. All of these drugs and bleomycin also have the ability to form complexes with iron [10, 11]. One of the proposed mechanisms of free radical formation relates the free radical production with iron complexes of these drugs [10, 12].

The bisdioxopiperazine, dexrazoxane, is the (+)-(*S*)-enantiomer of racemic ICRF-159 (razoxane). Dexrazoxane undergoes hydrolysis through intermediates with one open imide ring, to the product, ADR-925, with both imide rings open (Fig. 1.1) [13]. The intermediates of dexrazoxane and ADR-925 are potent chelating agents and they can remove iron from Fe-doxorubicin and Fe-bleomycin complexes [4, 14], as well as from transferrin and ferritin [15]. Dexrazoxane also has antitumor activity [16], probably through catalytic inhibition of topoisomerase II (see Chapter II).

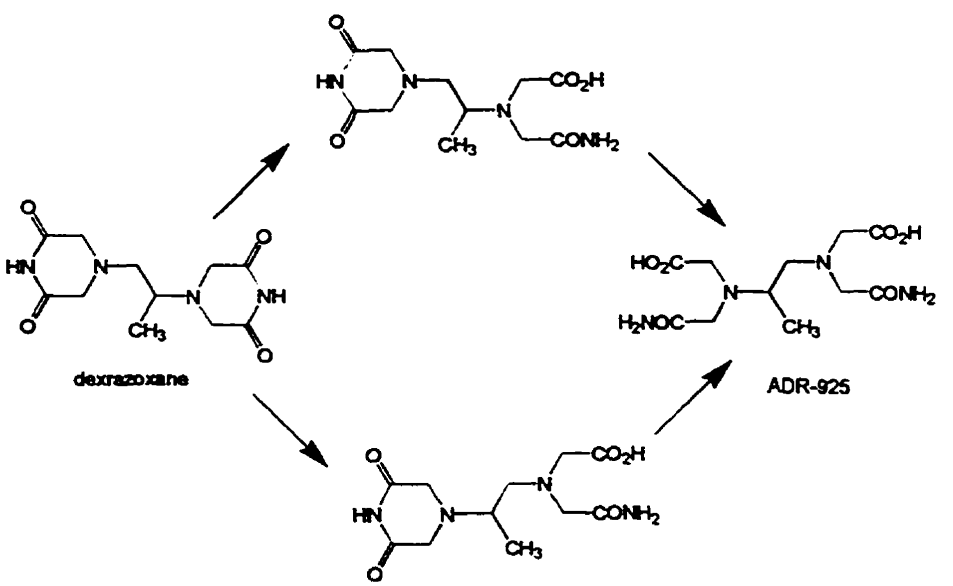

Fig. 1.1. Hydrolysis products of dexrazoxane.

The drugs studied in this project were chosen because they have been, or may be, a part of multidrug therapy with dexrazoxane. Multidrug chemotherapy was developed to achieve improved therapeutic results [17]. The desired effect of drug combination is synergy, or at least additivity; however, the combined drugs may affect each other's absorption, metabolism and excretion. One agent may also influence tissue sensitivity to

another drug [18]. Drug interactions may be sensitive to the time schedule [19]. Dexrazoxane is combined with other drugs to prevent free radical damage. It is hypothesised that dexrazoxane does not lower the therapeutic effect of its counterpart.

1.1.2. Methods for drug interaction studies

Drugs used in combination produce effects which may be smaller, equal or greater than expected. The expected combined effect is usually predicted on the basis of single agent effects [18], with the assumption that their combination does not alter their individual efficacies. The simplest approach is based on the summation of effects, where the predicted combined effect of two drugs is the sum of their effects when they act separately. All the methods presented below propose different models of additivity. Each of the methods theoretically defines the additivity of the effects and compares experimental results with the theoretical references.

The diversity of the methods for studying drug interaction is reflected in a broad range of nomenclature used by different research groups. Cancer chemotherapists, radiobiologists, pharmacologists, microbiologists, and immunologists use their own vocabulary of terms [18]. Many of these words describe the same phenomena, although sometimes they may introduce more subtle subdivisions. Synonyms which may be found in the literature for zero interaction between drugs are: additivism, independence and indifference. A positive interaction has been described as: synergy, supra-additiveness, potentiation and augmentation. A negative interaction has been described as: antagonism, sub-additiveness, negative synergy, depotentiation, desensitisation, or infra-additiveness.

Use of the terms "enhancement" for positive interaction, and "inhibition" for negative interaction express gradation of the effect and have weaker meaning than synergy and antagonism, respectively. The term "sensitisation" describes a positive interaction with a inactive agent, whereas "protection" describes a negative interaction [20].

1.1.2.1. Dose-response curves

The methods for studying drug combinations presented below are based on the analysis of dose-response curves. A dose-response curve shows dependence of an effect on a dose or concentration. Although the term "dose" is often reserved for the amount of drug administrated per unit of body weight, in this thesis, it is defined as a particular drug concentration in solution. Often the effect-concentration experimental data can be fitted to simple mathematical formulas, such as logistic, linear or exponential equations.

Equations developed to describe enzyme catalysed reactions have been applied to drug-effect relationships. The Michaelis-Menten equation is given as:

$$E = \frac{E_{max}\dfrac{D}{EC_{50}}}{1+\dfrac{D}{EC_{50}}} \tag{1.1}$$

where E is the effect, D is the drug concentration or dose, E_{max} is the maximal effect of the drug measured from zero effect, and EC_{50} is the concentration producing 50% of the maximal effect. In drug research, this relationship is known as E_{max} model [21, 22]. The shape of the curve expressed by equation (1.1) is hyperbolic. Most experimental data will

fit a more complicated model proposed by Hill to study the saturation of haemoglobin with oxygen [21]. This relation is called sigmoidal E_{max} or a logistic model [22-24]:

$$E = \frac{E_{max}\left(\frac{D}{EC_{50}}\right)^{m}}{1+\left(\frac{D}{EC_{50}}\right)^{m}} \tag{1.2}$$

where m is the Hill-type coefficient that influences the shape of a curve. For stimulatory drugs, $m > 0$ and the curve rises with drug concentration. For inhibitory drugs, $m < 0$ and the curve falls with drug concentration, and the variable EC_{50}, is replaced with IC_{50}, the median inhibitory concentration. If $|m| > 1$ the curve is sigmoidal; if $|m| < 1$ the curve is steeper at lower concentrations and shallower in the middle range of concentrations (Fig. 1.2, a). If there is a baseline effect, it is added to the equation (1.2), resulting in equation (1.3):

$$E = \frac{E_{max}\left(\frac{D}{EC_{50}}\right)^{m}}{1+\left(\frac{D}{EC_{50}}\right)^{m}} + B \tag{1.3}$$

where B is the constant baseline effect (for inhibitory drugs, B is the effect of an infinite drug concentration, when the effect levels off) and E_{max} is the value of a maximal effect measured from B (compare Fig. 1.2, d). Dose-response curves may be presented in different co-ordinate systems such as logarithmic (Fig. 1.2, b, c, d) and normalised as a percent of maximal effect (Fig. 1.2, c). Analysis of dose-response curves may give information about the efficacy of the compound (E_{max}, Fig. 1.2, b) and its potency (EC_{50},

Fig. 1.2, a, c). Parallel curves suggest the same mechanism of action (Fig. 1.2, b, c) and the ranges of different activities of the same agent may be found (Fig.1.2, a, b, c, d). The survival effects of inhibitory drug, presented in Fig. 1.2. (d), are expressed in absorbance units. Absorbance is often a parameter correlated with the effect of cell survival in tissue culture experiments. In this thesis, the survival of the cells under different drug concentrations was measured with a MTT assay (see Chapter II, Section 2.2.3).

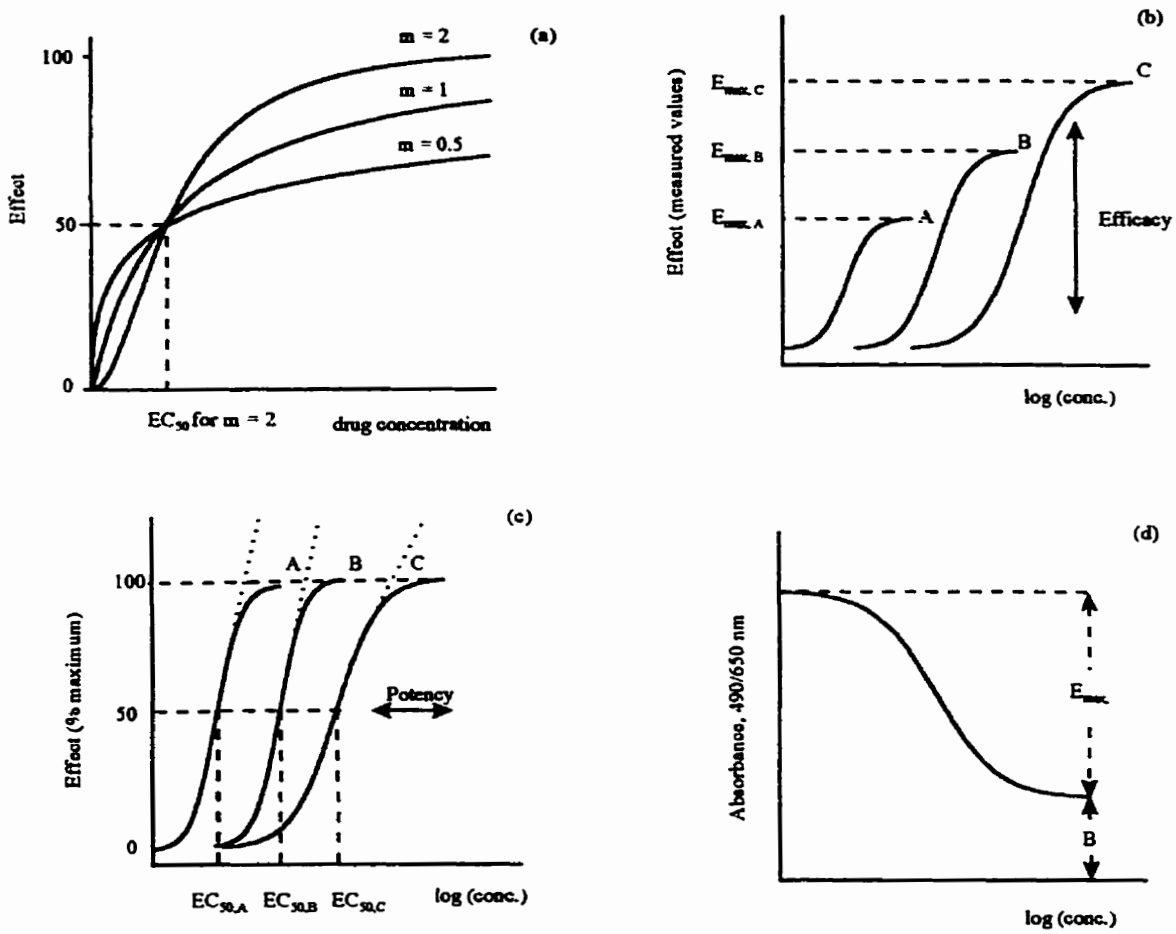

Fig. 1.2. Presentation of dose-response curves using different co-ordinates: (a) linear co-ordinates, (b) logarithmic scale of concentration, (c) effect expressed as % of the maximum effect, (d) effect expressed in absorbance units [22, 25].

1.1.2.2. Comparison of dose-response curves

A fixed dose of one drug may modify the shape of a dose-response curve of another drug [18, 20, 26]. In Fig. 1.3, some possible modifications of the dose-response curves are presented. These curves are presented as the logarithm of survival *versus* drug concentration.

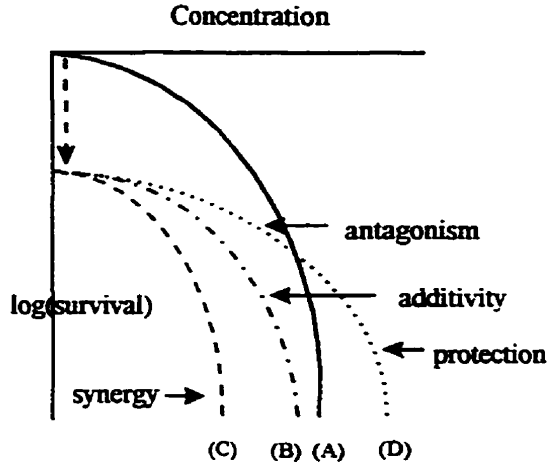

Fig. 1.3. Dose-response curve comparison of a drug alone, and a drug with a fixed dose of a second drug. Four different cases are illustrated: (A) dose-response curve for a single agent; (B), (C), and (D) the dose-response curves for A with fixed doses of the second drug. The dashed arrow represents the effect of the fixed dose of the second drug by itself [20].

If a fixed dose moves curve (A) downwards by a constant effect value (dashed arrow), the resulting dose-response curve (B) represents the additivity of the effects. If the fixed dose moves curve (A) by a value higher than that expected based on the activities of single agents, the combined effect is synergistic (curve C); that is, the interaction of the two drugs results in a reinforced combined effect. The shallower dose-response curve for the drug combination is an indication of antagonism (D). Curve (D) may even cross curve

(A) showing protection, meaning that "the administration of one agent allowed the other to be given at greater than single-dose level for the iso-effect" [27]. This type of analysis was used in a study of the combined effect of radiation with a fixed dose of a drug [26, 28].

1.1.2.3. Method based on summation of effects

If the effects of two single agents, A and B, are directly proportional to concentration, the effect of their combination may also be directly proportional to concentration [18]. The anticipated combined effect when there is no drug interaction is a sum of the effects of the agents acting alone (E_A and E_B). The zero-interaction case represents the only instance where additivity of the effects can be measured by straight summation:

$$E_{AB} = E_A + E_B \tag{1.4}$$

If the combined effect of two drugs is greater than expected (*i.e.* $E_{AB} > E_A + E_B$), there is positive interaction between the drugs and their effect is synergistic. If the combined effect of the drugs gives a smaller effect than anticipated (*i.e.* $E_{AB} < E_A + E_B$) the agents show an antagonistic relationship. The use of the summation method is limited to linear dose-response curves. The experimental data seldom fit this model, thus it is used only occasionally. This method has been used in the calculation of the expected combined effect of hypothermia and X-irradiation on sister chromatid exchange frequency [29].

1.1.2.4. Fractional product method

The fractional product method is based on an independence criterion. If two agents have independent modes of action, the expected combined effect is the product of the effects of the single agents. The fractional product method is valid only for exponential dose-response curves [24] that can be converted to the linear relationships by logarithmic transformation [18, 27, 30]. In this case the logarithm of survival, S, is directly proportional to drug concentration. Summation of logarithms leads to the equation for the additive effect of the combined drugs:

$$\log S_A + \log S_B = \log S_A \cdot S_B = \log S_{AB} \qquad (1.5a)$$

thus

$$S_A \cdot S_B = S_{AB} \qquad (1.5b)$$

where S_A, S_B and S_{AB} are the fractional survival effects for each agent and their combination, respectively. If $S_{AB} = S_A \cdot S_B$ the drugs do not interact with each other and their effect is additive. If $S_{AB} < S_A \cdot S_B$ the interaction of the drugs is positive, and the effect is synergistic. If $S_{AB} > S_A \cdot S_B$ drug interaction is negative and the effect of the combined drugs is antagonistic. The effect is expressed as fractional survival to avoid misleading conclusions. For instance, if a fractional mortality for one drug is 0.3 and the other 0.4 their product is $0.3 \cdot 0.4 = 0.12$, thus the additive effect would be smaller than that of a single agent. The same results expressed as fractional survival gives $(1-0.3)(1-0.4) = 0.42$; the expected effect of the drug combination is 42% survival. Simply stated, if one drug kills 30% of the cells, the other drug will act on the remaining 70%. If the second drug kills 40% of the remaining 70%, 42% of cells will survive [31]. Additional explanation has

been given by Berenbaum based on the probability of the sum of two independent events. [18].

According to Chou [19], the fractional product method is suitable only for hyperbolic curves where $m = 1$ (m is the Hill-type coefficient as described in Section 1.1.2.1), that is, for drugs with totally independent modes of action (mutually nonexclusive drugs). For higher order systems ($m > 1$), where drugs have similar modes of action (mutually exclusive drugs), this method cannot be used.

1.1.2.5. Loewe isobole method

An Loewe isobologram is a plot of an equi-potent combination of drug concentrations; that is the concentrations that produce the same effect [18, 32]. The abscissa of the isobologram graph is the concentration of drug A, and the ordinate is the concentration of drug B. If D_A and D_B are the doses of single agents, A and B, that produce the effect x%, the co-ordinates of the points (d_A and d_B) lying along the segment connecting D_A and D_B represent any concentrations of A and B in a mixture that also produce x% iso-effect. These concentrations should be obtained when A and B do not interact with each other. In Fig 1.4 (a), the chosen effect is 50% thus D_A and D_B are the median effective concentrations $EC_{50,A}$ and $EC_{50,B}$, respectively. The relationship between the doses of the single drugs and the combination which produces the same effect is described by the segmental equation:

$$\frac{d_A}{D_A} + \frac{d_B}{D_B} = I \qquad (1.6)$$

where D_A and D_B are the doses of single drugs A and B that produce effect x%, d_A and d_B are the doses of the these drugs in the mixture that produce the same combined effect x%, and I is an index of interaction. If I=1, the drugs do not modify each other's action, and their combined effect is additive. If $I > 1$, the drugs antagonise each other. Higher concentrations of the drugs are required to produce the iso-effect in a mixture. If $I < 1$, the drugs act synergistically. The relationships of additivity, antagonism and synergy are graphically illustrated in Fig. 1.4, b.

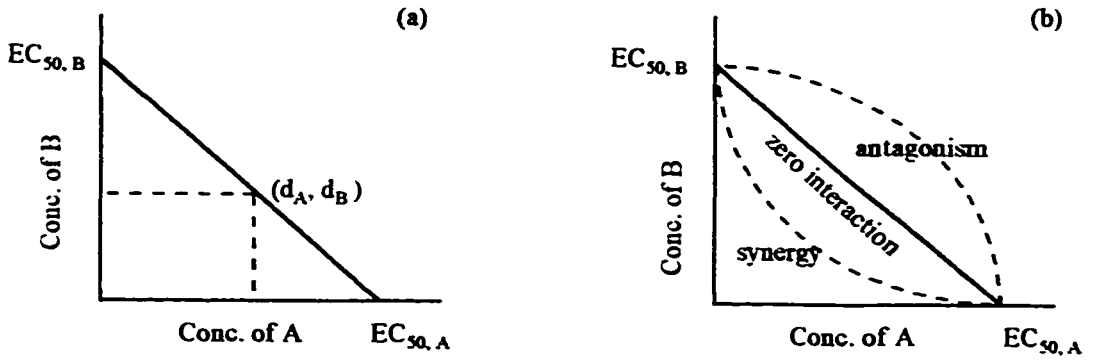

Fig. 1.4. Loew isobole. (a) The zero interaction isobole for 50% effect, (b) the 50% iso-effect lines showing additivity (solid line), antagonism and synergy (dashed lines).

The model of zero interaction between agents (I = 1) is based on the concept of two drugs being different lots of the same drug A. Drug A becomes drug B by adding an inert agent to A so that its potency is changed [18]. This assumption ensures no interaction between drugs and the linearity of additive isobole. The conceptual zero interaction model is also independent of the shape of the dose-response curves; thus it is universal.

1.1.2.6. Envelope of additivity

Steel [20, 27] has considered cases where the dose-response curves for single drugs are not linear, so their effects cannot be simply added. The doses of the drugs which, in combination, give a certain additive effect are derived from single drug dose-response curves. If the combined drugs produce an effect, E, part of this effect is due to action of the drug A (E_A), and the rest is contributed by drug B (E_B), (Fig. 1.5, a). There are three modes of finding the doses which produce the effects E_A and E_B, mode I, mode IIa and mode IIb [31]. For mode I, doses d_A and d_{B1} for the fractional effects E_A and E_B are measured from zero on the effect axis. For mode IIa, the dose of drug A is located as above but dose d_{B2} that produces the effect E_B is measured from the point where the effect of A ends. In practice, this dose can be calculated by subtracting the dose producing effect E_A from the dose producing full effect E. Both doses are calculated with the equation of a dose-response curve for drug B. Finally, for mode IIb, the doses for E_A and E_B are found as described in mode IIa, except now the curve for drug B is taken as the first one to find the ending point for this mode.

The full range of the possible combinations of doses of single agents that produce the combined effect E builds the envelope of additivity (Fig. 1.5, b). Mode I is derived from the assumption that drugs act independently, whereas in mode II it assumed that both drugs act by the same mechanism. The envelope of additivity is represented as a zone restricted by the confidence limits in which zero or almost zero interaction between the agents may be expected. The concept of the zone, originates from the uncertainty

associated with defining the constituent doses of the mixture when single drugs have non-linear dose-response curves.

If the experimental data fall to the left of the envelope of additivity, the combined agents action is synergistic. The data to the left of the mode I boundary indicates positive interaction, although the data inside the envelope may indicate enhancement. The points to the right of the envelope imply antagonism (Fig. 1.5, b). The order and shape of the lines defining the envelope may change with different shapes of dose response curves.

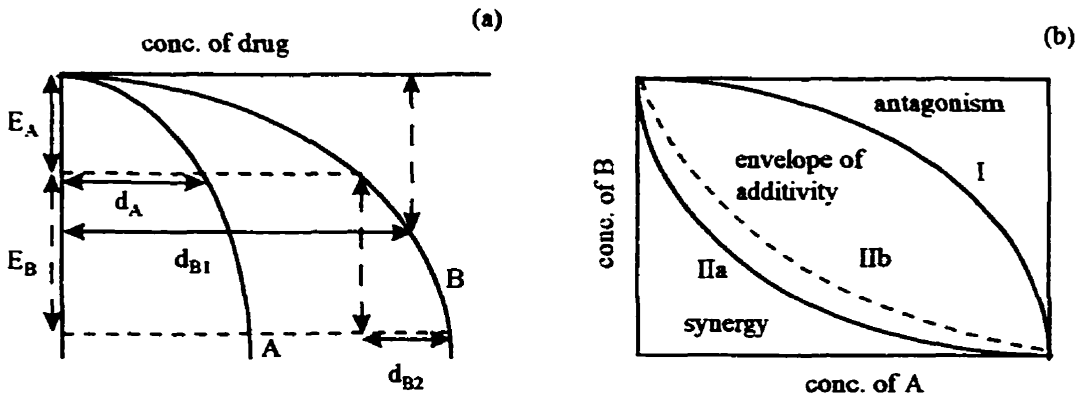

Fig. 1.5. Construction of envelope of additivity. (a) The envelope of additivity is constructed from the dose-response curves of drug A and B. Mode I: the doses that produce the final effect E are d_A and d_{B1}. Mode II: the doses that produce the effect E are d_A and d_{B2}. The full delimiting lines are obtained by finding the different combinations of doses that produce the effect E. (b) The envelope of additivity delimited by the lines of Mode I, Mode IIa, and Mode IIb. There is zero or almost zero interaction between agents inside the envelope.

When the dose-response curve for drug A follows first order kinetics, mode II b is identical to mode I. If both drugs follow first order kinetics the envelope becomes the classical Lowe isobole [33]. According to Shūnel [24] only an envelope constructed from linear-dose response curves leads to the classical Loewe isobole.

1.1.2.7. Combination index method

The combination index method is independent of the shape of the dose-response curves [34]. The type and degree of interaction between drugs is evaluated by a combination index, *CI*:

$$CI = \frac{d_A}{D_A} + \frac{d_B}{D_B} + \frac{\alpha \cdot d_A \cdot d_B}{D_A \cdot D_B} \tag{1.7}$$

where D_A and D_B are the doses of single drugs that produce the effect x, d_A and d_B are the constituents of a drug mixture that produce the same effect. The constant, α, may have a values of either 0 or 1, where $\alpha = 0$ corresponds to mutually exclusive agents (similar modes of action), and $\alpha = 1$ corresponds to mutually non-exclusive agents (independent modes of action). If $CI = 1$, the effect of the agents is additive and the combination index equation for the drugs with similar modes of action ($\alpha = 0$) becomes the classical isobologram formula (equation 1.6). If $CI < 1$, there is a synergy between drugs, if $CI > 1$, antagonism is observed.

Before this method can be used its applicability must be assessed. The median effect equation is used to evaluate the exclusivity of the drugs action (*i.e.* the value of α) is given as:

$$\frac{f_a}{f_u} = \left(\frac{D}{EC_{50}}\right)^m \tag{1.8}$$

where f_a and f_u are the fractions affected and unaffected by the dose D, and as such, $f_a + f_u = 1$; EC_{50} is the median effective concentration and m is the Hill-type coefficient. When f_a

is replaced by $E\,E_{max}$, this equation is equivalent to logistic equation (1.2). The non-linear relationship (1.8) can be transformed into a linear equation by taking logarithms of both sides:

$$\log\frac{f_a}{f_u} = m\cdot\log(D) - m\cdot\log(EC_{50}) \qquad (1.9)$$

The plot of $\log(f_a/f_u)$ against $\log(D)$ is a straight line obtained by linear regression with a slope equal to m and the X-intercept equal to $\log(EC_{50})$ (Fig. 1.6, a). The EC_{50} value may be calculated as: $EC_{50} = 10^{-b/m}$, where b is a Y-intercept and m is a slope. The resulting graph is called the median effect plot. If the regression lines for single agents and for their combination are parallel, then $\alpha = 0$ in equation (1.7). If the regression lines for single agents are parallel but the regression line for the combination is not, then $\alpha = 1$. When exclusivity of the drugs cannot be assessed, equation (1.7) should be used for both values of α.

Combination index experiments are designed to obtain at least three dose-response curves; one for each single agent, and another for their mixture at a constant ratio. The values of m and EC_{50} for the single agents and their combination obtained from the median effect plot enables the calculation of single drug doses D_A, D_B, and a combined dose of the mixture $D = (d_A + d_B)$, for any chosen value of the fraction affected:

$$D = EC_{50}\left(\frac{f_a}{1-f_a}\right)^{1/m} \qquad (1.10)$$

The constituent doses d_A and d_B of the mixture D are calculated from the known ratio of doses used in the experiment. The equi-potent (i.e. $d_A/d_B = EC_{50,A}/EC_{50,B}$) constant ratio of d_A and d_B is recommended for preliminary studies. In this case a comparable level of effect contribution is expected from both mixed drugs [30]. Other constant ratios with an excess of one drug are advised for more detailed studies. The CI value may be calculated for any fractional effect f_a and presented graphically as CI *vs.* f_a (Fig. 1.6, b). A computer program written in BASIC allows automatic calculation of CI values [35], although such calculations can be achieved using any spreadsheet software.

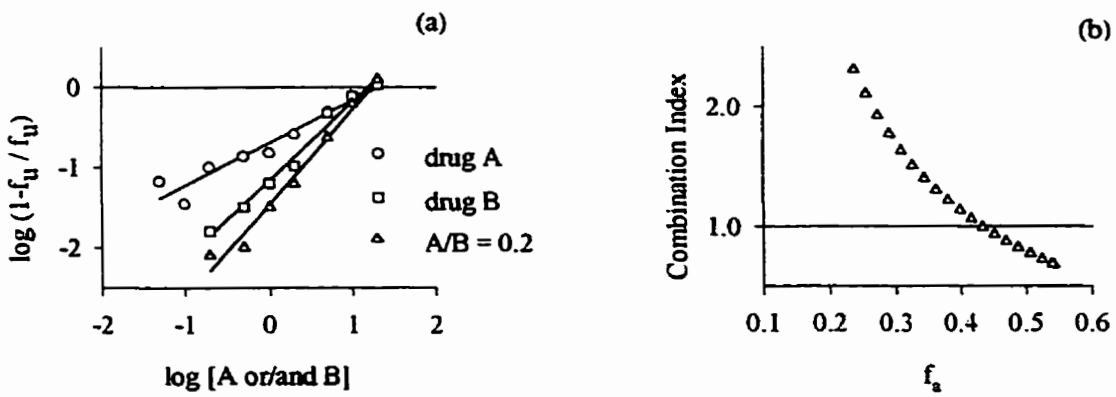

Fig. 1.6. Median effect and combination index plots. (a) The median effect plot for drug A, B and for their combination in the constant ratio A/B = 0.2, (b) the graph of the combination index *vs.* fraction affected for A/B = 0.2. Data below the value of one indicate synergy and above the value of one indicate antagonism between drug A and B.

Authors who criticised the combination index method argue that the mutually nonexclusive model was not adequately derived [23, 36]. The transformation of experimental data into a linear relationship by the median effect plot is often associated with large errors, producing inaccurate values of EC_{50} and m. There is also no solution for

data higher than the control effect (this is occasionally seen with concentration of drug close to zero, where the fractional survival is higher than 1). Another problem accrues for drugs with different m values, when the exclusivity of an effect is not possible to define. The confusion is also due to the lack of a proper statistical approach and assessment of the obtained values, such as interpretation of the combination index close to 1. Belen'kii and Schinazi improved the median effect method by introducing the confidence intervals for the combination index [37].

1.1.2.8. Response surface method

The methods described below use the microcomputer based isobole with three dimensional response surface for the interaction of two drugs [23, 24]. In the work by Greco [24], the parametric response surface equation has been fitted to experimental data. The response surface method evaluates the interaction between drugs based on experimental dose-response curves of single agents and their combinations. The sets of data obtained in the envelope of additivity and combination index experiments also may be examined using this method. The proposed model is valid for inhibitory drugs with logistic dose-response curves similar to equation (1.3). The logistic equation (1.3) must be modified for inhibitory drug by replacing EC_{50} with IC_{50}. From this equation, the doses of the single agents D_A and D_B, have been calculated and replaced in the classical isobole equation (1.6) for zero interaction between drugs ($I = 1$):

$$\frac{d_A}{IC_{50,A}\left(\frac{E-B}{E_{max}-E+B}\right)^{1/m_A}} + \frac{d_B}{IC_{50,B}\left(\frac{E-B}{E_{max}-E+B}\right)^{1/m_B}} = 1 \qquad (1.11)$$

Equation (1.11), relates constituent doses, d_A and d_B, of the agents in combination with their survival effect E, the median inhibitory concentrations $IC_{50,A}$ and $IC_{50,B}$, and the Hill-type coefficients m_A and m_B for the individual drugs A and B. If there is no interaction between the drugs, experimental data may be fitted with this equation and the zero interaction response surface may be plotted using three co-ordinates: effect, concentration of drug A, and concentration of drug B. Any deviation of experimental data from the zero interaction surface implies interaction between drugs. To fit general data, for drugs with and without interaction, a third term has been introduced to equation (1.11), [23]:

$$\frac{d_A}{IC_{50,A}\left(\frac{E-B}{E_{max}-E+B}\right)^{1/m_A}}+\frac{d_B}{IC_{50,B}\left(\frac{E-B}{E_{max}-E+B}\right)^{1/m_B}}+\frac{a'\cdot d_A\cdot d_B}{IC_{50,A}\cdot IC_{50,B}\left(\frac{E-B}{E_{max}-E+B}\right)^{(1/m_A+1/m_B)}}=1 \qquad (1.12)$$

Equation (1.12) has been derived as an empirical formula. The best fit of experimental data to equation (1.12) gives estimates of the seven parameters; E_{Max}, B, $IC_{50,A}$, $IC_{50,B}$, m_A, m_B, and α', along with standard errors. The term α', is a interaction parameter; $\alpha' = 0$ when there is additivity, $\alpha' > 0$ when there is synergy, and $\alpha' < 0$ when there is antagonism between drugs. Equation (1.12) has been fitted to experimental data for single drugs and for their combination with custom written software called SYNFIT using non-linear regression [38]. The results can be examined by plotting a three dimensional scatter plot of the measured data and a mesh plot constructed from equation (1.12). The theoretical, two dimensional plots of the single agents, their combination calculated from estimated best fit

parameters, along with experimental data can be plotted on one graph to evaluate the model. In Fig. 1.7, experimental data and the estimated surface based on equation (1.12) are presented [38]. The leukaemia L1210 cell line was used to test interaction of 1-ß-D-arabinofuranosylcytosine (ara-C) with cisplatin. The measured effect was cell density that decreased with drug concentration. In this particular experiment, the estimated $\alpha' = 3.08 \pm 0.96$; thus, the drug interaction shows synergy.

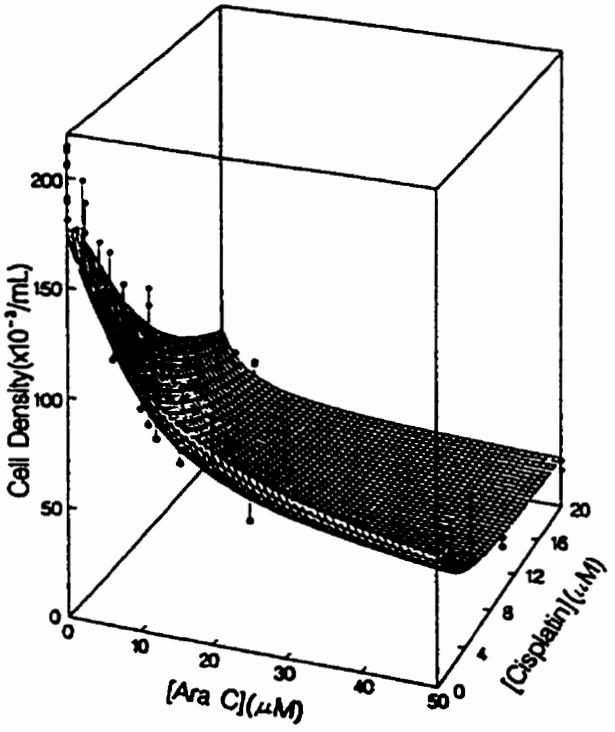

Fig. 1.7. Response surface for effect of 3 h exposure of L1210 cells to ara-C and cisplatin. Fishnet surface represents the response surface estimated from fitting equation (1.12) to the experimental data with non-linear regression; points above (•) and below (○) the surface represent the experimental data used to estimate the response surface. The plot is from [38].

Using an approach which is more general than Greco's model, Sühnel correlated the effects of single agents and their combined effect in the case of no interaction [24].

This was accomplished by substituting of the denominators of the isobole equation (1.6), with the terms for doses calculated from any equations (*i.e.* not only logistic) that describes the dose-response curves for the single agents, and replacing E_A and E_B by the effect of combined drugs E_{AB}. These rearrangements result in an equation that correlates d_A, d_B, E_{AB} and I. If the interaction index is set to 1, this isobole equation expresses a zero interaction response surface where E_{AB} becomes $E°_{AB}$. Transformation of the isobole equation leads to correlation of $E°_{AB}$ with E_A and E_B. For linear dose-response curves, $E = m_A \cdot d_A$, $E°_{AB} = m_A \cdot d_A + m_B \cdot d_B$ thus $E°_{AB} = E_A + E_B$. If the exponential dose-response curve has been used, the transformations give the equation for no interaction effect of the fractional product method, *i.e.* $S°_{AB} = S_A \cdot S_B$. This approach for the logistic function is given as [24]:

$$E(d) = \frac{1}{1 + \left(\frac{D}{IC_{50}}\right)^m} \tag{1.13}$$

Equation (1.13) is similar to equation (1.2), except that when applied to the inhibitory drug data $m > 0$ and $E_{Max} = 1$. For this type of dose-response curve the correlation between $E°_{AB}$, E_A and E_B cannot be obtained. The isobole equation with substituted denominators for logistic dose-response curves is given as:

$$\frac{d_A}{IC_{50,A}\left(\frac{1 - E°_{AB}}{E°_{AB}}\right)^{1/m_A}} + \frac{d_B}{IC_{50,B}\left(\frac{1 - E°_{AB}}{E°_{AB}}\right)^{1/m_B}} = 1 \tag{1.14}$$

Equation (1.14) can be solved analytically only when the slopes for the single agents are equal to each other. In other cases, when $m_A \neq m_B$, the equation must be solved by numerical iteration. The drug concentrations d_A, d_B, and calculated E°_{AB} defined the zero interaction surface. When the data from combined drug experiments are plotted, the positive deviations from zero interaction surface show synergy, antagonism is shown by data below the surface. The data may also be presented as a difference between the experimental and expected effects. In this case the plane of zero difference ($E_{AB} = E^\circ_{AB}$) divides equally the synergy and antagonism spaces where the points below the plane show antagonism ($E_{AB} - E^\circ_{AB} < 0$) and these above the plane show synergy ($E_{AB} - E^\circ_{AB} > 0$). Another approach of Shünel to the study of drug interaction is to fit an analytical function to the experimental data [36]. This may be done by piecewise fitting of spline functions. In such a case the procedure is independent of the shape of dose-response curves. The resulting empirical equation relates the doses to their experimental effects. The differences between E_{AB} (calculated from this equation) and E°_{AB} (gained from isobole equation) form the difference response surface that represents evaluation of synergy and antagonism for the broad range of dose combinations. The fitted function makes it easy to extract data for plotting the isoboles at any effect level.

From the literature methods described in this chapter, the combination index, envelope of additivity and response surface methods were studied in this thesis work. These three methods were chosen as the most complex in their approach to synergy, antagonism and additivity. The combination index method evaluates interaction between drugs based on the value of CI. There is no interaction when CI = 1. It tests the drugs

combined in a constant ratio of wide concentration range. The envelope of additivity method defines synergy, antagonism and additivity based on the location of the points on the envelope. The envelope is a area of no interaction. It tests the drugs in wide concentration range combined with the fixed doses of the second drug. The response surface method can be used for drugs in the concentration arrangements like for the both methods above. The evaluation of drug interaction is based on a value of the interaction parameter α'. Drugs were also tested with the method not described in the literature. The slope comparison method, described in Section 3.2.3.3, was developed by Dr. Brian Hasinoff. It was chosen for drug interaction study because of dexrazoxane low cell kill in 48 h cytotoxicity experiments. The method is simple and the results are easy to interpret.

References

1. Speyer JL, Green MD, Kramer E, Rey M, Sanger J, Ward C, Dubin N, Ferrans V, Stecy P, Zeleniuch-Jacquotte A, Wernz J, Feit F, Slater W, Blum R and Muggia F, Protective effect of the bispiperazinedione ICRF-187 against doxorubicin-induced cardiac toxicity in women with advanced breast cancer. *N Engl J Med* **319:** 745-752, 1988.

2. Lemez P and Maresova J, Protective effect of cardioxane against anthracycline induced cardiotoxicity in relapsed acute myeloid leukemias. *Neoplasma* **43:** 417-419, 1996.

3. Kolaric K, Bradamante V, Cervek J, Cieslinka A, Cisarz-Filipcak E, Denisov LE, Donat D, Drosik K, Gershanovic M, Hudziec P, Jelic S, Jurga L, Kalasiewicz M, Kowgird L, Kozacka M, Lichinitzer M, Machalski M, Mechl Z, Odintsov S, Pawlicki M, Rubach D, Roth A, Stabuc B, Tomczak J, Utracka B, Zborzil J and Rogan J, A phase II trial of cardioprotection with cardioxane (ICRF-187) in patients with advanced breast cancer receiving 5-fluorouracil, doxorubicin and cyclophosphamide. *Oncology 52:* 251-255, 1995.

4. Herman EH, Hasinoff BB, Zhang J, Raley LG, Zhang T-M, Fukada Y and Ferrans VJ, Morphologic and morphometric evaluation of the effect of ICRF-187 on bleomycin-induced pulmonary toxicity. *Toxicol* **98:** 163-175, 1995.

5. Demant EJF and Jensen PK, Destruction of phospholipids and respiratory-chain activity in pig-heart submitochondrial particles induced by an adriamycin-iron complex. *Eur J Biochem* **132:** 551-556, 1983.

6. Doroshow JH, Effect of anthracycline antibiotics on oxygen radical formation in rat heart. *Cancer Res* **43:** 460-472, 1983.

7. Doroshow JH and Davies JA, Redox cycling of anthracyclines by cardiac mitochondria. *J Biol Chem* **261:** 3068-3074, 1986.

8. Gianni L, Zweier JL, Levy A and Myers CE, Characterization of the cycle of iron-mediated electron transfer from adriamycin to molecular oxygen. *J Biol Chem* **260:** 6820-6826, 1985.

9. Rajagopalan S, Politi PM, Sinha BK and Myers CE, Adriamycin-induced free radical formation in the perfused rat heart: implications for cardiotoxicity. *Cancer Res* **48:** 4766-4769, 1988.

10. Malisza KL and Hasinoff BB, Production of hydroxyl radical by iron(III)-anthraquinone complexes through self-reduction and through reductive activation by the xanthine oxidase/hypoxanthine system. *Arch Biochem Biophys* **321:** 51-60, 1995.

11. Hecht SM, Bleomycin-group antitumor agents. In: *Cancer Chemotherapeutic Agents.* (Ed. Foye WO), pp. 369-388. American Chemical Society, Washington, DC, 1995.

12. Myers C, Gianni L, Zweier J, Muindi J, Sinha BK and Eliot H, Role of iron in adriamycin biochemistry. *Fed Proc* **45:** 2792-2797, 1986.

13. Buss JL and Hasinoff BB, The one-ring open hydrolysis product intermediates of the cardioprotective agent ICRF-187 (dexrazoxane) displace iron from iron-anthracycline complexes. *Agents Actions* **40:** 86-95, 1993.

14. Hasinoff BB, The interaction of the cardioprotective agent ICRF-187 ((+)-1,2-bis(3,5-dioxopiperazinyl-1-yl)propane), its hydrolysis product ICRF-198, and other chelating agents with the Fe(III) and Cu(II) complexes of adriamycin. *Agents Actions* **26:** 378-385, 1989.

15. Hasinoff BB and Kala SV, The removal of metal ions from transferrin, ferritin and ceruloplasmin by the cardioprotective agent ICRF-187 ((+)-1,2-bis(3,5-dioxopiperazinyl-1-yl)propane) and its hydrolysis product ADR-925. *Agents Actions* **39:** 72-81, 1993.

16. Von Hoff DD, Howser D, Lewis BJ, Holcenberg J, Weiss RB and Young RC, Phase I study of ICRF-187 using a daily for 3 days schedule. *Cancer Treat Rep* **65:** 249-252, 1981.

17. Frei E, Clinical Studies of Combination Chemotherapy for Cancer. In: *Synergism and Antagonism in Chemotherapy.* (Eds. Chou T-C and Rideout DC), pp. 103-108. Academic Press, San Diego, California, 1991.

18. Berenbaum MC, Criteria for analyzing interactions between biologically active agents. *Adv Cancer Res* **35:** 269-335, 1981.

19. Rideout DC and Chou T-C, Synergism and Antagonism, and Potentiation in Chemotherapy: an overview. In: *Synergism and Antagonism in Chemotherapy.* (Eds. Chou T-C and Rideout DC), pp. 3-59. 1st ed. Academic Press, San Diego, California, 1991.

20. Steel GG, Terminology in the description of drug-radiation interaction. *Int J Radiat Oncol* **5:** 1145-1150, 1979.

21. Nogrady T, Ed. *Medicinal Chemistry. 2nd ed.* Oxford University Press, Oxford, 1988; 514 p.

22. Holford HG and Sheiner LB, Understanding the dose-effect relationship: clinical application of pharmacokinetic-pharmacodynamic models. *Clin Pharmacokinet* **6:** 429-453, 1981.

23. Greco WR, Bravo G and Parsons JC, The search for synergy: a critical review from a response surface perspective. *Pharmacol Rev* **47:** 331-385, 1995.

24. Sühnel J, Zero interaction response surfaces, interaction functions and difference response surfaces for combinations of biologically active agents. *Arzneim-Forsch* **42(II):** 1251-1258, 1992.

25. Martin YC, Bush EN and Kyncl JJ, Quantitive Description of Biological Activity. In: *Comprehensive Medicinal Chemistry.* (Ed. Hansch C), pp. 349-373. Vol. 4. Pergamon Press, Oxford, 1990.

26. Han A and Elkind MM, Ultraviolet light and x-ray damage interaction in Chinese hamster cells. *Radiat Res* **74:** 88-100, 1978.

27. Steel GG, Exploitable mechanisms in combined radiotherapy-chemotherapy: The concept of additivity. *Int J Radiat Oncol* **5:** 85-91, 1979.

28. Waldren CA and Rasko I, Caffeine enhancement of x-ray killing in cultured human and rodent cells. *Radiat Res* **73:** 95-110, 1978.

29. Livingston GK and Dethlefsen LA, Effects of hyperthermia and x irradiation on sister chromatid ecxhange (SCE) frequency in Chinese hamster ovary (CHO) cells. *Radiat Res* **77:** 512-520, 1979.

30. Chou T-C and Talalay P, Applications of the Median-Effect Principle for the Assessment of Low-Dose Risk of Carcinogens and for the Quantitation of Synergism and Antagonism of Chemotherapeutic Agents. In: *New Avenues in Developmental Cancer Chemotherapy.* (Eds. Harrap KR and Connors A), pp. 37-64. Academic Press, Orlando, FL, 1987.

31. Merlin J-L, Concept of synergism and agnagonism. *Anticancer Res* **14:** 2315-2320, 1994.

32. Loewe S, The problem of synergism and antagonism of combined drugs. *Arzneim-Forsch* **3:** 285-320, 1953.

33. Kano Y, Ohnuma T, Okano T and Holland JF, Effect if vincristine in combination with methotrexate and other antitumor agents in human acute lymphoblastic leukemia cells in culture. *Cancer Res* **48:** 351-356, 1988.

34. Chou T-C and Talalay P, Quantitative analysis of dose-effect relationships: the combined effects of multiple drugs or enzyme inhibitors. *Adv Enz Regul* **22:** 27-55, 1984.

35. Chou T-C, Motzer RJ, Tong Y and Bosl GJ, Computerized quantitation of synergism and antagonism of taxol, topotecan, and cisplatin against human teratocarcinoma cell growth: a rational approach to clinical protocol design. *J Natl Cancer Inst* **86:** 1517-1524, 1994.

36. Sühnel J, Evaluation of synergism or antagonism for the combined action of antiviral agents. *Antiviral Res* **13:** 23-40, 1990.

37. Belen'kii MS and Schinazi RF, Multiple drug effect analysis with confidence interval. *Antiviral Res* **25:** 1-11, 1994.

38. Greco WR, Park HS and Rustum YM, Application of a new approach for the quantitation of drug synergism to the combination of cis-diamminedichloroplatinum and 1-β-D-arabinofuranosylcytosine. *Cancer Res* **50:** 5318-5327, 1990.

2. Mechanism of mitindomide cytotoxic activity

2.1. Introduction

The National Cancer Institute identified the bis imide, mitindomide, as a promising anticancer drug [1]. This drug has never been clinically tested because of difficulties with its formulation. Mitindomide (Fig. 2.1), has been shown to be active against a variety of tumour models such as the transplanted mouse tumours B16 melanoma, CD8F mammary, colon 38 and L1210 leukaemia [2]. Its mechanism of cytotoxicity was suggested to be the cross-linking of DNA [3]. Recently bis imides like dexrazoxane (ICRF-187), ICRF-154, ICRF-159, ICRF-193 and sobuzoxane were classified as anticancer drugs that act on topoisomerase II. Mitindomide bears some structural similarity to dexrazoxane. It has also been demonstrated to be cross-resistant in an ICRF-159 (racemic form of dexrazoxane) resistant cell line [4]. This evidence suggests that mitindomide and dexrazoxane may have a common mechanism of cytotoxicity. Inhibition of topoisomerase II and Chinese hamster ovary cell (wild type and dexrazoxane resistant) growth, by mitindomide and dexrazoxane were used to evaluate this hypothesis. Molecular modelling was used to compare structural parameters of mitindomide and dexrazoxane.

2.1.1. Topoisomerase II

DNA topoisomerase II is a homodimeric protein that catalyses changes in the topology of circular DNA [5]. Both eukaryotic and prokaryotic cells contain a comparable enzyme. DNA topology is important to many cellular processes, and a number of anticancer drugs exert their cytotoxicity by affecting DNA topoisomerase II. There are three general functions of the enzyme; the relaxation of closed circular double-stranded

DNA, formation and resolution of knotted DNA, and catenation and decatenation of circular DNA.

The catalytic cycle of topoisomerase II consist of six Steps [6]. The first Step is substrate recognition and binding. Several topoisomerase II recognition sites have been identified. They are determined by nucleotide sequences in DNA and also DNA topology (crossovers and nodes). The second Step is pre-strand passage DNA cleavage/religation equilibrium, which requires the presence of Mg^{2+} and ATP and it favours the religation event. Each subunit of the homodimeric enzyme mediates the breakage of one strand of the double helix. Some antitumor drugs exert their activity through stabilisation of the enzyme-DNA complex. In the third Step, the segment of DNA is passed through the break, and the DNA is relaxed. The fourth event is the post-strand-passage DNA cleavage/religation equilibrium. In this Step, religation is also favoured, but not as strongly as in Step two. In the fifth Step ATP is hydrolysed by topoisomerase II to ADP and orthophosphate. The last, sixth, event is enzyme turnover. In this Step, topoisomerase II restores its active conformation. It may dissociate from DNA, or, stay bound to carry on relaxation process on the same DNA molecule.

2.1.2. Anti-tumour drugs that act on topoisomerase II

There are two classes of anti-tumour drugs that act on topoisomerase II. The first consists of drugs which form complexes with the enzyme-DNA complex during the pre-strand equilibrium of topoisomerase II catalytic cycle (the second Step in Section 1.1) [7]. This class of drugs is known as cleavable complex forming poisons. Some examples from

his class are amsacrine, CP-115,953, daunorubicin, doxorubicin, epirubicin, etoposide, idarubicin and mitoxantrone [8].

The second class is known as catalytic inhibitors of topoisomerase II. This class of drugs includes such compounds as: dexrazoxane, ICRF-154, ICRF-159, ICRF-193, aclarubicin, sobuzoxane, merbarone and suramin [9]. These drugs do not stimulate cleavable complex formation; in the presence of ATP they convert the enzyme into a form incapable of binding circular DNA [10]. In a model proposed by Roca [11], topoisomerase II takes the form of protein clamp which opens and closes upon ATP-binding. The closed enzyme-DNA form may trap the second segment of DNA and transport it through enzyme-mediated DNA gate. The stabilisation of the closed clamp form of enzyme was proposed as a mechanism of the inhibitory effect of bis imide, ICRF-193 [10].

Proliferating cells have a higher level of topoisomerase II and they are more sensitive to drugs targeting this enzyme [7]. Topoisomerase II cleavable complex formation and catalytic inhibition results in effects leading to cell death or strong inhibition of cell growth [7, 10, 12].

2.1.3. Mitindomide

Mitindomide was first synthesised by Bradshaw in 1966 [13] as the imide analogue of the corresponding maleic anhydride photoproduct (Fig. 2.1). It is the product of 1,2-photoaddition and 1,4-Diels-Alder addition of maleimide to benzene.

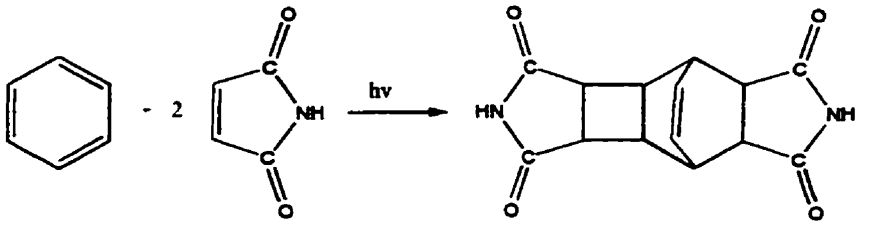

Fig. 2.1. Photochemical addition of maleimide to benzene leading to mitindomide product.

The solubility of mitindomide (M_w = 272.3 g/mol) is not satisfactory in any common solvents [14]. It is practically insoluble in water (< 1.8 mM) [14]. The disodium salt of mitindomide is freely soluble in water but it stays in solution only above pH 10 [15]. It has been demonstrated that some synthesised derivatives of mitindomide have improved aqueous solubility, and still retain anti-tumour activity [16, 17, 18]. Mitindomide has been shown to be the active form of the N-substituted mitindomide compound, fetindomide [19, 20].

The anticancer activity of mitindomide has motivated interest in determining its x-ray crystal structure [21, 22]. Attempts to obtain mitindomide in crystalline form from DMF-H_2O solution were unsuccessful. Also sodium and potassium salts of mitindomide have not given suitable crystals. Crystallisation of mitindomide from ammonium hydroxide [21] or as a diacetate of bis(hydroxymethyl) derivative [22] gave specimens suitable for crystallographic study. The crystal structure of mitindomide has verified that it is a totally rigid, nonplanar molecule, an unlikely candidate for intercalation.

(a) (b)

Fig. 2.2. Structures of mitindomide (a) and dexrazoxane (b).

The molecular structure of mitindomide has some common features with dexrazoxane (Fig. 2.2). Both compounds contain two imide groups and their crystal structures have approximately coplanar imide containing rings; the angles between plane normals are 2 and 4.1°, respectively [22, 23].

2.2. Materials and methods

Two kinds of Experiments were performed with mitindomide and dexrazoxane. An electrophoretic topoisomerase II decatenation assay was used to study the inhibitory properties of mitindomide and dexrazoxane toward topoisomerase II. Cytotoxicity studies on Chinese hamster ovary (CHO) and dexrazoxane resistant (DZR) cell lines were performed to compare the inhibitory effects of mitindomide and dexrazoxane on cell growth. Dexrazoxane resistant cell line was obtained by continuous exposure of wild type CHO cells into increasing concentration of dexrazoxane [9]. In addition, molecular modelling of mitindomide and dexrazoxane was performed to compare the structural features of both drugs.

2.2.1. Materials

Dexrazoxane (ICRF-187) used in this study was donated by Pharmacia & Upjohn (Columbus, OH). Mitindomide (NSC-284356) was obtained from the National Cancer Institute (Bethesda, MD). A topoisomerase II assay kit and human type II topoisomerase (p170 form) were obtained from TopoGen Inc. (Columbus, OH). CHO nuclear extract containing topoisomerase II was prepared by Joan Buss in our laboratory [24]. Agarose (ultra pure), sodium bicarbonate (cell culture tested, cat. No. 895-1810IO), minimum essential medium, alpha medium (cat. No. 12000-022), Fetal Bovine Serum (cat. No. 26140-087), penicillin-streptomycin (cat. No. 15140-122) and trypsin, 0.25% (w/v) with 1 mM Na_4EDTA (cat. No. 25200-072) were obtained from Gibco BRL, Life Technologies Inc. (Burlington, Ontario, Canada). Tris-HCl (cat. No. T-6666), bovine serum albumin (cat. No. A-6003), N-lauroylsarcosine free acid (cat. No. L 5000), HEPES (cell culture tested, cat. No. H-9136), ethidium bromide (95%, cat. No. E-8751), MTT (98%, TLC, cat. No. M-5655), DMSO (used to dissolve drugs, 99.5%, cat. No. D-5879), Dulbecco's phosphate buffered saline (cell culture, cat. No. D-5652), bromophenol blue sodium salt (cat. No. B8026), dithiothreitol (cat. No. D-0632) and phenylmethylsulfonyl fluoride (cat. No. P-7626) were obtained from Sigma Chemical Co. (St. Louis, MO, USA). KCl (cat. No. 37,885-2), $MgCl_2 \cdot 6 \cdot H_2O$ (cat. No. 20,895-7), Na_2EDTA volumetric standard, 0.0997 M in water (cat. No. 31,888-4) were obtained from Aldrich Chemical Company (Milwaukee, WI, USA). Adenosine 5'-triphosphate (cat. No. 0-1076) and glycerol (cat. No. G-32) were obtained from Fisher Scientific Company (Fair Lawn, New Jersey, USA). Dithiothreitol (cat. No. 2697-XI) and DMSO (used for MTT assay, cat. No. 4948) were

obtained from Mallinckrodt Baker Inc. (Paris, Kentucky, USA). Tris (cat. No. 604205) was obtained from Boehinger Mannheim Co. NaCl (cat. No. ACS 783) and Na_2EDTA (99.5%, cat. No. 10093) were obtained form BDH Chemical (Toronto, Canada). Boric acid (cat. No. AC-1308) was obtained from Anachemia Ltd. (Montreal, Canada).

2.2.2. Topoisomerase II decatenation assay and agarose gel electrophoresis

A topoisomerase II decatenation assay [25-27] was performed to determine if mitindomide, like dexrazoxane, has the ability to inhibit the catalytic activity of topoisomerase II. This project consisted of three major Steps. The first was the assay itself. The second was the detection of decatenation products of topoisomerase II by agarose gel electrophoresis. The third was the quantitative analysis of nicked open circular monomers.

2.2.2.1. Topoisomerase II assay

Topoisomerase II decatenates kinetoplast DNA (kDNA). kDNA is a network of catenated mini- and maxicircles of mitochondrial DNA from a parasitic protozoa. The products of catalytic activity of eukaryotic topoisomerase II on kDNA are decatenated monomers of nicked, open circular DNA (NOC) and covalently closed circular, relaxed DNA (CC). The decatenation is dependent on ATP and Mg(II). Besides kDNA and the enzyme, the assay contained the assay buffer, consisting of ATP, Mg(II), Tris-HCl, KCl, dithiothreitol and bovine serum albumin. The assay was incubated for 30 min at 37° C. The degree of decatenation was dependent on the amount of the enzyme and incubation time. Drugs targeting topoisomerase II, such as dexrazoxane, decrease its activity [28], and thus the amount of decatenation product.

Both purified, human and crude, CHO nuclear extract topoisomerases II were used. The assay was prepared in 1.5 mL microcentrifuge tubes. The total volume of a single assay was 20 μL. The assay mixture consisted of water (to make up to 20 μL), 2.0 μL assay buffer (final concentrations: 50 mM Tris-HCl, 120 mM KCl, 10 mM $MgCl_2$, 0.5 mM ATP, 0.5 mM dithiothreitol, 30 μg BSA/mL), appropriate volumes of drug, kDNA and topoisomerase II. Authentic topoisomerase II decatenation markers, controls with no enzyme and no drug were also included. When DMSO was used, the usual volume of the drug added was 1.0 μL. A DMSO control was typically included in the experiment. After mixing all the components of the assay, added in the order: water, assay buffer, drug, kDNA and enzyme, the solutions were incubated for 30 min in a 37° C water bath. The reaction was stopped by mixing the assay with 5.0 μL of the stop buffer.

Drug dissolution: The ability of mitindomide to inhibit topoisomerase II was examined along with the topoisomerase II catalytic inhibitor, dexrazoxane. Stock solutions of mitindomide were prepared in DMSO or in 2.1 equivalents aqueous solution of sodium hydroxide (to titrate the two imide hydrogen atoms). Dexrazoxane solutions were prepared in water. Five different concentrations of mitindomide or dexrazoxane were prepared as separate stock solutions (compare example 1 and 2 below), such that the same volume of solution was used for each assay sample.

Assay buffer: Ten times concentrated assay buffer was prepared as follows: 0.1789 g of KCl, 0.0406 g of $MgCl_2$, 0.006 g of ATP, 0.0015 g of dithiothreitol and 0.0006 g of bovine serum albumin were dissolved in 2 mL of Tris-HCl. Tris-HCl was prepared by

dissolving 0.788 g of Tris-HCl in 10 mL of double distilled water and adjusting the pH of the solution to 8.

Storage conditions: The assay buffer, in 30 µL aliquots, was stored in microcentrifuge tubes at -80°C. Thawed, unused portions of buffer were discarded. The buffer was prepared in our laboratory because decatenation of kDNA did not consistently occur when the TopoGen assay buffer was used. The kDNA, stop buffer and markers shipped frozen from TopoGen were stored in the refrigerator (4°C). Human topoisomerase II and CHO nuclear extract were stored at -80°C. The activity of the enzyme was partly lost by repeated freezing and thawing.

Assay optimisation: One unit of topoisomerase II decatenates 0.2 µg of kDNA in 15 min at 37° C [29]. The amounts of kDNA used in this study were 0.2, 0.3 and 0.4 µg, depending on the original concentration of DNA and enzyme activity. The amounts of the enzyme and kDNA were optimised to get 80-90% decatenation. Higher levels of enzyme activity did not permit the detection of drug inhibition; lower levels of enzyme activity decreased the sensitivity of the assay.

Enzyme dilution: The concentration of the enzyme was adjusted by dilution with Tris-HCl, pH 7.5 or dilution buffer. The dilution buffer (10 mM Tris-HCl; pH 7.5, 500 mM KCl, 1 mM phenyl methyl sulfonyl fluoride, 2 mM dithiothreitol, 50 µg/mL of bovine serum albumin, and 1 mM Na_2EDTA) was prepared by dissolving 0.3728 g of KCl, 0.0018 g phenylmethyl sulfonyl fluoride, 0.0031 g dithiothreitol, 0.0005 g bovine serum albumin and 100 µL of 0.0997 M Na_2EDTA in 10 mL Tris-HCl, with the pH adjusted to 7.5 by titration with 2 M NaOH. When the dilution buffer was used for CHO nuclear

extract, KCl was not added to the buffer. Too high of a concentration of the salt inhibits topoisomerase II [24].

Stop buffer: Two kinds of stop buffer were used. The first stop buffer was obtained from TopoGen (5% (w/v) Sarkosyl, 0.125% (w/v) bromophenol blue, 25% (v/v) glycerol) and the second was prepared in our laboratory. Five times concentrated stop buffer was prepared by mixing 0.05 g of N-lauroylsarcosnine free acid dissolved in 368 μL 0.5 N NaOH with 250 μL of 0.5% (w/v) bromophenol blue (0.005 g/1 mL), 250 μL glycerol and 132 μL double distilled water. The final volume of buffer was 1.0 mL.

Examples of two typical Experiments are presented below. In the first Experiment mitindomide was dissolved in DMSO, in the second Experiment mitindomide was dissolved in NaOH.

Example 1. In this example, the CHO nuclear extract of topoisomerase II was used. The enzyme was 25 times diluted: 2.0 μL enzyme was added to 48 μL of Tris-HCl buffer, pH 7.5. The concentration of kDNA was 110 ng/μL. Mitindomide (Mid) was dissolved in DMSO. The concentrated stock solution of mitindomide was 20 mM: 0.0020 g of mitindomide was dissolved in 371 μL DMSO and sonicated until the drug was dissolved (approximately 20 min). More dilute stock solutions were obtained by appropriate dilution with DMSO as shown in Table 2.1.

Table 2.1. Example of mitindomide solutions used in Experiment with the CHO nuclear extract of topoisomerase II.

No.	Mitindomide final standard concentration µM	Concentration of mitindomide stock solution µM	Volume of mitindomide stock solution µL	Volume of 100% DMSO µL
1	1000	20 000	-	-
2	300	6000	33 of No. 1	67
3	100	2000	10 of No. 1	90
4	30	600	10 of No. 2	90
5	10	200	10 of No. 3	90

The types of the assay samples and the volumes of solutions used in this Experiment are given in Table 2.2.

Table 2.2. Example of samples used in CHO nuclear extract of topoisomerase II decatenation assay.

No.	Final sample	Water µL	Buffer µL	Mid µL	kDNA µL	Enzyme µL
1	No DMSO	15.2	2	0	1.8	1
2	No enzyme	16.2	2	0	1.8	0
3	DMSO, 1 µL	14.2	2	0	1.8	1
4	Mid, 1000 µM	14.2	2	1	1.8	1
5	Mid, 300 µM	14.2	2	1	1.8	1
6	Mid, 100 µM	14.2	2	1	1.8	1
7	Mid, 30 µM	14.2	2	1	1.8	1
8	Mid, 10 µM	14.2	2	1	1.8	1

Example 2. In this example, mitindomide was dissolved in NaOH: 0.2214 g of mitindomide was dissolved in 248 μL of 42 mM NaOH. The resulting stock solution was 20 mM. The kDNA concentration was 50 ng/μL. Human topoisomerase II concentration was 1 U/μL. The enzyme was diluted two times with dilution buffer for the human topoisomerase II. More diluted stock solutions were prepared by dilution of the 20 mM stock solution with double distilled water as shown in Table 2.3.

Table 2.3. Example of mitindomide solutions used in Experiment with human topoisomerase II.

No.	Mitindomide final standard concentration μM	Concentration of mitindomide stock solution μM	Volume of mitindomide stock solution μL	Volume of H_2O μL
1	1000	20 000	-	-
2	500	10 000	50 of No. 1	50
3	200	4000	40 of No. 2	60
4	100	2000	50 of No. 3	50
5	50	1000	50 of No. 4	50

In Table 2.4, the types of assay samples and the volumes of solutions used in this Experiment are given. An aqueous solution of 21 mM HCl was used to maintain the pH of the samples with the highest drug concentrations (No. 7 and 8, HCl:NaOH concentration ratio 1:1).

Table 2.4. Example of the samples used with the human topoisomerase II decatenation assay.

No.	Final sample	Water µL	Buffer µL	MID µL	kDNA µL	21mM HCl µL	Topo II µL
1	Marker	19	0	0	0	0	0
2	No enzyme	14	2	0	4	0	0
3	No drug	13	2	0	4	0	1
4	MID, 50 µM	12	2	1	4	0	1
5	MID, 100 µM	12	2	1	4	0	1
6	MID, 200 µM	12	2	1	4	0	1
7	MID, 500 µM	11	2	1	4	1	1
8	MID, 1000 µM	10	2	1	4	2	1

The assays from examples 1 and 2 were incubated for 30 min in a 37°C water bath. The reaction was stopped first by putting the test tubes on ice, and next mixing the assay samples with 5 µL of the stop buffer. The stop buffer contained detergent Sarcosyl, recommended by TopoGen company for stopping the activity of the enzyme [29]. The final sample volumes were 25 µL.

2.2.2.2. Agarose gel electrophoresis

Under electrophoretic conditions the large kDNA network cannot enter the gel and remains in the well. The faster moving bands are genomic DNA and the products of topoisomerase II activity (compare Fig. 2.3). The bands move to the positive electrode.

Besides decatenated monomers of kDNA (NOC and CC), topoisomerase II also produces kDNA decatenated trimers and dimers. They move only a short distance from the gel origin. Between the wells and the nicked, open circular band, a genomic DNA band was seen. If the assay is nuclease-contaminated, linear DNA can be seen as a nuclease ATP independent reaction. If bacterial topoisomerase II, namely DNA gyrase, is present, decatenated, supercoiled DNA is produced. None of the bands corresponding to nuclease or gyrase activity were seen in these Experiments. Enzyme activity was inhibited by mitindomide and dexrazoxane; thus, lower levels of decatenated, nicked open circular; and decatenated, covalently closed products were observed. The level of nicked open circular monomers was suitable for quantitative analysis.

Agarose gel: The 25 μL volumes of single topoisomerase II decatenation assay samples were loaded into wells in a 1% (w/v) agarose gel (15 x 7 cm), immersed in running buffer (0.1 M TRIS-base, 0.1 M boric acid, 2 mM Na_2EDTA, pH 8.3). The running buffer and agarose gel contained the intercalator ethidium bromide to visualise the bands under UV light. The agarose gel was prepared by weighing 1 g of agarose in a beaker and adding 100 mL of running buffer. The mixture was heated on a hot plate and stirred constantly with a magnetic stirrer until the boiling point. It was then cooled to about 60°C. Two μL of ethidium bromide was added with stirring and the gel was poured into a levelled gel caster with the 20-tooth comb in place. All the air bubbles were moved to the sides with a Pasteur pipette and the gel was left to set for at least 60 min.

10xTBE buffer: Tris-boric acid-Na_2EDTA (TBE) buffer was prepared ten times concentrated: 121.1 g of Tris, 61.8 g of boric acid and 7.4 g Na_2EDTA were dissolved in

1 L of double distilled water. The pH of the buffer was adjusted with 5 N aqueous solution of NaOH to 8.3 at room temperature. The buffer was stored in the refrigerator.

Ethidium bromide: Ethidium bromide solution was prepared by dissolving of 0.01 g of ethidium bromide in 1 mL of double distilled water. The solution was stored at room temperature and wrapped in aluminium foil. The ethidium bromide solution is light sensitive. The solution was used not longer than one month. Ethidium bromide has the ability to fluoresce under UV light. The fluorescence is enhanced by intercalation of planar ethidium bromide molecules between DNA bases.

Running buffer: The running buffer was prepared by ten times dilution of 100 mL of TBE buffer with double distilled water on the day of Experiment. The running buffer with 0.2 μg/mL of ethidium bromide (for 900 mL volume of running buffer, 18 μL ethidium bromide was added) was poured into the chamber until its level was about 0.5 cm above the gel surface. All the air bubbles were removed. The same running buffer was used for multiple gels run on the same day.

Running the gel: After the gel was set, the comb was removed, and the gel on the tray was transferred into the electrophoresis chamber (Sub-Cell GT Agarose Gel Electrophoresis System, Bio-Rad Laboratories Inc., Hercules, California, USA). The 25 μL assay samples were delivered to every, or every second well. The chamber was covered with the lid with the electrodes attached. The 100 V potential was slowly applied and gel was run for 40 - 45 min. The negative potential (black end) was applied on the loading wells side. The gel was examined under UV light on a VWR, bench transilluminator (model M-20E) using single 302 nm ultraviolet wavelength. The gel was

destained in 1 L of double distilled water until a good contrast was obtained; generally, the optimal destaining time was 4 h.

Gel photography: A Polaroid direct screen instant camera DS34, with ISO3000, type 667 Polaroid film was used to photograph the gel under UV light. Typical conditions for photography were as follows: 1/8 s exposure and 5.6 F-stop, 30 s development time.

2.2.2.3. Quantitative analysis

The photographs were scanned with a digital Hewlett-Packard ScanJet 4P scanner. The white frame on the photograph was omitted in scanning. The intensities of the bands formed by nicked, open circular (NOC) DNA were measured on SigmaGel (Jandel Scientific, San Rafael CA). A square covering the band was used for integration (see Fig. 2.3). Typically, 27 pixels size square was applied to cover the band. The intensity of the measured square included some level of the background (square "a" in Fig. 2.3). The level of the background was measured on the gel in a place without bands (square "b"). The background "b" was subtracted from the intensity of the square "a".

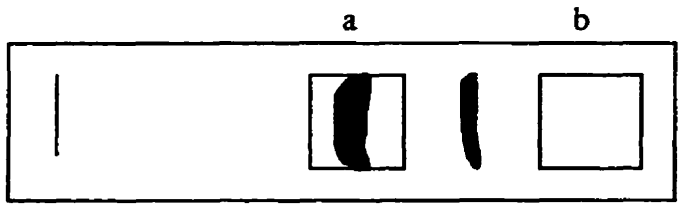

Fig. 2.3. Integration of kDNA decatenation products with SigmaGel. Squares were chosen to cover the bands; (a) represents the square with the band and (b) represents the background square.

The intensities of the bands and corresponding concentrations were fitted to a four-parameter logistic (2.1) equation on SigmaPlot software (Jandel Scientific, San Rafael CA):

$$I = \frac{a-d}{1+\left(\frac{D}{IC_{50}}\right)^{b}} + d \qquad (2.1)$$

where I is the intensity of the band, D is the drug concentration, a is the estimated maximal intensity, b is Hill-type exponential factor (> 0), d is the estimated background intensity obtained at the highest drug concentrations, and IC_{50} is the median inhibitory drug concentration.

2.2.3. Cytotoxicity experiments

Two cell lines were used in the cytotoxicity Experiments: a wild type Chinese hamster ovary (CHO) cell line (type AA8; ATCC CRL-1859) obtained from the American Type Culture Collection (Rockville, MD) and CHO-derived, a dexrazoxane resistant (DZR) cell line. The DZR cell line is 1500 fold more resistant to dexrazoxane than the parent Chinese hamster ovary cells (48 h continuous exposure to dexrazoxane gave an IC_{50} of 2800 μM for the DZR cell line and 1.8 μM for the CHO cell line [9]). The DZR cell line was obtained in our laboratory by exposure of CHO cell line to increasing concentrations of dexrazoxane. Its resistance to the drug is probably due to an alteration in topoisomerase II [9].

Culturing the cells: Both cell lines were cultured in T-flasks (25 cm^2, cat. No. 25100-25, Corning Inc., New York, USA) in α–MEM (this medium is recommended by ATCC for propagation) containing 20 mM HEPES, 100 units/mL penicillin G, 100 μg/mL

streptomycin, 10% (v/v) fetal bovine serum in an atmosphere of 5% (v/v) CO_2 and 95% (v/v) air at 37°C (pH 7.4). Cell culture medium was prepared by dissolving one pack (10.1 g) of α-MEM, 4.76 g of HEPES and 2.2 g of $NaHCO_3$ in 700 mL of double distilled water. The pH of the solution was adjusted to 7.2 with 5 N NaOH. Ten mL of penicillin with streptomycin (the flask was opened under sterile conditions), along with about 200 mL of double distilled water were added to make up to 900 mL. The solution was filtered with a 0.2 μm Nalgene bottle top filter (Nalgene Company, Rochester, New York) and divided equally into two sterile 500 mL flasks in the laminar flow hood (Envirco Safety Cabinet, model ESC, Albuquerque, New Mexico, USA). The solution was kept in a refrigerator up to one month. Before the cell medium was used, 50 mL (10% (v/v) of final medium volume) of fetal bovine serum was added under sterile conditions. The contamination for mycoplasma was not tested during the Experiments.

Harvesting and seeding the cells: Cells in exponential growth were harvested. The cell culture medium was removed from the flask and the cells were washed with 10 mL of Dulbecco's phosphate buffered saline. One mL of 0.25 % (w/v) trypsin with 1 mM EDTA was added and left for a few minutes to detach the cells from the bottom of the culture flask. The cells were transferred to a 10 mL sterile centrifuge tube with 9 mL of complete cell culture medium and centrifuged at 5000 *g* for 6 min. The supernatant was removed and cells were resuspended in 10 mL of the cell culture medium. A hemocytometer was used to count a sample of the cells and estimate the total amount. The cells were seeded on 96-well, sterile tissue culture plates (flat bottom with lid, cat. No. 831835, Sarstedt Inc., Newton, NC, USA) in 100 μL cell culture medium per well. CHO cells were seeded

at 2000 cells/well, and DZR cells at 5000 cells/well, and allowed to attach for 24 h before the drug solutions were added.

Drug delivery: Dexrazoxane was dissolved in cell culture medium and filtered through a 0.2 μm sterile cellulose acetate syringe filter (25 mm, cat. No. 831826001, Sarstedt Inc., Newton, NC, USA). Mitindomide was dissolved either in DMSO or in 2.1 equivalents of NaOH in aqueous solution. When DMSO was used, its final concentration in the cell culture medium was 0.5% (v/v), and controls were included in Experiments to ensure that DMSO did not affect cell growth. When mitindomide was used in alkaline solution, appropriate amounts of hydrochloric acid were added to wells with the highest drug concentrations to maintain the pH and appropriate controls were included.

MTT assay: Appropriate volumes of cell culture medium were added to the wells with cells for a final volume of 200 μL/well. Six replicates were performed at each drug concentration. Cells were incubated with drugs for another 72 h. Cell survival was measured by the MTT assay [30-32], in which the yellow tetrazolium salt MTT (3-(4,5-dimethylthiazol-2-yl)-2,5-diphenyltetrazolium bromide) is converted into water-insoluble blue formazan crystals by the mitochondrial dehydrogenase of viable cells. After the 72 h drug incubation period, 20 μL of 0.25% (w/v) tetrazolium salt in PBS was added to each well, and the plates were returned to the incubator. The tetrazolium solution was prepared by dissolving 0.25 g of MTT in 100 mL of phosphate buffered saline. This buffer was prepared by dissolving 0.44 g of NaCl and 1.03 g of $NaH_2PO_4 \cdot H_2O$ in 100 mL of double distilled water and adjusting the pH to 7.2 with 5 N NaOH. The MTT-buffer solution is light sensitive and kept wrapped in aluminium foil in the refrigerator. After 4 h, the cell

culture medium was removed and 100 µL of DMSO was added to dissolve the crystals. A plate reader (Molecular Devices, Menlo Park, CA) was used to measure absorbance at 490 nm in the wells. Absorbance was corrected for non-specific, scattered light by subtracting the absorbance at 650 nm from the absorbance at 490 nm.

Dose-response curves: Non-linear, least-squares fitting of the absorbance-drug concentration data to a three- or four-parameter logistic equation (2.2) was performed using SigmaPlot (Jandel Corp., San Rafael CA):

$$A_{490/650} = \frac{a-d}{1+\left(\frac{D}{IC_{50}}\right)^{b}} + d \qquad (2.2)$$

where $A_{490/650}$ is the absorbance at 490 nm minus the absorbance at 650 nm, D is the drug concentration, IC_{50} is the median inhibitory concentration, b is a Hill-type exponential factor, a is the estimated maximal absorbance and d is the estimated background absorbance at the highest drug concentration. When the background absorbance is close to zero d is set equal to 0 in the equation (2.2) giving three-parameter logistic equation.

2.2.4. Molecular modelling

Molecular modelling of mitindomide and dexrazoxane structures was performed with PCModel versions 4 and 5 (Serena Software, Bloomington, IN). The MM2 Allinger algorithm was used [33].

2.3. Results

2.3.1. Inhibition of topoisomerase II decatenation activity

Dexrazoxane is a catalytic inhibitor of topoisomerase II [28]. Both human p170 and CHO nuclear extract topoisomerases II were used to compare the inhibitory

properties of mitindomide with dexrazoxane. Topoisomerase II activity using kDNA as a substrate, produces nicked, opened circular and relaxed, covalently closed decatenated DNA monomers [25]. Topoisomerase II inhibitors lower the decatenation rate. As shown in Fig. 2.4, mitindomide and dexrazoxane inhibited the catalytic decatenation activity of topoisomerase II. Dexrazoxane and mitindomide were each used at five different concentrations to observe their inhibitory effect. Lanes 3 and 9 are lanes without inhibitory drugs. The bands of the nicked, open circular (NOC) and covalently closed circular (CC) DNA in these lanes show the highest decatenation rate. With increasing concentration of the drugs in lanes 4 to 8 for dexrazoxane, and 10 to 14 for mitindomide, decatenated products are significantly decreased, compared to the bands without the drugs. For the highest concentrations of dexrazoxane (50 μM, lane 8) and mitindomide (1000 μM, lane 14), the formation of covalently closed circular monomers is completely inhibited. The position of the decatenated bands could be recognised by comparing them with authentic decatenated kDNA markers which consisted of NOC and CC monomers (line 1 and 15). In lane 2 the enzyme was not added to the sample with kDNA and assay buffer. Under this condition contamination with gyrase could be evaluated. Decatenated supercoiled DNA, the product of gyrase activity was not seen. If the contamination was present, a band would appear before the relaxed DNA band. The intensities of the nicked, opened circular DNA bands were integrated with SigmaGel (Jandel Scientific, San Rafael CA). Examples of the intensities of the NOC labelled bands plotted against concentrations of the drugs are presented in Fig. 2.5. The experimental data were fitted to a four-parameter logistic equation (2.1). The solid lines represent the results of the curve fits. The median inhibitory

concentrations ● SEM of mitindomide for human and CHO nuclear extract topoisomerases II were 264 ± 24.9 μM and 247 ● 62.0 μM, respectively (Fig. 2.5, a and c). Analogously, dexrazoxane inhibition of human and CHO nuclear extract topoisomerases II, expressed in median inhibitory concentrations ● SEM were 13.0 ± 3.8 μM and 6.2 ● 1.8 μM, respectively (Fig. 2.5, b and d). The results from all topoisomerase II inhibitory Experiments are presented in Table 2.5. The average values of the median inhibitory concentrations ± SEM for mitindomide were 199.3 ± 36.3 μM and 152.0 ± 52.0 μM on human and CHO nuclear extract topoisomerases II, respectively. The corresponding values for dexrazoxane were 10.0 ● 4.2 μM and 6.2 ± 1.8 μM.

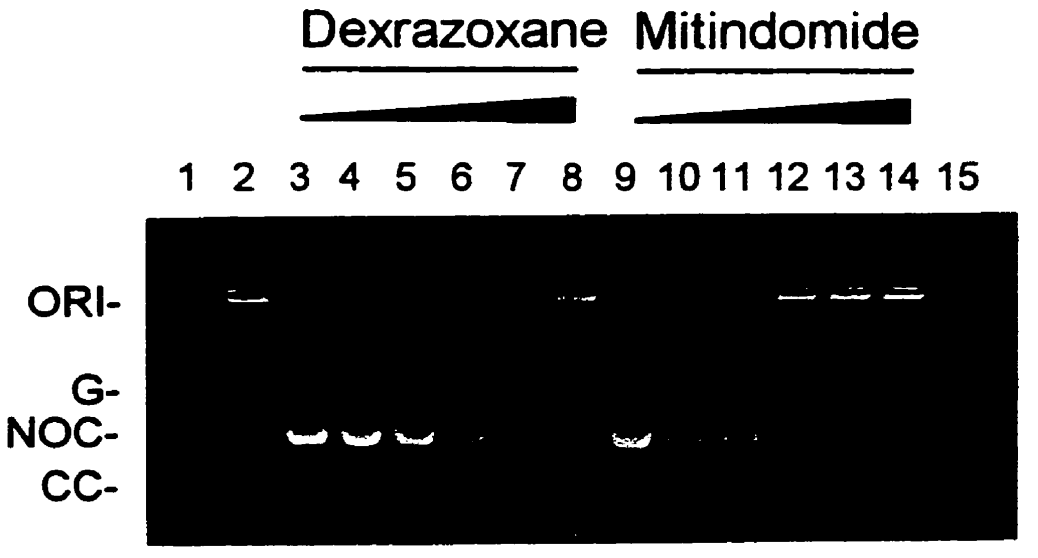

Fig. 2.4. Electrophoresis of kDNA decatenation products under human topoisomerase II activity. Decatenation activity of topoisomerase II is inhibited by dexrazoxane (line 3-8) and mitindomide (line 10-14). Wells 2-14 contain 4 μL of kDNA (50 ng/μL) and 2 μL of assay buffer. Wells 3-14 contain 1 μL of human topoisomerase II (1 unit/μL). The following bands are seen on the gel: ORI - loading well origin, G - genomic DNA (a contaminant of kDNA), NOC - nicked, open circular decatenated DNA, CC - covalently closed circular decatenated DNA. The contents of the wells are as follows: 1 - kDNA marker, 2 - no enzyme, 3 - no drug; dexrazoxane: 4 - 2 μM, 5 - 5 μM, 6 - 10 μM, 7 - 20 μM, 8 - 50 μM, 9 - no drug; mitindomide: 10 - 50 μM, 11 - 100 μM, 12 - 200 μM, 13 - 500 μM, 14 -1000 μM; 15 - kDNA marker. The bands between the origin and genomic bands likely correspond to incompletely decatenated kDNA products [25].

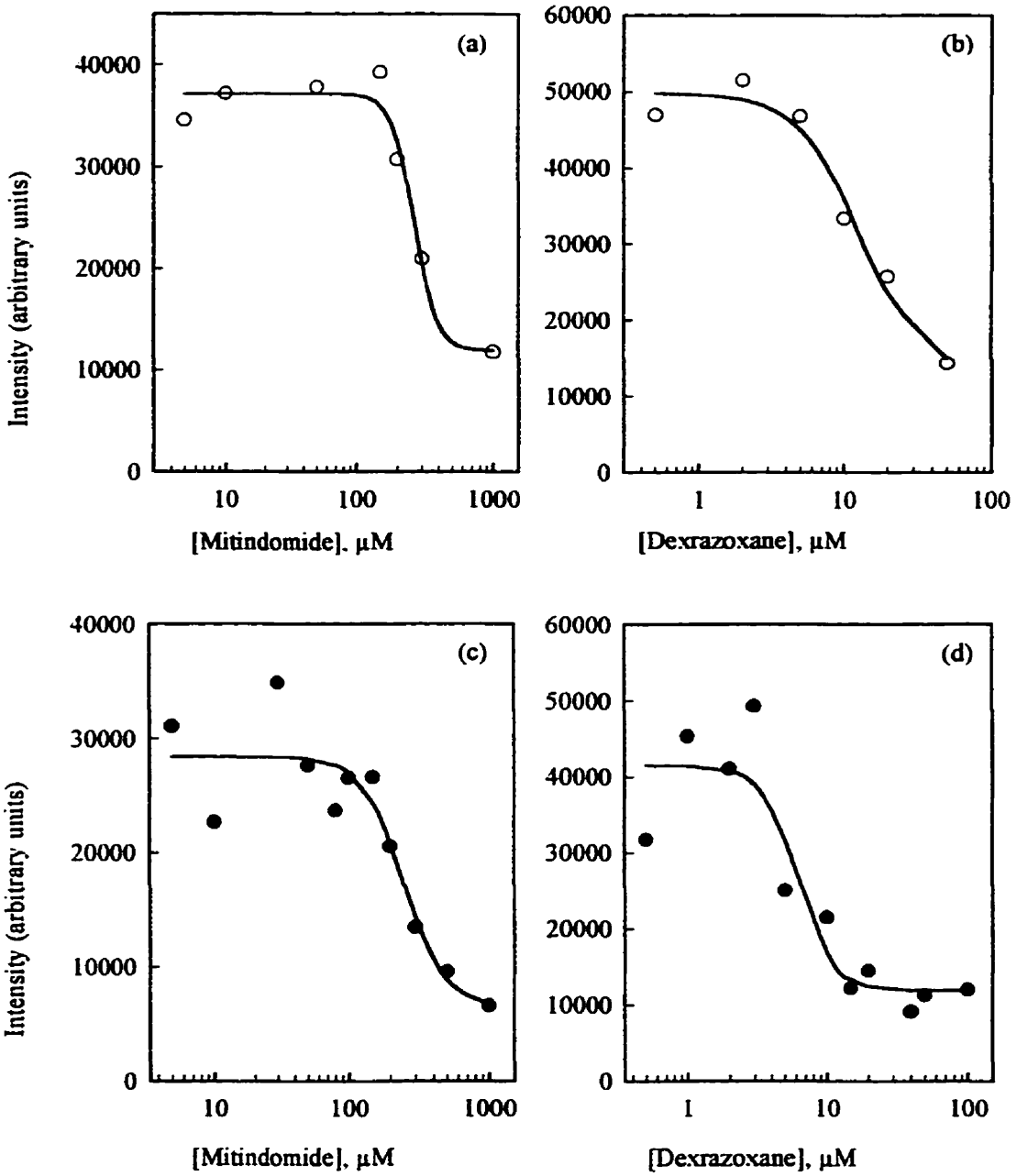

Fig. 2.5. Inhibition of human (○) and CHO nuclear extract (●) topoisomerase II by mitindomide (a, c) and dexrazoxane (b, d). The intensity values were obtained from scanned photographs of gels by integration of the NOC-bands (Fig. 2.3) on SigmaGel. The solid lines represent the results of least square non-linear regression fits of measured values to a four-parameter logistic equation on each graph. The lowest concentrations plotted correspond to zero concentration of drug, plotted for convenience on the

logarithmic scale with an arbitrary given value. The IC_{50} values ● SEM for these Experiments are given in the text above.

Table 2.5. Mitindomide and dexrazoxane inhibitory effect on human and CHO nuclear extract topoisomerase II

	IC_{50} ± SEM[a], μM			
	Mitindomide		Dexrazoxane	
Experiment No.	human p170 topo II	CHO nuclear extract topo II	human p170 topo II	CHO nuclear extract topo II
1	200.0 ± 4.6	247.2 ± 62.0	4.4 ± 4.63	6.2 ± 1.8
2	295.0 ± 37.21	66.3 ± 16.3	20.4 ± 164.8	-
3	123.0 ± 10.4	142.4 ± 0.001	2.0 ± 47.0	-
4	114.3 ± 0.004	-	13.0 ± 3.8	-
5	264.0 ± 24.9	-		
Mean ± SEM[b]	199.3 ± 36.3	152.0 ± 52.0	10.0 ± 4.2	6.2 ± 1.8[c]

[a] The individual median inhibitory concentrations, of mitindomide and dexrazoxane and their means ● SEM towards human p170 topoisomerase II. The individual IC_{50} values ● SEM were obtained from a non-linear least squares regression fit of integrated intensity to a three- or four-parameter logistic equation.

[b] The average IC_{50}-values ± SEM are the means from corresponding individual values.

[c] This value represents the standard error from the least squares, non-linear regression fit of integrated intensity from a single Experiment to a four-parameter logistic equation.

2.3.2. Cytotoxicity experiments

Mitindomide (Mid) was examined for cross-resistance with dexrazoxane using the dexrazoxane resistant (DZR) cell line. The cytotoxicity of mitindomide and dexrazoxane toward CHO and DZR cell lines was studied. The examples of the results from single Experiments are given in Fig. 2.6. Dexrazoxane used in these Experiments was dissolved in cell culture medium. The poor solubility of mitindomide caused experimental difficulties; we found mitindomide solubility in DMSO to be 20 mg/mL. DMSO shows cytotoxicity above 0.5% (v/v) thus the highest concentration of mitindomide was limited to 400 μM. When mitindomide was dissolved in sodium hydroxide (1:2.1 molar ratio of mitindomide to sodium hydroxide), and 5 μL volumes of mitindomide standards were added to wells with 195 μL of the cell culture medium, the crystals were observed in the wells above 1000 μM (Fig. 2.7.(b) for DZR cell line). Based on these observations, the solubility of mitindomide in the cell culture medium is 0.25 mg/mL (about 1 mM). The individual values of median inhibitory concentration for each cytotoxicity Experiment and their means are presented in Table 2.6. The median inhibitory concentrations for mitindomide towards the CHO cell line was about 25 times smaller than towards the DZR cell line; the corresponding median inhibitory concentrations ± SEM were 92.3 ± 13.6 μM and 2300 ± 200 μM. The mitindomide IC_{50}-value on DZR cell line was estimated since it was above the limit of its solubility.

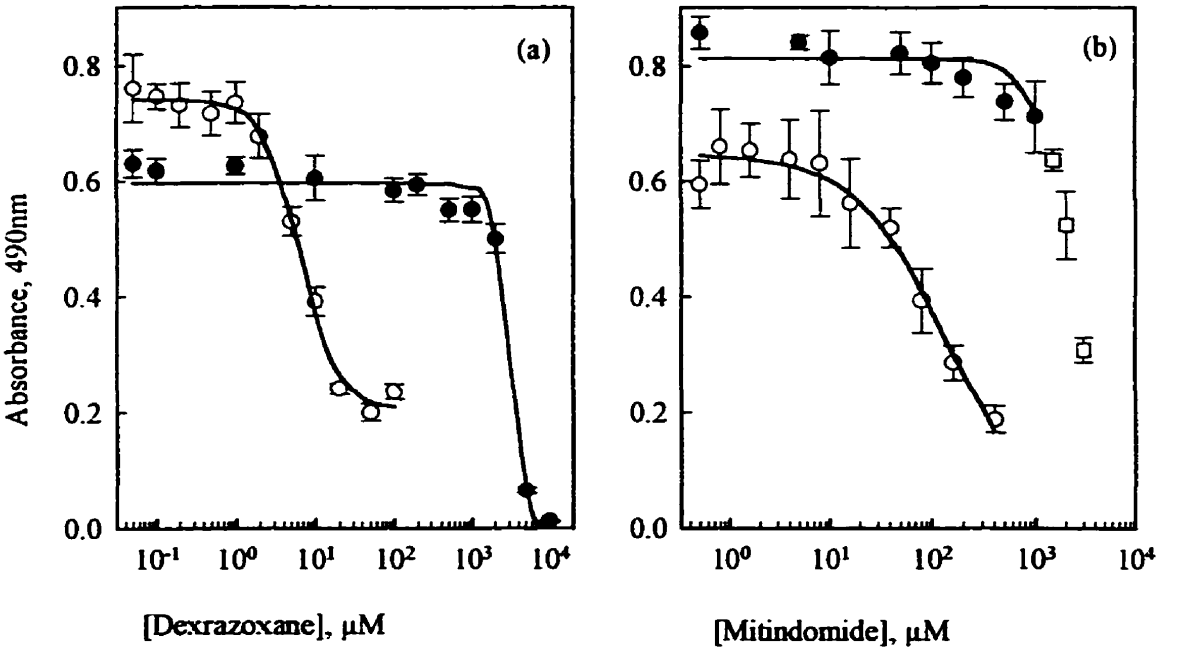

Fig. 2.6. Inhibition of cell growth by dexrazoxane and mitindomide. Dexrazoxane and mitindomide were incubated for 72 h with CHO (○) and DZR (●) cell lines; (a) IC_{50} ± SEM of dexrazoxane were 6.5 ± 0.5 μM and 2982 ± 213 μM on CHO and DZR cell lines, respectively; (b) IC_{50} ± SEM of mitindomide were 139.2 ± 15.8 μM and 2523 ± 137 μM on CHO and DZR cell lines, respectively; points (□) - represent absorbance measured above the solubility limit of mitindomide. The curves represent the results of least squares non-linear regression fits of measured values to three- or four-parameter logistic equations. The error bars represent standard deviations. The lowest concentrations are the zero values, plotted for convenience on a logarithmic scale with arbitrary given values.

Table 2.6. Cytotoxicity of mitindomide and dexrazoxane toward CHO and DZR cell lines.

	$IC_{50} \pm SEM^a$, μM			
	Mitindomide		Dexrazoxane	
Experiment No.	CHO	DZR	CHO	DZR
1	71.2 ± 3.1	2115 ± 75.2	5.4 ± 0.5	2803 ± 555
2	70.0 ± 16.9	2523 ± 137	3.1 ± 0.4	2387 ± 193
3	139.2 ± 15.8	-	8.2 ± 0.5	3290 ± 512
4	118.0 ± 13.0	-	6.5 ± 0.5	2982 ± 213
5	87.4 ± 5.4	-		
Mean ± SEM[b]	92.3 ± 13.6	2300 ± 200	5.8 ± 1.0	2900 ± 180
Resistance factor[c]	25		500	

[a] The individual median inhibitory concentrations of mitindomide and dexrazoxane on CHO and DZR cell lines and their means ● SEM. The single IC_{50} values were obtained by fitting the data to three- or four-parameter logistic equations. The IC_{50} values for inhibitory effect of mitindomide on DZR cells were obtained by including the absorption of wells containing drug above its solubility limit. Thus, these values are only estimated.
[b] The average IC_{50}-values ± SEM are the means from corresponding individual values.
[c] Resistance factor: the ratio of mean median inhibitory concentrations of mitindomide or dexrazoxane on CHO and DZR cells.

2.3.3. Molecular modelling

Molecular modelling was used to compare structure of mitindomide and dexrazoxane. Since both drugs inhibited topoisomerase II, these studies were conducted to examine which common structural elements might be important for topoisomerase II

inhibition. Crystal structure parameters were obtained from x-ray data of dexrazoxane [23], a N-substituted analogue of mitindomide [22] and a one-ring open mitindomide derivative [21]. The molecular modelling data obtained are presented in Table 2.7.

Table 2.7. Structural parameters of mitindomide and dexrazoxane obtained from molecular modelling

Parameter	Mitindomide	Dexrazoxane
imide N-to-imide N distance (Å)[a]	7.8	9.0
Co-planarity of imide rings (°)[a, b]	7.3	1.3
N-to-plane distance (Å)[a]	3.0	3.7
Non-polar surface area ($Å^2$)[c]	127	135
Polar surface area ($Å^2$)[c]	135	141
Total surface area ($Å^2$)[c]	262	276
Molecular volume ($Å^3$)[c]	326	351
Human p170 topoisomerase II inhibition, IC_{50} (μM)	200	9.3
CHO topoisomerase II inhibition, IC_{50} (μM)	152	6.2

[a] From x-ray crystal structures from a N-substituted derivative of mitindomide [22] and dexrazoxane [23].
[b] The imide ring plane was defined by the nitrogen imide atom and the two adjacent carbonyl carbon atoms. The co-planarity was measured by the angle that the normals of the two planes have to each other.
[c] Calculated from the van der Waals surfaces by molecular modelling. Non-polar surface area includes contributions from both unsaturated (mitindomide only) and saturated areas.

The ball and stick structures of mitindomide and dexrazoxane (Fig. 2.7) are based on the x-ray crystal structures of mitindomide [22] and dexrazoxane [23] and have been energy minimised by the molecular modelling.

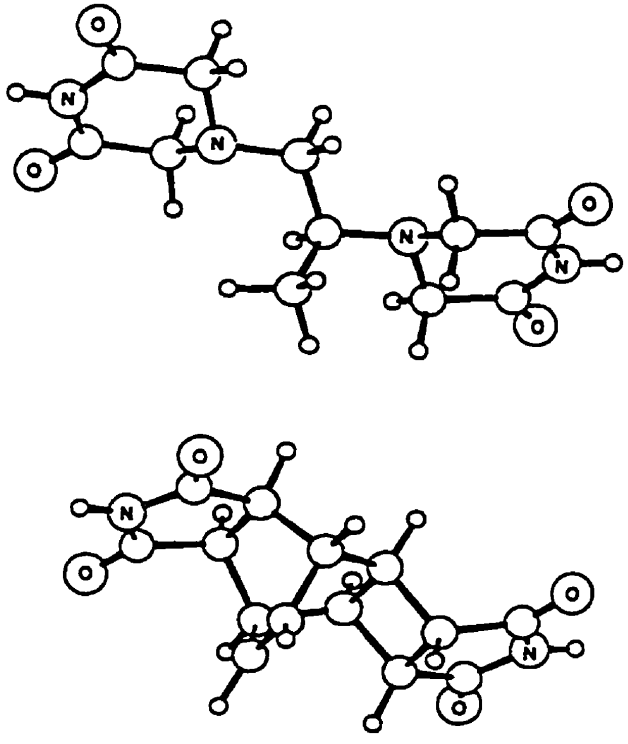

Fig. 2.7. Ball and stick structure of energy minimised mitindomide (top) and dexrazoxane (bottom).

2.4. Conclusions

Mitindomide, like dexrazoxane, was able to inhibit mammalian topoisomerase II as shown by the topoisomerase II decatenation assay (Table 2.5 and Fig. 2.5). Mitindomide median inhibitory concentrations ± SEM were 199.3 ± 36.3 μM and 152 ± 52.0 μM on human p170 and CHO nuclear extract topoisomerases II, respectively. Dexrazoxane

inhibition of topoisomerase II examined by the same assay resulted in 10.0 ± 4.2 μM and 6.2 ± 1.8 μM median inhibitory concentrations ± SEM for human and CHO topoisomerase II, respectively. Both mitindomide and dexrazoxane inhibited human and CHO enzymes to a comparable degree. This indicates a close relation between human and CHO topoisomerases II. There are two kinds of topoisomerase II inhibition mechanisms; catalytic inhibition shown by bisdioxopiperazines and stabilisation of a topoisomerase II-DNA complex (cleavable complex) shown by the anthracyclines, etoposide and amsacrine [8]. Since mitindomide targets topoisomerase II, a study was conducted to show which mechanism is more likely for mitindomide. Yalowich [34] has measured the level of cleavable complexes in CHO and DZR cells in the presence of mitindomide and the cleavable complex forming drug, etoposide. Unlike etoposide, mitindomide did not elevate cleavable complexes in CHO or DZR cells [34]. Furthermore, like the bisdioxopiperazines ICRF-154 and ICRF-193 [35], mitindomide was able to inhibit cleavable complex formation by etoposide in CHO cells [34]. This effect was not seen in DZR cells. Inhibition of etoposide cleavable complex formation in CHO, but not in DZR, cells was also shown with dexrazoxane [9]. These results indicate that mitindomide and dexrazoxane have similar mechanisms of action on topoisomerase II. The differences in the inhibition of etoposide-topoisomerase II-DNA complexes on CHO compared with DZR cells for mitindomide and dexrazoxane suggest that both drugs act on the same site of topoisomerase II. It has been shown that the cytotoxicity of bisdioxopiperazenes toward CHO and mouse-L cells is highly correlated with topoisomerase II inhibition [28]. The DZR cell line is highly resistant to dexrazoxane and cross-resistant to other

bispiperazines such as ICRF-193, ICRF-154, ICRF-186 [9]. The mean median inhibitory concentrations of dexrazoxane on CHO cells were 5.8 ± 1.0 μM and on DZR cells 2900 ● 180 μM. The corresponding values for mitindomide were 92.3 ± 13.6 μM and 2300 ● 200 μM, thus the DZR cell line also showed cross-resistance toward mitindomide (Table 2.6 and Fig. 2.6). The resistance factors, towards the DZR cell line compared with the parent CHO cell line, were 25 and 500 for mitindomide and dexrazoxane, respectively. In fact, the dexrazoxane-resistant cell line shows specific resistance to dexrazoxane probably through an alternation in topoisomerase II [9]. DZR cells' resistance to mitindomide suggests a common site of binding with bisdioxopiperazines.

The mitindomide and dexrazoxane structural parameters obtained from molecular modelling are given in Table 2.7. The distances between the two imide nitrogen atoms in the crystal structures of mitindomide and dexrazoxane are similar: 7.8 Å and 9 Å, respectively. Both mitindomide and dexrazoxane have approximately coplanar imide-containing rings: 7.3° and 1.3°, respectively. The offset of the rings is 3.0 Å in mitindomide and 3.7 Å in dexrazoxane. Other molecular parameters such as total, polar and non-polar surface areas, and molecular volumes have similar values for both drugs. Dexrazoxane is a conformationally flexible molecule which can rotate around its chain connecting the rings. Dexrazoxane, in crystallographic form, appears to be in an extended conformation [23]. The mitindomide molecule is extremely conformationally restricted. Its parameters such as co-planarity and nitrogen to nitrogen distance are very similar to those of dexrazoxane in an extended conformation. These findings suggest that rigid mitindomide and flexible dexrazoxane and presumably other bisdioxopiperazines, bind

topoisomerase II in their extended conformations (Fig.2.7). The mechanism of action on cells and topoisomerase II of both these drugs is similar; therefore, mitindomide can be classified as a topoisomerase II catalytic inhibitor.

References

1. Lomax NL and Narayanan VL, Chemical structures of interest to the division of cancer treatment. In: *Compounds in development. Drugs with clinical activity.* National Cancer Institute, National Institutes of Health, April 1981.

2. Narayanan VL, Strategy for the discovery and development of novel anticancer agents. In: *Structure-activity relationships of anti-tumour agents.* (Eds. Reinhoudt DN, Connors TA, Pinedo HM and van de Poll LW), pp. 5-22. Martinus Nijhoff, The Hague, 1983.

3. Moore DJ, Powis G, Melder DC, Deutsch HM and Zalkow LH, Cross-linking of DNA by diimide antitumor agents and the relationship to cytotoxicity in A204 rhabdomyosarcoma cells. *J Cell Pharmacol* **1:** 103-108, 1990.

4. Kenwrick SJ and Creighton AM, Isolation and characterization of a subline of CHO cells with induced resistance to ICRF 159. *Br J Cancer* **46:** 504-505, 1982.

5. Maxwell A and Gellert M, Mechanistic aspects of DNA topoisomerases. *Adv Protein Chem* **38:** 69-107, 1986.

6. Osheroff N, Zechiedrich EL and Gale KC, Catalytic function of DNA topoisomerase II. *Bioessays* **13:** 269-275, 1991.

7. D'Arpa P and Liu LF, Topoisomerase-targeting antitumor drugs. *Biochim Biophys Acta* **989:** 163-177, 1989.

8. Pommier Y, DNA topoisomerase II inhibitors. In: *Cancer Therapeutics: Experimental and Clinical Agents.* (Ed. Teicher B), pp. 153-174. Humana Press Inc., Totowa, NJ, 1997.

9. Hasinoff BB, Kuschak TI, Creighton AM, Fattman CL, Allan WP, Thampatty P and Yalowich JC, Characterization of a Chinese hamster ovary cell line with acquired resistance to the bisdioxopiperazine dexrazoxane (ICRF-187) catalytic inhibitor of topoisomerase II. *Biochem Pharmacol* **53:** 1843-1853, 1997.

10. Roca J, Ishida R, Berger JM, Andoh T and Wang JC, Antitumor bisdioxopiperazines inhibit yeast DNA topoisomerase II by trapping the enzyme in the form of a closed protein clamp. *Proc Natl Acad Sci USA* **91:** 1781-1785, 1994.

11. Roca J and Wang JC, The capture of a DNA double helix by an ATP-dependent protein clamp: A key step in DNA transport by type II DNA topoisomerases. *Cell* **71:** 833-840, 1992.

12. Sengupta SK, Topoisomerase II inhibitors. In: *Cancer chemotherapeutic agents.* (Ed. Foye WO), pp. 205-291. 1st ed. American Chemical Society, Washington, DC, 1995.

13. Bradshaw JS, The photosensitized addition of maleimide to benzene in the absence of a charge-transfer complex. *Tetr Lett* : 2039-2042, 1966.

14. Choudhari KB, Labhasetwar V and Dorle AK, Liposomes as a carrier for oral administration of insulin: effect of formulation factor. *J Microencapsul* **11:** 319-325, 1994.

15. Vishnuvajjala BR and Cradock JC, Tricyclo[4.2.2.$0^{2,5}$]dec-9-ene-3,4,7,8-tetracarboxylic acid diimide: formulation and stability studies. *J Pharm Sci* **75:** 301-303, 1986.

16. Neighbors RP and Riden JR, Use of a tricyclodecene-3,4,7,8-tetracarboxylic acid diimide as an anti-murine tumor agent. US Patent US 4,877,806 31 Oct 1989., 1989.

17. Deutsch HM, Gelbaum LT, McLaughlin M, Fleischmann TJ, Earnhart LL, Haugwitz RD and Zalkow LH, Synthesis of congeners and prodrugs of the benzene maleimide photoadduct, mitindomide, as potential antitumor agents. 2. *J Med Chem* **29:** 2164-2170, 1986.

18. Haugwitz RD, Narayanan V, Zalkow LH, Deutch HM and Gelbaum L, Substituted N-methyl derivatives of mitindomide. US Patent US 4803202, 1984.

19. Umprayn K, Stella VJ and Riley CM, Stability indicating assay for fetindomide (NSC 373965), a potential prodrug of mitindomide (NSC 284356), employing high-performance liquid chromatography. *J Pharm Biomed Anal* **5:** 675-685, 1987.

20. Sendo F, Riley CM and Stella VJ, Kinetics of hydrolysis of fetindomide (NSC-373965), bis-N,N'-phenylalanyloxymethyl prodrug of mitindomide (NSC-284356); an unexpected catalytic effect of generated formaldehyde. *Int J Pharm* **45:** 207-216, 1988.

21. Pettit GR, Paull KD, Herald CL, Herald DL and Riden JR, Antineoplastic agents. 90. The structure of the benzene-maleimide photosynthetic product (mitindomide). *Can J Chem* **61:** 2291-2294, 1983.

22. Deutsch HM, McGowan L, Van Derveer DG, Gelbaum LT and Zalkow LH, Structure of a derivative of mitindomide, the maleimide-benzene photoadduct, $C_{20}H_{20}N_2O_8$. *Acta Crystallogr C* **C40:** 1925-1927, 1984.

23. Hempel A, Camerman N and Camerman A, Stereochemistry of the antitumor agent 4,4'-(1,2-propanediyl)bis(4-piperazine-2,6-dione): Crystal and molecular structures of the racemate (ICRF-159) and a soluble enantiomer (ICRF-187). *J Am Chem Soc* **105:** 3453-3456, 1982.

24. Danks MK, Schmidt CA, Cirtain MC, Suttle DP and Bect WT, Altered catalytic activity of and DNA cleavage by DNA topoisomerase II from human leukemic cells selected for resistance to VM-26. *Biochemistry* **27:** 8861-8869, 1988.

25. Sahai BM and Kaplan JG, A quantitative decatenation assay for type II topoisomerases. *Anal Biochem* **156:** 364-379, 1986.

26. Marini JC, Miller KG and Englund PT, Decatenation of kinetoplast DNA by topoisomerases. *J Biol Chem* **255:** 4976-4979, 1980.

27. Ryan KA, Shapiro TA, Rauch CA and Englund PT, Replication of kinetoplast DNA in trypanosomes. *AnnRevMicrobiol* **42:** 339-358, 1988.

28. Hasinoff BB, Kuschak TI, Yalowich JC and Creighton AM, A QSAR study comparing the cytotoxicity and DNA topoisomerase II inhibitory effects of bisdioxopiperazine analogs of ICRF-187 (dexrazoxane). *Biochem Pharmacol* **50:** 953-958, 1995.

29. A decatenation-supercoiling assay using kinetoplast DNA suitable for prokaryotic and eukaryotic type II topoisomerases. TopoGen Inc., Columbus, OH, USA, 1996; 4 p.

30. Vistica DT, Skehan P, Scudiero D, Monks A, Pittman A and Boyd MR, Tetrazolium-based assays for cellular viability: a critical examination of selected parameters affecting formazan production. *Cancer Res* **51:** 2515-2520, 1991.

31. Sobottka SB and Berger MR, Assessment of antineoplastic agents by MTT assay: partial underestimation of antiproliferative properties. *Cancer Chemother Pharmacol* **30:** 385-393, 1992.

32. Carmichael J, DeGraff WG, Gazdar AF, Minna JD and Mitchell JB, Evaluation of a tetrazolium-based semiautomated colorimetric assay: assessment of chemosensitivity testing. *Cancer Res* **47:** 936-942, 1987.

33. Burkert U and Allinger NL. *Molecular Mechanics. ACS Monograph 177.* American Chemical Society, Washington, 1982.

34. Hasinoff BB, Creighton AM, Kozlowska H, Thampatty P, Allan WP and Yalowich JC, Mitindomide is a catalytic inhibitor of DNA topoisomerase II that acts at the bisdioxopiperazine binding site. *Mol Pharmacol* **:** 839-845, 1997.

35. Ishida R, Miki T, Narita T, Yui R, Sato M, Utsumi KR, Tanabe K and Andoh T, Inhibition of intracellular topoisomerase II by antitumor bis(2,6-dioxopiperazine) derivatives: mode of cell growth inhibition distinct from that of cleavable complex-forming type inhibitors. *Cancer Res* **51:** 4909-4916, 1991.

3. Effect of dexrazoxane on growth inhibition of Chinese hamster ovary cells in the combination with mafosfamide, 5-fluorouracil and vinblastine

3.1. Introduction

Dexrazoxane is clinically used to prevent the cardiotoxicity of the anticancer drug doxorubicin (Chapters I and IV) [1, 2]. Doxorubicin is often given in an anticancer multi-drug schedule with cyclophosphamide, 5-fluororacil and vinblastine [3, 4]. Besides its cardioprotective properties, dexrazoxane also has anticancer activity, probably through topoisomerase II inhibition [5]. A detailed description of dexrazoxane topoisomerase II inhibition is given in Chapter II. Cyclophosphamide, 5-fluorouracil, and vinblastine are anticancer drugs with different mechanisms of cytotoxicity.

The objective of this study was to analyse the effect of the combined action of dexrazoxane with each of these drugs on Chinese hamster ovary cell growth. The experiments were designed to use different evaluation methods of drug interaction. Combination index, envelope of additivity, response surface and slopes comparison methods were used in the data analysis.

3.1.1. Mechanisms of cyclophosphamide, 5-fluorouracil and vinblastine cytotoxicity

Cyclophosphamide (Fig. 3.1.a) exerts its cytotoxicity by reacting chemically with DNA [6]. The strongest effect of cyclophosphamide is observed on proliferating tissue, but like other alkylating agents, its toxicity is not cell-cycle dependent [6]. This drug belongs to the same class as nitrogen mustards. Cyclophosphamide is a prodrug which is activated *in vivo*, mostly in the liver [7] to 4-hydroxycyclophosphamide. Non-enzymatic

conversion of 4-hydroxycylophosphamide leads to phosphoramide mustard and acrolein. It has been demonstrated that phosphoramide mustard is responsible for the therapeutic activity of cyclophosphamide [6]. It is not clear whether phosphoramide mustard or 4-hydroxycyclophosphamide is a major blood transport form that enters tumour cells. Phosphoramide mustard and 4-hydroxycyclophosphamide have different levels of cytotoxicity towards different types of cancer, for instance 4-hydroxycyclophosphamide shows greater cytotoxicity than phosphoramide mustard toward lymphoproliferative tumours. Since Chinese hamster ovary cells are not able to convert cyclophosphamide to its active forms, the cyclohexylamine salt of mafosfamide (Fig. 3.1.c) is often used in *in vitro* studies. Hydrolysis of this salt yields the active compound, 4-hydroxycyclophosphamide (Fig. 3.1.d), as well as 2-mercaptoethanesulfonic acid and cyclohexylamine.

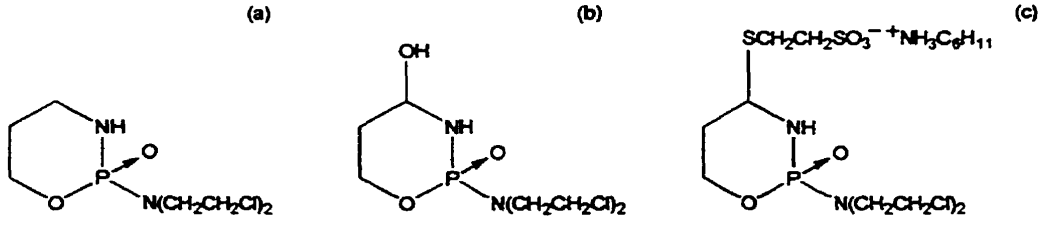

Fig. 3.1. Structures of (a) cyclophosphamide, (b) 4-hydroxycyclophosphamide, and (c) cyclohexylamine salt of mafosfamide.

5-Fluorouracil (Fig. 3.2) is an antimetabolite which interferes with the synthesis of new DNA [8]. 5-Fluorouracil cytotoxicity is most expressed in the S phase of the cell cycle [8]. 5-Fluorouracil itself is not active; but it is metabolically activated in cells to

fluororibonucleotides and fluorodeoxyribonucleotides [8]. Cytotoxicity of 5-fluorouracil is exerted through incorporation of fluorouridine triphosphate (FUTP) into RNA, incorporation of fluorodeoxyuridine triphosphate (FdUTP) into DNA and inhibition of thymidylate synthase enzyme by fluorodeoxyuridine monophosphate (FdUMP) [9]. These processes cause disruptions in the function and synthesis of RNA and DNA.

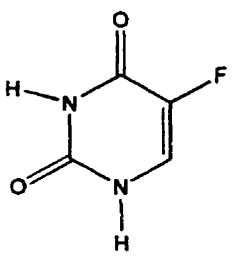

Fig. 3.2. Structure of 5-fluorouracil.

Vinblastine (Fig. 3.3) is an antimitotic agent that interferes with cell division [10]. Vinblastine is a natural product obtained from *Vinica rosea*. The biochemical mechanism of vinblastine cytotoxicity is not well known. Vinblastine binds with high affinity to microtubules. There are probably two vinblastine high affinity binding sites per microtubule. The binding seems to be dependent on the ionic interaction between the tubulin (an acidic protein) and vinblastine (a basic molecule) [10]. Normal cellular function is dependent on microtubule assembly and disassembly. At low concentrations (10 nM - 1.0 μM), vinblastine binds to the growing end of the microtubules and inhibits their growth. Above 10 μM, tubulin aggregation occurs, resulting in the formation of tubulin paracrystals [10].

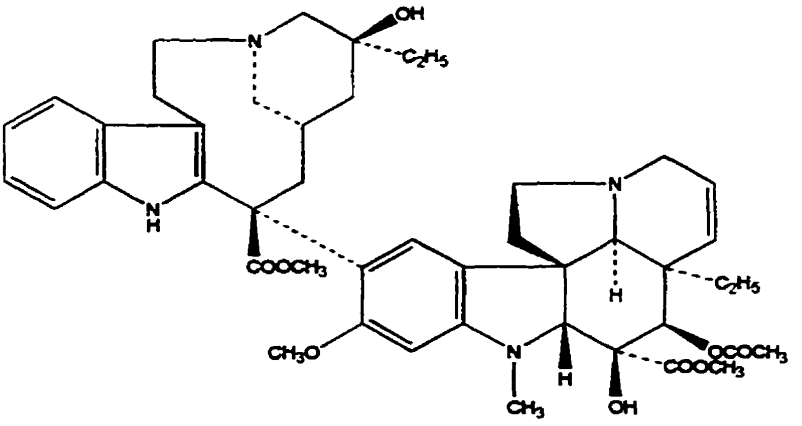

Fig. 3.3. Structure of vinblastine.

3.2. Materials and methods

Chinese hamster ovary cells were used to study the influence of drug combinations. The cells were seeded at 2000 cells in 100 μL of cell culture medium on 96-well plates and allowed to attach for a specified time. After this period of time, drugs were delivered and the volume of cell culture medium was increased to 200 μL/well. The cells were incubated for another 72 or 48 h as indicated in descriptions of the particular experiments. The MTT assay was used to quantify the effects of cell exposure to the drugs. A detailed description of cytotoxicity experiments and the MTT assay is given in Chapter II, Section 2.2.3. The growth inhibition of Chinese hamster ovary cells by dexrazoxane with mafosfamide and dexrazoxane with 5-fluorouracil was examined using the combination index (Section 3.2.4.1), envelope of additivity (Section 3.2.4.2), response surface (Section 3.2.4.3), and slope comparison (Section 3.2.4.4) methods. The slope comparison method was also used to study the interaction of vinblastine and dexrazoxane.

3.2.1. Materials

Dexrazoxane (ICRF-187) was a gift from Pharmacia & Upjohn (Columbus, OH). Mafosfamide cyclohexylamine salt was a gift from Asta Medica (Frankfurt, Germany). Vinblastine sulphate salt and 5-fluorouracil (99%) were obtained from Sigma Chemical Co., DMSO (used to dissolve drugs, 99.5%, cat. No. D-5879) was obtained from Sigma Chemical Co.

3.2.2. Solubility of mafosfamide, 5-fluorouracil, vinblastine and dexrazoxane

New stock solutions of all drugs were prepared 15 min before each experiment. The solubility of cyclohexylamine salt of mafosfamide (M_w = 50.5 g/mol) in water is 160 mg/mL [11]. In water, mafosfamide is converted to its active unstable form, 4-hydroxycyclophosphamide. For this reason, the cyclohexylamine salt of mafosfamide was dissolved in DMSO to avoid problems of instability. It was delivered in 1 μL volume to plate wells. The final concentration of DMSO in the wells was 0.5% (v/v). Each mafosfamide concentration was prepared as a separate stock solution.

5-Fluorouracil (M_w = 130.08 g/mol) is sparingly soluble in water [12]. For experiments, 5-fluorouracil was dissolved in 1.00 equivalent of an aqueous solution of NaOH. The stock solution was filter sterilised with a previously sterilised 4 mm syringe filter with PVDF filter media, 0.2 μm pore size (Whatman Laboratory Division, cat. No. 6777-0402). The dilution of stock solution was made with sterilised 0.9% (w/v) NaCl or water. Each concentration of 5-fluorouracil was prepared as a separate stock solution and delivered to the wells in 1 μL volume.

Vinblastine (M_w = 811 g/mol) was used in the form of its sulphate salt (M_w = 909.1 g/mol) that also contained 1.5 mol water per mol of vinblastine, and 7.8% (wt/wt) ethanol. The mass corrected for 1.5 mol of water and 7.8% (wt/wt) ethanol that contained 1 mol of vinblastine was 1015.2 g/mol. The sulphate salt of vinblastine is freely soluble in water [12]. Vinblastine used for experiments was highly diluted. The highest stock solution concentration was 10 μM. For these experiments, vinblastine was dissolved in one equivalent of aqueous solution of 1 mM HCl to maintain an acidic environment. 0.9% (w/v) NaCl was used for further dilution. The stock solution was filter sterilised with a 0.2 μm sterile cellulose acetate syringe filter (Sarstedt Inc., Cat. No. 831826001). Each stock solution was prepared separately. 10 μL of stock solution volume was delivered to the wells. One experiment (not shown) was performed with vinblastine dissolved in DMSO and delivered in 1 μL aliquots. The obtained results were similar to those in which vinblastine was dissolved in HCl indicating that vinblastine cytotoxicity is maintained in HCl.

Dexrazoxane (M_w = 268.28 g/mol) was dissolved in cell culture medium and it was filter sterilised with a 0.2 μm cellulose acetate filter. Dexrazoxane was delivered in 10-60 μL volumes. When dexrazoxane was used with mafosfamide for combination index experiments both drugs were dissolved in DMSO and delivered separately as single agents, or as a mixture in 1 μL aliquots.

3.2.3. Design of the experiments for the combination of dexrazoxane with mafosfamide, 5-fluorouracil and vinblastine

3.2.3.1. Design of the combination index experiments for the combination of dexrazoxane with mafosfamide and 5-fluorouracil

The combination index experiments were performed for dexrazoxane with either mafosfamide or 5-fluorouracil. The concentrations of drugs were chosen to obtain a wide range of effect, from 100% to 20% of survival. Continuous, 72 h exposure of Chinese hamster ovary cells to the drugs was selected for the combination index experiments. This length of time resulted in 80% cell death for 50 μM dexrazoxane; 48 h exposure to 50 μM dexrazoxane produced only a 20% cell death. Five plates with seeded cells were used for one combination index experiment. The first plate was used for wide range dose-response curve of dexrazoxane (0.05-50 μM), the second, for wide range dose-response curve of either mafosfamide (0.05-50 μM) or 5-fluorouracil (0.05-50 μM), and the remaining three plates were used for dose-response curves of drug mixtures.

The ratio of the two drugs was kept constant through the whole range of concentrations. Three ratios of drugs were chosen. One was the ratio of drug concentrations that contribute equally to the effect of their combination (an equipotent combination). The equipotent ratio was calculated as $D_A/D_B = d_A/d_B$ where D_A and D_B, the doses of single drugs that produce the same effect as d_A and d_B, the doses of drugs in combination. For the other two ratios, an excess of one or the other drugs was used.

The volume of 1 μL of stock solutions of dexrazoxane and mafosfamide and their mixtures in DMSO were delivered to wells. DMSO was also added in 1 μL aliquots to the

first column of six wells as a control. In the experiment with dexrazoxane and 5-fluorouracil, the drugs were delivered separately to the wells assigned for the mixture of the drugs. Dexrazoxane dissolved in the cell culture medium was always added first, immediately followed by 1 μL of 5-fluorouracil stock solution.

3.2.3.2. Design of the envelope of additivity experiments for the combination of dexrazoxane with mafosfamide and 5-fuorouracil

The envelope of additivity experiments were performed for the combination of dexrazoxane with either mafosfamide or 5-fluorouracil. The inhibitory effects of a 72 h exposure of Chinese hamster ovary cells to the drugs were measured. Experiments were designed to obtain wide range dose-response curves for dexrazoxane (0.1-100 μM) and mafosfamide (0.05-50 μM) or 5-fluorouracil (0.1-100 μM) and four additional dose-response curves for each of mafosfamide and 5-fluorouracil with different fixed concentrations of dexrazoxane for each curve *e.g.* 1.5, 2.0, 2.5 and 4.0 μM. The fixed concentrations of dexrazoxane were selected to include the effect of the planned envelope. Dexrazoxane was dissolved in the cell culture medium and delivered 20 min before the second drug was added. The time gap between drugs delivery was arranged to give dexrazoxane a chance to enter the cells and bind topoisomerase II. Mafosfamide was dissolved in DMSO to reduce hydrolysis. 5-Fluorouracil was dissolved in one equivalent of aqueous solution of NaOH. Both drugs were delivered in a 1 μL aliquots.

3.2.3.3. Design of the slope comparison experiments for the combination of dexrazoxane with mafosfamide, 5-fluorouracil and vinblastine

The slope comparison experiments were designed to obtain dose-response curves for a wide range of dexrazoxane concentrations (0.5-500 μM) as a single agent and as its combinations with fixed doses of mafosfamide, 5-fluorouracil or vinblastine. The Chinese hamster ovary cells were incubated for 24 h without the drugs. Then the drugs were delivered and incubated with the cells for another 48 h. The 48 h incubation of the cells with dexrazoxane gave only 20% kill as a maximal effect. Five to eight fixed concentrations of the drugs were used. The fixed concentrations of drugs were selected to cover a broad range of cell survival *i.e.* to obtain the combined drug dose-response curves for many different cell survival levels. Dexrazoxane was added one hour before the second drug. Mafosfamide, as with the other experiments, was dissolved in DMSO. Although dexrazoxane was dissolved in the cell culture medium, 1 μL of DMSO was also added to plate with dexrazoxane (only in experiments with mafosfamide) to keep the same conditions for all dose-response curves. 5-Fluorouracil was dissolved in NaOH solution and vinblastine in HCl as described in Chapter II, Section 3.2.2.

3.2.4. Data analysis with the combination index, envelope of additivity, response surface and slope comparison methods

3.2.4.1. Data analysis with the combination index method

The combination index method [13] was described in Chapter I, Section 1.1.2.7. In this Section the individual experimental and calculation Steps are given in an example for

dexrazoxane and mafosfamide. All the Steps below are undertaken to obtain the variables for the equation (3.1) and to calculate the combination index CI :

$$CI = \frac{d_{Dex}}{D_{Dex}} + \frac{d_{Maf}}{D_{Maf}} + \frac{\alpha \cdot d_{Dex} \cdot d_{Maf}}{D_{Dex} \cdot D_{Maf}} \qquad (3.1)$$

where D_{Dex} and D_{Maf} are the doses of dexrazoxane and mafosfamide alone that produce given effect x and d_{Dex} and d_{Maf} are the doses of dexrazoxane and mafosfamide in combination that produce the same effect x; $\alpha = 0$ or 1, as described in Chapter I, Section 1.1.2.7.

The analysis with the combination index method consist of following Steps:

1. In the preliminary cytotoxicity experiment, the 72 h dose-response curves for mafosfamide and dexrazoxane on Chinese hamster ovary cells were defined. The MTT assay was used to measure the effect (absorbance 490-650 nm) of different drug concentrations on the survival of the cells. The absorbance-concentration data were fitted to a three- or four-parameter logistic equation (3.4a and b) as appropriate. The IC_{50} values were calculated; thus the equipotent ratio of dexrazoxane to mafosfamide was calculated: $IC_{50,Dex}/IC_{50,Maf}$ = 4.1 μM/6.0 μM = 0.683. The other two ratios of dexrazoxane to mafosfamide chosen were 5.0 and 0.2.

2. The appropriate cytotoxicity experiment was designed. The experiment consisted of five 72 h dose-response curves: the dose-response curves for dexrazoxane and mafosfamide alone and their three ratios 0.683, 5.0 and 0.2. The concentrations D_{Dex} and D_{Maf} of single drugs and their combinations (d_{Dex}+d_{Maf}) were in the range 0.05-50 μM.

The results for single agents and their equipotent combination are given in Table 3.1. These raw data are also plotted in Fig. 3.5.

Table 3.1. Effect-dose data of dexrazoxane, mafosfamide and their mixture in equipotent ratio obtained from 72 h cytotoxicity experiment on Chinese hamster ovary cells.

D^a	Absorbance at 490 - 650 nm		
μM	Maf	Dex	Dex/Maf=0.683
0.00	0.7622	0.6857	0.6557
0.05	0.7752	0.712	0.6895
0.1	0.7908	0.7445	0.6947
0.2	0.7678	0.7277	0.6983
0.5	0.758	0.7255	0.6892
1.0	0.7775	0.7353	0.7062
2.0	0.6982	0.626	0.6213
5.0	0.3967	0.408	0.4687
10.0	0.1207	0.2508	0.189
20.0	0.2002	0.163	0.1935
50.0	0.0108	0.1385	0.0828

[a] Concentration of single and combined drugs

3. The equation (3.1) includes the parameter α. For mutually exclusive drugs α = 0 and mutually nonexclusive drugs α = 1. The median effect plot (equation 3.2) was used to assess the exclusivity of the drugs and determine the value of α:

$$\log\frac{1-f_u}{f_u} = m\cdot\log(D) - m\cdot\log(IC_{50}) \qquad (3.2)$$

where f_u is the fraction unaffected by the dose D (D is D_{Maf}, D_{Dex} or $D = d_{Dex}+d_{Maf}$), IC_{50} is a median effective concentration and m is a Hill-type coefficient. The calculated f_u values for the data presented in Table 3.1 are given in Table 3.2. They were determined by dividing each absorbance by the corresponding values of absorbance obtained from the wells without the drugs (first row in Table 3.1).

Table 3.2. Fractions of the cells unaffected (fractional survival) by mafosfamide, dexrazoxane and their equipotent mixture calculated for the example from Table 3.1.

D^a	fraction unaffected, f_u		
μM	Maf	Dex	Dex/Maf=0.683
0.00	1.0000	1.0000	1.0000
0.05	1.0171	1.0384	1.0515
0.1	1.0375	1.0858	1.0595
0.2	1.0073	1.0613	1.0650
0.5	0.9945	1.0580	1.0511
1.0	1.0201	1.0723	1.0770
2.0	0.9160	0.9129	0.9475
5.0	0.5205	0.5950	0.7148
10.0	0.1584	0.3658	0.2882
20.0	0.2627	0.2377	0.2951
50.0	0.0142	0.2020	0.1263

[a] Concentration of single and combined drugs

The values from Table 3.2 were used to calculate the left side of equation (3.2): $\log(1-f_u)/f_u$ for corresponding $\log D$. The results of calculations are given in Table 3.3.

Table 3.3. Log D and log $(1-f_u)/f_u$ for data from Table 3.2.

D	log D	log $(1-f_u)/f_u$		
μM		Maf	Dex	Dex/Maf=0.683
0.00				
0.05	-1.3010			
0.1	-1.0000			
0.2	-0.6990			
0.5	**-0.3010**	**-2.2564**		
1.0	0.0000			
2.0	**0.3010**	**-1.0378**	**-1.0206**	**-1.2567**
5.0	**0.6990**	**-0.0356**	**-0.1671**	**-0.3991**
10.0	**1.0000**	**0.7255**	**0.2391**	**0.3926**
20.0	1.3010	0.4483	0.5061	0.3781
50.0	1.6990	1.8424	0.5967	0.8400

The log $(1-f_u)/f_u$ was not calculated for D in a range 0.0-1.0 μM because $(1-f_u)/f_u = 0$ or $<$ 0. A median effect plot was generated from the data in Table 3.3. The responses of 20.0

μM and 50.0 μM were not used to construct the median effect plot because they were not linear. Only the data in bold font from Table 3.3 were used to construct the plot shown in Fig. 3.6, Section 3.3.1.1. These data are from the steepest part of the dose-response curve (Fig.3.5). When median effect plots for single agents and their combination are parallel, the drugs are mutually exclusive and $\alpha = 0$ in equation (3.1). When the single agent median effect plots are parallel, but their combination is not, the drugs are mutually nonexclusive; then $\alpha = 1$ in equation (3.1). None of the median effect plots for single agents used in these experiments were parallel. The value of median effect plot slopes presented in Fig.3.6 were 2.3 and 1.8 for mafosfamide and dexrazoxane, respectively. Because exclusivity of the drugs could not be determined, both equations *i.e.* for $\alpha = 0$ and $\alpha = 1$ were used for combination index calculations.

4. The equation (3.1) requires the calculation of the doses of single agents and the combination that produce given effect x. The parameters (IC_{50} and m) that defined the concentration-effect relationship given as equation (3.3) were obtained from the median effect plot (equation 3.2). In equation (3.2) m is the slope and ($-m \cdot \log IC_{50}$) is the Y-intercept b; thus $IC_{50} = 10^{-b/m}$. The calculated parameters are given in Table 3.4.

Table 3.4. The linear parameters (Hill-type coefficient *m* and Y-intercept *b*) of median effect plot and calculated IC_{50} values for mafosfamide and dexrazoxane combination index experimental data.

	Maf[a]	Dex[b]	Dex/Maf=0.683[c]
m	2.2924	1.8201	2.349
b	-1.6248	-1.5296	-1.987
IC_{50}, μM	5.1142	6.9246	7.0128

[a] Parameters for mafosfamide
[b] Parameters for dexrazoxane
[c] Parameters for combination of dexrazoxane with mafosfamide in equipotent ratio

5. The doses d_{Dex}, d_{Maf}, D_{Dex} *and* D_{Maf} at any chosen effect x (expressed as the fraction affected, f_a, where $f_a + f_u = 1$) were calculated with the equation below:

$$D = IC_{50}\left(\frac{f_a}{1-f_a}\right)^{\frac{1}{m}} \tag{3.3}$$

where D is D_{Dex}, D_{Maf} or $D = d_{Dex} + d_{Maf}$. The IC_{50} and m values were taken from Table 3.4. The f_a values were chosen in the range of data used to construct the median effect plot *i.e.* 0.03-0.65. The values obtained for D_{Dex}, D_{Maf}, $D = d_{Dex} + d_{Maf}$, d_{Dex} and d_{Maf} are given in Table 3.5. The doses d_{Dex} and d_{Maf} were calculated from the known ratio d_{Dex}/d_{Maf} = 0.683 and the value of D.

Table 3.5. Calculated doses of mafosfamide, dexrazoxane and their combination at each given fraction affected level.

f_u[a]	f_a[b]	D_{Maf}[c] μM	D_{Dex}[d] μM	D[e] Dex/Maf=0.683 μM	d_{Maf}[f] μM	d_{Dex}[g] μM
0.97	0.03	1.1226	1.0256	1.5967	0.9487	0.6480
0.94	0.06	1.5399	1.5270	2.1736	1.2915	0.8821
0.91	0.09	1.8641	1.9424	2.6190	1.5562	1.0629
0.88	0.12	2.1444	2.3173	3.0028	1.7842	1.2186
0.85	0.15	2.3997	2.6699	3.3511	1.9912	1.3600
0.82	0.18	2.6394	3.0101	3.6774	2.1850	1.4924
0.79	0.21	2.8693	3.3439	3.9896	2.3706	1.6191
0.76	0.24	3.0932	3.6758	4.2932	2.5509	1.7423
0.73	0.27	3.3139	4.0093	4.5920	2.7285	1.8635
0.7	0.3	3.5339	4.3473	4.8892	2.9051	1.9842
0.67	0.33	3.7550	4.6926	5.1875	3.0823	2.1052
0.64	0.36	3.9790	5.0478	5.4893	3.2616	2.2277
0.61	0.39	4.2076	5.4158	5.7968	3.4443	2.3525
0.58	0.42	4.4425	5.7993	6.1125	3.6319	2.4806
0.55	0.45	4.6855	6.2017	6.4386	3.8257	2.6129
0.52	0.48	4.9387	6.6267	6.7779	4.0273	2.7506
0.49	0.51	5.2042	7.0785	7.1333	4.2384	2.8948
0.46	0.54	5.4847	7.5623	7.5082	4.4612	3.0470
0.43	0.57	5.7833	8.0844	7.9068	4.6981	3.2088
0.4	0.6	6.1037	8.6525	8.3341	4.9519	3.3821
0.35	0.65	6.6997	9.7298	9.1273	5.4232	3.7041

[a] Fraction unaffected
[b] Fraction affected
[c] Doses of mafosfamide that as the single agent produce an effect f_a
[d] Doses of dexrazoxane that as the single agent produce an effect f_a
[e] Doses of combination of dexrazoxane with mafosfamide that produce an effect f_a
[f] Doses of mafosfamide that contribute to D
[g] Doses of dexrazoxane that contribute to D

6. Based on the calculated values of D_{Dex}, D_{Maf}, d_{Dex} and d_{Maf} from Table 3.5, the combination index was calculated using the equation (3.1) for each value of f_a. The combination index was calculated with equation for $\alpha = 1$ or 0.

Table 3.6. Combination index calculated for dexrazoxane and mafosfamide ratio = 0.683.

f_a[a]	$CI, \alpha = 0$	$CI, \alpha = 1$
0.03	1.4769	2.0108
0.06	1.4163	1.9008
0.09	1.3820	1.8388
0.12	1.3579	1.7954
0.15	1.3391	1.7618
0.18	1.3236	1.7341
0.21	1.3104	1.7104
0.24	1.2987	1.6896
0.27	1.2881	1.6708
0.3	1.2785	1.6537
0.33	1.2695	1.6377
0.36	1.2610	1.6228
0.39	1.2530	1.6086
0.42	1.2453	1.5950
0.45	1.2378	1.5818
0.48	1.2305	1.5690
0.51	1.2234	1.5565
0.54	1.2163	1.5440
0.57	1.2093	1.5317
0.6	1.2022	1.5193
0.65	1.1902	1.4983

[a] Fraction affected was chosen in a range of linearity of the median effect plot *i.e.* for the effect of 2.0 to 10.0 μM of dexrazoxane and mafosfamide; the increment was chosen arbitrarily

The combination index plotted against the f_a value for $\alpha = 0$ and 1, is presented in Figs. 3.7 and 3.8. The values of $CI > 1$ indicate antagonism, $CI < 1$ indicate synergy and $CI = 0$ indicate additivity between combined drugs.

3.2.4.2. Data analysis with the envelope of additivity method

The envelope of additivity method [14] is described in Chapter I, Section 1.1.2.6. The construction of the envelope, presented in Fig. 3.13, is described for the experiment with mafosfamide and dexrazoxane.

1. The experiment for evaluation with the envelope of additivity was designed to obtain dose-response curves for dexrazoxane alone in the range (0.1-100 μM), for mafosfamide alone in a range (0.05-50 μM) and for mafosfamide in a range (0.05-50 μM) with 1.5, 2.0, 2.5, 4.0 μM fixed doses of dexrazoxane.

2. The experimental data obtained were fitted to four- or three-parameter logistic equations (3.4a) and (3.4b) given below using SigmaPlot (Jandel Corp., San Rafael CA):

$$A_{490/650} = \frac{a-d}{1+\left(\frac{D}{IC_{50}}\right)^{b}} + d \qquad (3.4a)$$

$$A_{490/650} = \frac{a}{1+\left(\frac{D}{IC_{50}}\right)^{b}} \qquad (3.4b)$$

where $A_{490/650}$ is the absorbance ($A_{490/650} = A_{490} - A_{650}$), D is the drug concentration; IC_{50} is the median inhibitory concentration, b is the exponential factor, a is the estimated maximal effect and d is the estimated baseline effect. When the background absorbance, d, is close to zero in equation (3.4a), this parameter can be eliminated giving the equation (3.4b). The experimental data were normalised to the absorbance obtained for a control well on each plate to correct for an error related to the number of cells seeded. For dexrazoxane, the control value was the absorbance without the drug. For mafosfamide, and mafosfamide with fixed doses of dexrazoxane, it was the absorbance without the drug but with 1 μL DMSO. The normalised data of dexrazoxane were fitted into the four-parameter equation (3.4a) and the data of mafosfamide and mafosfamide with fixed doses with dexrazoxane

into the three-parameter equation (3.4b). The best fit parameters obtained are presented in Table 3.7. The 72 h dose-response curves for this experiment are plotted in Fig. 3.13.

Table 3.7. Parameters obtained from non-linear least square fit of dexrazoxane, mafosfamide and mafosfamide with fixed doses of dexrazoxane experimental data to four- or three-parameter logistic equation 3.4.

	Dex alone	Maf alone	Maf +1.5 μM Dex	Maf +2.0 μM Dex	Maf +2.5 μM Dex	Maf +4.0 μM Dex
a^a	1.000	1.000	0.930	0.876	0.830	0.719
b^b	1.989	1.411	1.264	1.332	1.321	1.259
IC_{50}^c, μM	4.221	7.040	6.969	6.552	8.298	7.036
d^d	0.389					

[a] Maximal estimated survival
[b] Exponential factor
[c] 50% effect
[d] Minimal estimated survival

3. The effect for which the envelope was constructed was chosen arbitrarily as 0.5 survival. The three lines limiting the envelope were calculated with three different modes I, IIa and IIb. The lines were defined by the combinations of the dexrazoxane and mafosfamide doses which produce 0.5 survival. The doses were calculated with transformed equations (3.4) for dexrazoxane and mafosfamide alone. For mode I the concentrations of mafosfamide and dexrazoxane were calculated for the effects starting at 100% survival for both drugs. For mode IIa the doses for dexrazoxane were also calculated for the effect starting at 100% survival, but the doses of mafosfamide were calculated starting at the survival where the effect of dexrazoxane ends (compare Chapter I, Section 1.1.2.6). The calculated doses of dexrazoxane and mafosfamide by mode I and mode IIa are given in Table 3.8. In these calculations the dexrazoxane dose-response curve was considered first.

Table 3.8. Calculated with mode I and mode IIa doses of dexrazoxane and mafosfamide (in bold) for 0.5 survival envelope of additivity.

S	S_{Dex}	S_{Maf}	$D_{Dex,I}$ μM	$D_{Maf,I}$ μM	$D_{Maf,II}$ μM	$D_{Maf,IIa}$ μM
0.5	0.5000	1.0000	**8.9943**	**0.0000**	7.0400	**0.0000**
0.5	0.5001	0.9999	**8.9894**	**0.0103**	7.0380	**0.0020**
0.5	0.5026	0.9974	**8.8670**	**0.1038**	6.9883	**0.0517**
0.5	0.5076	0.9924	**8.6332**	**0.2229**	6.8899	**0.1501**
0.5	0.5176	0.9824	**8.2039**	**0.4070**	6.6972	**0.3428**
0.5	0.5676	0.9324	**6.5831**	**1.0962**	5.8054	**1.2346**
0.5	0.6176	0.8824	**5.4666**	**1.6876**	5.0122	**2.0278**
0.5	0.6676	0.8324	**4.6125**	**2.2608**	4.2947	**2.7453**
0.5	0.7176	0.7824	**3.9112**	**2.8424**	3.6352	**3.4048**
0.5	0.7676	0.7324	**3.3024**	**3.4489**	3.0187	**4.0213**
0.5	0.8176	0.6824	**2.7470**	**4.0942**	2.4313	**4.6087**
0.5	0.8676	0.6324	**2.2121**	**4.7928**	1.8576	**5.1824**
0.5	0.9176	0.5824	**1.6579**	**5.5615**	1.2757	**5.7643**
0.5	0.9676	0.5324	**0.9909**	**6.4214**	0.6340	**6.4060**
0.5	0.9876	0.5124	**0.6010**	**6.7968**	0.3164	**6.7236**
0.5	0.9881	0.5119	**0.5885**	**6.8064**	0.3072	**6.7328**
0.5	0.9886	0.5114	**0.5757**	**6.8161**	0.2978	**6.7422**
0.5	0.9986	0.5014	**0.1989**	**7.0121**	0.0669	**6.9731**
0.5	1	0.5	**0.0000**	**7.0400**	0.0000	**7.0400**

S - combined survival effect for which the envelope is constructed, $S = S_{Dex} + S_{maf} - 1$

S_{Dex} - contribution of dexrazoxane to combined effect S

S_{Maf} - contribution of mafosfamide to combined effect S, $S_{Maf} = 1 + S - S_{Dex}$

$D_{Dex,I}$ - doses of dexrazoxane that produce survival S_{Dex} calculated with equation: $D_{Dex,I} = IC_{50,Dex}[(1-S_{Dex})/(S_{Dex}-d)]^{1/b}$, the parameters $IC_{50,Dex}$, d and b were given in Table 3.7

$D_{Maf,I}$ - doses of mafosfamide that produce survival S_{Maf} calculated with equation: $D_{Maf,I} = IC_{50,Maf}[(1-S_{Maf})/S_{Maf}]^{1/b}$, the parameters $IC_{50,Maf}$, d and b were given in Table 3.7

$D_{Maf,II}$ - doses of mafosfamide calculated for dexrazoxane survival with equation: $D_{Maf,II} = IC_{50,Maf}[(1-S_{Dex})/S_{Dex}]^{1/b}$

$D_{Maf,IIa}$ - doses of mafosfamide calculated for the survival that starts from the end of dexrazoxane survival: $D_{Maf,IIa} = D_{0.5,Maf} - D_{Maf,II}$ where $D_{0.5,Dex}$ is a dose of mafosfamide that produce 0.5 survival effect (the highest effect of mafosfamide was 100% kill thus $D_{0.5,Maf} = IC_{50,Maf}$)

Columns $D_{Dex,I}$ and $D_{Maf,I}$ form the mode I line, and the columns $D_{Dex,I}$ and $D_{Maf,IIa}$ form the mode IIa line in the envelope of additivity presented in Fig. 3.4.

4. In Step 3, the doses of dexrazoxane were calculated for arbitrary incremented contribution to 0.5 survival effect based on its dose-response curve. Next, corresponding mafosfamide doses were calculated by mode I and mode IIa. If the mafosfamide doses were calculated for arbitrary incremented contribution to 0.5 effect with its dose-response curve equation, the dexrazoxane doses are the same with mode I but different with mode IIa. To distinguish between the order of the curves used for calculations this mode is called IIb. The doses calculated by mode IIb are given in Table 3.9 (values in bold font).

Table 3.9. Doses of dexrazoxane calculated by mode IIb for 0.5 survival.

S	S_{Maf}	S_{Dex}	$D_{Maf,I}$ μM	$D_{Dex,I}$ μM	$D_{Dex,II}$ μM	$D_{Dex,IIb}$ μM
0.5	0.5000	1.0000	**7.0400**	0.0000	8.9943	**0.0000**
0.5	0.5001	0.9999	**7.0380**	0.0527	8.9894	**0.0050**
0.5	0.5026	0.9974	**6.9883**	0.2718	8.8670	**0.1273**
0.5	0.5076	0.9924	**6.8899**	0.4680	8.6332	**0.3612**
0.5	0.5176	0.9824	**6.6972**	0.7199	8.2039	**0.7905**
0.5	0.5676	0.9324	**5.8054**	1.4802	6.5831	**2.4112**
0.5	0.6176	0.8824	**5.0122**	2.0525	5.4666	**3.5278**
0.5	0.6676	0.8324	**4.2947**	2.5880	4.6125	**4.3818**
0.5	0.7176	0.7824	**3.6352**	3.1340	3.9112	**5.0832**
0.5	0.7676	0.7324	**3.0187**	3.7234	3.3024	**5.6919**
0.5	0.8176	0.6824	**2.4313**	4.3923	2.7470	**6.2474**
0.5	0.8676	0.6324	**1.8576**	5.1928	2.2121	**6.7822**
0.5	0.9176	0.5824	**1.2757**	6.2151	1.6579	**7.3364**
0.5	0.9676	0.5324	**0.6340**	7.6461	0.9909	**8.0035**
0.5	0.9876	0.5124	**0.3164**	8.4211	0.6010	**8.3933**
0.5	0.9881	0.5119	**0.3072**	8.4427	0.5885	**8.4059**
0.5	0.9886	0.5114	**0.2978**	8.4644	0.5757	**8.4187**
0.5	0.9986	0.5014	**0.0669**	8.9253	0.1989	**8.7954**
0.5	1.0000	0.5000	**0.0000**	8.9943	0.0000	**8.9943**

S - combined survival effect for which the envelope is constructed, $S = S_{Dex} + S_{maf} - 1$

S_{Maf} - contribution of mafosfamide to combined effect S

S_{Dex} - contribution of dexrazoxane to combined effect S, $S_{Dex} = 1 + S - S_{Maf}$

$D_{Maf,I}$ - doses of mafosfamide that produce survival S_{Maf} calculated with equation: $D_{Maf} = IC_{50,Maf}[(1-S_{Maf})/(S_{Maf}-d)]^{1/b}$, the parameters $IC_{50,Maf}$, d and b were given in Table 3.7

$D_{Dex,I}$ - doses of dexrazoxane that produce survival S_{Dex} calculated with equation: $D_{Dex,I} = IC_{50,Dex}[(1-S_{Dex})/S_{Dex}]^{1/b}$, the parameters $IC_{50,Dex}$, d and b were given in Table 3.7

$D_{Dex,II}$ - doses of dexrazoxane calculated for mafosfamide survival with equation: $D_{Dex,II} = IC_{50,Dex}[(1-S_{Maf})/S_{Maf}]^{1/b}$

$D_{Dex,IIb}$ - doses of dexrazoxane calculated for the survival that starts from the end of mafosfamide survival: $D_{Dex,IIb} = D_{0.5,Dex} - D_{Dex,II}$ where $D_{0.5,Dex}$ is a dose of dexrazoxane that produces 0.5 survival effect starting effect from zero on effect axis (dexrazoxane highest effect is $\neq 0$ thus $D_{0.5,Dex} \neq IC_{50,Dex}$)

5. All three sets of dexrazoxane-mafosfamide doses that define the 50% effect envelope of additivity were calculated and the envelope was constructed (Fig. 3.4). The zones of additivity, synergy and antagonism were defined. The last Step was to define the interaction between the drugs based on the dose-response curves for mafosfamide with fixed doses of dexrazoxane. The doses of mafosfamide used in combination with fixed doses of dexrazoxane that produce survival $S = 0.5$ were calculated based on the three-parameter logistic equation: $D_{Maf} = IC_{50,Maf}[(1-S)/S]^{1/b}$. The parameters obtained from the least square non-linear fit of experimental data to the equation (3.4) with $d = 0$, are given in Table 3.7. Since the experiment for the envelope of additivity was designed to obtain the dose-response curves of mafosfamide with fixed doses of dexrazoxane, the concentrations of dexrazoxane D_{Dex} were known for each curve: 1.5, 2.0, 2.5, 4.0 μM. If the points fall to the left of envelope of additivity, the interaction of drugs is synergistic. If they are inside the envelope, there is no interaction between the drugs and their effect is additive. If the points fall to the right of the envelope, the interaction between the drugs is antagonistic.

Table 3.10. The doses of dexrazoxane and corresponding doses of mafosfamide which combined produce a 50% effect.

D_{Dex} μM	D_{Maf} μM
1.5000	6.1805
2.0000	5.2944
2.5000	6.0631
4.0000	3.6577

The points with co-ordinates presented in Table 3.10 are plotted along with envelope of additivity in Fig. 3.4. The three points inside the envelope indicate additivity of the drug effects, the point to the right of the envelope indicates antagonism.

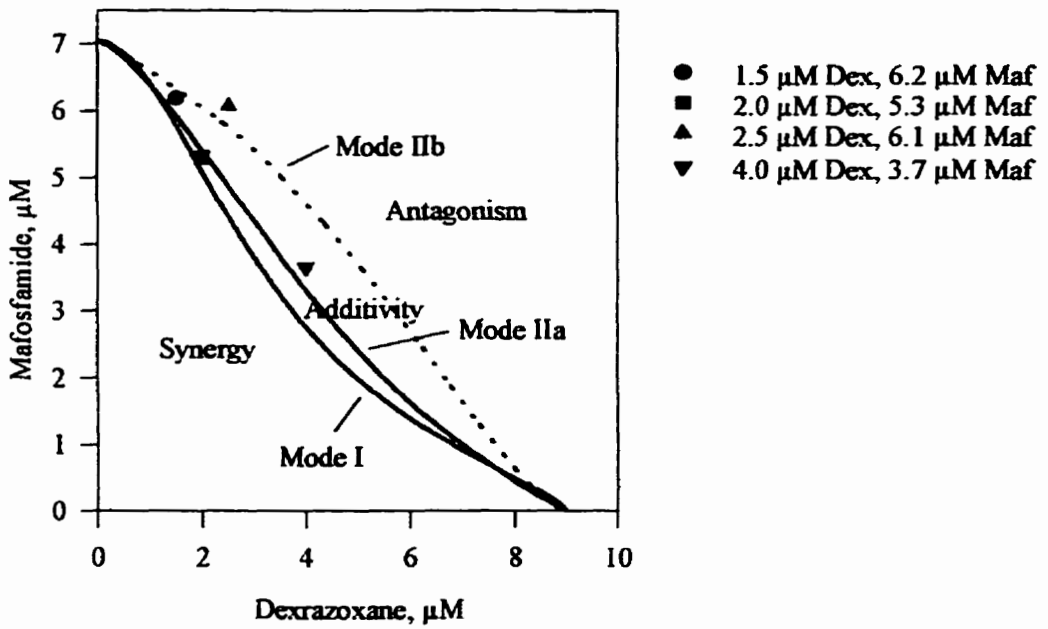

Fig. 3.4. Envelope of additivity for the dexrazoxane-mafosfamide experiment illustrated in Fig. 3.13.

3.2.4.3. Data analysis with the response surface method

The combined effect of drugs was also evaluated with the response surface method. The data obtained in the combination index and envelope of the additivity experiments were fitted to a seven parameter equation (3.5) [15].

$$\frac{d_A}{IC_{50,A}\left(\frac{E-B}{E_{max}-E+B}\right)^{1/m_A}}+\frac{d_B}{IC_{50,B}\left(\frac{E-B}{E_{max}-E+B}\right)^{1/m_B}}+\frac{\alpha' \cdot d_A \cdot d_B}{IC_{50,A}\cdot IC_{50,B}\left(\frac{E-B}{E_{max}-E+B}\right)^{(1/m_A+1/m_B)}}=1 \qquad (3.5)$$

where d_A and d_B, are the doses of the agents, alone and in combination; E is their survival effect; E_{max} is a maximal survival effect, B is a baseline (compare Fig. 1.2.(d) in Chapter I); $IC_{50,A}$ and $IC_{50,B}$, are the median inhibitory concentrations; m_A and m_B are the Hill-type coefficients; and α' is the interaction parameter. The value of α' provides information about the type of interaction between drugs. If $\alpha' = 0$, there is no interaction between drugs and their effects are additive. If $\alpha' < 0$, the interaction is antagonistic, and if $\alpha' > 0$, the interaction is synergistic. SigmaPlot was used for calculations and curve fitting. The highest effect (100% survival for d_A and $d_B = 0$) was not included in the fitting for all data sets used for evaluation with the response surface method, although this effect was calculated based on obtained best fit parameters. The data for the fitting process were moved to three columns: one column for the concentration of drug A (d_A = col(1)), the second for the concentration of drug B (d_B = col(2)) and the third column for the normalised effects (E = col(3)). The initial parameters E_{max}, $IC_{50,A}$, $IC_{50,B}$, m_A, m_B and B

were set to values from non-linear least square logistic fits of individual drug effects. The value of B is an averaged end effect (the lowest survival) produced by the highest drug concentrations, thus its initial value was estimated from both dose-response curves of the studied drugs. The value of E_{max} was set to a value higher than the highest measured effect (for normalised data this value was around 1.0). The initial value of α' was set to a variety of estimates usually starting with a value close to zero. The SigmaPlot curve fit file below was used to obtain best fit seven parameters: variable

[Parameters]

$E_{max} = 0.83$
$m_A = -1.10$
$m_B = -1.41$
$IC_{50,A} = 2.45$
$IC_{50,B} = 4.36$
$B = 0.25$
$a' = -0.35$

} initial estimates

[Variables]

$d_A = \text{col}(1)$
$d_B = \text{col}(2)$
$E = \text{col}(3)$

} independent variables

$y = 1$ } dependent variable

[Equations]

$$f = \frac{d_A}{IC_{50,A}\left(\frac{E-B}{E_{max}-E+B}\right)^{1/m_A}} + \frac{d_B}{IC_{50,B}\left(\frac{E-B}{E_{max}-E+B}\right)^{1/m_B}} + \frac{a' \cdot d_A \cdot d_B}{IC_{50,A} \cdot IC_{50,B}\left(\frac{E-B}{E_{max}-E+B}\right)^{(1/m_A + 1/m_B)}}$$

} fitting equation

fit f to y

[Constraints]

$B > 0$

The obtained best fit values of seven parameters: E_{max}, $IC_{50,A}$, $IC_{50,B}$, m_A, m_B, B, and α', were used to calculate the theoretical effects for single and combined drug concentrations using a bisection root finder [15, 16]. These effects, plotted on the same plot with measured values, gave a visual evaluation of the quality of the fit (Figs. 3.17, 3.18, 3.19 and 3.20). The following SigmaPlot file, written by Sam Hasinoff, was used to calculate the theoretical effects. The text after semicolon are the comments.

```
; !SAM.XFM
; June 5, 1997
; error tolerance = 1.5e-4
; number of dA, dB ordered pairs
n =51
; parameters
Emax =1.137
IC50,A =5.489
mA = -1.406
IC50,B =8.651
mB =-1.205
α' = -0.2264
B = 0
; Do NOT edit anything below this line!
; ═══════════════════════════════
; columns where dA and dB are found
dAcol =30
dBcol =31
; column where E should be placed
Ecol = 33
; cells for temp storage space
; limitations with "variable redefinition")
Lcol =34
Lrow = 1
Ucol = 35
Urow = 1
for i = 1 to n do
dA = cell(dAcol,i)
```

d_B = cell(d$_B$col,i)
; test for the control case, to avoid divide by zero
if (d_A = 0) and (d_B = 0) then
cell(Ecol,i) = E_{max}+B
; solve by bisection (with a fixed number of iterations)
else
cell(Lcol, Lrow) = B
cell(Ucol, Urow) = E_{max} + B
for j = 1 to 25 do
M = (cell(Lcol, Lrow) + cell(Ucol,Urow))/2
Part1 = $IC_{50,A}$ * ((M-B) / (E_{max}-M+B)) ** (1/m_A)
Part2 = $IC_{50,B}$ * ((M-B) / (E_{max}-M+B)) ** (1/m_B)
Part3 = $IC_{50,A}$ * ((M-B) / (E_{max}-M+B)) ** (0.5/m_A)
Part4 = $IC_{50,B}$ * ((M-B) / (E_{max}-M+B)) ** (0.5/m_B)
G = d_A /Part1 + d_B /Part2 + α'*d_A *d_B /(Part3*Part4) - 1
if (G < 0) then
cell(Lcol, Lrow) = M
else
cell(Ucol, Urow) = M
end if
end for
cell(Ecol,i) = M
end if
end for
; pretty up the spreadsheet by erasing the temporary cells
cell(Lcol, Lrow) = 0/0
cell(Ucol, Urow) = 0/0

3.2.4.4. Data analysis with the comparison of slopes method

The 48 h continuous exposure of Chinese hamster ovary cells to dexrazoxane produced a low cell kill even at high drug concentrations (20% for 500 μM dexrazoxane). For these data, presented in log-log scale, the linear equation was a good fitting model. A logarithmic Y-axis scale gave the same change in cell survival represented by constant vertical differences, in the other words, the changes were relative to the effected cell population. When dexrazoxane was used in a wide range of concentrations (0.5-500 μM)

with fixed doses of the other drug, linearity of the curve was observed. The fixed dose of the other drug influenced the y-intercept (b) and slope (a) of the dexrazoxane dose-response curves. Based on these observations, the drug interactions were defined by changes in the slope and y-intercept of the dexrazoxane dose-response curves under fixed doses of a second drug. In experiments presented in this Chapter, the dose-response curve of dexrazoxane was compared with the dose-response curves of dexrazoxane with fixed doses of mafosfamide, 5-fluorouracil and vinblastine. The statistical evaluation of the slopes and, if necessary, intercepts, was performed with the Student's t-test. A transform program in SigmaPlot (file name: com2reg.xfm) was used. The linear regression coefficients: intercept a and slope b, were computed ($\log A = a + b \cdot \log D$, where A is an absorbance from the MTT assay and D is a drug concentration). The t value Tb and the degree of freedom Vb, were obtained for the slope and Ta and Va for the intercept. Differences in the slopes of the regression line of dexrazoxane alone and dexrazoxane combined with the second drug were considered significant when $P < 0.05$. If the slopes were significantly different, the intercept a was not compared with the statistical test.

3.3. Results

3.3.1. Results for the combination of dexrazoxane with mafosfamide and 5-fluorouracil obtained with the combination index method

3.3.1.1. Results for the combination of dexrazoxane with mafosfamide obtained with the combination index method

The combination index experiments were performed for dexrazoxane (Dex) with mafosfamide (Maf). The 72 h inhibitory effect of the drugs on Chinese hamster ovary cells

was measured. The cells were seeded at 2000 cells/100 μL/plate well. The cells were allowed to attache for 24 h. After this period of time, the drugs were delivered, the volume of the cell culture medium was increased to 200 μL/well, and the drugs were incubated with cells for another 72 h. Five plates were used: one plate for dexrazoxane alone, one plate for mafosfamide alone and three plates for the drug combination in three constant ratios. The equipotent ratio of dexrazoxane (Dex) to mafosfamide (Maf) was calculated as follows: $IC_{50,Dex}/IC_{50,Maf}$ = 4.1 μM/6.0 μM = 0.683, where $IC_{50,Dex}$ and $IC_{50,Maf}$ are the median inhibitory concentrations of dexrazoxane and mafosfamide, respectively. The IC_{50}-values were obtained from preliminary experiments in which the dose-response curve for dexrazoxane was fitted to a four-parameters equation (3.4a) and for mafosfamide to a three-parameter equation (3.4b). The two other chosen ratios of dexrazoxane to mafosfamide were 5.0 and 0.2. These ratios were selected to expose the cells to combinations with an excess of dexrazoxane or excess of mafosfamide. Mafosfamide and dexrazoxane were dissolved in DMSO and delivered as single drugs or as a mixture in 1 μL aliquots to each well. The control wells with DMSO only were included. An example of dose-response curves for mafosfamide and dexrazoxane alone and for their three combinations is given in Fig. 3.5. This graph represents one combination index experiment. This experiment was repeated three times under the same conditions. The effect of drugs was measured as the absorbance, obtained from the MTT assay, correlated with survival of the cells. The absorbance was measured at 490 nm and 650 nm. The absorbance at 650 nm was subtracted from absorbance at 490 nm to correct

for a non-specific absorption and scattered light; this is a meaning of "Absorbance 490/650 nm" given on the graph ordinate.

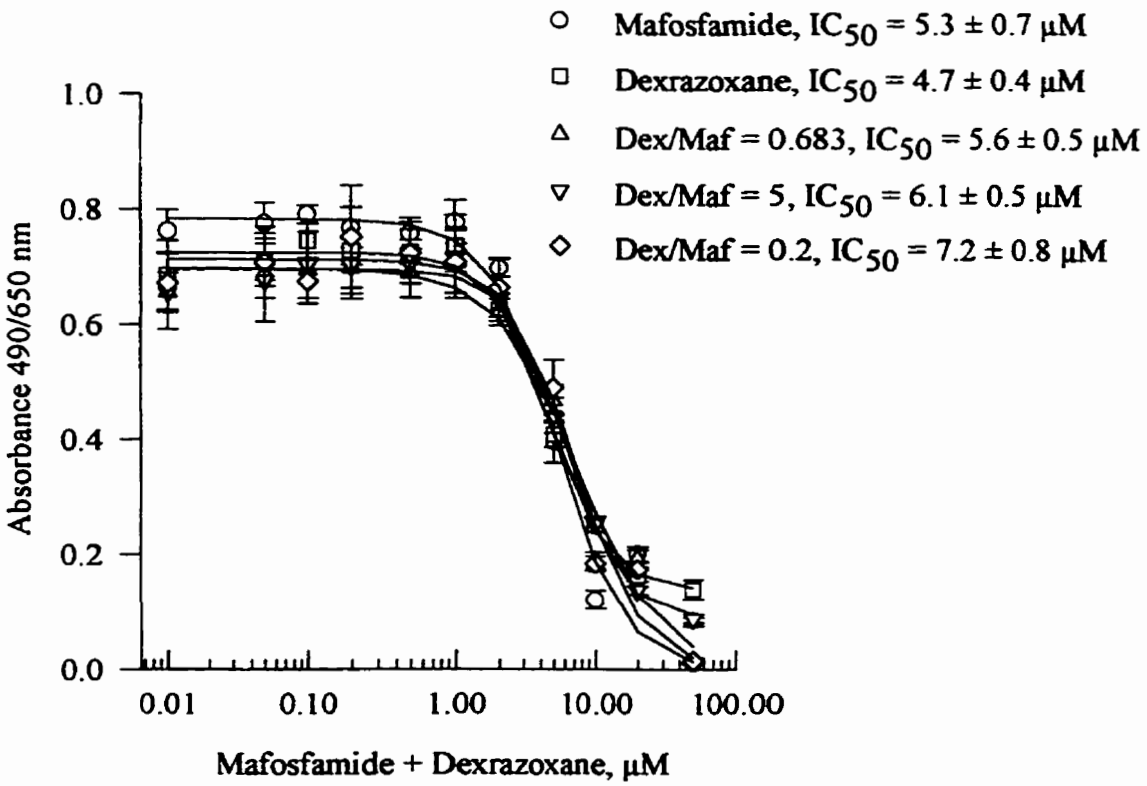

Fig. 3.5. Combination index experiment for the combination of dexrazoxane with mafosfamide. Chinese hamster ovary cells were incubated with the drug for 72 h. The points represent absorbance means ● SD from six replicates at each concentration. The lines represent the non-linear least squares fit of the experimental data to three- or four-parameter logistic equations. The lowest concentration corresponds to zero concentration of drugs plotted for convenience on a logarithmic scale with an arbitrary given value.

Only a portion of the data from the experiment above (Fig 3.5) were used for the median effect plots. The logarithm of data with higher values of absorbance than the control could not be defined. The data which did not fit the linear median effect plot were also not used (solid symbols in Fig.3.6). Data from the steepest part of the dose-response

curves, specifically 2.0, 5.0 and 10 μM and for mafosfamide also 0.5 μM, were used for the median effect plot presented in Fig. 3.6 (compare Table 3.3, data printed in bold font).

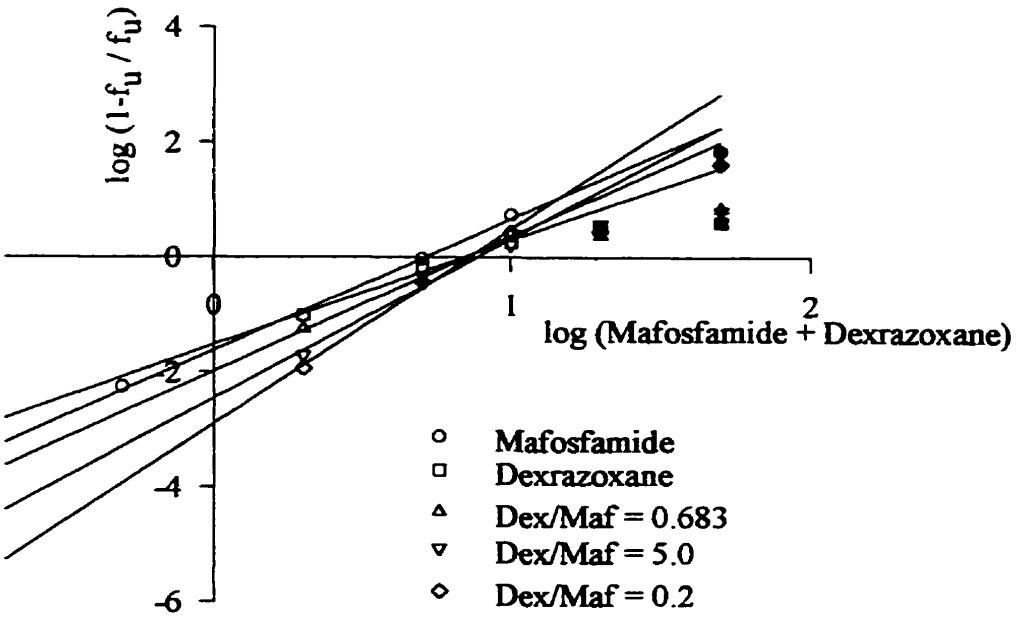

Fig. 3.6. Median effect plot for dexrazoxane-mafosfamide combination index experiment presented in Fig. 3.5. The effects for 20 and 50 μM and higher than the control, were not used to construct the plot (solid symbols).

The slopes of median effect plots for mafosfamide was 2.3 and for dexrazoxane 1.8; thus the median effect plots are not parallel to one another. Similar results were obtained for two other experiments (data not shown). The exclusivity of the drugs could not be specified; thus two equations for $\alpha = 0$ and $\alpha = 1$ were used to calculate the combination index. The combination index presented in Fig. 3.7 was calculated with an equation for mutually exclusive drugs where $\alpha = 0$.

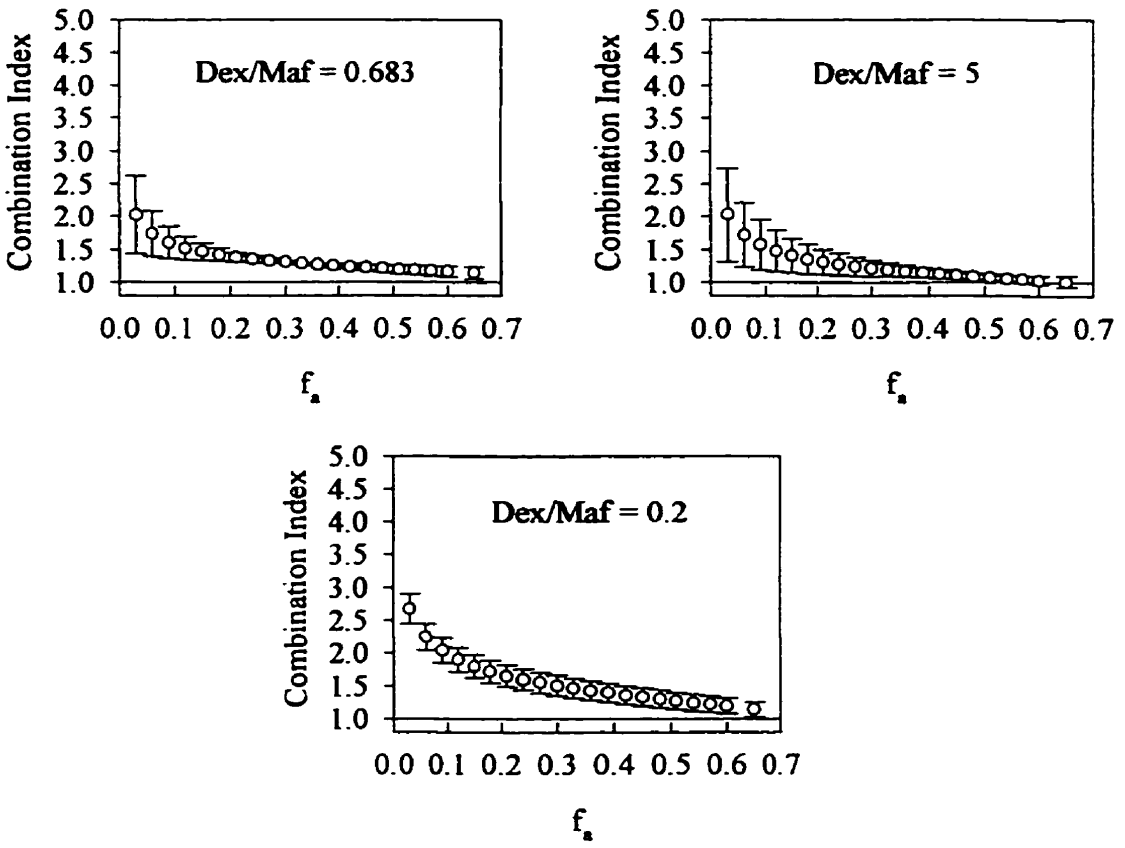

Fig. 3.7. Plots of combination index against fraction affected for the assumption of the same modes of action (mutually exclusive drugs, $\alpha = 0$) for mafosfamide and dexrazoxane at three concentration ratios. Every point represents the combination index mean ● SEM from three different experiments.

The combination index for all three ratios of dexrazoxane to mafosfamide was higher than one over the whole range of f_a (0.03-0.65). This result shows that interaction of mafosfamide with dexrazoxane was negative and their combined effect was antagonistic.

When drugs have different modes of action (drugs mutually nonexclusive, $\alpha = 1$) the equation for combination index contains a third term. The calculated values of the combination index, plotted against the fraction affected, are presented in Fig. 3.8.

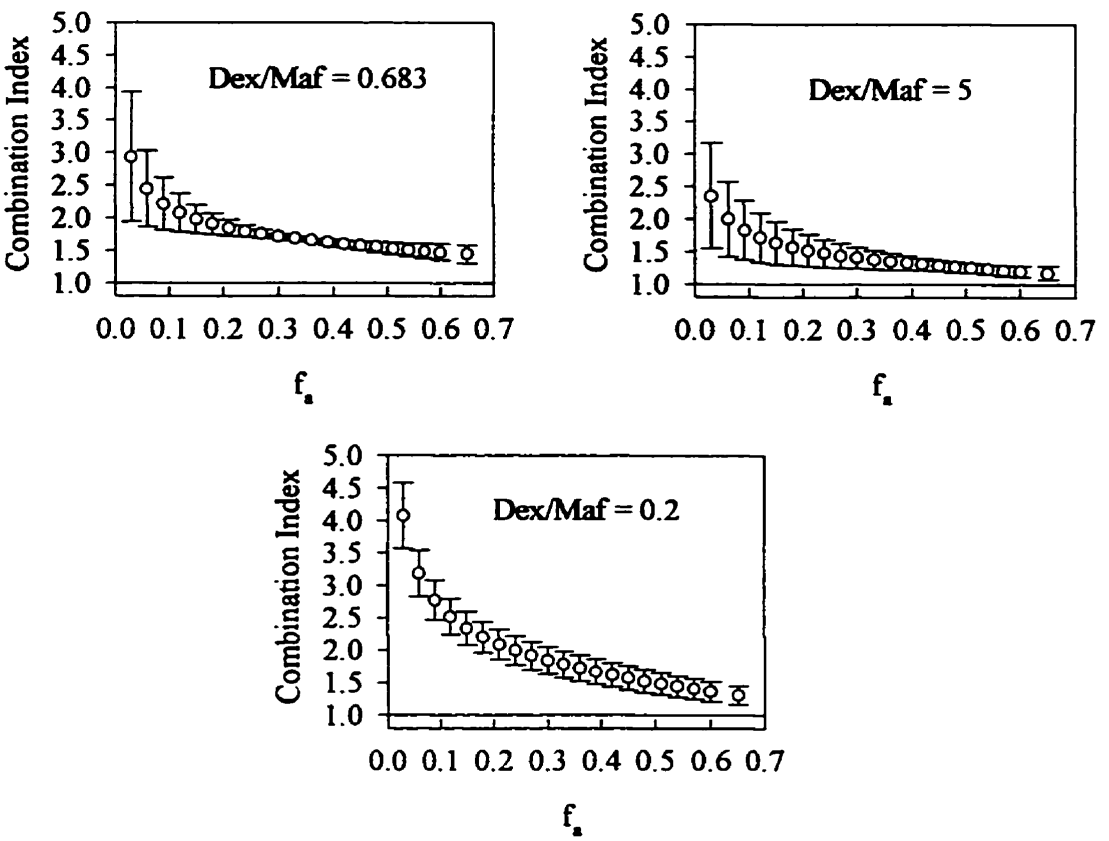

Fig. 3.8. Plots of combination index against fraction affected for the assumption of different modes of action (mutually nonexclusive drugs, $\alpha = 1$) for mafosfamide and dexrazoxane at three different concentration ratios. Each point represents the combination index mean ± SEM from three different experiments.

The combination index calculated with the equation for mutually nonexclusive drugs was higher than one for the whole range of f_a (0.03-0.65) at every ratio studied. Thus dexrazoxane and mafosfamide show antagonism when used in combination.

In Table 3.11, the mean and the single values of combination index (CI) and corresponding fraction affected (f_a) ranges are given for three separate experiments.

Table 3.11. Mean and single values of combination index (CI) and corresponding ranges of fraction affected (f_a) for three mafosfamide-dexrazoxane combination index experiments[a].

α	0						1			
Ratio	0.683		5.0		0.2		0.683	5.0		0.2
Effect	Ant[b]	Syn[b]	Ant	Syn	Ant	Syn	Ant	Ant	Syn	Ant
CI_{mean}[c]	**2.03-1.14**		**2.03-1.01**		**2.67-1.15**		**2.94-1.44**	**2.36-1.18**		**4.08-1.30**
$f_{a,mean}$[d]	0.03-0.65		0.03-0.65		0.03-0.65		0.03-0.65	0.03-0.65		0.03-0.65
CI_1[c]	**1.39-1.27**		**1.0-1.12**	**0.76-1.00**	**3.10-1.29**		**1.87-1.65**	**1.00-1.31**	**0.82-1.00**	**4.83-1.50**
$f_{a,1}$[d]	0.03-0.65		0.3-0.65	0.03-0.36	0.03-0.65		0.03-0.65	0.30-0.65	0.03-0.30	0.03-0.65
CI_2[c]	**1.48-1.19**		**2.11-1.06**		**2.34-1.22**		**2.01-1.50**	**2.69-1.25**		**3.14-1.38**
$f_{a,2}$[d]	0.03-0.65		0.03-0.65		0.03-0.65		0.03-0.65	0.30-0.65		0.03-0.65
CI_3[c]	**3.2-1.00**	**1.00-0.97**	**3.22-1.00**	**1.00-0.85**	**2.56-1.00**	**1.00-0.93**	**4.93-1.18**	**3.57-1.00**	**1.00-0.97**	**4.20-1.02**
$f_{a,3}$[d]	0.03-0.60	0.60-0.65	0.03-0.51	0.51-0.65	0.03-0.54	0.54-0.65	0.03-0.65	0.30-0.61	0.61-0.65	0.03-0.65

[a] The combination index was calculated with two equations for α = 0 and α = 1 for three ratios of dexrazoxane to mafosfamide 0.683, 5.0 and 0.2. The value of 1.0 is only a cross point between synergy and antagonism and it is not recognised as an additivity effect

[b] Ant and Syn mean synergy and antagonism, respectively

[c] CI_{mean}, CI_1, CI_2 and CI_3 are the mean combination index from three experiments and combination indexes for three single experiments (1, 2 and 3), respectively

[d] f_a^{mean}, f_a^1, f_a^2 and f_a^3 are fractions affected corresponding to mean combination index and combination indexes for three separate experiments, respectively

When α = 0 the mean combination index CI_{mean} for the 0.683 equipotent ratio of dexrazoxane to mafosfamide showed antagonism ($CI > 1$). The single Experiments CI_1, CI_2 and CI_3, also showed antagonism; although, CI_3 defined synergy for f_a in a range 0.60-

0.65. For the ratio 5.0 (excess of dexrazoxane), the second Experiment (CI_2) showed antagonism for the whole range of f_a. The first (CI_1) and the third (CI_3) Experiments showed both antagonism and small synergy for different ranges of f_a. For the ratio of 0.2 (excess of mafosfamide), CI_{mean} showed antagonism, as did the first and the second Experiments. The third Experiment showed small synergy for f_a in a range 0.54-0.65. When $\alpha = 1$ was used in the equation, CI_{mean} showed antagonism for the entire range of f_a and each ratio. All single Experiments for ratio 0.683 and 0.2 and the second Experiment for ratio 5.0 also showed antagonism for the whole range of f_a. The first and the third single Experiments, with an excess of dexrazoxane (ratio 5.0), were not consistent with this result. They showed antagonism for higher effects and small synergy for low effects.

3.3.1.2. Results for the combination of dexrazoxane with 5-fluorouracil obtained with the combination index method

The combination index Experiments were performed also for dexrazoxane with 5-fluorouracil (5-Fu). The 72 h inhibitory effect of the drugs on Chinese hamster ovary cells was measured. Five plates were used: one plate for dexrazoxane alone, one plate for 5-fluorouracil alone and three plates for the drug combination in three constant ratios. The equipotent ratio of dexrazoxane to 5-fluorouracil (5-Fu) was calculated as follows: $IC_{50,Dex}/IC_{50,5\text{-}Fu}$= 4.6 μM/2.3 μM = 2.0, where $IC_{50,5\text{-}Fu}$ is a median inhibitory concentration of 5-fluorouracil. The IC_{50}-values were obtained from preliminary Experiments in which the dose-response curves for single drugs were prepared and the median inhibitory concentrations were estimated by fitting experimental data to four-parameter equation (3.4a). The two other chosen ratios of dexrazoxane to 5-fluorouracil

were 5.0 and 0.2. These ratios were selected to expose the cells to combinations with an excess of dexrazoxane or excess of 5-fluorouracil. The drugs were delivered separately to the wells. Dexrazoxane was delivered dissolved in the cell culture medium and it was followed by 1 μL of 5-fluorouracil dissolved in one equivalent of NaOH. The combination index Experiment for dexrazoxane and 5-fluorouracil is shown in Fig. 3.9. Five dose-response curves are plotted; one for 5-fluorouracil, one for dexrazoxane and three for different ratios of dexrazoxane with 5-fluorouracil.

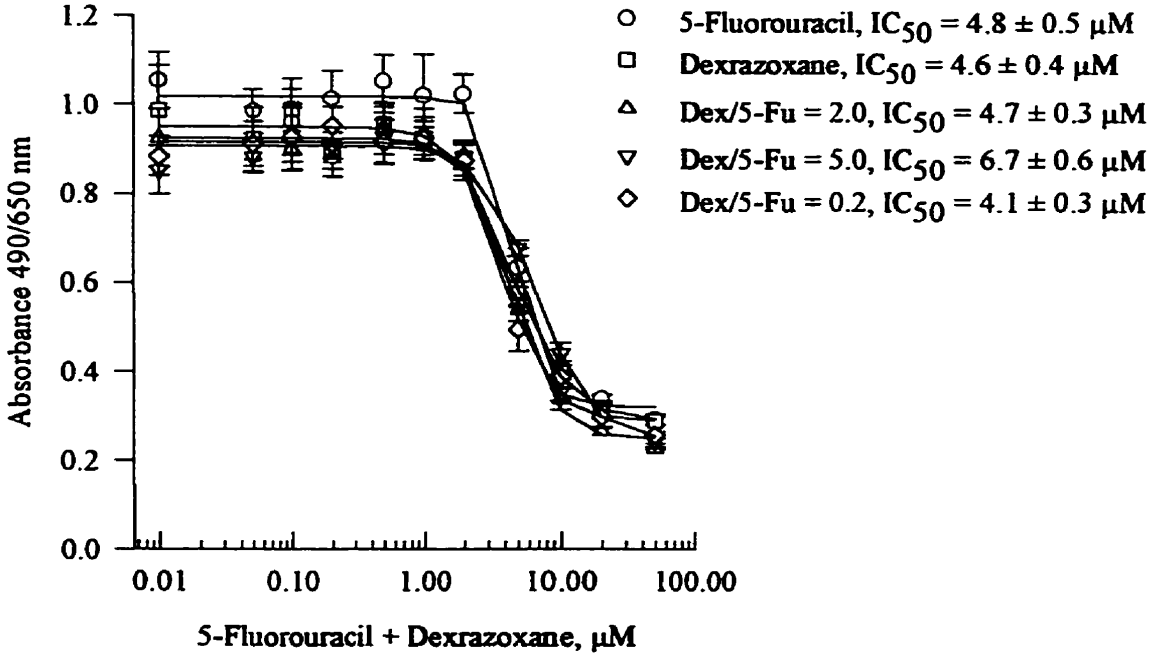

Fig. 3.9. Combination index Experiment for the combination of dexrazoxane with 5-fluorouracil. Chinese hamster ovary cells were incubated with the drug for 72 h. The symbols represent absorbance means ● SD from six replicates at each concentration. The lowest concentrations plotted for convenience on a logarithmic scale with an arbitrary given values, correspond to zero concentration of the drugs. The curves are the best fit of experimental data to a four-parameter logistic equation.

The median effect plot for 5-fluorouracil and dexrazoxane is given in Fig. 3.10. The plots were defined by data points given in white symbols. The data points plotted as black symbols were not linear and they were not included in calculations. Some data points were also lost because $(1-f_u/f_u) < 0$.

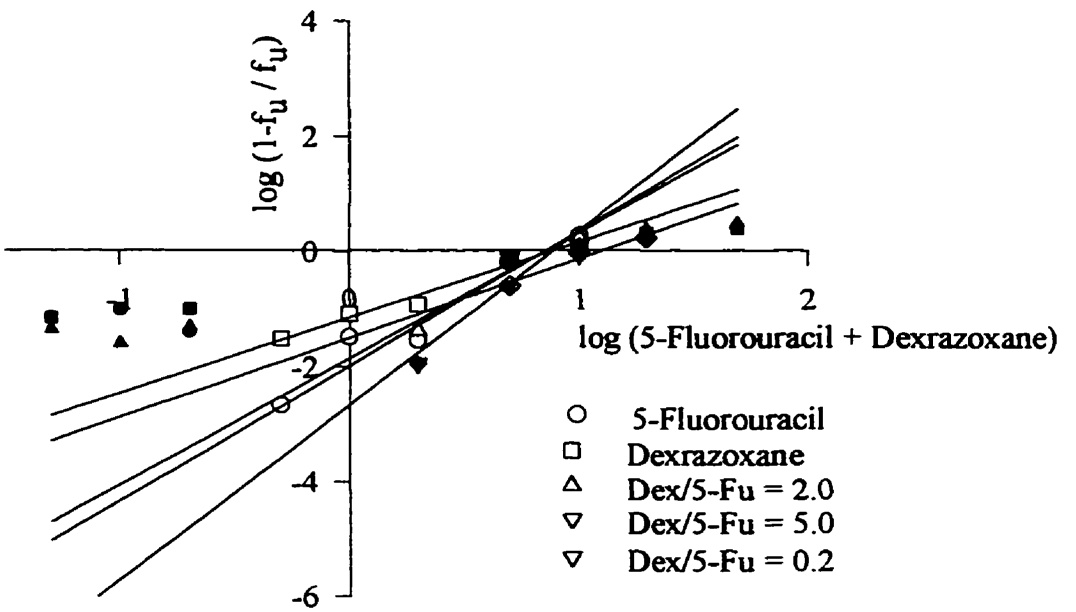

Fig. 3.10. Median effect plot for the dexrazoxane-5-fluorouracil combination index experiment presented in Fig. 3.9. The plots are limited to the points that are linear in median effect plot (white symbols). The data that were not included in calculations are given in solid symbols.

The combination index for 5-fluorouracil with dexrazoxane was calculated using both equations for drugs which are mutually exclusive (Fig. 3.11) and mutually nonexclusive (Fig. 3.12). The combination index was not calculated for Dex/5-Fu = 5.0 because only two data points defined the median effect plot.

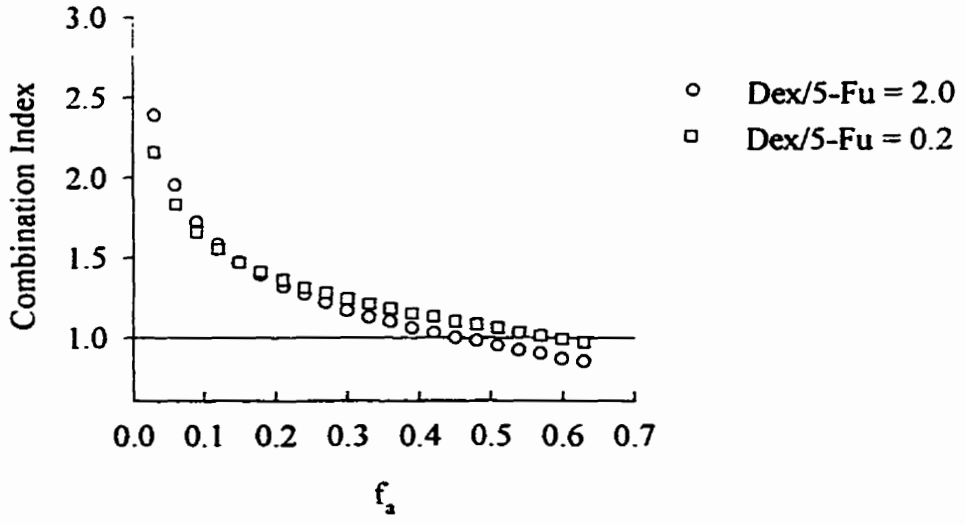

Fig. 3.11. Plot of combination index against fraction affected for 5-fluorouracil and dexrazoxane two different ratios. The combination index was calculated for single experiment with the equation for $\alpha = 0$.

The combination index for $\alpha = 0$, calculated for 5-fluorouracil and dexrazoxane showed similar values at each f_a in both studied ratios. The effect of the drugs was antagonistic up to values of $f_a = 0.46$ and 0.57 for ratios of 2.0 and 0.2, respectively. Above $f_a = 0.46$ for ratio 2.0, and above $f_a = 0.57$ for ratio 0.2, they showed synergy.

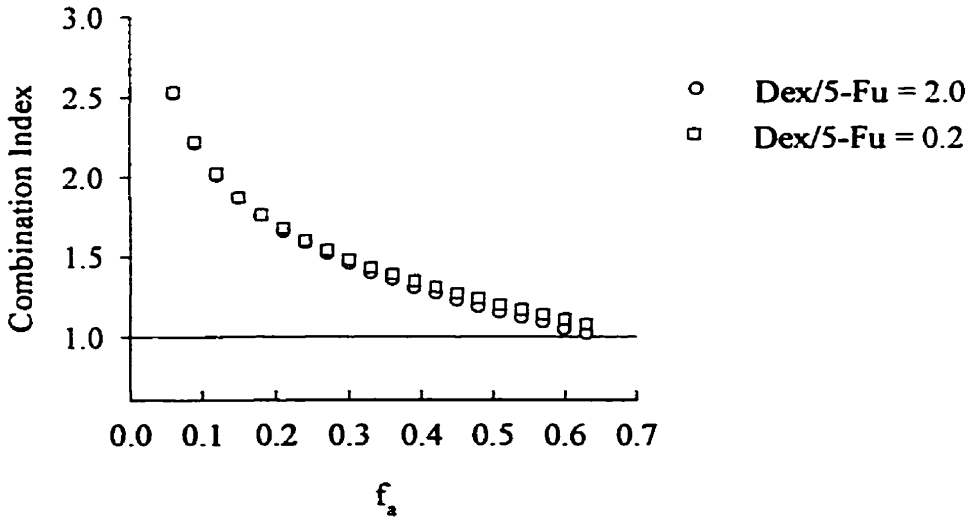

Fig. 3.12. Plot of combination index against fraction affected for 5-fluorouracil and dexrazoxane two different ratios. Nonexclusivity of the two drugs is assumed ($\alpha = 1$). The combination index was calculated for single experiment.

The combination index calculated with $\alpha = 1$ (Fig. 3.12) was greater than one for the whole range of effect studied (0.03-0.63). 5-Fluoruouracil and dexrazoxane showed antagonism for both ratios, Dex/5-Fu = 2.0 and Dex/Fu = 0.2. In Table 3.12, the values of combination index and corresponding fraction affected are given.

Table 3.12. Values of combination index (*CI*) and corresponding ranges of fraction affected (f_a) for one 5-fluorouracil-dexrazoxane combination index experiments[a].

α	0				1	
Ratio	2.0		0.2		2.0	0.2
Effect	Ant[b]	Syn[b]	Ant	Syn	Ant	Ant
CI[c]	**2.39-1.00**	**1.00-0.85**	**2.16-1.00**	**1.00-0.97**	**3.14-1.02**	**3.22-1.08**
f_a[d]	0.03-0.45	0.45-0.63	0.03-0.57	0.57-0.63	0.03-0.63	0.03-0.63

[a] The combination index was calculated with two equations for α =0 and α = 1 for two ratios of dexrazoxane to 5-fluorouracil 2.0 and 0.2. The value of 1.00 is a cross point between synergy and antagonism; thus it is not recognised as an additivity effect
[b] Ant and Syn mean antagonism and synergy, respectively
[c] *CI* is the combination indexes
[d] f_a is the fraction affected corresponding to combination indexes

3.3.2. Results for the combination of dexrazoxane with mafosfamide and 5-fluorouracil obtained with the envelope of additivity method

3.3.2.1. Results for the combination of dexrazoxane with mafosfamide obtained with the envelope of additivity method

The effect of 72 h continuous exposure of mafosfamide with dexrazoxane on Chinese hamster ovary cell growth was measured for the envelope of additivity experiments as described in Section 3.2.3.2. Experiments were designed to obtain a wide range of dose-response curves of dexrazoxane (0.1-100 μM) and mafosfamide (0.05-50 μM) and four dose-response curves of mafosfamide with different fixed concentrations of dexrazoxane for each curve *e.g.* 1.5, 2.0, 2.5 or 4.0 μM. Dexrazoxane was dissolved in the cell culture medium and delivered 20 min before mafosfamide was added. The time gap between drugs delivery was established to introduce mafosfamide into established conditions of interaction between dexrazoxane and topoisomerase II. Mafosfamide was

dissolved in DMSO and delivered in 1 μL aliquots. The control values for DMSO were also included. The envelope of additivity experiments for mafosfamide and dexrazoxane were repeated four times under the same conditions. The results of one single experiment of mafosfamide with dexrazoxane are presented in Fig. 3.13. The dose-response curves of mafosfamide and dexrazoxane alone and four dose-response curves of mafosfamide with fixed doses of dexrazoxane are plotted.

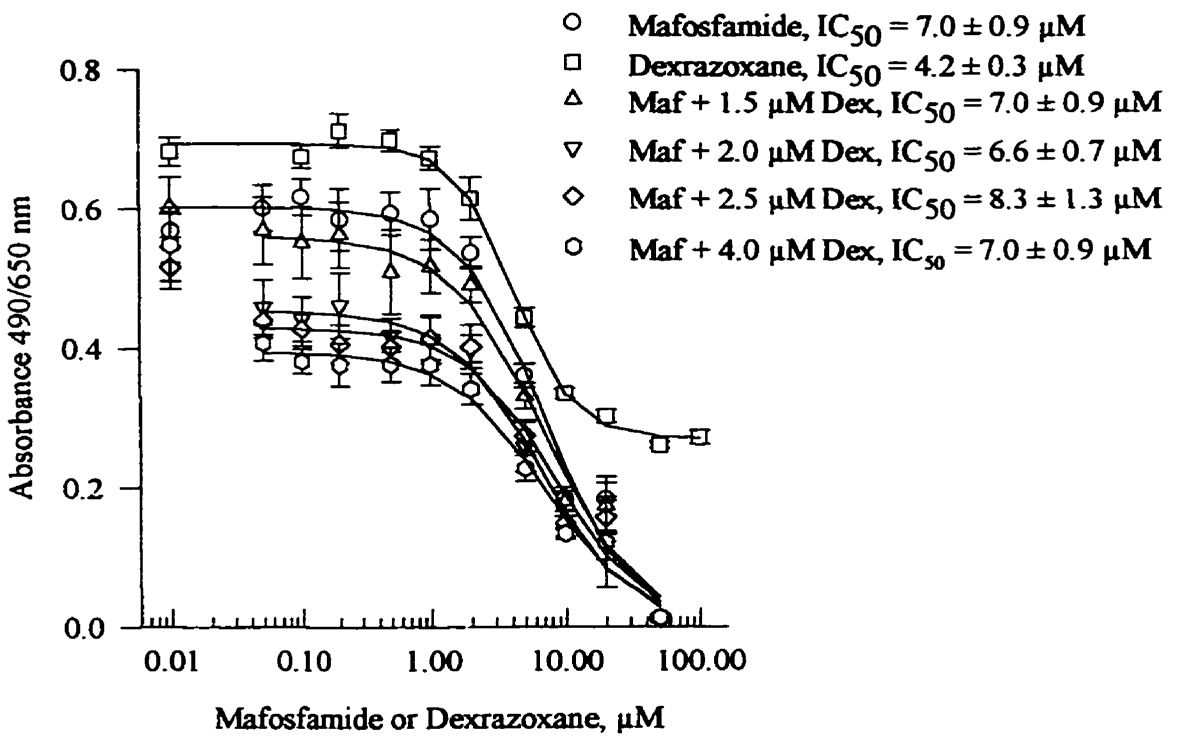

Fig. 3.13. Envelope of additivity experiment for the combination of dexrazoxane with mafosfamide. Chinese hamster ovary cells were incubated with the drug for 72 h. The points represent the mean absorbance ± SD from six replicates at each concentration. The curves represent non-linear least squares fits of experimental data to three- or four-parameter logistic equations. The lowest concentration values correspond to zero concentration of drugs (control values) plotted for convenience with an arbitrary given value on a logarithmic scale.

The envelope of additivity was constructed from the mafosfamide and dexrazoxane dose-response curves at 50% effect as described in Section 3.2.4.2. The 50% effect was chosen because the potency of the drugs is often expressed as the concentration that produces 50% effect, called the median inhibitory concentration. The envelope was constructed for each of four experiments. The four sets of theoretical combination of doses that defined envelope for each experiment were averaged and the SEM was calculated for each mean dose of dexrazoxane and mafosfamide. Since mean doses were determined for mafosfamide and dexrazoxane separately, the SEM bars are in both directions: parallel to the mafosfamide and dexrazoxane axis. The envelope in Fig. 3.14 obtained from the combinations of mean doses that produce 50% effect. The experimental data that in combination produces 50% effect (black symbols on the envelope) include SEM bars only for doses of mafosfamide. The doses of dexrazoxane were known as the fixed concentrations.

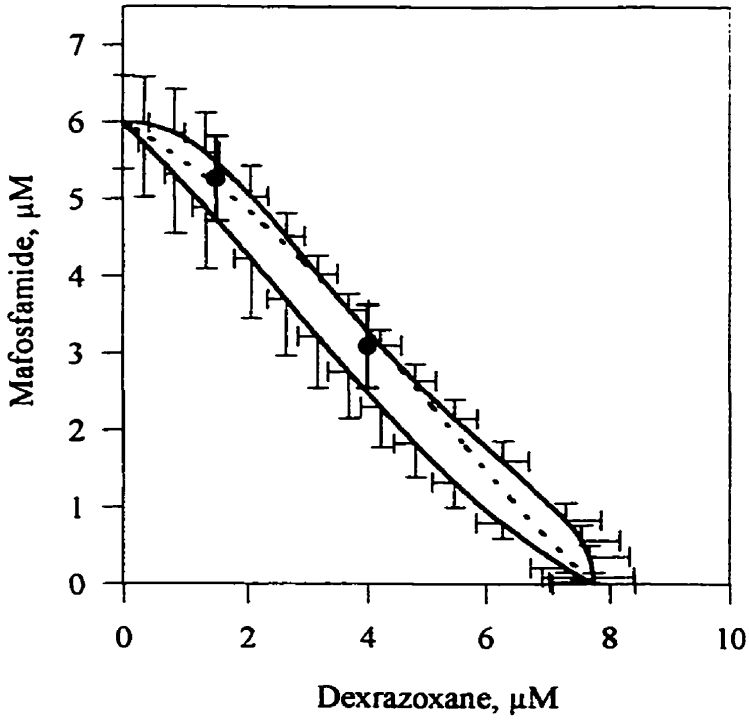

Fig. 3.14. Envelope of additivity for the combination of dexrazoxane with mafosfamide constructed for 50% effect from four experiments. The solid line to the left was calculated by mode I, the solid line to the right was calculated by mode IIa and the dotted line was calculated by mode IIb. The bars represent SEM for every mean concentration. The bars of SEM for mode IIb as well as the bars that entered the envelope are not shown to obtain a clearer graph. The co-ordinates of the points (•) represent concentrations of mafosfamide and dexrazoxane in the combination that produce 50% effect. The concentrations of dexrazoxane are 1.5 and 4 μM for the upper and lower point, respectively. The concentrations of mafosfamide were 5.3 and 3.1 μM and they were calculated from equation for dose-response curves with 1.5 and 4 μM fixed doses of dexrazoxane for 50% effect (compare Fig. 3.13). The points represent the mean concentration of mafosfamide ± SEM from four determinations.

The points of 50% effect of the drug combinations are inside the envelope of additivity. This result suggests an additive effect of mafosfamide and dexrazoxane. The results from single experiments and their means are given in Table 3.13.

Table 3.13. Calculated doses of mafosfamide in combination with dexrazoxane that give 50% effect.

Dexrazoxane μM	Mafosfamide μM				
	Mean ± SEM	Experiment 1	Experiment 2	Experiment 3	Experiment 4
1.5	5.3 ± 0.5 Ad[a]	4.1 Ad	6.2 Ant[c]	4.6 Ad	6.2 Ad
2.0					5.3 Ant
2.5					6.1 Ad
4.0	3.1 ± 0.5 Ad	1.5 Syn[b]	3.6 Ant	3.6 Ad	3.6 Ad

The effects were estimated based on the position of the points on the envelope of additivity for the mean envelope (Fig.3.14) and for single Experiments not shown here.
[a] Additivity
[b] Synergy
[c] Antagonism

As shown in Table 3.13, the common effect of mafosfamide and dexrazoxane was determined to be additive by the mean envelope from all Experiments. The single Experiments, 3 and 4, also showed additive effects for the same doses of dexrazoxane (1.5 and 4.0 μM). Experiment 1 gave additivity for 1.5 μM dose of dexrazoxane but for dose 4.0 the effect was slightly synergistic. Experiment 2 showed that the combined effect of mafosfamide and dexrazoxane was antagonistic.

3.3.2.2. Results for the combination of dexrazoxane with 5-fluorouracil obtained with the envelope of additivity method

The effect of 72 h continuous exposure of 5-fluorouracil with dexrazoxane on Chinese hamster ovary cell growth was measured for the envelope of additivity experiments as described in Section 3.2.3.2. Experiments were designed to obtain the wide range dose-response curves for dexrazoxane (0.1-100 μM) and 5-fluorouracil (0.1-100 μM), and four dose-response curves of 5-fluorouracil with different fixed concentrations

of dexrazoxane for each curve *e.g.* 1.5, 2.0, 2.5 or 4.0 μM. Dexrazoxane was dissolved in the cell culture medium and was delivered 20 min before 5-fluorouracil was added. The time gap between drugs delivery was established to introduce 5-fluorouracil into established conditions of interaction between dexrazoxane and topoisomerase II. 5-Fluorouracil was dissolved in one equivalent of aqueous solution of NaOH and it was delivered in 1 μL aliquots. An example of the experiment for envelope of additivity for 5-fluorouracil and dexrazoxane is given in Fig. 3.15. This experiment was conducted three times under the same conditions.

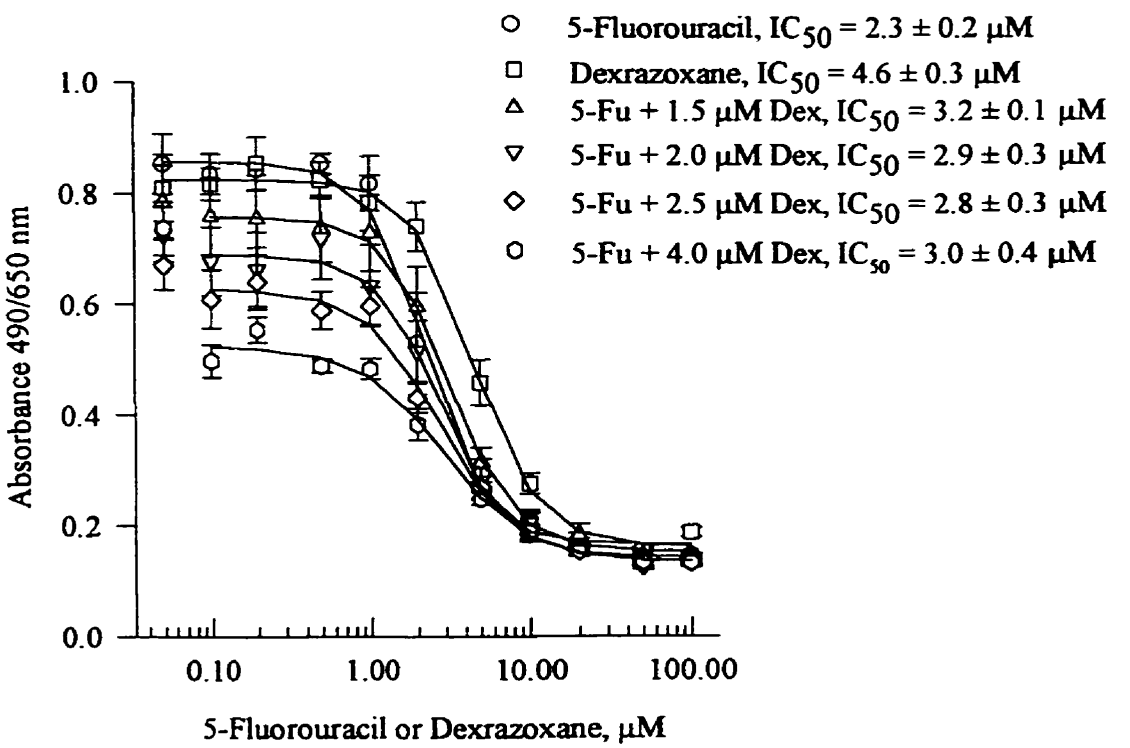

Fig. 3.15. Envelope of additivity experiment for the combination of dexrazoxane with 5-fluorouracil. Chinese hamster ovary cells were incubated with the drug for 72 h. The points represent the mean absorbance ± SD from six replicates at each concentration. The curves represent non-linear least square best fit of experimental data to a four-parameter logistic equation. The lowest concentration values correspond to zero concentration of

drugs (control values) plotted for convenience with an arbitrary given value on a logarithmic scale.

The 50% effect envelope of additivity for 5-fluorouracil and dexrazoxane is shown in Fig. 3.16. The envelope was constructed from the means of three separate experiments.

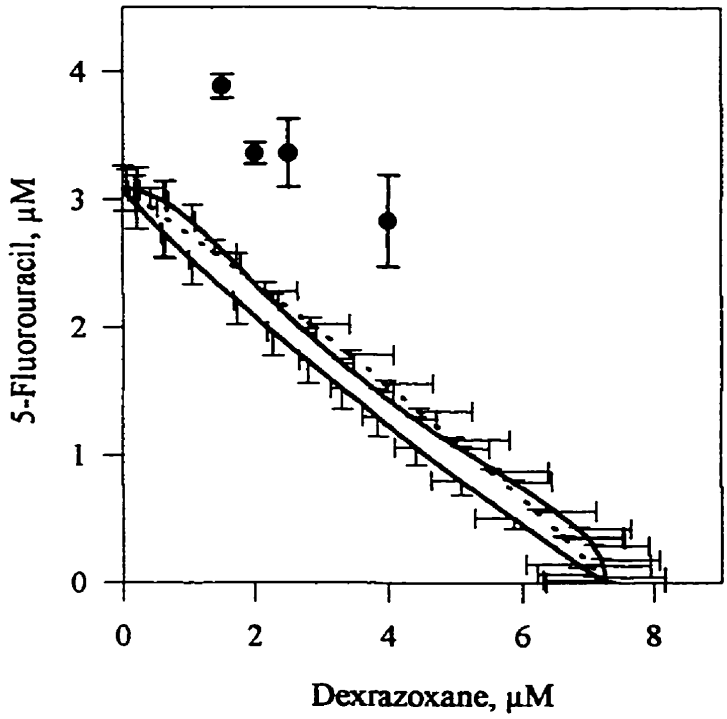

Fig. 3.16. Envelope of additivity for the combination of dexrazoxane with 5-fluorouracil constructed for 50% effect from three experiments. The solid line to the left was calculated by mode I, the solid line to the right was calculated by mode IIa, and the dotted line was calculated by mode IIb. The bars represent standard error of the mean concentrations obtain from three experiments. The parts of the bars that entered the envelope were not plotted to give a clearer graph. The bars of SEM for mode IIa are not shown. The four points (•) represent the concentrations of 5-fluorouracil and dexrazoxane that produce 50% effect when used as a mixture. The co-ordinates (dexrazoxane: 5-fluorouracil) of the points starting from the left are as follows: (1.5 μM: 3.9 μM), (2.0 μM: 3.4 μM), (2.5 μM: 3.4 μM), (4.0 μM: 2.8 μM). The error bars for the points are standard errors of the 5-fluorouracil concentration means obtained from three experiments.

Four points corresponding to the effects of drug combination are to the right of the envelope of additivity; thus, the interaction of 5-fluorouracil with dexrazoxane for their 50% effect was antagonistic.

The single Experiments results and their means are given in Table 3.14.

Table 3.14. Calculated doses of 5-fluorouracil that in combination with dexrazoxane give 50% effect. All combinations showed antagonism[a].

Dexrazoxane μM	5-Fluorouracil μM			
	Mean ± SEM	Experiment 1	Experiment 2	Experiment 3
1.5	3.9 ± 0.1	4.0	3.7	3.9
2.0	3.4 ± 0.1		3.3	3.5
2.5	3.4 ± 0.3	3.8	2.9	3.4
4.0	2.8 ± 0.4	3.5	2.7	2.3
7.5		1.6		

[a] All single envelope Experiments and their mean showed antagonism for each combination with dexrazoxane. The results were evaluated based on position of the points on the mean envelope presented in Fig. 3.16 and the envelopes constructed for single Experiments not showed here

3.3.3. Results for the combination of dexrazoxane with mafosfamide and 5-fluorouracil obtained with the response surface method

Drug interactions were also evaluated with the response surface method (Section 3.2.4.3). The data obtained from experiments designed for the combination index and the envelope of additivity methods were used to determine the interaction parameter α' in the equation (3.5). The obtained survival effects were normalised to the control effects *i.e.* the data were divided by the mean absorbance corresponding to the wells without drugs; thus, the maximal survival, E_{max}, is 1.0. Each dose-response curve had individual controls. The

control effect was not included in the data fit because of poor fitting results (for the control $d_A = d_B = 0$; the zero value would have to appear in numerators of equation (3.5)). For some dose-response curves, data which did not fit to the equation (3.5) well were also omitted (data in Fig. 3.18 and 3.20).

3.3.3.1. Results for the combination of dexrazoxane with mafosfamide obtained with the response surface method

The data for mafosfamide and dexrazoxane from the three combination index experiments described in Section 3.3.1.1 were also fitted to a modified Greco equation (3.6) [15]. The mafosfamide dose-response curves showed 100% kill for the highest concentrations; thus, the mafosfamide term does not include the background parameter *B*. This equation gave a better fit than equation (3.5).

$$\frac{d_{Maf}}{IC_{50,Maf}\left(\frac{E}{E_{max}-E}\right)^{1/m_{Maf}}}+\frac{d_{Dex}}{IC_{50,Dex}\left(\frac{E-B}{E_{max}-E+B}\right)^{1/m_{Dex}}}+\frac{a'\cdot d_{Maf}\cdot d_{Dex}}{IC_{50,Dex}\cdot IC_{50,Maf}\left(\frac{E-B}{E_{max}-E+B}\right)^{\left(1/m_{Dex}+1/m_{Maf}\right)}}=1 \qquad (3.6)$$

The meaning of the variables is given in Section 3.2.4.3. The best fit parameter estimates obtained for each experiment and their means ± standard error are presented in Table 3.15.

Table 3.15. Best fit parameter estimates ± SEM from fitting mafosfamide-dexrazoxane combination index experimental data to equation (3.6) for three single experiments and their means.

Experiment	α' ± SEM	$IC_{50,Maf}$ ± SEM μM	$IC_{50,Dex}$ ± SEM μM	m_{Maf} ± SEM	m_{Dex} ± SEM	E_{max} ± SEM	B ± SEM
1	-0.243 ± 0.248[a]	5.454 ± 1.802[a]	4.627 ± 2.590[a]	-2.056 ± 0.433[a]	-0.695 ± 0.126[a]	1.209 ± 0.140[a]	0.019 ± 0.148[a]
2	-0.205 ± 0.244[a]	5.473 ±1.165[a]	7.901 ± 3.979[a]	-1.390 ± 0.246[a]	-1.159 ± 0.205[a]	1.138 ± 0.036[a]	0.014 ± 0.078[a]
3	-0.395 ± 0.135[a]	5.310 ± 1.102[a]	7.234 ± 3.030[a]	-1.392 ± 0.228[a]	-0.829 ± 0.114[a]	1.121 ± 0.039[a]	0.019 ± 0.064[a]
Mean	-0.281 ± 0.058[b]	5.412 ± 0.052[b]	6.587 ± 0.999[b]	-1.613 ± 0.222[b]	-0.894 ± 0.138[b]	1.156 ± 0.027[b]	0.017 ± 0.002[b]

[a] Standard error of the mean from SigmaPlot fitting
[b] Standard error of the mean from three results

Based on the parameters obtained, the theoretical effects were calculated by a bisection root finder (file given in Section 3.2.4.3). The real experimental data and calculated curves were plotted together. The experimental data presented in Fig. 3.6 is used in the example given in Fig. 3.17. Visual inspection of the plots showed good agreement between measured and calculated values.

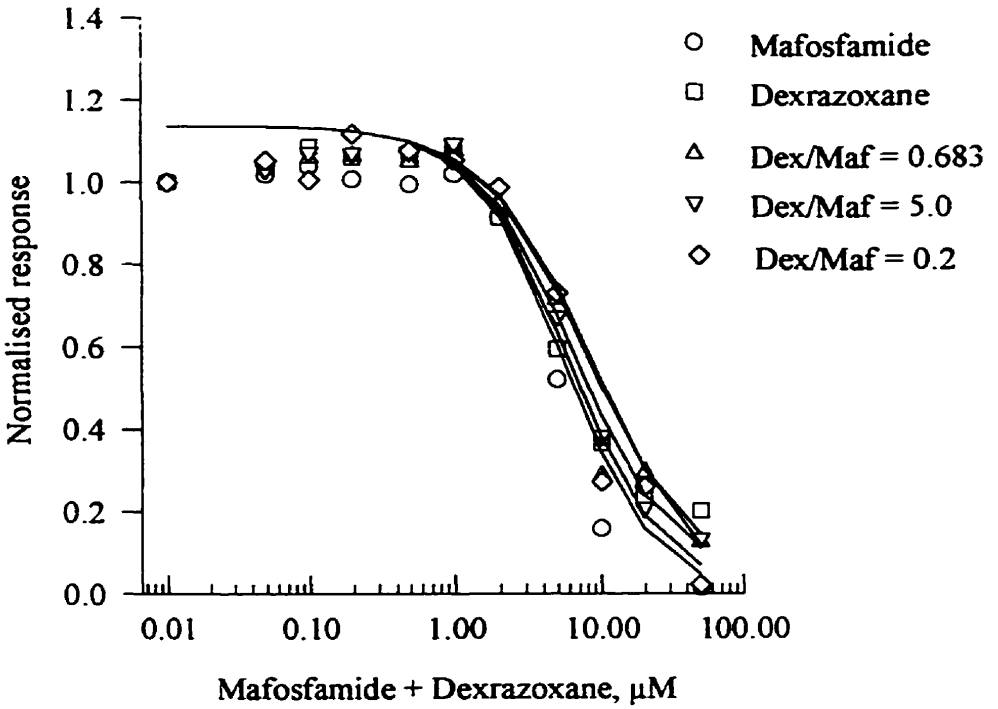

Fig. 3.17. Evaluation of the results from the response surface method used for the dexrazoxane-mafosfamide combination index experiment. The measured (symbols) and calculated (lines) effects are plotted. The effects were calculated based on seven parameters obtained from the four dimensional fit of equation (3.6) to combination index experimental data (Fig.3.6). The lowest concentration values correspond to zero concentration of drugs (control values) plotted for convenience on a logarithmic scale with an arbitrary given value.

The mean interaction parameter α' is -0.281 ± 0.058. The value of α' was less than zero; thus, the combined effect of mafosfamide and dexrazoxane calculated with response surface methodology is slightly antagonistic. The single Experiment calculations shown in Table 3.15 also gave negative values of interaction parameters; but, only the result from Experiment 3 can be defined as antagonistic within SEM. The large standard errors for Experiment 1 and 2 classified the interaction effect as additive ($\alpha' = 0$).

The data for mafosfamide and dexrazoxane from the three Experiments for the envelope of additivity described in Section 3.3.2.1 were also analysed with the response surface method. The modified Greco equation (3.6) was used. The response of 50 and 100 μM of dexrazoxane were excluded from the fit to obtain better results. The best fit parameter estimates obtained for single Experiments and their means ± standard error are presented in Table 3.16.

Table 3.16. Best fit parameter estimates ● SEM from fitting the mafosfamide-dexrazoxane envelope of additivity experimental data to equation (3.6) for single experiments and their mean.

Experiment	$\alpha' \pm$ SEM	$IC_{50,Maf} \pm$ SEM μM	$IC_{50,Dex} \pm$ SEM μM	$m_{Maf} \pm$ SEM	$m_{Dex} \pm$ SEM	$E_{max} \pm$ SEM	$B \pm$ SEM
1	0.004 ± 0.228[a]	4.094 ± 0.437[a]	5.712 ± 1.636[a]	-1.685 ± 0.111[a]	-1.290 ± 0.150[a]	1.114 ± 0.002[a]	$3x10^{-10}$ ± 0.078[a]
2	-0.474 ± 0.134[a]	7.581 ± 1.153[a]	6.210 ± 0.509[a]	-2.138 ± 0.272[a]	-1.398 ± 0.145[a]	1.088 ± 0.012[a]	0.0142 ± 0.0007[a]
3	-0.022 ± 0.330[a]	5.238 ± 0.763[a]	7.076 ± 1.183[a]	-2.097 ± 0.175[a]	-1.394 ± 0.206[a]	1.119 ± 0.011[a]	0.012 ± 0.042[a]
4	-0.483 ± 0.608[a]	6.878 ± 0.797[a]	8.941 ± 1.540[a]	-1.632 ± 0.133[a]	-0.880 ± 0.118[a]	1.087 ± 0.001[a]	0.017 ± 0.038[a]
Mean	-0.244 ± 0.136[b]	5.948 ± 0.789[b]	6.985 ± 0.710[b]	-1.888 ± 0.133[b]	-1.241 ± 0.123[b]	1.102 ± 0.008[b]	0.011 ± 0.004[b]

[a] Standard error of the mean from SigmaPlot fitting
[b] Standard error of the mean from four single results

The calculated effects based on estimated parameters showed good fit to the measured effect. As an example, the graph with calculated and measured effects for data from Fig. 3.13 is given in Fig. 3.18. The seven parameter fit to the Greco equation was satisfied.

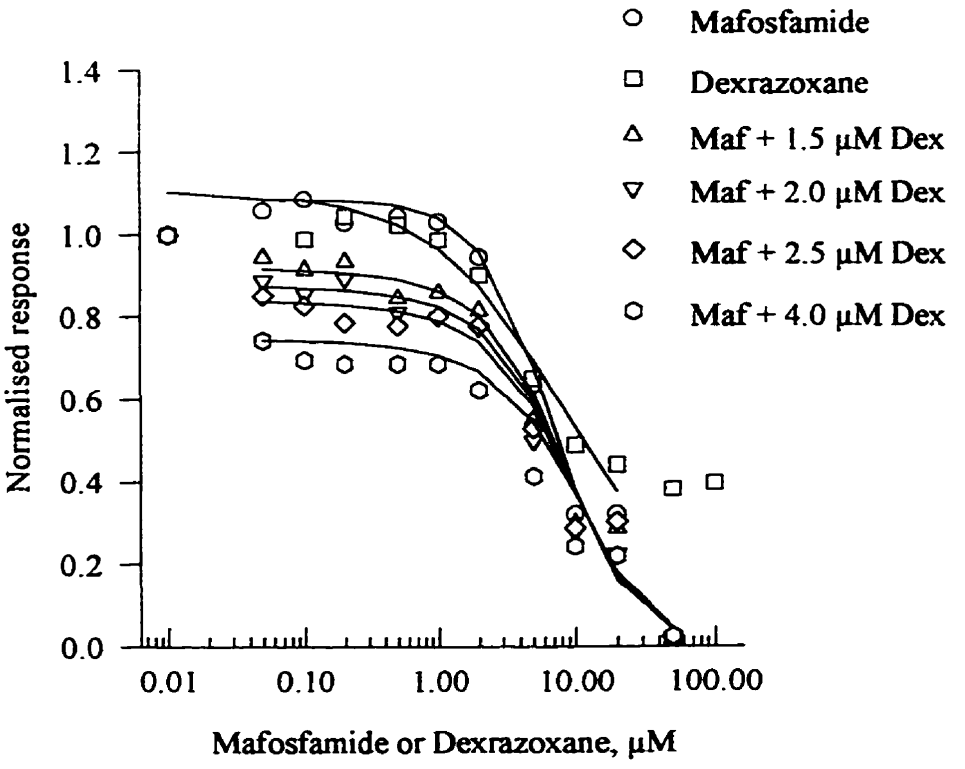

Fig. 3.18. Evaluation of the results from the response surface method used for the dexrazoxane-mafosfamide envelope of additivity experiment. The measured (symbols) and calculated (lines) effects are plotted. The effects were calculated based on seven parameters obtained from the four dimensional fit of the equation (3.6) to envelope of additivity experimental data (Fig. 3.13). The lowest concentration values correspond to zero concentration of drugs (control values) plotted for convenience with an arbitrary given value on a logarithmic scale.

The mean value of the interaction parameter, α', obtained from the three envelope of additivity Experiments was -0.244 ● 0.136. Thus, the effect of mafosfamide and dexrazoxane was slightly antagonistic. The results for single Experiments presented in Table 3.16 showed additivity for Experiments 1, 3 and 4. Experiment 2 showed antagonism.

3.3.3.2. Results for the combination of dexrazoxane with 5-fluorouracil obtained with the response surface method

The response surface methodology was used to calculate the effect of 5-fluorouracil and dexrazoxane combined action. Since both 5-fluorouracil and dexrazoxane have background B, the combination index data described in Section 3.3.1.2, were fitted to the Greco equation with all terms containing parameter B (3.7).

$$\frac{d_{5\text{-}Fu}}{IC_{50,5\text{-}Fu}\left(\frac{E-B}{E_{max}-E+B}\right)^{1/m_{5\text{-}Fu}}}+\frac{d_{Dex}}{IC_{50,Dex}\left(\frac{E-B}{E_{max}-E+B}\right)^{1/m_{Dex}}}+\frac{a'\cdot d_{Dex}\cdot d_{5\text{-}Fu}}{IC_{50,Dex}\cdot IC_{50,5\text{-}Fu}\left(\frac{E-B}{E_{max}-E+B}\right)^{\left(1/m_{Dex}+1/m_{5\text{-}Fu}\right)}}=1 \qquad (3.7)$$

The obtained seven best fit parameters are presented in Table 3.17.

Table 3.17. Best fit parameter estimates ± SEM from fitting the 5-fluorouracil-dexrazoxane combination index experimental data (Fig.3.9) to equation (3.7).

α' ± SEM	$IC_{50,5\text{-}Fu}$ ± SEM μM	$IC_{50,Dex}$ ± SEM μM	$m_{5\text{-}Fu}$ ± SEM	m_{Dex} ± SEM	E_{max} ± SEM	B ± SEM
-0.306 ± 0.262	5.667 ± 1.578	10.06 ± 3.383	-1.449 ± 0.311	-2.246 ± 1.212	0.871 ± 0.061	0.207 ± 0.053

The data calculated from the best fit parameters (lines) and measured data (symbols) are plotted on the same graph (Fig. 3.19). Visual comparison of the data showed good agreement. This indicates a good fit to the Greco equation (3.7).

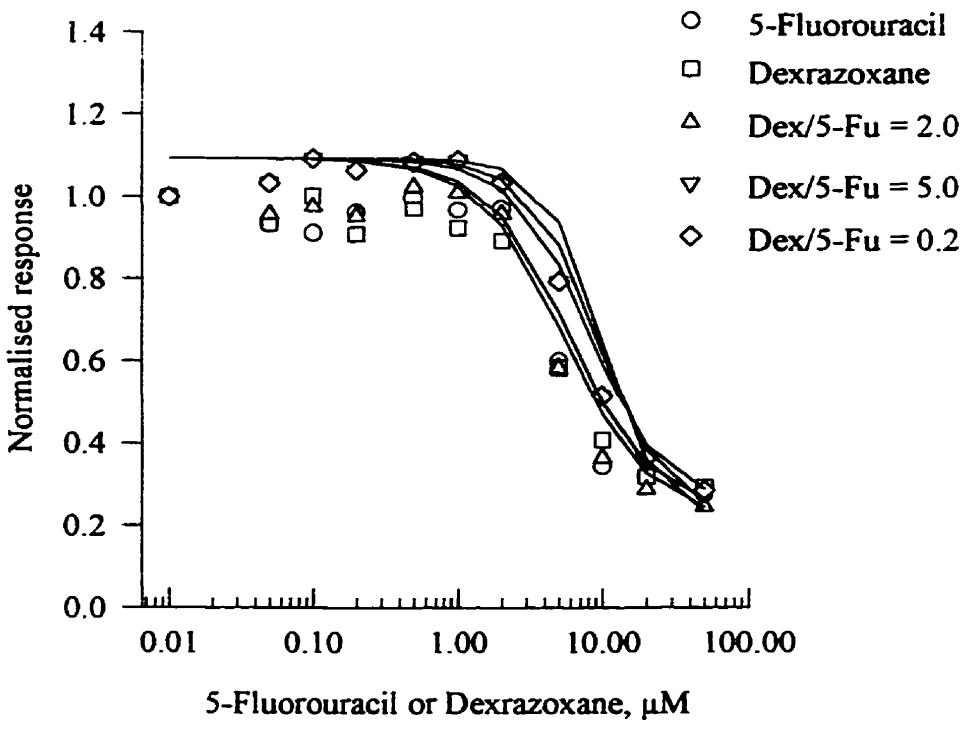

Fig. 3.19. Evaluation of the results from the response surface method used for the dexrazoxane-5-fluorouracil combination index experiment. The measured (symbols) and calculated (lines) effects are plotted. The effects were calculated based on seven parameters obtained from the four dimensional fit of the equation (3.7) to combination index experimental data (Fig. 3.9). The lowest concentration values correspond to zero concentration of drugs (control values) plotted for convenience with an arbitrary given value on a logarithmic scale.

A value of -0.306 ± 0.262 was obtained for the interaction parameter, α'. Because α' was less than zero, the interaction between 5-fluorouracil and dexrazoxane is slightly antagonistic.

The three sets of data from the dexrazoxane-5-fluorouracil experiment for envelope of additivity, described in Section 3.3.2.2, were fitted to the Greco equation

(3.7). The data for 50 and 100 μM for each of the curves were excluded from the fit. The best fit parameter estimates and their means ● standard errors are presented in Table 3.18.

Table 3.18. Best fit parameter estimates ± SEM from fitting the 5-fluorouracil-dexrazoxane envelope of additivity experimental data to equation (3.7) for single experiments and their mean.

Experiment	α' ± SEM	$IC_{50,5\text{-}Fu}$ ± SEM μM	$IC_{50,Dex}$ ± SEM μM	$m_{5\text{-}Fu}$ ± SEM	m_{Dex} ± SEM	E_{max} ± SEM	B ± SEM
1	-0.156 ± 0.167[a]	2.983 ± 0.332[a]	5.255 ± 0.391[a]	-1.682 ± 0.134[a]	-1.597 ± 0.137[a]	0.775 ± 0.015[a]	0.283 ± 0.014[a]
2	-0.533 ± 0.245[a]	3.211 ± 0.438[a]	5.431 ± 0.544[a]	-2.161 ± 0.276[a]	-2.436 ± 0.276[a]	0.751 ± 0.014[a]	0.251 ± 0.013[a]
3	-0.599 ± 0.214[a]	3.028 ± 0.446[a]	4.951 ± 0.562[a]	-2.022 ± 0.296[a]	-2.570 ± 0.405[a]	0.871 ± 0.019[a]	0.185 ± 0.016[a]
Mean	-0.429 ± 0.138[b]	3.074 ± 0.070[b]	5.212 ± 0.140[b]	-1.955 ± 0.142[b]	-2.201 ± 0.305[b]	0.799 ± 0.037[b]	0.240 ± 0.029[b]

[a] Standard error of the mean from SigmaPlot fitting
[b] Standard error of the mean from three results

The data calculated from the obtained best fit parameters (lines) and measured data (symbols) are plotted on the same graph (Fig. 3.20). Visual comparison of the data showed good agreement. This indicates a good fit to the Greco equation (3.7).

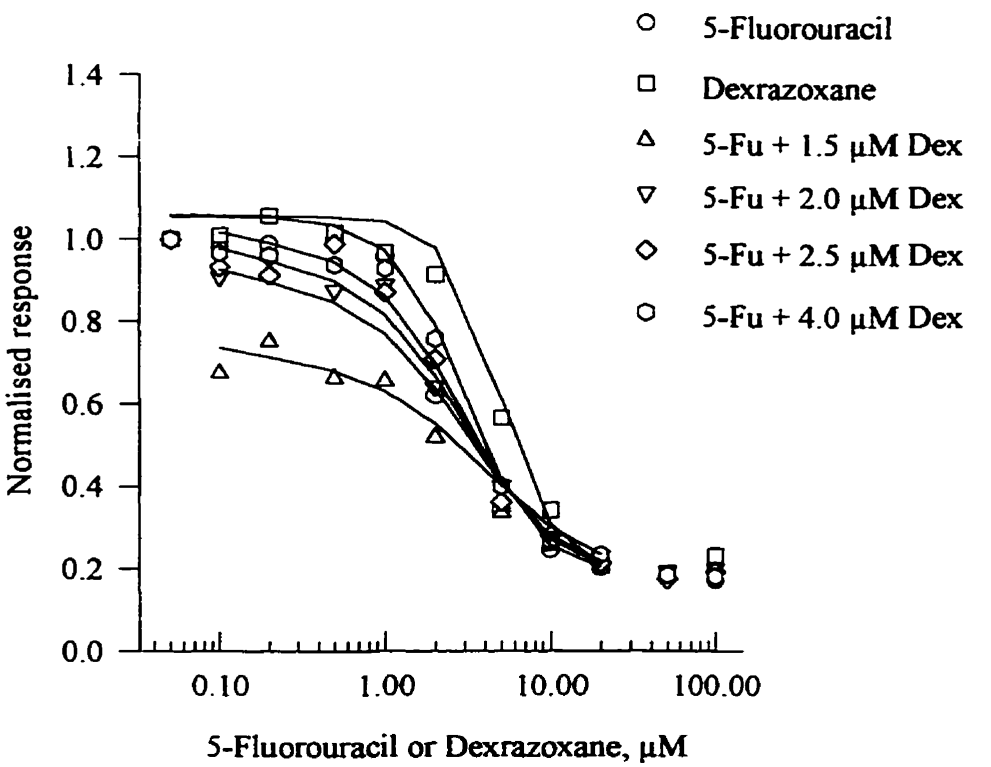

Fig. 3.20. Evaluation of the results from the response surface method used for the dexrazoxane-5-fluorouracil envelope of additivity experiment. The measured (symbols) and calculated (lines) effects are plotted. The effects were calculated from seven parameters obtained from the three dimensional fit of the equation (3.7) to envelope of additivity experimental data presented in Fig. 3.15. The data for 50 and 100 μM were not used in calculations. The lowest concentration values correspond to zero concentration of drugs (control values) plotted for convenience with an arbitrary given value on a logarithmic scale.

The mean interaction index, α', from the three Experiments was -0.429 ± 0.138. Thus, the interaction between 5-fluorouracil and dexrazoxane was negative and the effect was antagonistic. The results of single Experiments presented in Table 3.18 indicate an antagonistic effect for Experiment 2 and 3; but, Experiment 1 showed additivity.

3.3.4. Results for the combination of dexrazoxane with mafosfamide, 5-fluorouracil and vinblastine obtained with the slope comparison method

The 48 h effects of dexrazoxane alone and dexrazoxane combined with fixed concentrations of mafosfamide, 5-fluorouracil or vinblastine on Chinese hamster ovary cell growth were measured. A 500 μM concentration of dexrazoxane gave a cell kill of about 20 % in 48 h exposure experiments; whereas, 100 μM produced an 80% cell kill in 72 h exposure experiments. A linear equation was a good model to fit the 48 h cytotoxicity data. The results of the dexrazoxane (Dex) with mafosfamide (Maf) experiment are given in Fig. 3.21. In this experiment, nine different concentrations of mafosfamide were used (10, 12, 15, 18, 20, 30, 40, 50 μM) with a wide range of dexrazoxane concentrations (0.5-500 μM). The 48 h median inhibitory concentration of mafosfamide obtained in a preliminary experiment was 9.0 ± 0.7 μM (three-parameter fit). Dexrazoxane was preincubated 1 h before the mafosfamide was added. Dexrazoxane was dissolved in the cell culture medium. Mafosfamide was dissolved in DMSO; 1 μL aliquots of DMSO were also added to the plate for the dexrazoxane dose-response curve. The results of the slope comparison for the experiment from Fig. 3.21 are given in Table 3.19.

Table 3.19. Slope comparison of dexrazoxane and dexrazoxane with fixed doses of mafosfamide linear dose-response curves presented in Fig. 3.21.

Parameters	Doses of Mafosfamide, μM								
	0	10	12	15	18	20	30	40	50
a ● SEM	-0.104 ● 0.019	-0.312 ± 0.020	-0.380 ± 0.024	-0.370 ± 0.034	-0.487 ± 0.021	-0.447 ± 0.029	-1.227 ● 0.094	-1.419 ± 0.032	-1.309 ± 0.011
b ● SEM	-0.073 ± 0.012	0.001 ± 0.012	0.017 ± 0.014	0.009 ± 0.020	0.037 ± 0.013	0.012 ● 0.017	0.016 ± 0.056	0.071 ± 0.019	0.015 ± 0.007
Tb		-4.552	-4.880	-3.531	-6.484	-4.105	-6.967	-6.485	-6.635
Vb		12	12	12	12	12	12	12	12
P		< 0.001	< 0.001	< 0.01	< 0.001	< 0.001	< 0.001	< 0.001	< 0.001

Listing of the variables used in the t-test:

a - y-intercept

b - slope

Tb - *t* value computed for comparing the two slopes

Vb - the degrees of freedom for the slope comparison

Ta - *t* value computed for comparing the intercepts

Va - the degrees of freedom for the intercept comparison

P - statistical significance

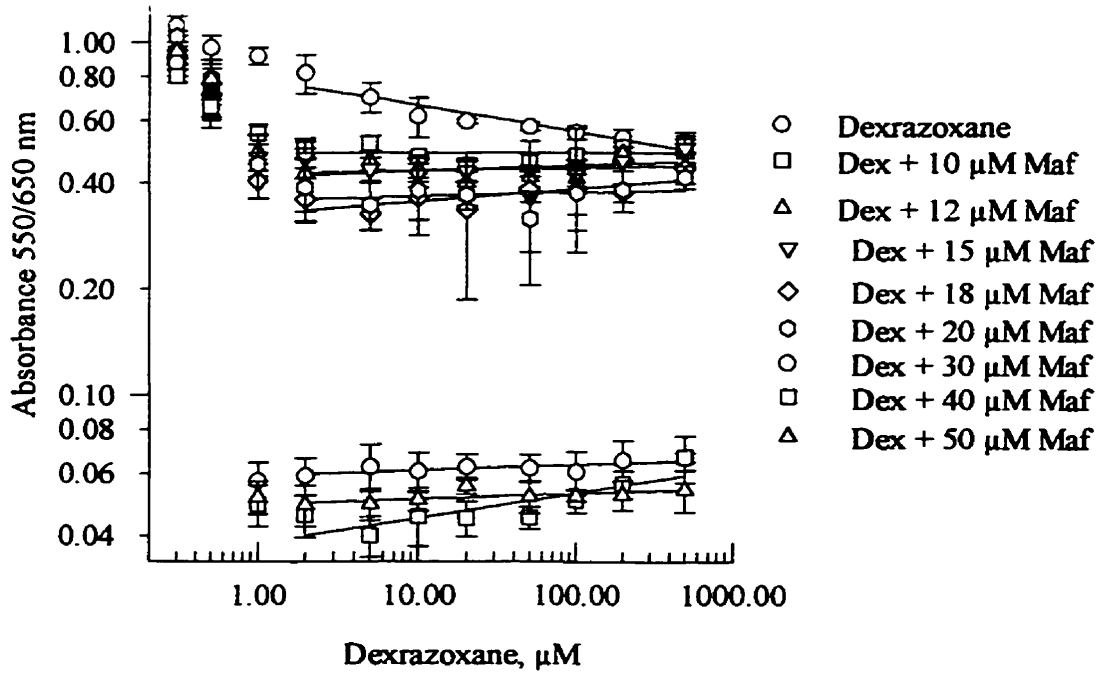

Fig. 3.21. Slope comparison experiment for the combination of dexrazoxane with mafosfamide. The 48 h inhibitory effect of dexrazoxane alone and dexrazoxane with fixed doses of mafosfamide on Chinese hamster ovary cell growth is presented in log-log scale. The points represent the means of absorbance ± SD from six replicates at each concentration. The lowest concentrations correspond to control values with zero concentration of drugs and without DMSO. The data, next to the lowest concentration of the drugs, are the data for control with 1 μL of DMSO. The third set of control data represent the control with mafosfamide only (this control is for dexrazoxane with mafosfamide dose-response curves).

The slopes obtained and corresponding mafosfamide concentrations are plotted in Fig. 3.22.

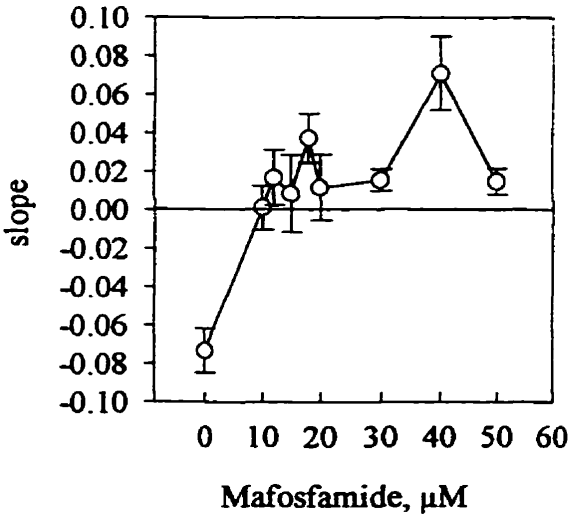

Fig. 3.22. Slopes obtained from the dexrazoxane-mafosfamide slope method experiment. The slopes of linear dose-response curves are plotted *vs.* concentration of mafosfamide. The slopes of dexrazoxane with fixed doses of mafosfamide are significantly different from the slope of dexrazoxane alone.

All the regression line slopes for dexrazoxane with fixed doses of mafosfamide were significantly different from dexrazoxane alone ($P < 0.01$, Table 3.19). The slope of the dexrazoxane regression line was negative and the slopes for dexrazoxane with mafosfamide were positive. The highest slope value was produced by the combination of dexrazoxane with 40 μM of mafosfamide. The growth of Chinese hamster ovary cells steadily increased with higher concentrations of dexrazoxane compared to the control with mafosfamide only. Thus, the interaction of dexrazoxane with mafosfamide shows antagonism.

The effect of 48 h exposure of Chinese hamster ovary cells to dexrazoxane with 5-fluorouracil (5-Fu) is given in Fig. 3.23. In this experiment, six different concentrations of 5-fluorouracil were used (2.0, 5.0, 20, 500, 2000, 5000 μM) with a wide range of

dexrazoxane concentrations (0.5-500 μM). The 48 h median inhibitory concentration of 5-fluorouracil obtained in the preliminary experiment was 160.0 ± 76.7 μM. The three-parameter logistic equation was used to fit the absorbance for 0.01-20.0 mM; although, the curve fitting was not satisfactory because of the presence of a plateau at 50, 100 and 200 μM. Dexrazoxane was preincubated for 1 h before the 5-fluorouracil was added. Dexrazoxane was dissolved in the cell culture medium. 5-Fluorouracil was dissolved in one equivalent of aqueous solution of NaOH and delivered to the wells in 1 μL aliquots. The results of slope comparison for the experiment shown in Fig. 3.23 are given in Table 3.20.

Table 3.20. Slope comparison of linear dose-response curves of dexrazoxane and dexrazoxane with fixed doses of 5-fluorouracil presented in Fig. 3.23.

Parameters	Doses of 5-Fluorouracil, μM						
	0	2	5	20	500	2000	5000
a ± SEM	-0.136 ± 0.008	-0.297 ± 0.006	-0.340 ± 0.006	-0.353 ± 0.008	-0.382 ± 0.008	-0.466 ± 0.007	-0.586 ± 0.012
b ± SEM	-0.062 ± 0.005	-0.045 ± 0.004	-0.034 ± 0.039	-0.033 ± 0.005	-0.025 ± 0.005	-0.022 ± 0.004	-0.006 ± 0.008
Tb		-2.683	-4.330	-3.904	-5.121	-5.912	-5.939
Vb		14	14	14	14	14	14
P		< 0.05	< 0.001	< 0.01	< 0.001	< 0.001	< 0.001

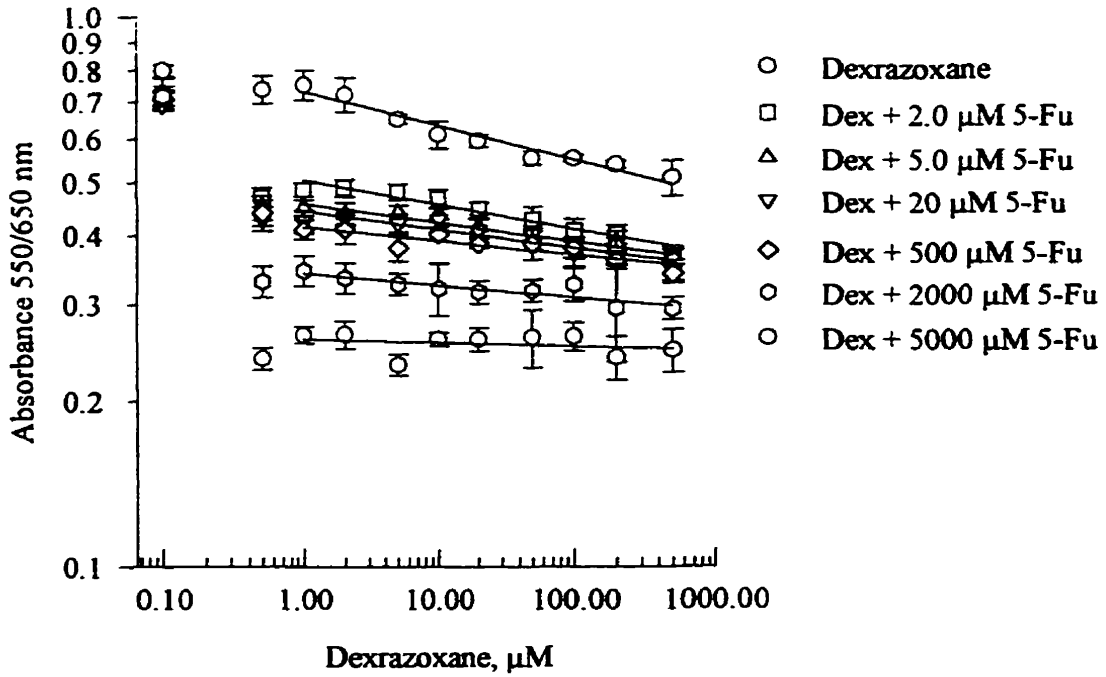

Fig. 3.23. Slope comparison experiment for the combination of dexrazoxane with 5-fluorouracil. The 48 h inhibitory effect of dexrazoxane alone and dexrazoxane with fixed doses of 5-fluorouracil on Chinese hamster ovary cells is presented in log-log scale. The points represent the means of absorbance ± SD from six replicates at each concentration. The lowest concentrations correspond to control values with zero concentration of drugs. The second control value is an effect of 5-fluorouracil by itself (this control is for dexrazoxane with 5-fluorouracil dose-response curves).

The obtained slopes were plotted against the concentration of 5-fluorouracil in Fig. 3.24.

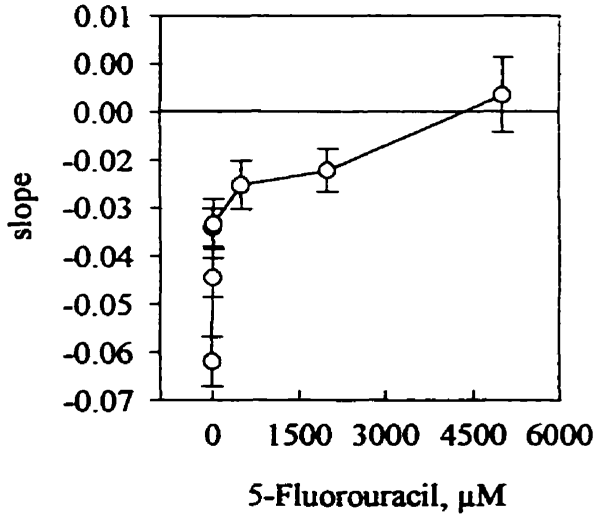

Fig. 3.24. Slopes obtained from the dexrazoxane-5-fluorouracil slope method experiment. The slopes of linear dose-response curves are plotted *vs.* concentration of 5-fluorouracil. The slopes of dexrazoxane with fixed doses of 5-fluorouracil are significantly different from the slope of dexrazoxane alone.

All regression line slopes for dexrazoxane with fixed doses of 5-fluorouracil were different from the slope of dexrazoxane alone with a probability greater than or equal to 95% (Table 3.20). The value of the slopes increases steadily with the concentration of 5-fluorouracil, although, the effect was not very strong (Fig. 3.24). Thus, the interaction of dexrazoxane with 5-fluorouracil was slightly antagonistic.

A third experiment was performed for dexrazoxane with vinblastine. The effect of 48 h exposure of Chinese hamster ovary cells to dexrazoxane with vinblastine (Vin) is given in Fig. 3.25. In this experiment, six different concentrations of vinblastine were used (0.005, 0.01, 0.02, 0.03, 0.04, 0.05 μM) with a wide range of dexrazoxane concentrations (0.5-500 μM). The 48 h median inhibitory concentration of vinblastine obtained in a preliminary experiment was 0.01 ± 0.002 μM (four-parameter fit). Dexrazoxane was

delivered 1 h before the vinblastine was added. Dexrazoxane was dissolved in the cell culture medium. Vinblastine was dissolved in 1 equivalent of aqueous solution of HCl and delivered to the wells in 10 μL aliquots. The results of the slope comparison for the experiment from Fig. 3.25 are given in Table 3.20.

The dose-response curves for dexrazoxane with vinblastine consisted of two data sets for dexrazoxane with concentrations 1.0 - 10 μM and 10-500 μM. Each set of data could be fitted to a linear equation with different slopes. Thus, the comparison of slopes was divided into two parts: the first for 1.0-10 μM and the second for 10-500 μM concentration ranges of dexrazoxane. In the range 1.0-10 μM, the slopes of the linear regression lines increase with the concentration of vinblastine (Table 3.21); although, the slopes for 0.005, 0.01 and 0.02 μM of vinblastine were not significantly different from the slope of dexrazoxane alone. The slops of dexrazoxane with 0.03, 0.04 and 0.05 μM doses of vinblastine were significantly different from dexrazoxane alone with a probability 95% or higher. These three concentrations of vinblastine showed antagonism with dexrazoxane. In the range 10-500 μM, the slopes were not significantly different from dexrazoxane alone (Table 3.22). The data for 10-500 μM of dexrazoxane were normalised to the absorbance of wells without any drugs, representing 100% survival. The comparison of intercepts was conducted to evaluate their changes (Table 3.23). The intercepts of dexrazoxane with 0.005, 0.04, and 0.05 μM of vinblastine were not significantly different from that of dexrazoxane alone. Vinblastine showed cytotoxicity by itself, thus lack of increased effect of vinblastine-dexrazoxane combination can be interpreted as antagonism.

Table 3.21. Slope comparison of linear dose-response curves of dexrazoxane (1.0-10 μM) and dexrazoxane with fixed doses of vinblastine presented in Fig. 3.25.

Dexrazoxane 1.0-10 μM							
Parameters	Doses of Vinblastine, μM						
	0	0.005	0.01	0.02	0.03	0.04	0.05
$a \pm$ SEM	-0.059 ● 0.011	-0.132 ± 0.012	-0.152 ● 0.008	-0.190 ± 0.012	-0.202 ± 0.011	-0.219 ± 0.007	-0.448 ● 0.025
$b \pm$ SEM	-0.050 ± 0.017	-0.045 ● 0.019	-0.030 ± 0.013	0.002 ± 0.020	0.022 ● 0.017	0.042 ± 0.012	0.170 ● 0.040
Tb		-0.185	-0.902	-1.981	-2.978	-4.399	-4.998
Vb		4	4	4	4	4	4
P					< 0.05	< 0.05	< 0.01

Table 3.22. Slope comparison of linear dose-response curves of dexrazoxane (10-500 μM) and dexrazoxane with fixed doses of vinblastine presented in Fig. 3.25. All the slopes were not significantly different from dexrazoxane alone.

Dexrazoxane 10-500 μM							
Parameters	Doses of Vinblastine, μM						
	0	0.005	0.01	0.02	0.03	0.04	0.05
a ± SEM	-0.037 ± 0.023	-0.109 ● 0.0018	-0.112 ± 0.041	-0.126 ± 0.025	-0.091 ± 0.018	-0.096 ± 0.024	-0.188 ± 0.030
b ± SEM	-0.079 ± 0.012	-0.061 ± 0.009	-0.056 ± 0.021	-0.047 ± 0.013	-0.069 ± 0.010	-0.066 ± 0.013	-0.067 ± 0.016
Tb		-1.220	-0.970	-1.806	-0.654	-0.746	-0.627
Vb		8	8	8	8	8	8

Table 3.23. Intercept comparison of normalised linear dose-response curves of dexrazoxane (10-500 μM) and dexrazoxane with fixed doses of vinblastine.

Dexrazoxane 10-500 μM							
Parameters	Doses of Vinblastine, μM						
	0	0.005	0.01	0.02	0.03	0.04	0.05
a ● SEM	-0.020 ± 0.023	-0.031 ● 0.0018	-0.021 ● 0.041	-0.003 ± 0.025	0.022 ± 0.018	-0.010 ± 0.024	0.016 ± 0.030
Ta		2.045	-3.167	-3.069	-2.406	0.673	-1.662
Va		9	9	9	9	9	9
P			< 0.05	< 0.05	< 0.05		

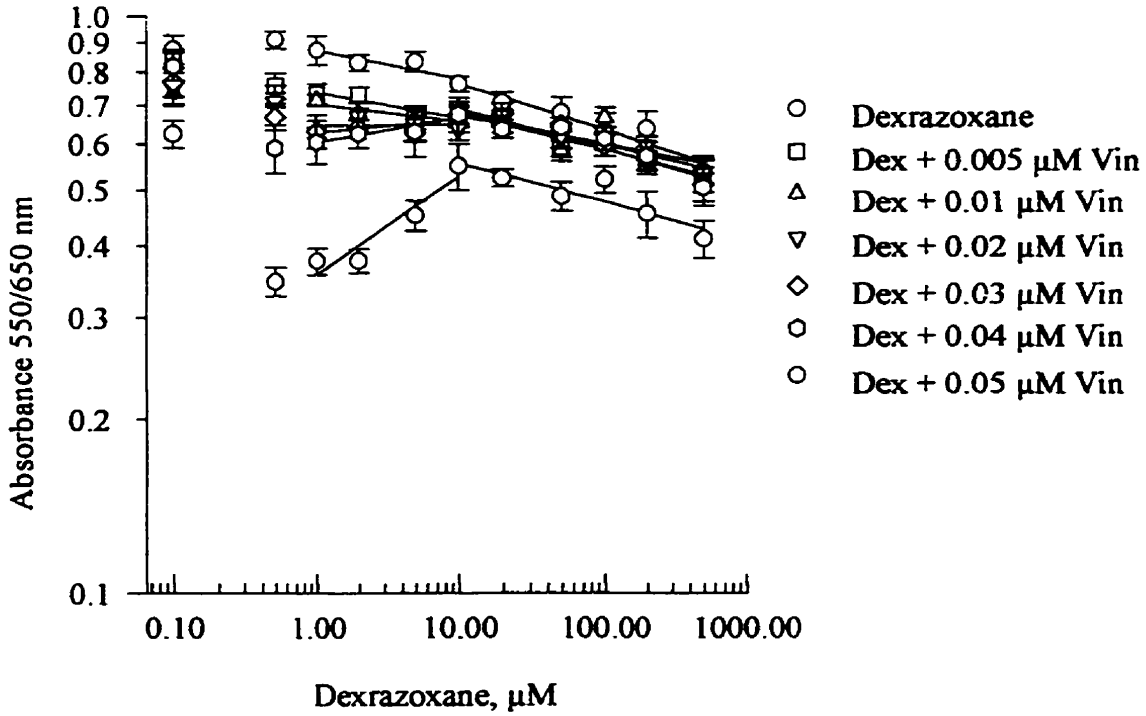

Fig. 3.25. Slope comparison experiment for the combination of dexrazoxane with vinblastine. The 48 h inhibitory effect of dexrazoxane alone and dexrazoxane with fixed doses of vinblastine on Chinese hamster ovary cells is presented in log-log scale. The points represent the means of absorbance ± SD from six replicates at each concentration. The lines represent the result of the fit of experimental data to linear equation The lowest concentrations correspond to control values with zero concentration of drugs. The second control value is an effect of vinblastine by itself (this control is for dexrazoxane with vinblastine dose-response curves).

The obtained slopes were plotted against the concentration of vinblastine in Fig. 3.26.

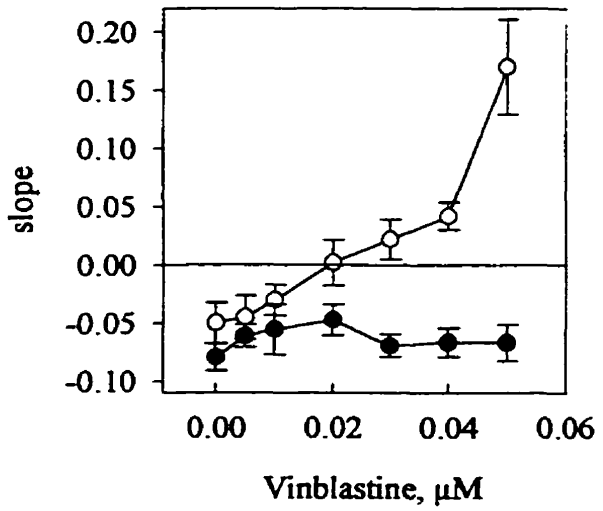

Fig. 3.26. Slopes obtained from the dexrazoxane-vinblastine slope method experiment. The slopes of linear dose-response curves are plotted against the concentration of vinblastine. The slopes of dexrazoxane in a range 1.0-10 μM (○) with 0.05, 0.04, 0.03 and 0.02 μM fixed doses of vinblastine are significantly different from the slope of dexrazoxane alone. The slopes of dexrazoxane in a range 10-500 μM (●) with all fixed doses of vinblastine are not significantly different from dexrazoxane alone.

3.3.5. Combined results from the combination index, envelope of additivity, response surface and slope comparison methods for the combination of dexrazoxane with mafosfamide and 5-fluorouracil

The results obtained from all evaluating methods are combined for dexrazoxane with mafosfamide in Table 3.24 and for dexrazoxane with 5-fluorouracil in Table 3.25.

Table 3.24. Combined effect of dexrazoxane and mafosfamide on Chinese hamster ovary cell growth evaluated with different methods for single experiments and their means.

	Dexrazoxane with Mafosfamide										
	Combination Index[a]						Envelope[b] for 50% effect		Response Surface[c]		Slope[d]
	α = 0			α = 1							
	Dex/Maf 0.683	Dex/Maf 5.0	Dex/Maf 0.2	Dex/Maf 0.683	Dex/Maf 5.0	Dex/Maf 0.2	Dex 1.5 μM	Dex 4.0 μM	CI	Env.	
Exp. 1	Ant[f]	Syn[g] (0.36)[e] Ant	Ant	Ant	Syn (0.30) Ant	Ant	Ad[h]	Syn	Ad	Ad	Ant
Exp. 2	Ant	Ant	Ant	Ant	Ant	Ant	Ant	Ant	Ad	Ant	
Exp. 3	Ant (0.60) Syn	Ant (0.51) Syn	Ant (0.54) Syn	Ant	Ant (0.61) Syn	Ant	Ad	Ad	Ant	Ad	
Exp. 4							Ad	Ad		Ad	
Mean	Ant	Ant	Ant	Ant	Ant	Ant	Ad	Ad	Ant	Ant	Ant

[a] This method was used to evaluate the effects of 72 h exposure of the cells to dexrazoxane and mafosfamide at three concentration ratios Dex/Maf = 0.683, 5.0 and 0.2; the equations (3.1) for α = 0 and 1 were used. The type of interaction was evaluated for three single experiments (Exp. 1, Exp. 2 and Exp. 3) and as their mean (Mean)

[b] 72 h exposure to the drugs with 20 min preincubation to 1.5 and 4.0 μM concentrations of dexrazoxane (Dex)

[c] Response surface method was used with combination index (CI) and envelope of additivity (Env.) experimental data

[d] 48 h exposure of cells to the drugs with 1 h preincubation with dexrazoxane (0.5-500 μM)
[e] The value of fraction affected from the range 0.03-0.65, where $CI \approx 1.0$
[f] Antagonism
[g] Synergy
[h] Additivity

Table 3.25. Combined effect of dexrazoxane and 5-fluorouracil on Chinese hamster ovary cell growth evaluated with different methods for single experiments and their means.

	Dexrazoxane with 5-Fluorouracil										
	Combination Index[a]				Envelope[b] 50 % effect				Response Surface[c]		Slope[d]
	α = 0		α = 1								
	Dex/Fu 2.0	Dex/Fu 0.2	Dex/Fu 2.0	Dex/Fu 0.2	Dex 1.5 μM	Dex 2.0 μM	Dex 2.5μM	Dex 4.0 μM	CI	Env.	
Exp. 1	Ant[f] (0.45)[e] Syn[g]	Ant (0.57) Syn	Ant	Ant	Ant	Ant	Ant	Ant	Ant	Ad[h]	Ant
Exp. 2					Ant	Ant	Ant	Ant		Ant	
Exp. 3					Ant	Ant	Ant	Ant		Ant	
Mean	Ant (0.45) Syn	Ant (0.57) Syn	Ant	Ant	Ant	Ant	Ant	Ant	Ant	Ant	Ant

[a] This method was used to evaluate the effects of 72 h exposure of the cells to dexrazoxane and 5-fluorouracil at three concentration ratios Dex/Maf = 0.7, 5.0 and 0.2; the equations (3.1) with $\alpha = 0$ and 1 were used. The type of interaction was evaluated for three single experiments (Exp. 1, Exp. 2 and Exp. 3) and for their mean (Mean)
[b] 72 h exposure to the drugs with 20 min preincubation to 1.5, 2.0, 2.5 and 4.0 μM concentrations of dexrazoxane (Dex)
[c] Response surface method was used for combination index (CI) and envelope of additivity (Env.) experimental data
[d] 48 h exposure of cells to the drugs with 1 h preincubation with dexrazoxane (0.5-500 μM)
[e] The value of fraction affected from the range 0.03-0.63, where $CI \approx 1.0$
[f] Antagonism
[g] Synergy
[h] Additivity

3.4. Conclusions

The mean combination index values from the three Experiments have shown that the combined action of dexrazoxane and mafosfamide was antagonistic (Tables 3.11 and 3.24). The equations for mutually exclusive and mutually nonexclusive drugs gave the same results. The combined drug effect in single experiments was not always consistent with the means. Experiment 1 showed synergy for ratio 5.0 up to $f_a = 0.36$ for $\alpha = 0$ and up to $f_a = 0.30$ for $\alpha = 1$. In Experiment 3, synergy was shown for all three ratios of dexrazoxane to mafosfamide for higher f_a values ($f_a > 0.5$) when the equation with $\alpha = 0$ was used. When $\alpha = 1$, synergy was evaluated for ratio 5.0 above $f_a = 0.61$. Only Experiment 2 showed antagonism for each ratio with both equations.

The mean envelope of additivity constructed from the four single Experiments showed that mafosfamide and dexrazoxane do not interact with each other (Tables 3.13, 3.24 and Fig. 3.14). The single Experiments 3 and 4 (Tables 3.13 and 3.24) indicated additivity for mafosfamide with dexrazoxane concentrations 1.5 and 4.0 μM. Experiment 1 showed additivity and synergy for 1.5 μM and for 4.0 μM doses of dexrazoxane, respectively. Experiment 2 showed antagonism for both dexrazoxane concentrations. Additive effects evaluated by the envelope of additivity method is in agreement with clinical findings that dexrazoxane does not reduce the anticancer activity of cyclophosphamide, 5-fluorouracil and doxorubicin used in multi-drug therapy [17].

The mean effect of dexrazoxane combined with mafosfamide evaluated by the response surface method (Tables 3.15 and 3.24) for three combination index experimental data sets was antagonistic ($\alpha' = -0.281 \pm 0.058$). This result is in agreement with the mean

result of the combination index method (Tables 3.11 and 3.24). Although, the response surface method used with single Experiments gave additivity for Experiments 1 and 2 with α' = -0.243 ● 0.248 and -0.205 ± 0.244, respectively. Whereas Experiment 3 showed antagonism with α' = -0.395 ± 0.135. The mean interaction parameter of the response surface method used with the envelope of additivity data also showed antagonism with α' = -0.244 ● 0.136 (Tables 3.16 and 3.24). This method used with single Experiments showed additivity for Experiments 1, 3 and 4 with α' = 0.004 ± 0.228; -0.022 ± 0.330 and -0.483 ± 0.608, respectively. Experiment 2 showed antagonism with α = -0.474 ± 0.134. The same data evaluated with the envelope of additivity method showed additivity as a mean from all four Experiments (Tables 3.13, 3.24 and Fig. 3.14).

The slope method (Tables 3.19, 3.24 and Figs. 3.23, 3.24) showed antagonism between dexrazoxane and mafosfamide for all mafosfamide doses used. The highest antagonistic effect was seen for 40 μM of mafosfamide.

The mean results from the combination index, response surface and slope methods showed antagonism between dexrazoxane and mafosfamide; whereas, the envelope of additivity implicated additive effect. The combination index was calculated for a wide range of f_a (0.03-0.65) and three ratios of the drugs. The values of the combination index calculated with α = 0 and 1 were much higher than 1.0 for low values of f_a and approached 1.0 for higher f_a. The antagonistic effect at f_a = 0.5 calculated with the equation for α = 0 was small with combination index values of 1.19 ± 0.08, 1.05 ± 0.07 and 1.22 ± 0.10 for dexrazoxane to mafosfamide ratios of 0.683, 5.0 and 0.2, respectively. The combination index calculated with the equation with α = 1 for f_a = 0.5 was 1.52 ±

0.12, 1.22 ± 0.10 and 1.42 ± 0.12 for the corresponding 0.683, 5.0 and 0.2 ratios of the drugs. The envelope of additivity was calculated for 50% effect. Only two concentrations of dexrazoxane were tested for interaction with mafosfamide. The points of 50% combined effect of dexrazoxane and mafosfamide fell inside the envelope of additivity (Fig. 3.14); although, the standard error values showed that a small degree of antagonistic interaction was possible (standard errors of mafosfamide mean concentrations crossed the right boundary of the envelope). These results are closer to those obtained by the combination index method with $\alpha = 0$. The response surface method evaluates interaction of the drugs with single value of interaction index, α'. The values for mafosfamide and dexrazoxane were small (for the combination index experimental data $\alpha' = -0.281 \bullet 0.058$ and for the envelope of additivity $\alpha' = -0.244 \pm 0.136$); thus, the antagonistic effect was small. The slope method tested the 48 h inhibitory effect of a wide range of dexrazoxane concentrations with eight fixed doses of mafosfamide. In this experiment, cells were preincubated 1 h with dexrazoxane. In the combination index experiment, the drugs were added simultaneously, and, in the envelope of additivity experiment, there was only a 20 min gap between drug deliveries. The 40 μM fixed dose of mafosfamide changed the slope of dexrazoxane from -0.073 ± 0.012 to 0.071 ± 0.019. The effect of inhibition was changed to stimulation of cell growth. In conclusion, the effect of the combined action of mafosfamide and dexrazoxane on the growth of Chinese hamster ovary cells, evaluated with the combination index, envelope of additivity, response surface and slope comparison methods, was from very small antagonistic to additive.

Dexrazoxane and 5-fluorouracil showed antagonism with most methods of analysis used in this study, except the combination index method (Table 3.25). When the combination index (Table 3.12) was calculated with the equation for mutually exclusive drugs, the combination index was higher than one for the ratio 2.0, up to $f_a = 0.45$. Above $f_a = 0.45$, the effect was slightly synergistic (the lowest value of combination index was 0.85). For the ratio 0.2, the effect of dexrazoxane and 5-fluorouracil was antagonistic up to $f_a = 0.57$. Above $f_a = 0.57$, the effect was slightly synergistic (the lowest value of combination index was 0.97). When the combination index was calculated with the equation for mutually nonexclusive drugs, the effect for both ratios of dexrazoxane to 5-fluorouracil was antagonistic. Only one Experiment was performed for the combination index method; thus, the statistical evaluation of the result could not be performed.

The 50% envelope of additivity constructed from the results of four Experiments (Tables 3.14, 3.25 and Fig. 3.16) showed antagonism for each concentration of dexrazoxane used. Based on the position of the points on the envelope of additivity (Fig. 3.16), the antagonistic effect of the drugs was strong. The same effect was obtained for each single Experiment. The combination index values for $f_a = 0.5$ were 0.96 and 1.06 for $\alpha = 0$ and 1.17 and 1.22 for $\alpha = 1$, for 2.0 and 0.2 ratios of dexrazoxane to 5-fluorouracil respectively. Based on these values, the antagonistic effect ($CI > 1$) was small. The 20 min time gap between dexrazoxane and 5-fluorouracil delivery to the cells might have contributed to the strong antagonistic effect evaluated by the envelope of additivity method.

The response surface method (Tables 3.17 and 3.25) used with combination index experimental data showed small antagonism ($\alpha' = -0.306 \pm 0.262$). The same Experiment evaluated with the combination index method showed antagonism and synergy dependent on f_a with $\alpha = 0$ and antagonism with $\alpha = 1$ (Tables 3.12 and 3.25). The mean value of the interaction index determined by the response surface method for the envelope of additivity data also showed antagonism ($\alpha' = -0.429 \pm 0.138$). The mean result was not consistent with the results of the single Experiment data fitting. Experiment 1 (Tables 3.18 and 3.25) showed additivity ($\alpha' = -0.156 \pm 0.167$) whereas Experiments 2 and 3 showed antagonism ($\alpha' = -0.533 \pm 0.245$ and -0.599 ± 0.214, respectively). The same data with the envelope of additivity method showed antagonism for all Experiments.

The results of 48 h inhibition of cell growth by dexrazoxane and 5-fluorouracil evaluated with the slope comparison method showed antagonism (Tables 3.20, 3.25 and Figs. 3.23, 3.24). The value of the slope changed from -0.062 for dexrazoxane alone to -0.006 for dexrazoxane with 5000 μM of 5-fluorouracil. The effect of drug combination was still inhibitory but the inhibition was smaller than for dexrazoxane alone.

The mean values from the combination index, envelope of additivity, response surface and slope comparison methods show the inhibitory effect of dexrazoxane and 5-fluorouracil on Chinese hamster ovary cell growth was antagonistic. This result was also obtained with most single Experiments. This finding is not in agreement with the clinical study of Koning, previously mentioned [17]. The interaction of dexrazoxane with 5-fluorouracil has not been studied on cells. In the study by Kano [18], the bisdioxopiperazine, ICRF-154 was used with 5-fluorouracil. The results of 72 h

cytotoxicity Experiments were analysed by the 50% envelope of additivity method. ICRF-154 and 5-fluorouracil showed an additive effect on all cell lines used (MOLT-3, HSB-2, BALL-2 and K-562).

The combined effect of vinblastine and dexrazoxane was studied with the slope comparison method (Figs. 3.25, 3.26 and Tables 3.21, 3.22, 3.23). Combined drugs showed antagonism up to 10 μM of dexrazoxane with 0.03, 0.4 and 0.05 μM of vinblastine (Table 3.21). The slope of dexrazoxane was significantly different from the slopes of dexrazoxane with fixed doses of vinblastine. The slopes from 10-500 μM of dexrazoxane with vinblastine (Table 3.22) were not significantly different from dexrazoxane alone. Furthermore, the intercepts for normalised data, were not significantly different for 0.005, 0.04 and 0.05 μM of vinblastine compared to dexrazoxane alone (Table 3.23). The lack of vinblastine effect above 10 μM of dexrazoxane suggest that dexrazoxane completely blocked the binding sites for vinblastine. The combined effect of dexrazoxane in a range 10-500 μM with 0.005, 0.04 and 0.05 μM of vinblastine was antagonistic.

In summary, the inhibitory effect of mafosfamide and dexrazoxane on Chinese hamster ovary cell growth was slightly antagonistic or additive. The effect of 5-fluorouracil and dexrazoxane was antagonistic. The effect of vinblastine and dexrazoxane was antagonistic up to 10 μM of dexrazoxane and additive for the 10-500 μM range of dexrazoxane concentration, as shown in the 48 h Experiment.

References

1. Speyer JL, Green MD, Zeleniuch-Jacquotte A, Wernz JC, Rey M, Sanger J, Kramer E, Ferrans V, Hochster H, Meyers M, Blum RH, Feit F, Attubato M,

Burrows W and Muggia FM, ICRF-187 permits longer treatment with doxorubicin in women with breast cancer. *J Clin Oncol* **10:** 117-127, 1992.

2. *Compendium of Pharmaceuticals and Specialties. 32nd ed.* Canadian Pharmaceutical Association, Ottawa, Ontario, Canada, 1997:1798; 1032 p.

3. Roth BJ, Sledge GW, Williams SD, Meyer SC, Ansari R and Fisher WB, Methotrexate, vinblastine, doxorubicin, and cisplatin in metastatic breast cancer. *Cancer* **68:** 248-252, 1991.

4. Hudis C, Seidman A, Raptis G, Fennelly D, Gilewski T, Baselga J, Theodoulou M, Sklarin N, Moynahan M, Surbone A, Currie V, Lebwohl D, Uhlenhopp M, Crown J and Norton L, Sequential adjuvant therapy: the Memorial Sloan-Kettering Cancer Center Experience. *Semin Oncol* **23:** 58-64, 1996.

5. Pommier Y, DNA topoisomerase II inhibitors. In: *Cancer Therapeutics: Experimental and Clinical Agents.* (Ed. Teicher B), pp. 153-174. Humana Press Inc., Totowa, NJ, 1997.

6. Struck RF, Agents that react wiht DNA. In: *Cancer Chemotherapeutic Agents.* (Ed. Foye O), pp. 112-120. American Chemical Society, Washingron, DC, 1995.

7. Remers WA, Antineoplastic Agents. In: *Wilson and Gisvold's Textbook of Organic Medicinal and Pharmaceutical Chemistry.* (Eds. Delgado JN and Remers WA), 9th ed.,, 1991.

8. Mini E and Bertino JR, Biochemical modulation of 5-fluorouracil by metabolites and antimetabolites. In: *Synergism and Antagonism in Chemotherapy.* (Eds. Chou T-C and Rideout DC), pp. 449-488. Academic Press, Inc., San Diego, California, 1991.

9. Anathan S, Antimetabolites. In: *Cancer Chemotherpeutic Agents.* (Ed. Foye O), pp. 49-56. American Chemical Society, Washington, DC, 1995.

10. Lu MC, Antimitotic agents. In: *Cancer Chemotherapeutic Agents.* (Ed. Foye WO), pp. 345-368. American Chemical Society, Washington, DC, 1995.

11. Pohl J. Mafosfamide information sheet. ASTA Medica AG, P.O. Box 100105, D-80001 Frankfurt am Main, Germany.

12. *Drug Information for the Health Care Professional. 9th ed.* The United States Pharmacopeial Convention, Inc., Harrisonburg, Virginia, USA, 1989.

13. Chou T-C and Talalay P, Applications of the Median-Effect Principle for the Assessment of Low-Dose Risk of Carcinogens and for the Quantitation of Synergism and Antagonism of Chemotherapeutic Agents. In: *New Avenues in Developmental Cancer Chemotherapy.* (Eds. Harrap KR and Connors A), pp. 37-64. Academic Press, Orlando, FL, 1987.

14. Steel GG, Exploitable mechanisms in combined radiotherapy-chemotherapy: The concept of additivity. *Int J Radiat Oncol* **5:** 85-91, 1979.

15. Greco WR, Park HS and Rustum YM, Application of a new approach for the quantitation of drug synergism to the combination of cis-diamminedichloroplatinum and 1-b-D-arabinofuranosylcytosine. *Cancer Res* **50:** 5318-5327, 1990.

16. Thisted RA. *Elements of statistical computing.* Chapman and Hall, New York, NY, 1988:427; 427 p.

17. Koning J, Palmer P, Franks CR, Mulder DE, Speyer JL, Green MD and Hellmann K, Cardioxane-ICRF-187, towards anticancer drug specificity through selective toxicity reduction. *Cancer Treat Rev* **18:** 1-19, 1991.

18. Kano Y, Narita T, Suzuki K, Akutsu M, Suda K, Sakamoto S and Miura Y, The effects of ICRF-154 in combination with other anticancer agents in vitro. *Br J Cancer* **66:** 281-286, 1992.

4. Inhibitory effect of dexrazoxane in the combination with doxorubicin, daunorubicin and mitoxantrone on Chinese hamster ovary cell growth

4.1. Introduction

Doxorubicin, daunorubicin and mitoxantrone are anticancer drugs with a cardiotoxic side effect [1]. Dexrazoxane is an agent with protective properties against doxorubicin cardiotoxicity [2]. Dexrazoxane also has anticancer activity through catalytic inhibition of topoisomerase II (compare Chapter II) [3]. These studies were designed to determine the combined cytotoxic effect of dexrazoxane with doxorubicin, daunorubicin and mitoxantrone on Chinese hamster ovary cells. Comparisons of linear dose-response curve slopes and the response surface method were used to evaluate the results.

4.1.1. Anti-tumour activity and cardiotoxicity of doxorubicin, daunorubicin and mitoxantrone

Doxorubicin and daunorubicin are anthracycline antibiotics isolated from a *Streptomyces* species [4]. They contain an anthraquinone ring system, with an attached amino sugar (Fig. 4.1).

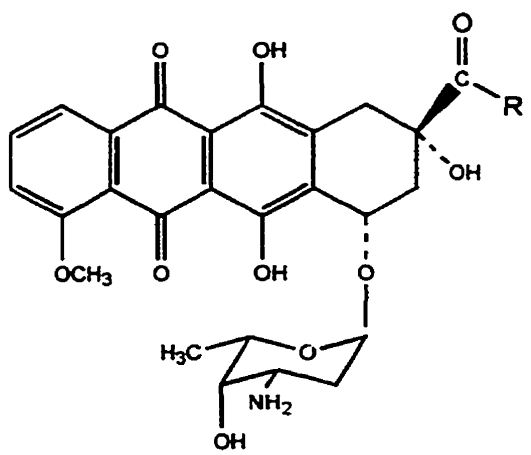

Fig. 4.1. Structure of doxorubicin (R = CH_2OH) and daunorubicin (R = CH_3).

The anthraquinone, mitoxantrone, is a synthetic chemotherapeutic agent. Like the anthracyclines, mitoxantrone has a hydroxyquinone function on its ring structure (Fig. 4.2).

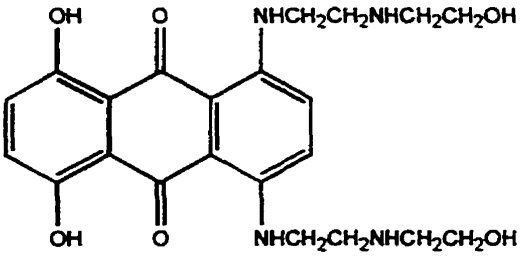

Fig. 4.2. Structure of mitoxantrone.

One of the proposed mechanisms for the cytotoxicity of doxorubicin, daunorubicin and mitoxantrone is an interaction with topoisomerase II [5, 6]. It has been proposed that these drugs form ternary complexes with topoisomerase II and DNA, thus disturbing mitotic activity, cell growth and proliferation. Another hypothesis links the anthracyclines' anticancer activity to free radical formation. It has been demonstrated that anthracyclines are able to undergo one- or two-electron reduction promoted by enzymes such as cytochrome P450 reductase, xanthine oxidase, and cytochrome B5 reductase [7]. The reduced drugs may reduce molecular oxygen to a reactive species, such as superoxide ions, hydrogen peroxides and hydroxyl radicals. Certain tumour cell lines are sensitive to anthracycline-induced free radicals [8, 9]. Free radicals produced by the reduction of anthracyclines cause lipid peroxidation and cell membrane lesions. Since the cardiac muscle has low levels of enzymes which protect it against free radical damage,

anthracycline therapy causes cardiomyopathy. The most damaging free radical species is hydroxyl radical. It has been reported that 550 to 600 mg/m^2 cumulative doses of doxorubicin caused congestive heart failure [10]. Doxorubicin has stimulated superoxide formation in cardiac mitochondria [11]. Doxorubicin and daunorubicin induced NADPH-dependent mouse heart microsomal lipid peroxidation with their strongest effect at 100-200 μM. Some reactive oxygen scavengers and EDTA diminished lipid peroxidation [12]. Doxorubicin, daunorubicin and mitoxantrone form complexes with Fe(III). Iron complexes of doxorubicin, daunorubicin and mitoxantrone mediate the production of strong oxidants, such as hydroxyl radicals, in the presence of xanthine oxidase, although mitoxantrone does so to a lesser extent. Under aerobic conditions, iron catalyses the free radical formation of doxorubicin, but not daunorubicin or mitoxantrone [13, 14]. Dexrazoxane allows for longer treatments and higher cumulative doses of doxorubicin to be used. Patients with cardiac risk were able to receive anthracycline therapy when dexrazoxane was used [15]. It has been shown that dexrazoxane lowers the cardiotoxic effect of anthracyclines in animals [16]. Dexrazoxane reduced the cardiotoxicity of mitoxantrone, and to a lesser extent, doxorubicin, on isolated neonatal rat heart myocytes [17]. In a study on mice, dexrazoxane was cardioprotective to doxorubicin damage but not mitoxantrone [18]. In an experiment on adult rat heart myocytes loaded with iron, dexrazoxane was capable of chelating and transporting the iron out of the cells. The iron-loaded cells were sensitive to the toxic effect of doxorubicin [19]. The hydrolysis products of dexrazoxane removed iron from iron-anthracycline complexes [20], thereby reducing

free radical production by anthracyclines. This is likely the mechanism of dexrazoxane cardioprotection [19].

4.1.2. Bisdioxopiperazines in combination with doxorubicin, daunorubicin and mitoxantrone *in vitro*

Dexrazoxane has cardioprotective and limited anticancer activities [21]. The anticancer activity of dexrazoxane is probably due to the catalytic inhibition of topoisomerase II [6]. Since dexrazoxane, doxorubicin, daunorubicin and mitoxantrone exert their anticancer activity through interaction with topoisomerase II, it is likely that when used together they compete for a common target. A previous study [22] has shown that preincubation of Chinese hamster ovary cells with dexrazoxane antagonised the cytotoxicity of doxorubicin and daunorubicin. Dexrazoxane inhibition of DNA single strand break formation and induction of DNA cross links by doxorubicin and daunorubicin has been shown by the alkaline elution technique [23]. In the same study, dexrazoxane was used in non-toxic doses simultaneously with daunorubicin on OC-NYH cells in a clonogenic assay. Although the effect of 1 h incubation of the two drugs was antagonistic, when dexrazoxane was incubated for two hours on OCI/AML-3 and NB-4 cell lines it did not change the sensitivity of the cells to doxorubicin [24]. The antitumor activity of mitoxantrone was not altered by dexrazoxane in human tumour cells [17]. The bisdioxopiperazines ICRF-159, and ICRF-186, antagonised daunorubicin against HeLa cell growth when a clonogenic assay was used; doxorubicin was not affected [25]. The interaction between ICRF-154 and doxorubicin over 72 h was studied on MOLT-3, HSB and B-ALL cell lines [26]. A synergistic (supra-additive) effect was observed for these cell

lines. The same study on the K-562 cell line showed additivity of the effect of dexrazoxane and doxorubicin. When mitoxantrone was studied with ICRF-193, the effect of these drugs on rat neurons was antagonistic when added simultaneously. This effect has not been observed when ICRF-193 was added two hours later [27].

4.2. Materials and methods

Chinese hamster ovary cells were used to study the influence of drug combinations on cell growth. The cells were seeded at 2000 cells in 100 μL of cell culture medium on 96-well plates and allowed to attach for 24 h. After this period of time, the drugs were delivered, the volume of cell culture medium was increased to 200 μL/well, and the cells were incubated for another 48 h. The MTT assay was used to quantify the effects of cell exposure to the drugs. A detailed description of the cytotoxicity experiments and the MTT assay is given in Chapter II, Section 2.2.3. The interactions of dexrazoxane with doxorubicin, daunorubicin and mitoxantrone were studied with the response surface and slope comparison methods described in Chapter III, Section 3.2.4.3 and 3.2.4.4, respectively.

4.2.1. Materials

Dexrazoxane (ICRF-187) was a gift from Pharmacia & Upjohn (Columbus, OH). Doxorubicin hydrochloride was a gift from Adria-SP Inc. (Columbus, OH). Daunorubicin hydrochloride was a gift from Rhone-Poulenc Pharma (Montreal, Canada). Mitoxantrone dihydrochloride was obtained from Lederle Laboratories Division, American Cyanamid Company (Pearl River, New York).

4.2.2 Solubility of dexrazoxane, doxorubicin, daunorubicin and mitoxantrone

Dexrazoxane was dissolved in cell culture medium. Doxorubicin hydrochloride (M_w = 579.99 g/mol), daunorubicin hydrochloride (M_w = 563.99 g/mol) and mitoxantrone dihydrochloride (M_w = 516.9 g/mol) were dissolved in 0.9% (w/v) aqueous NaCl.

4.2.3. Design of experiments for the combination of dexrazoxane with doxorubicin, daunorubicin and mitoxantrone

4.2.3.1. Design of the response surface experiments for the combination of dexrazoxane with doxorubicin, daunorubicin and mitoxantrone

The results of 48 h continuous exposure of Chinese hamster ovary cells to combinations of dexrazoxane with doxorubicin, daunorubicin and mitoxantrone were analysed by the response surface method [28]. The concentrations of doxorubicin, daunorubicin and mitoxantrone ranged between 0.05 and 50 μM. The dose-response curves for the single drugs and for doxorubicin, daunorubicin and mitoxantrone with fixed doses of dexrazoxane were prepared. The fixed doses of dexrazoxane used for the doxorubicin experiment were 5, 20, 50 and 100 μM. The fixed doses of dexrazoxane used with daunorubicin and mitoxantrone were 5, 20, 50, 100, 200 μM. A dose-response curve for dexrazoxane in an experiment with doxorubicin was also prepared. The dexrazoxane concentration range was 0.05-50 μM. The dose-response curves of dexrazoxane in the experiment with daunorubicin and mitoxantrone were not prepared. Dexrazoxane, as a single agent, was included as control of the daunorubicin or mitoxantrone dose-response curves with fixed doses of dexrazoxane. For all experiments, dexrazoxane was added 20 min before the second drug. Dexrazoxane was dissolved in cell culture medium.

Doxorubicin, daunorubicin and mitoxantrone were dissolved in 0.9% (w/v) aqueous solution of NaCl and stock solutions were added to the wells in volumes of 2.0 - 11.0 μL. The absorbance for the doxorubicin and daunorubicin experiments was measured at 490 nm, with the reference at 650 nm. The absorbance of mitoxantrone experiments was measured at 490 nm without a reference wavelength because mitoxantrone absorbs at 650 nm. In the wells with a high concentration of mitoxantrone (50 μM), some residue of the drug was visibly present before DMSO was added for the MTT assay.

4.2.3.2. Design of the slope comparison experiment for the combination of dexrazoxane with doxorubicin, daunorubicin and mitoxantrone

The highest effect of dexrazoxane obtained in the 48 h cytotoxicity experiment was 20% cell kill at 500 μM. The relationship between the logarithms of the absorbance and the corresponding concentration was linear. This observation was used to design the slope comparison experiments. Seven dose-response curves were prepared for a comparison of slopes. One dose-response curve was prepared for dexrazoxane alone and six for dexrazoxane in a wide concentration range with fixed doses of doxorubicin, daunorubicin or mitoxantrone. Fixed doses of doxorubicin, daunorubicin and mitoxantrone were chosen to start the combined drug dose-response curves at different effect levels. The cells were allowed to attached for 24 h. Dexrazoxane, dissolved in cell culture medium, was added 1 h before the second drug was delivered. Doxorubicin, daunorubicin and mitoxantrone were dissolved in 0.9% (w/v) NaCl and added to the wells in 10 μL volumes as individual stock solutions. The 48 h inhibitory effects of drugs were measured by the MTT. The

absorbances for all drugs were measured at 550 nm wavelength, with a 650 nm reference line (the highest concentration of mitoxantrone used was 20 μM).

4.2.4. Data analysis with the response surface and slope comparison methods

The results of experiments for the dexrazoxane, combined with each of doxorubicin, daunorubicin and mitoxantrone, were evaluated with the response surface method described in Chapter III, Section 3.2.4.3. A modified Greco equation (4.1) was used to fit the data. The parameter B was not applied to the first term of the equation to obtain a better fit. Equation (4.1) is given for the specific combination of doxorubicin and dexrazoxane and was also used for other drugs.

$$\frac{d_{Dox}}{IC_{50,Dox}\left(\frac{E}{E_{max}-E}\right)^{1/m_{Dox}}}+\frac{d_{Dex}}{IC_{50,Dex}\left(\frac{E-B}{E_{max}-E+B}\right)^{1/m_{Dex}}}+\frac{a'\cdot d_{Dox}\cdot d_{Dex}}{IC_{50,Dex}\cdot IC_{50,Dox}\left(\frac{E-B}{E_{max}-E+B}\right)^{\left(1/m_{Dex}+1/m_{Dox}\right)}}=1 \qquad (4.1)$$

The slope comparison method was used as described in Chapter III, Section 3.2.4.4. The slopes were considered different when the value of $P < 0.05$.

4.3. Results

4.3.1. Results for the combination of dexrazoxane with doxorubicin, daunorubicin and mitoxantrone with the response surface method

The results of cell growth inhibition by doxorubicin (Dox), daunorubicin (Dnr) and mitoxantrone (Mit) in combination with fixed doses of dexrazoxane are presented in Fig. 4.3 (a), (b) and (c).

(a)

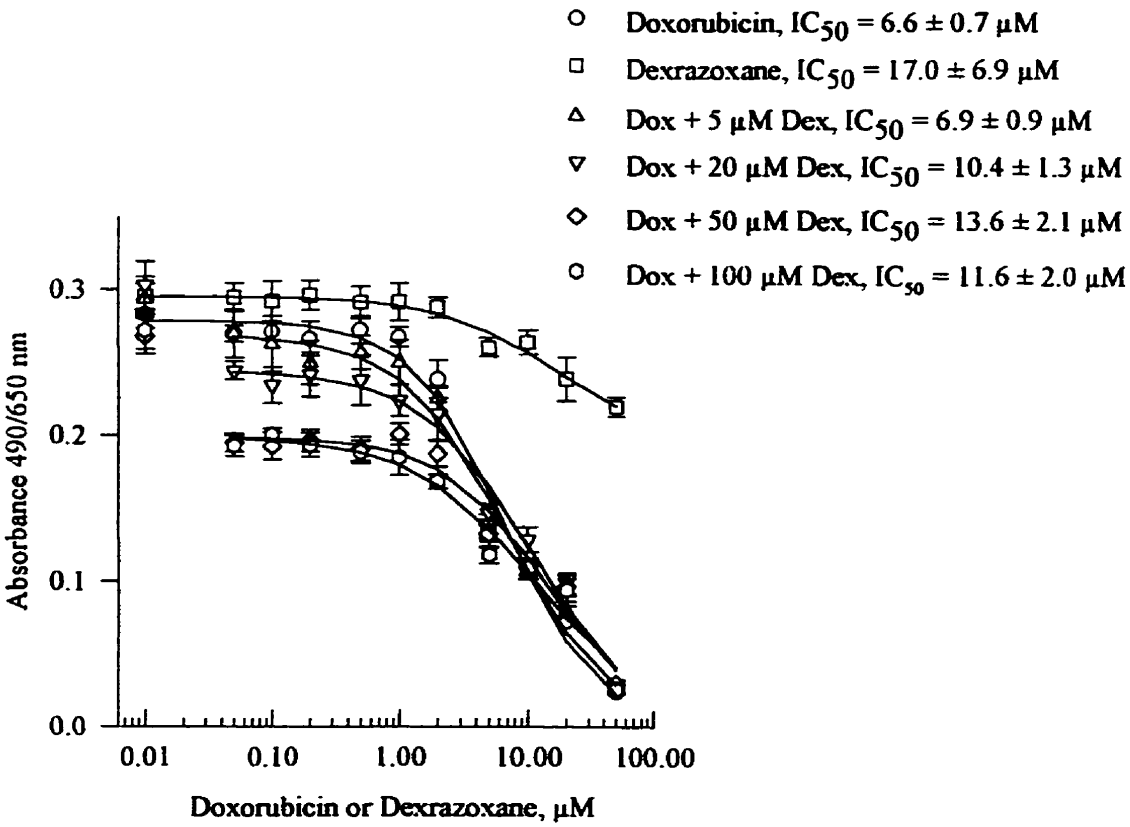
Doxorubicin, IC50 = 6.6 ± 0.7 μM
Dexrazoxane, IC50 = 17.0 ± 6.9 μM
Dox + 5 μM Dex, IC50 = 6.9 ± 0.9 μM
Dox + 20 μM Dex, IC50 = 10.4 ± 1.3 μM
Dox + 50 μM Dex, IC50 = 13.6 ± 2.1 μM
Dox + 100 μM Dex, IC50 = 11.6 ± 2.0 μM
Absorbance 490/650 nm
0.0
0.1
0.2
0.3
0.01
0.10
1.00
10.00
100.00
Doxorubicin or Dexrazoxane, μM

(b)

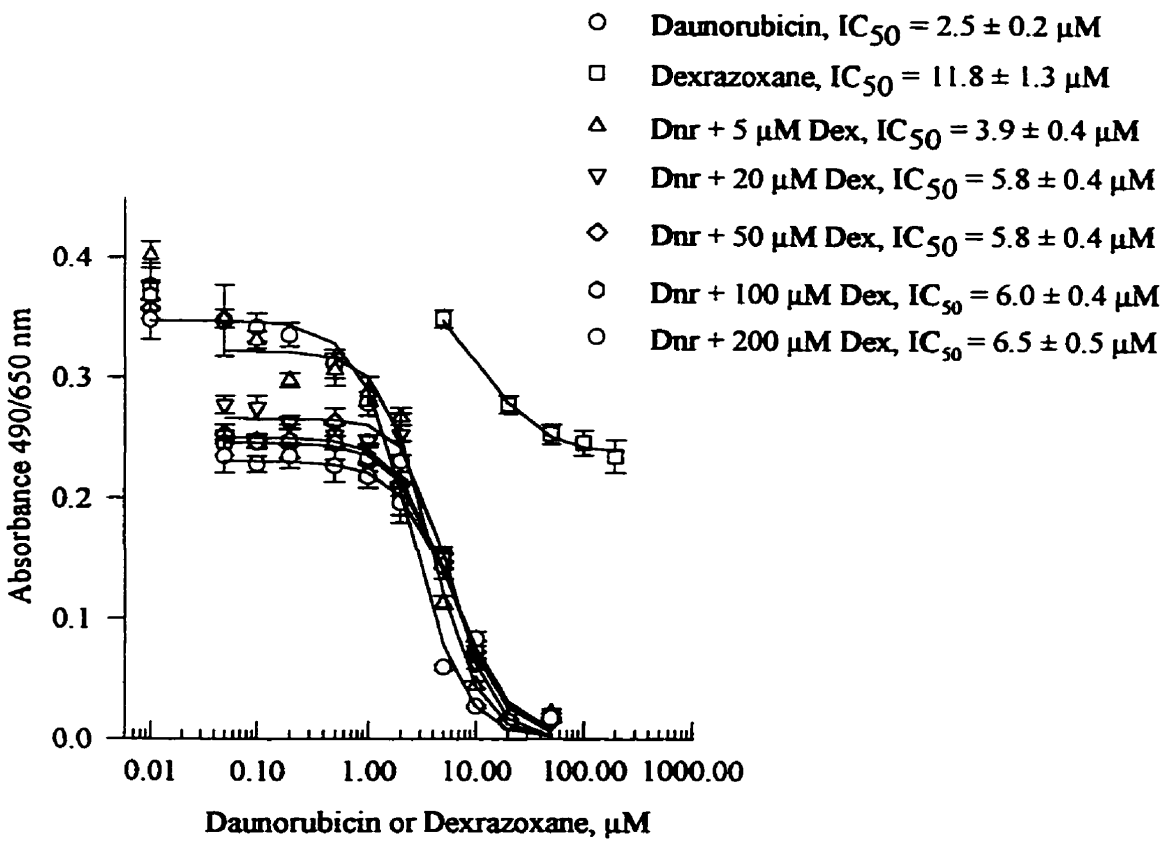
Daunorubicin, IC_{50} = 2.5 ± 0.2 μM
Dexrazoxane, IC_{50} = 11.8 ± 1.3 μM
Dnr + 5 μM Dex, IC_{50} = 3.9 ± 0.4 μM
Dnr + 20 μM Dex, IC_{50} = 5.8 ± 0.4 μM
Dnr + 50 μM Dex, IC_{50} = 5.8 ± 0.4 μM
Dnr + 100 μM Dex, IC_{50} = 6.0 ± 0.4 μM
Dnr + 200 μM Dex, IC_{50} = 6.5 ± 0.5 μM
Absorbance 490/650 nm
0.0
0.1
0.2
0.3
0.4
0.01
0.10
1.00
10.00
100.00
1000.00
Daunorubicin or Dexrazoxane, μM

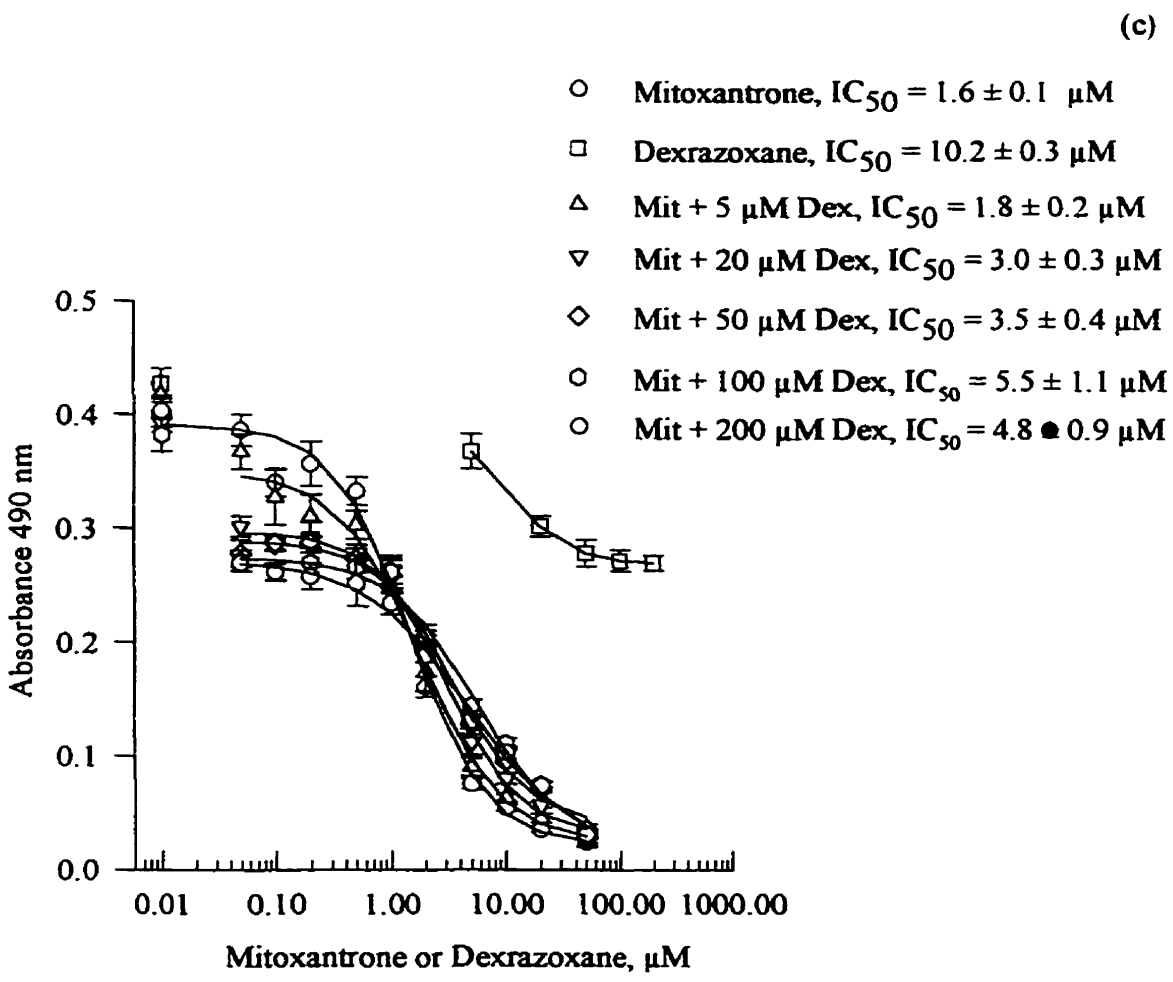

Fig. 4.3. Response surface experiment for the combination of dexrazoxane with doxorubicin (a), daunorubicin (b) and mitoxantrone (c). Chinese hamster ovary cells were incubated with the drugs for 48 h. The symbols represent the mean absorbance ± SD from six replicates at each concentration. The lines represent the non-linear least square fit of experimental data to three- or four-parameter logistic equations. The lowest concentration values correspond to zero concentration of drug (control values). The second-lowest values for dose-response curves with fixed concentrations of dexrazoxane are the values with dexrazoxane as a single drug. These values were also used to plot dexrazoxane dose-response curves for the (b) daunorubicin and (c) mitoxantrone experiments. For (a) doxorubicin experiment, dexrazoxane dose-response curve was prepared separately.

The data from the Experiments in Fig. 4.3 were divided by the values from the wells without drugs; thus, the control values were always 1.0. Each curve contained one

blank value. The normalised results were fitted to equation (4.1). The best fit parameters obtained (Table 4.1) were then used to calculate the theoretical dose-response curves using the bisection root finder method [29] described in Chapter III, Section 3.2.4.3. The theoretical calculated dose-response curves and normalised experimental results are plotted together in Fig. 4.4.(a), (b) and (c). The doxorubicin and daunorubicin experimental data showed good agreement with the theoretical data (Fig. 4.4.(a) and (b)). The fit for mitoxantrone was less satisfactory (Fig. 4.4.(c)).

Table 4.1. Best fit parameter estimates ± SEM obtained from fitting doxorubicin, daunorubicin and mitoxantrone with dexrazoxane experimental data to equation (4.1).[a]

Experiment	α' ± SEM	IC_{50} ± SEM μM	$IC_{50,Dex}$ ± SEM μM	m ± SEM	m_{Dex} ± SEM	E_{max} ± SEM	B ± SEM
Dox	-1.423 ± 0.870	6.711 ± 1.302	350 ± 81.6	-1.105 ● 0.126	-0.545 ± 0.070	1.021 ± 0.040	$5 \cdot 10^{-11}$ ± 0.040
Dnr	-2.171 ± 1.171	3.220 ± 0.300	1007 ± 410	-1.153 ± 0.055	-0.394 ± 0.168	0.932 ± 0.040	0.034 ± 0.093
Mit	-3.213 ● 0.790	2.171 ± 0.264	933 ± 193	-0.825 ● 0.041	-0.470 ± 0.085	0.948 ± 0.020	0.003 ● 0.032

[a] Experimental data were obtained from 48 h exposure of the cells to doxorubicin, daunorubicin and mitoxantrone with fixed doses of dexrazoxane. The cells were preincubated with dexrazoxane for 20 min before the anthracycline was added

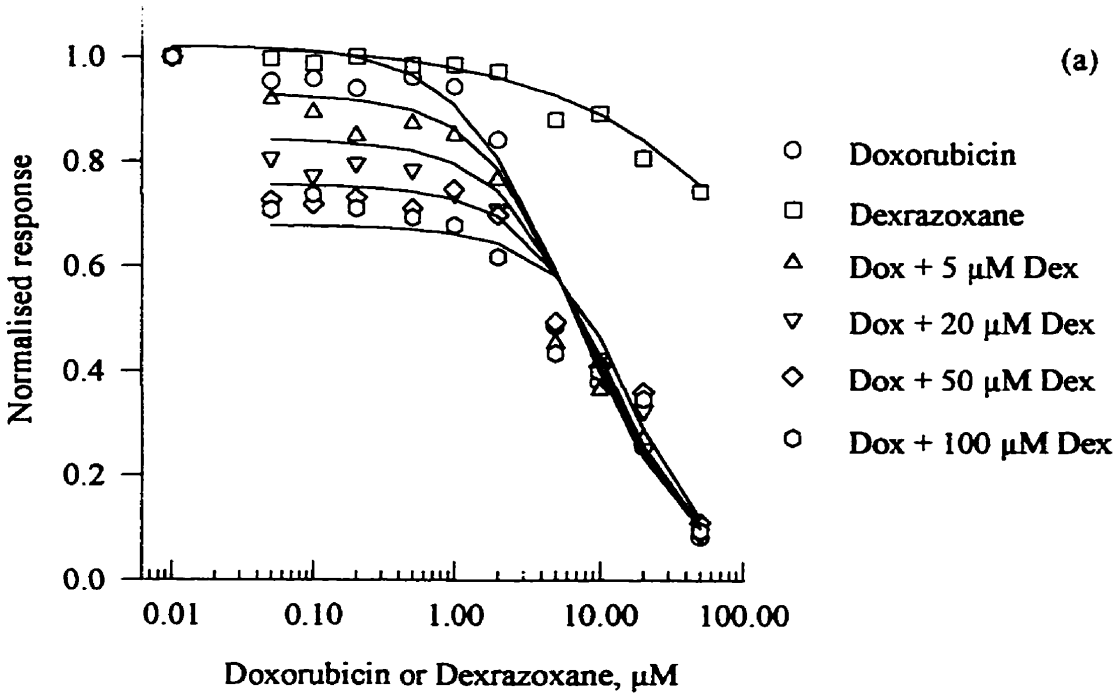
(a)
Normalised response
1.0
0.8
0.6
0.4
0.2
0.0
0.01
0.10
1.00
10.00
100.00
Doxorubicin or Dexrazoxane, μM
Doxorubicin
Dexrazoxane
Dox + 5 μM Dex
Dox + 20 μM Dex
Dox + 50 μM Dex
Dox + 100 μM Dex

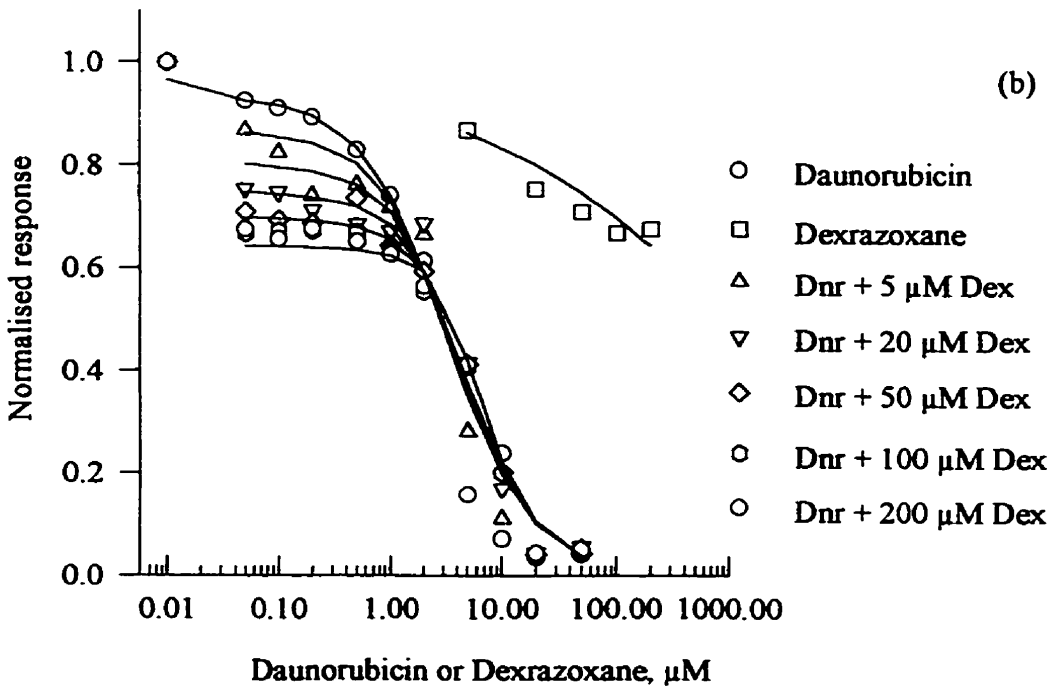
(b)
Normalised response
1.0
0.8
0.6
0.4
0.2
0.0
0.01
0.10
1.00
10.00
100.00
1000.00
Daunorubicin or Dexrazoxane, μM
Daunorubicin
Dexrazoxane
Dnr + 5 μM Dex
Dnr + 20 μM Dex
Dnr + 50 μM Dex
Dnr + 100 μM Dex
Dnr + 200 μM Dex

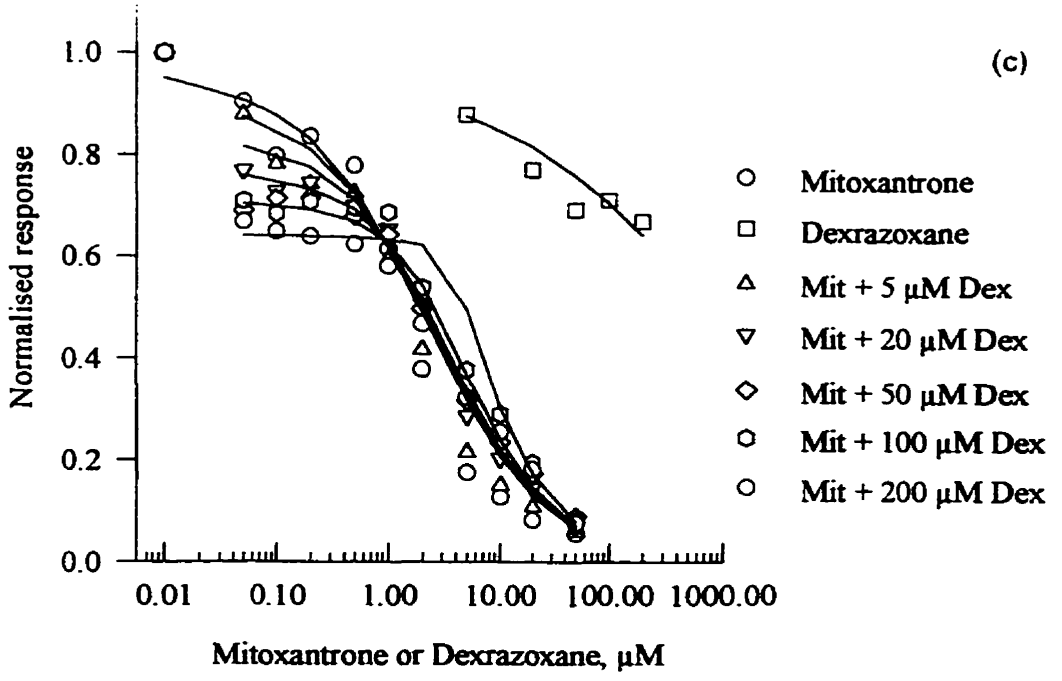

Fig. 4.4. Evaluation of the results from the response surface method used for the combination of dexrazoxane with doxorubicin (a), daunorubicin (b) and mitoxantrone (c). Normalised to an absorbance of 1.0 measured (symbols) and calculated (lines) effects are plotted. The effects were calculated based on the seven parameters obtained from fitting the experimental data presented in Fig. 4.3 to equation (4.1).

The value of the interaction index α', for the doxorubicin Experiment was -1.423 ± 0.870, for daunorubicin α' was -2.171 ± 1.171, and, for mitoxantrone α' was -3.213 ± 0.790. These results indicate antagonism between dexrazoxane and doxorubicin, daunorubicin and mitoxantrone.

4.3.2. Results for the combination of dexrazoxane with doxorubicin, daunorubicin and mitoxantrone with the comparison of slopes method

The inhibitory effects of 48 h continuous exposure of dexrazoxane and dexrazoxane with fixed doses of doxorubicin, daunorubicin and mitoxantrone on Chinese hamster ovary cell growth are presented in Fig. 4.5. (a), (b) and (c) (see pages 156-157).

The slopes of the linear dose-response curves of dexrazoxane and dexrazoxane with the fixed doses of the second drug were compared with the Student *t*-test described in Chapter III, Section 3.2.4.4. The results of the *t*-test along with the regression parameters are presented in Table 4.2. (a), (b) and (c). The median inhibitory concentrations obtained in the 48 h preliminary cytotoxicity Experiments for doxorubicin, daunorubicin and mitoxantrone were as follows: $IC_{50,Dox}$ = 6.6 ± 0.7 μM (three-parameter fit), $IC_{50,Dnr}$ = 2.5 ± 0.2 μM (three-parameter fit) and $IC_{50,Mit}$ = 1.6 ± 0.1 μM (four-parameter fit). These values were used in the design of the Experiments.

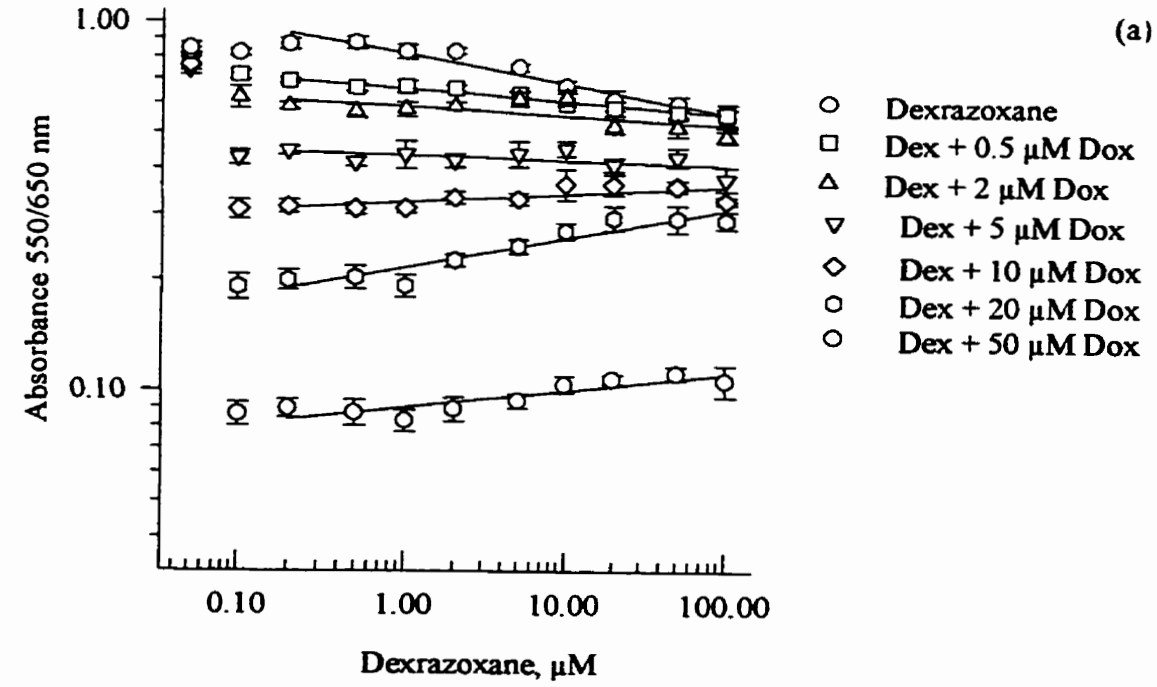
(a)
1.00
0.10
Absorbance 550/650 nm
0.10
1.00
10.00
100.00
Dexrazoxane, μM
Dexrazoxane
Dex + 0.5 μM Dox
Dex + 2 μM Dox
Dex + 5 μM Dox
Dex + 10 μM Dox
Dex + 20 μM Dox
Dex + 50 μM Dox

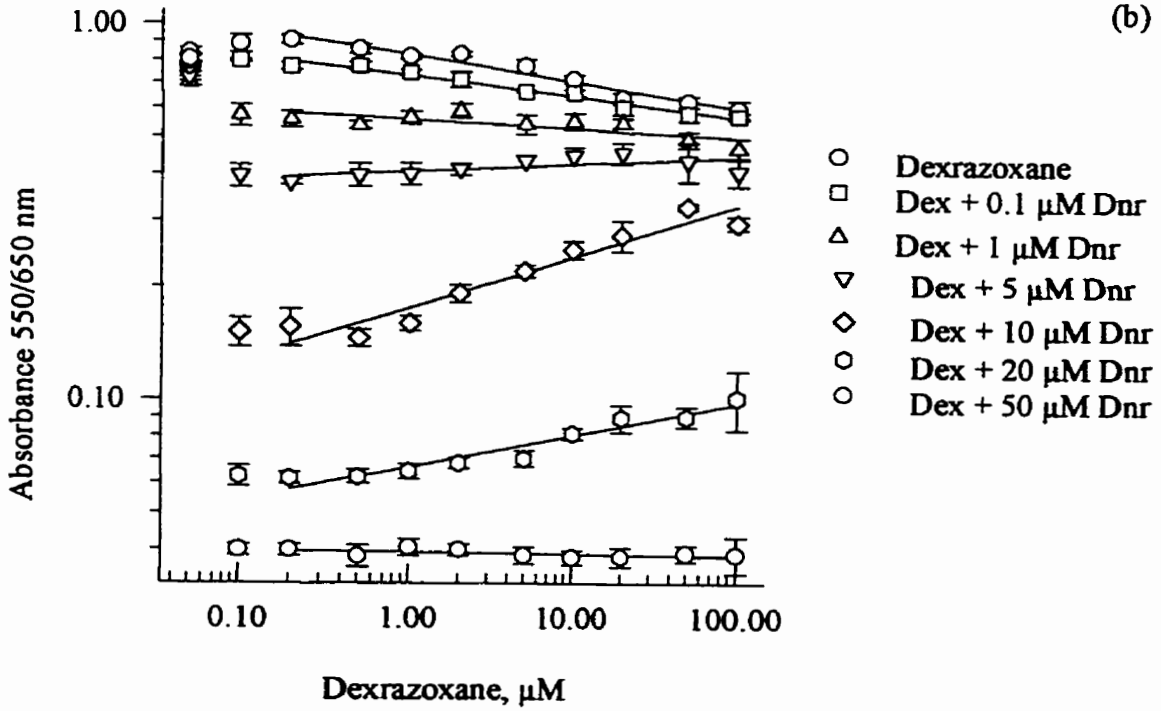
(b)
1.00
0.10
Absorbance 550/650 nm
0.10
1.00
10.00
100.00
Dexrazoxane, μM
Dexrazoxane
Dex + 0.1 μM Dnr
Dex + 1 μM Dnr
Dex + 5 μM Dnr
Dex + 10 μM Dnr
Dex + 20 μM Dnr
Dex + 50 μM Dnr

(c)

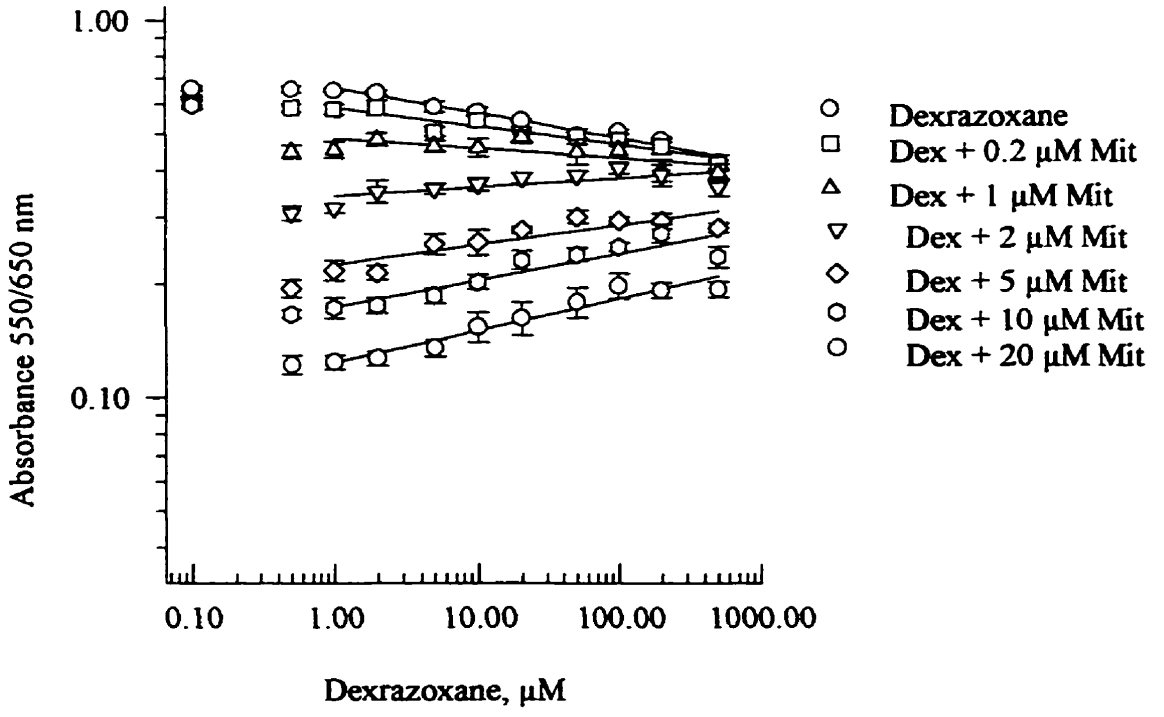

Fig. 4.5. Slope comparison experiments for the combination of dexrazoxane with doxorubicin (a), daunorubicin (b) and mitoxantrone (c). The 48 h inhibitory effect of dexrazoxane alone and dexrazoxane with fixed doses of doxorubicin, daunorubicin and mitoxantrone on Chinese hamster ovary cell growth are presented in log-log scale. The symbols represent the means of absorbance ± SD from six replicates at each concentration. The lines represent the result of the fit of experimental data to a linear equation (log $A_{550/650} = a + b \cdot \log D$, where $A_{550/650}$ is an absorbance at 550 nm minus absorbance at 650 nm and D is a drug concentration). The lowest concentrations correspond to control values with zero concentration of the drugs. The second control value for the mixed drugs is an effect of doxorubicin (a), daunorubicin (b) or mitoxantrone (c) by itself.

The listing of the variables used in the *t*-test is given in Chapter III, Section 3.3.4.

Table 4.2 Slope comparison of linear dose-response curves of dexrazoxane and dexrazoxane with fixed doses of doxorubicin (a), daunorubicin (b) and mitoxantrone (c) presented in Fig. 4.5.

(a)

Parameters	Doses of Doxorubicin, μM						
	0	0.5	2.0	5.0	10	20	50
$a \pm$ SEM	-0.086 ± 0.008	-0.180 ± 0.003	-0.230 ± 0.013	-0.362 ± 0.009	-0.489 ● 0.009	-0.667 ± 0.011	-1.047 ± 0.010
$b \pm$ SEM	-0.080 ± 0.008	-0.035 ± 0.003	-0.025 ± 0.012	-0.013 ● 0.009	0.022 ± 0.008	0.079 ± 0.011	0.046 ± 0.009
Tb		-5.534	-3.988	-5.858	-9.066	-12.196	-10.658
Vb		14	14	14	14	14	14
P		< 0.001	< 0.01	< 0.001	< 0.001	< 0.001	< 0.001

(b)

Parameters	Doses of Daunorubicin, μM						
	0	0.1	1.0	2.0	5.0	10	20
a ± SEM	-0.081 ± 0.006	-0.137 ± 0.004	-0.253 ± 0.009	-0.391 ± 0.009	-0.755 ± 0.015	-1.179 ± 0.009	-1.406 ± 0.004
b ± SEM	-0.071 ± 0.006	-0.055 ± 0.004	-0.233 ± 0.009	0.020 ± 0.008	0.137 ± 0.014	0.085 ± 0.009	-0.005 ± 0.004
Tb		-2.188	-4.526	-8.986	-13.502	-14.976	-9.514
Vb		14	14	14	14	14	14
P		< 0.05	< 0.001	< 0.001	< 0.001	< 0.001	< 0.001

(c)

Parameters	Doses of Mitoxantrone, μM						
	0	0.2	1.0	2.0	5.0	10	20
$a \pm$ SEM	-0.179 ± 0.008	-0.232 ± 0.010	-0.313 ± 0.014	-0.466 ± 0.015	-0.648 ± 0.018	-0.760 ± 0.019	-0.907 ± 0.014
$b \pm$ SEM	-0.066 ± 0.005	-0.048 ± 0.007	-0.025 ± 0.009	0.024 ± 0.009	0.053 ± 0.011	0.072 ± 0.012	0.085 ± 0.009
Tb		-2.178	-3.970	-8.721	-9.659	-10.651	-15.358
Vb		14	14	14	14	14	14
P		< 0.05	< 0.01	< 0.001	< 0.001	< 0.001	< 0.001

The values of the slopes are also plotted against the fixed doses of doxorubicin, daunorubicin and mitoxantrone in Fig. 4.6.

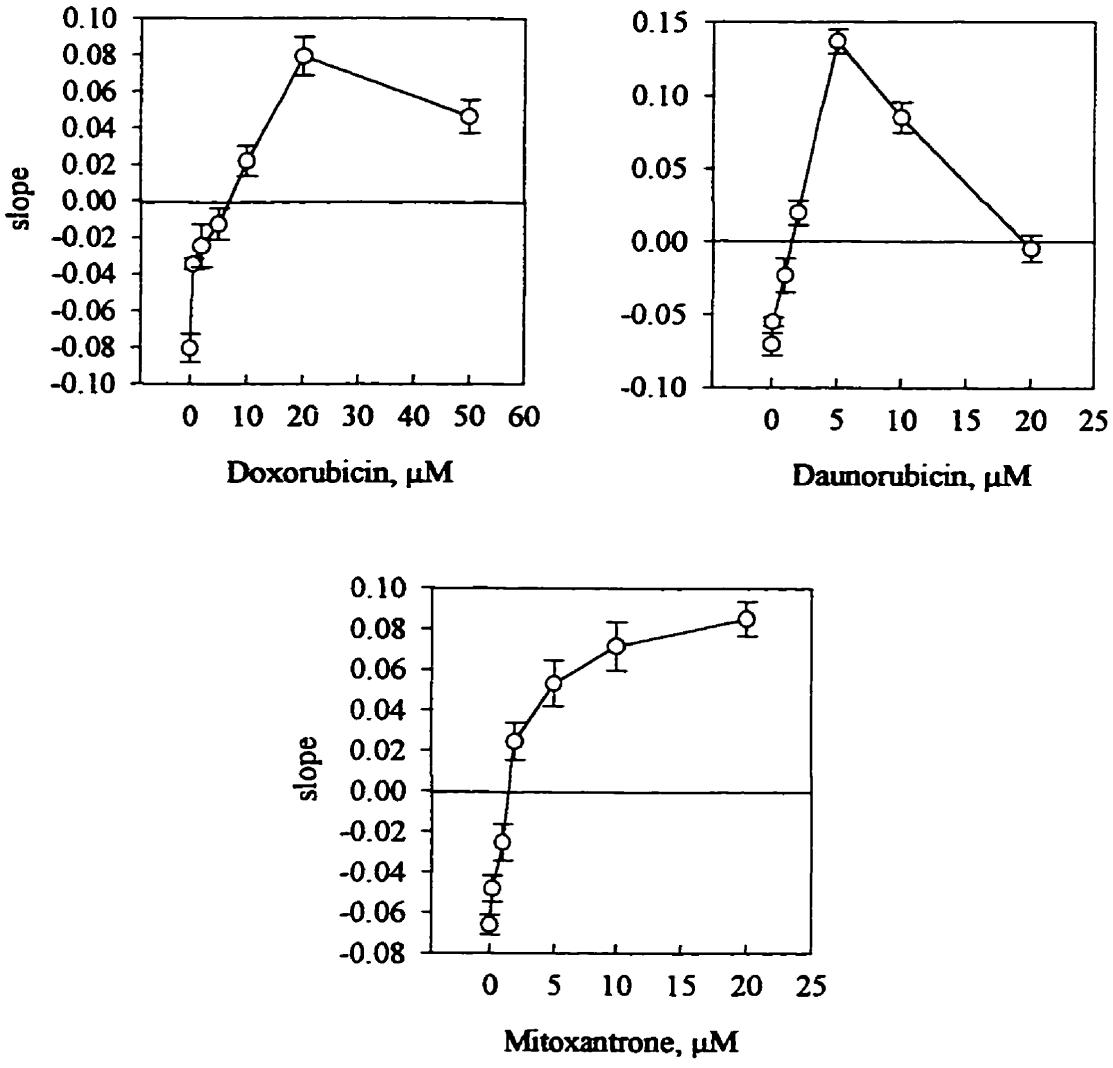

Fig. 4.6. Slopes obtained from the experiments for dexrazoxane with doxorubicin, daunorubicin and mitoxantrone analysed with the slope method. The slopes of linear dose-response curves were plotted against the concentrations of doxorubicin, daunorubicin and mitoxantrone. The first values are the slopes of the dose-response curve of dexrazoxane alone. The error bars represent SEM from SigmaPlot curve fit.

The slopes of the dexrazoxane dose-response curves were significantly different from the slopes of dexrazoxane with fixed doses of doxorubicin, daunorubicin and mitoxantrone (Table 4.2). The value of the dexrazoxane slope steadily increased with the

dose of the second drug (Fig. 4.6). Although, at the highest concentrations of doxorubicin and daunorubicin, the slopes began to decrease due to very low cell survival levels at these concentrations. The cell proliferation was almost completely inhibited; thus, the level of topoisomerase II was very low.

4.4. Conclusions

The inhibitory effect of doxorubicin, daunorubicin, and mitoxantrone in combination with dexrazoxane, on Chinese hamster ovary cell growth was antagonistic, as shown by the response surface and slope comparison methods. The cells were exposed to the drugs for 48 h and the time gap between dexrazoxane and the second drug was 20 min (response surface Experiments) or 60 min (slope comparison Experiments). The values of the interaction parameters, α', obtained with the response surface method were as follows: -1.423 ± 0.870 for doxorubicin, -2.171 ± 1.171 for daunorubicin, and, -3.213 ● 0.790 for mitoxantrone (Table 4.1). The interaction parameters of all three drugs were smaller than zero, which indicates antagonism with dexrazoxane. The low value of the interaction index obtained for the mitoxantrone Experiment seems to indicate a stronger antagonistic effect than either doxorubicin or daunorubicin, although, the results of mitoxantrone data fit were less satisfactory than for other drugs. The dexrazoxane linear dose-response curve slope was significantly different ($P < 0.05$) from those of dexrazoxane with fixed doses of either doxorubicin, daunorubicin or mitoxantrone (Table 4.2). The slope of the dexrazoxane dose-response curve was negative but it increased with the concentration of the second drug to positive values (Fig. 4.6). The slopes increased with doses of doxorubicin up to 20 μM, daunorubicin up to 5 μM, and for all mitoxantrone doses

studied up to 20 μM. These results indicate antagonism between dexrazoxane and doxorubicin, daunorubicin and mitoxantrone. The strongest antagonism, expressed as the highest slope, was for 5 μM of daunorubicin, where the slope change from -0.07 for dexrazoxane alone to 0.14 for dexrazoxane with 5 μM of daunorubicin. Strong antagonism was also observed for 20 μM doxorubicin and mitoxantrone; although, the change of the slopes was about 25% smaller than for 5 μM daunorubicin.

The antagonistic effect of dexrazoxane with doxorubicin, daunorubicin and, mitoxantrone may be explained by the theory of an ATP-modulated protein clamp [30]. Similar to the proposed mechanism for ICRF-193, dexrazoxane may stabilise a closed clamp form of topoisomerase II. The trapped enzyme is not available to form ternary complexes with DNA and the cleavable complex form poisons doxorubicin, daunorubicin and mitoxantrone (compare Section 2.1.2).

Although dexrazoxane may be beneficial as cardioprotective drug, its antagonistic cytotoxic effect with anticancer drugs such as doxorubicin, daunorubicin and mitoxantrone may lower cytotoxic effect of these drugs toward cancer cells.

References

1. *Compendium of Pharmaceuticals and Specialties. 32nd ed.* Canadian Pharmaceutical Association, Ottawa, Ontario, Canada, 1997; 1032 p.

2. Speyer JL, Green MD, Kramer E, Rey M, Sanger J, Ward C, Dubin N, Ferrans V, Stecy P, Zeleniuch-Jacquotte A, Wernz J, Feit F, Slater W, Blum R and Muggia F, Protective effect of the bispiperazinedione ICRF-187 against doxorubicin-induced cardiac toxicity in women with advanced breast cancer. *N Engl J Med* **319:** 745-752, 1988.

3. Sehested M and Jensen PB, Mapping of DNA topoisomerase II poisons (etoposide and clerocidin) and catalytic inhibitors (aclarubicin, ICRF-187) to four distinct

steps in the topoisomerase II catalytic cycle. *Biochem Pharmacol* **51:** 879-886, 1996.

4. Sengupta SK, Topoisomerase II inhibitors. In: *Cancer chemotherapeutic agents.* (Ed. Foye WO), pp. 205-291. 1st ed. American Chemical Society, Washington, DC, 1995.

5. D'Arpa P and Liu LF, Topoisomerase-targeting antitumor drugs. *Biochim Biophys Acta* **989:** 163-177, 1989.

6. Pommier Y, DNA topoisomerase II inhibitors. In: *Cancer Therapeutics: Experimental and Clinical Agents.* (Ed. Teicher B), pp. 153-174. Humana Press Inc., Totowa, NJ, 1997.

7. Myers CE, Mimnaugh EG, Yeh GC and Sinha BK, Biochemical mechanisms of tumor cell kill by the anthracyclines. In: *Anthracycline and anthracenedione-based anticancer agents.* (Ed. Lown JW), pp. 527-569. Vol. 6. Elsevier, Amsterdam, 1988.

8. Bredehorst R, Panneerselvam M and Vogel C-W, Doxorubicin enhances complement susceptibility of human melanoma cells by extracellular oxygen radical formation. *J Biol Chem* **262:** 2034-2041, 1987.

9. Doroshow JH, Role of hydrogen peroxide and hydroxyl radical formation in the killing of Ehrlich tumor cells by anticancer quinones. *Proc Natl Acad Sci USA* **83:** 4514-4518, 1986.

10. Carter SK, Adriamycin-a review. *J Natl Cancer Inst* **55:** 1265-1274, 1975.

11. Doroshow JH, Effect of anthracycline antibiotics on oxygen radical formation in rat heart. *Cancer Res* **43:** 460-472, 1983.

12. Mimnaugh EG, Gram TE and Trush MA, Stimulation of mouse heart and liver microsomal lipid peroxidation by anthracyclin anticancer drugs: characterization and affects of reactive oxygen scavengers. *J Pharmacol Exp Ther* **226:** 806-816, 1983.

13. Malisza KL and Hasinoff BB, Production of hydroxyl radical by iron(III)-anthraquinone complexes through self-reduction and through reductive activation by the xanthine oxidase/hypoxanthine system. *Arch Biochem Biophys* **321:** 51-60, 1995.

14. Myers C, Gianni L, Zweier J, Muindi J, Sinha BK and Eliot H, Role of iron in adriamycin biochemistry. *Fed Proc* **45:** 2792-2797, 1986.

15. Kolaric K, Bradamante V, Cervek J, Cieslinka A, Cisarz-Filipcak E, Denisov LE, Donat D, Drosik K, Gershanovic M, Hudziec P, Jelic S, Jurga L, Kalasiewicz M, Kowgird L, Kozacka M, Lichinitzer M, Machalski M, Mechl Z, Odintsov S, Pawlicki M, Rubach D, Roth A, Stabuc B, Tomczak J, Utracka B, Zborzil J and Rogan J, A phase II trial of cardioprotection with cardioxane (ICRF187) in patients with advanced breast cancer receiving 5-fluorouracil, doxorubicin and cyclophosphamide. *Oncology* **52:** 251-255, 1995.

16. Imondi AR, Torre PD, Mazue G, Sullivan TM, Robbins TL, Hagerman IM, Podesta A and Pinciroli G, Dose-response relationship of dexrazoxane for the prevention of doxorubicin-induced cardiotoxicity in mice rats and dogs. *Cancer Res* **56:** 4200-4204, 1996.

17. Shipp NG, Dorr RT, Alberts DS, Dawson BV and Hendrix M, Characterization of experimental mitoxantrone cardiotoxicity and its partial inhibition by ICRF-187 in cultured neonatal rat heart cells. *Cancer Res* **53:** 550-556, 1993.

18. Alderton PM, Gross J and Green MD, Comparative study of doxorubicin, mitoxantrone, and epirubicin in combination with ICRF-187 (ADR-529) in a chronic cardiotoxicity animal model. *Cancer Res* **52:** 194-201, 1992.

19. Doroshow JH, Role of reactive oxygen metabolism in cardiac toxicity of anthracycline antibiotics. In: *Anthracycline Antibiotics, New Analogues, Methods of Delivery, and Mechanisms of Action.* (Ed. Priebe W), pp. 259-267. American Chemical Society, Washington, 1995.

20. Buss JL and Hasinoff BB, The one-ring open hydrolysis product intermediates of the cardioprotective agent ICRF-187 (dexrazoxane) displace iron from iron-anthracycline complexes. *Agents Actions* **40:** 86-95, 1993.

21. Von Hoff DD, Howser D, Lewis BJ, Holcenberg J, Weiss RB and Young RC, Phase I study of ICRF-187 using a daily for 3 days schedule. *Cancer Treat Rep* **65:** 249-252, 1981.

22. Hasinoff BB, Yalowich JC, Ling Y and Buss JL, The effect of dexrazoxane (ICRF-187) on doxorubicin and daunorubicin-mediated growth inhibition of Chinese hamster ovary (CHO) cells. *Anticancer Drugs* **7:** 558-567, 1996.

23. Sehested M, Jensen PB, Sorensen BS, Holm B, Friche E and Demant EJF, Antagonistic effect of the cardioprotector (+)-1,2-bis(3,5-dioxopiperazinyl-1-yl)propane (ICRF-187) on DNA breaks and cytotoxicity induced by the topoisomerase II directed drugs daunorubicin and etoposide (VP-16). *Biochem Pharmacol* **46:** 389-393, 1993.

24. Pearlman ML, Pagliaro LC, Liu B and Freireich EJ, Dexrazoxane is cytotoxic to AML blasts and does not abrogate sensitivity to doxorubicin in vivo. *AACR* **38:** 608, 1997.

25. Supino R, Influence of ICRF-159 or ICRF-186 on cytotoxicity of daunorubicin and doxorubicin. *Tumori* **70:** 121-126, 1984.

26. Kano Y, Narita T, Suzuki K, Akutsu M, Suda K, Sakamoto S and Miura Y, The effects of ICRF-154 in combination with other anticancer agents in vitro. *Br J Cancer* **66:** 281-286, 1992.

27. Tomkins CE, Edwards SN and Tolkovsky AM, Apoptosis is induced in post-mitotic rat sympathetic neurons by arabinosides and topoisomerase II inhibitors in the presence of NGF. *J Cell Sci* **107:** 1499-1507, 1994.

28. Greco WR, Park HS and Rustum YM, Application of a new approach for the quantitation of drug synergism to the combination of cis-diamminedichloroplatinum and 1-β-D-arabinofuranosylcytosine. *Cancer Res* **50:** 5318-5327, 1990.

29. Thisted RA. *Elements of statistical computing.* Chapman and Hall, New York, NY, 1988:170; 427 p.

30. Roca J and Wang JC, The capture of a DNA double helix by an ATP-dependent protein clamp: A key step in DNA transport by type II DNA topoisomerases. *Cell* **71:** 833-840, 1992.

5. Effect of dexrazoxane and ADR-925 in the combination with bleomycin on Chinese hamster ovary cell growth

5.1. Introduction

Bleomycin is a glycopeptidic antibiotic with anticancer activity [1]. Bleomycin can be used as a single agent or as part of multidrug chemotherapy with doxorubicin and other anticancer drugs [2]. The major side effect of bleomycin is pulmonary toxicity [3]; but dexrazoxane lowers bleomycin pulmonary toxicity in animals [4]. Since dexrazoxane can be beneficial when used with bleomycin, these studies were designed to investigate the combined effect of dexrazoxane with bleomycin on Chinese hamster ovary cell growth. The combination index, envelope of additivity, response surface and slope comparison methods were used to evaluate the results. Besides dexrazoxane, its hydrolysis product, ADR-925, was also studied in combination with bleomycin.

5.1.1. Bleomycin an anticancer drug

Clinically used bleomycin sulphate (Blenoxane®) is a mixture of glycopeptide antibiotics isolated from a strain of *Streptomyces verticilus* [1], which differ only in their terminal amine part (R, Fig. 5.1). Bleomycin binds transition metal ions. Bleomycin-Fe(II) forms a ternary complex with O_2 and it is believed that binding of this complex to DNA is involved in bleomycin antitumor activity. The oxidation of iron and subsequent generation of oxygen radicals cause DNA strand scission [1]. Metal chelators and hypoxia inhibit bleomycin antitumor activity [1]. Patients exhibiting bleomycin pulmonary toxicity express a low level of bleomycin hydrolase, the enzyme inactivating bleomycin, in their lungs [1]. Lung fibrosis is induced when a cumulative dose of bleomycin is 300 mg/m^2 [5].

Bleomycin does not diffuse through the plasma membrane and only 0.1% of the drug reaches the cell interior through interaction with plasma membrane proteins [5].

Dexrazoxane enters the cell [6], where it may hydrolyse to one ring open intermediates and its two rings open hydrolysis product, ADR-925 [7]. Dexrazoxane and ADR-925, were able to remove iron from the bleomycin-Fe(III) complex *in vitro* [4]. Under non-saturating conditions, the ADR-925 reacted with the bleomycin-Fe(III) complex 47 times faster than dexrazoxane [4]. Unlike dexrazoxane, ADR-925 does not have a cytotoxic effect on the cells [8]. The ability of dexrazoxane to protect bleomycin pulmonary toxicity might be linked to its iron chelation properties [4]. The half-life for dexrazoxane and ADR-925 at pH 7.38 and 37°C is 9.3 and 23.0 h, respectively.

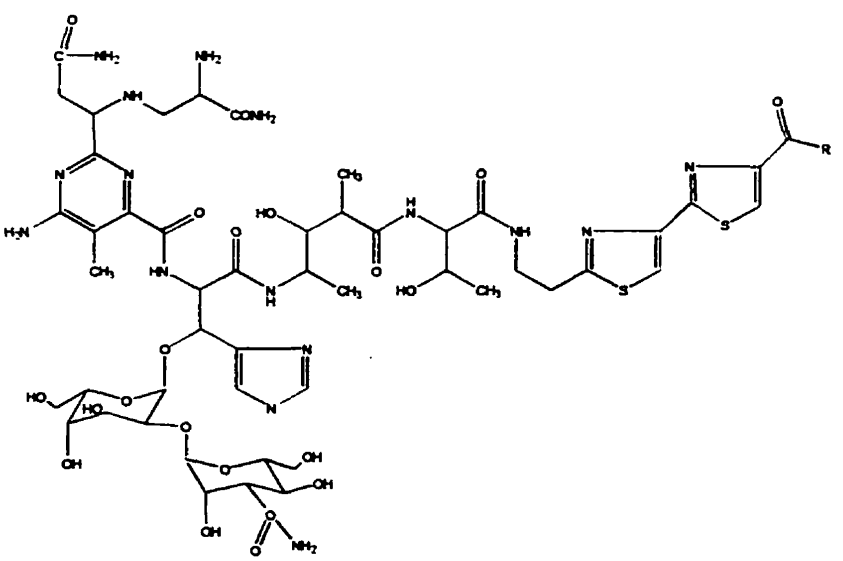

Fig. 5.1. Structure of bleomycin, R = substituent, positively charged at physiological pH; *e.g.* for bleomycin A_5, R = $-NH(CH_2)_3NH(CH_2)_4NH_2$.

There are contradictory studies either iron is necessary for anticancer activity of bleomycin. In a study on mice, iron deficiency did not change bleomycin antitumor activity

[9]. The cytotoxic effect of bleomycin toward Ehrlich cells was not altered by the Fe^{2-} chelator, 1,10-phenanthroline; however, bleomycin cytotoxicity was significantly reduced with 1,10-phenanthroline on rat alveolar type 2 cells (T2) [10]. In a study of HeLa cells, the presence of 1,10-phenanthroline suppressed the inhibitory activity of bleomycin [11]. Bleomycin-induced cleavage of DNA and the appearance of chromosome aberrations in Chinese hamster ovary cells were inhibited by 1,10-phenanthroline [12]. Bleomycin cytotoxicity on *Saccharomyces cerevisiae* cells was inhibited by EDTA, which is structurally similar to dexrazoxane [13]. Since some study indicated, that perhaps iron is a cofactor in the antitumor activity of bleomycin, and the hydrolysis products of dexrazoxane are iron chelators, an antagonistic cytotoxic effect of bleomycin and dexrazoxane could be expected.

5.2. Materials and methods

Chinese hamster ovary cells were used to study the influence of the combination of dexrazoxane and bleomycin on cell growth. Two thousand cells were seeded in 100 μL of cell culture medium on 96-well plates and allowed to attach for 24 or 6 h, according to experiment. After this period of time, drugs were delivered, the volume of cell culture medium was increased to 200 μL/well and cells were incubated for another 72 or 48 h. The MTT assay was used to quantify the effects of drug exposure to the cells. A detailed description of cytotoxicity experiments and the MTT assay is given in Chapter II, Section 2.2.3. The interactions of dexrazoxane with bleomycin were studied with the combination index, response surface, envelope of additivity and slope comparison methods. The

interaction of bleomycin with ADR-925 was evaluated by a simple comparison of the 72 h median inhibitory concentrations.

5.2.1. Materials

Dexrazoxane (ICRF-187) and ADR-925 were gifts from Pharmacia & Upjohn (Columbus, OH). Bleomycin sulphate (Blenoxane®) was obtained from Nippon Kayaku Co. Ltd. (Tokyo, Japan).

5.2.2. Solubility of bleomycin, dexrazoxane and ADR-925

Bleomycin sulphate (M_w = 1511.61 g/mol) is highly soluble in water [14]. Stock solutions of bleomycin were prepared in a 0.9% (w/v) aqueous solution of NaCl and delivered in volumes of 5-20 µL to the plate wells. Dexrazoxane (M_w = 268.3 g/mol) and ADR-925 (M_w = 302.3 g/mol) were dissolved in cell culture medium and filter sterilised with a 0.2 µm acetate filter.

5.2.3. Design of experiments for the combination of dexrazoxane and ADR-925 with bleomycin

5.2.3.1. Combination index experiments for the combination of dexrazoxane with bleomycin

Two experiments with different drug delivery schedules were performed for analysis with the combination index method. In the first experiment, dexrazoxane and bleomycin were delivered to the wells simultaneously and the cells were exposed to the drugs for 72 h. In the second experiment, there was an 18 h time gap between the addition of the two drugs. Dexrazoxane was added 6 h after the cells were seeded. After an 18 h cell incubation with dexrazoxane, bleomycin was added and the cells were incubated with

both drugs for another 72 h. Bleomycin as a single agent was added after 24 h growth of the cells. The half-life of dexrazoxane is 9.3 h; after 18 h of incubation 75% of the dexrazoxane should be hydrolysed to forms able to bind iron. Chinese hamster ovary cells do not contribute to dexrazoxane hydrolysis (not published data performed in our laboratory by Mukhtiar Singh). Five dose-response curves in a 0.05-50 μM range were prepared for each experiment: one dose-response curve for bleomycin (Bl), one for dexrazoxane (Dex) and three for their combinations. In both experiments, three ratios of dexrazoxane and bleomycin were used. One ratio was equipotent calculated as $IC_{50,Dex}/IC_{50,Bl}$ = 6.4 μM/4.6 μM = 1.4, where $IC_{50,Dex}$ and $IC_{50,Bl}$ are the median inhibitory concentrations for dexrazoxane and bleomycin, respectively. The IC_{50} values were obtained from preliminary 72 h dose-response curves. The two other ratios were Dex/Bl = 5 and Dex/Bl = 0.2 with the ratio of dexrazoxane and bleomycin remaining constant through the whole range of concentrations.

5.2.3.2. Envelope of additivity experiments for the combination of dexrazoxane with bleomycin

The envelope of additivity experiment was prepared with an 18 h time gap between the addition of dexrazoxane and bleomycin. Six hours after cells were seeded, dexrazoxane was added to the plates. After 18 h cell incubation with dexrazoxane, bleomycin was added to the wells designed for combination of drugs and cells were incubated with both drugs for another 72 h. At the same time, a bleomycin dose-response curve was also prepared. Six dose-response curves were prepared: one for dexrazoxane alone (0.2-200 μM), one for bleomycin alone (0.2-200 μM) and four for a wide range of

bleomycin concentrations (0.5-200 μM) with fixed doses of dexrazoxane: 1.0, 2.0, 3.0 and 4.0 μM. The fixed doses of dexrazoxane were chosen to include the 50% effect for the intended envelope of additivity.

5.2.3.3. Slope comparison experiments for the combination of dexrazoxane with bleomycin

For the slope comparison experiment, seven dose-response curves were prepared; one for dexrazoxane alone (0.5-500 μM), and six for a wide concentration range (0.5-500 μM) of dexrazoxane with fixed doses of bleomycin of 10, 20, 50, 100, 200 and 500 μM. Dexrazoxane was added one hour before the bleomycin. Cells were incubated with the drugs for 48 h. Due to the large quantities of bleomycin required for this experiment, only three wells were prepared for each data point.

5.2.4. Data analysis with the combination index, envelope of additivity, response surface and slope methods for dexrazoxane and ADR-925 combined with bleomycin

The combination index was calculated as described in Chapter III, Section 3.2.4.1. The envelope of additivity method was described in Chapter III, Section 3.2.4.2. The dose-response curves used with the envelope of additivity method were limited to the 0.2-100 μM range due to a non-logistic fit above 100 μM concentration of bleomycin. The response surface method was described in Chapter III, Section 3.2.4.3. The comparison of slopes was described in Chapter III, Section 3.2.4.4.

5.3. Results

5.3.1. Results from the combination index method for the dexrazoxane-bleomycin experiments

The results of 72 h exposure of Chinese hamster ovary cells to bleomycin (Bl), dexrazoxane (Dex) and their three mixtures (Dex/Bl) are presented in Fig. 5.2. Both drugs were added at the same time.

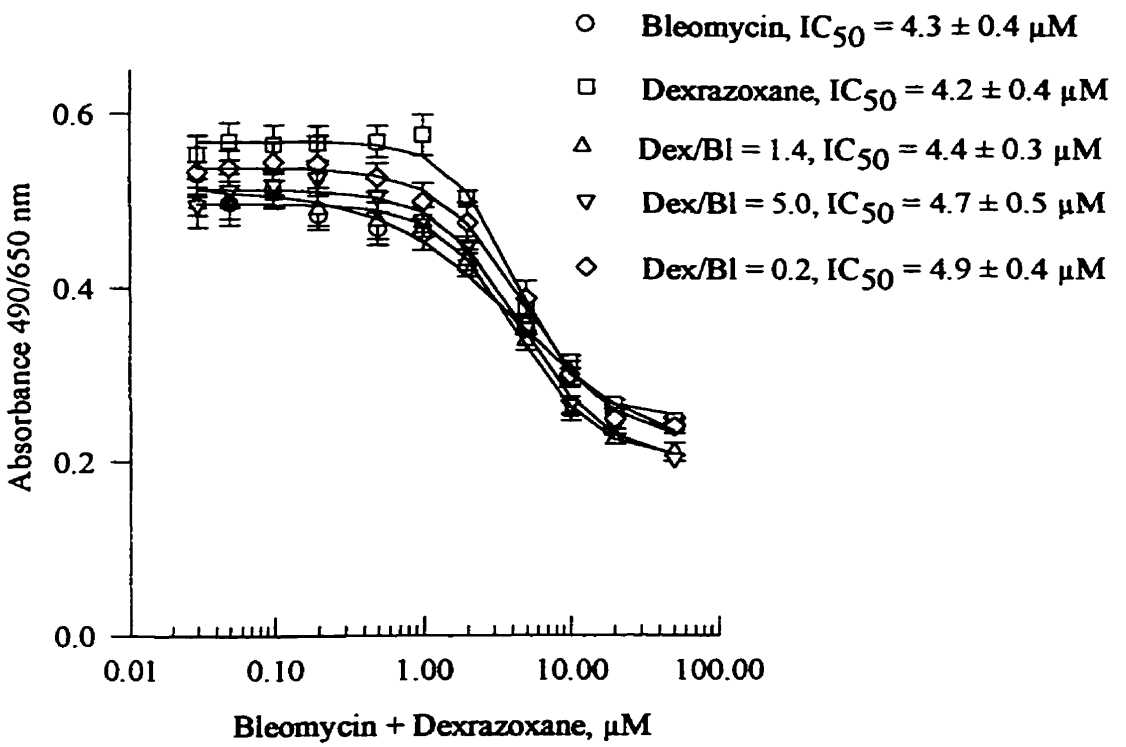

Fig. 5.2. Combination index experiment for bleomycin and dexrazoxane added simultaneously. Chinese hamster ovary cells were incubated with the drugs for 72 h. The points represent absorbance means ± SD from six repetitions at each concentration. The lines represent the non-linear least squares fit of the experimental data to a four-parameter logistic equation. The lowest concentration corresponds to zero concentration of drugs plotted for convenience on a logarithmic scale with an arbitrary given value.

Some data from the Experiment shown in Fig. 5.2 were used to construct a median effect plot, presented in Fig. 5.3. Absorbances that did not fit linear equations (black symbols in Fig. 5.3) as well as absorbances higher than the blank were not included.

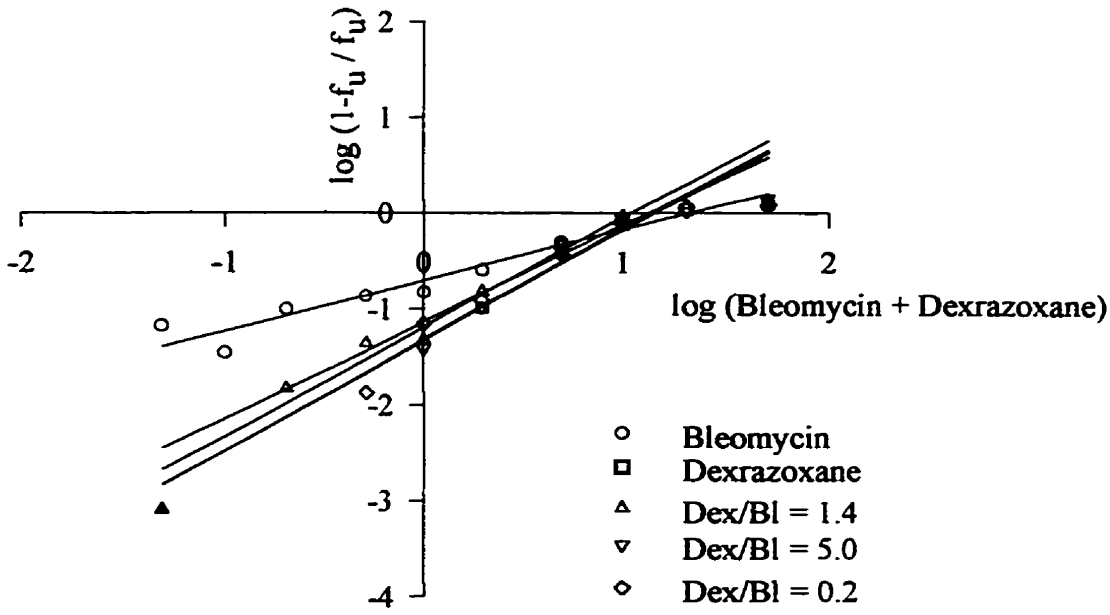

Fig. 5.3. Median effect plot for the dexrazoxane-bleomycin combination index experiment presented in Fig. 5.2. The data represented by solid symbols were not used to construct the plot. The plot of dexrazoxane is almost identical with Dex/Bl = 1.4, also the plot for Dex/Bl = 5.0 and Dex/Bl = 0.2 overlap each other.

Exclusivity of the drugs could not be evaluated from the median effect plot; the slopes of regression lines were 0.5 and 1.0 for bleomycin and dexrazoxane, respectively. The combination index was calculated using equations for mutually exclusive (Fig. 5.4, α = 0) and mutually nonexclusive drugs (Fig. 5.5, α = 1) in the 0.2-0.54 range of fraction affected (the range of experimental points defining the median effect plot).

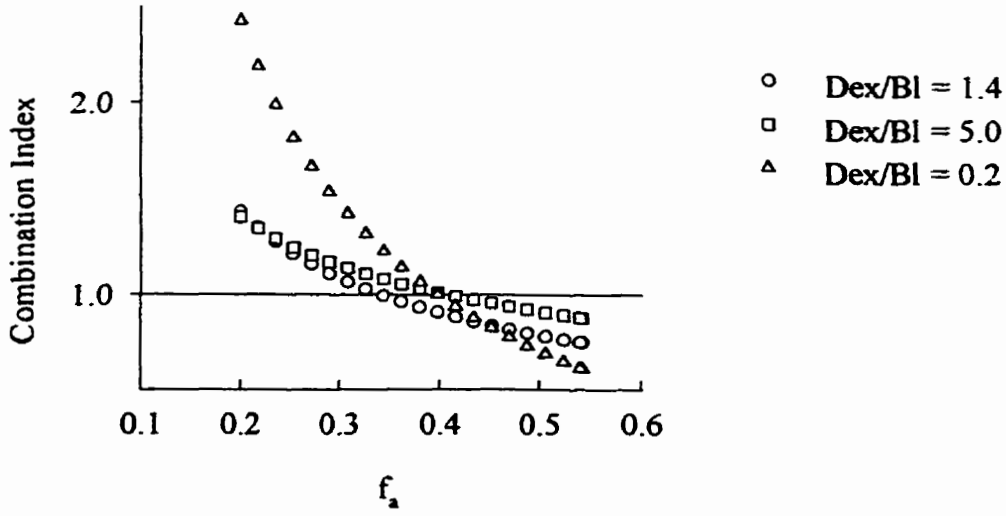

Fig. 5.4. Plot of combination index against fraction affected for three combinations of dexrazoxane and bleomycin added simultaneously. The combination index was calculated for $\alpha = 0$.

An antagonistic effect ($CI > 1$) between dexrazoxane and bleomycin was indicated up to $f_a = 0.34$ for Dex/Bl = 1.4 (equipotent ratio), and up to $f_a = 0.4$ for Dex/Bl = 5.0 and 0.2. At higher ranges of fraction affected the interaction of these drugs was synergistic ($CI < 1$).

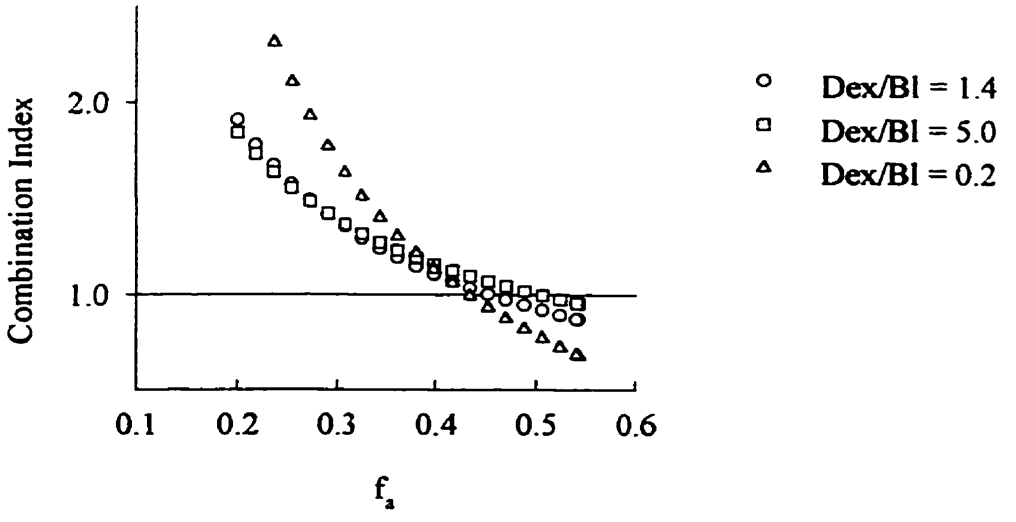

Fig. 5.5. Plot of combination index against fraction affected for three combinations of dexrazoxane and bleomycin added simultaneously. Combination index was calculated for $\alpha = 1$.

When the equation for mutually non-exclusive drugs was used, antagonism ($CI >$ 1) between dexrazoxane and bleomycin was observed up to $f_a = 0.45$ for the equipotent ratio Dex/Bl = 1.4, up to $f_a = 0.51$ and 0.42 for Dex/Bl = 5 and Dex/Bl = 0.2, respectively. Above these values, dexrazoxane and bleomycin showed synergy ($CI < 1$).

In the second combination index Experiment, dexrazoxane was added 18 h before bleomycin and both drugs were incubated another 72 h. The 18 h preincubation allowed dexrazoxane to hydrolyse to its metal chelating forms. The results of this Experiment are presented in Fig. 5.6.

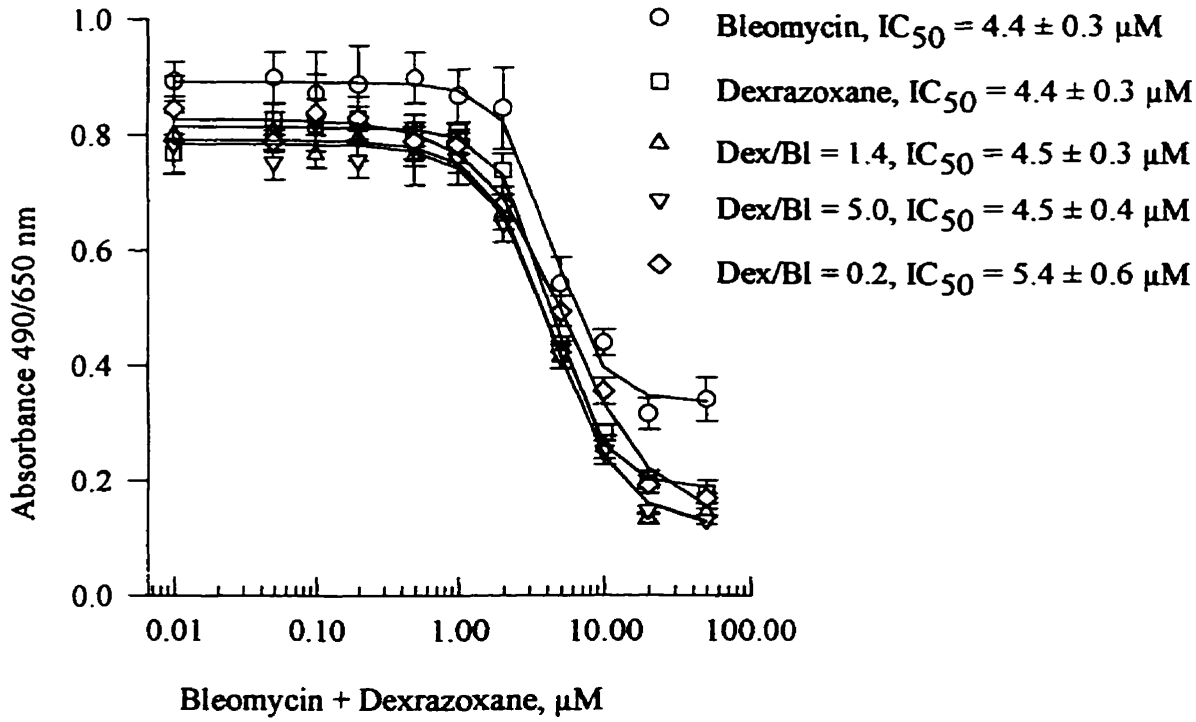

Fig. 5.6. Combination index experiment for bleomycin and dexrazoxane with 18 h preincubation of dexrazoxane. Chinese hamster ovary cells were incubated with both drugs for 72 h. The points represent absorbance means ● SD from six repetitions at each concentration. The lines represent the non-linear least squares fit of the experimental data to a four-parameter logistic equation. The lowest concentration corresponds to the zero concentration of drugs plotted for convenience on a logarithmic scale with an arbitrary given value.

The median effect plot for the Experiment in Fig.5.6 is presented in Fig. 5.7. The slope of the bleomycin plot was 1.5 and the dexrazoxane plot was 1.9. The linear median effect plots were not parallel to each other so exclusivity of the drugs could not be determined.

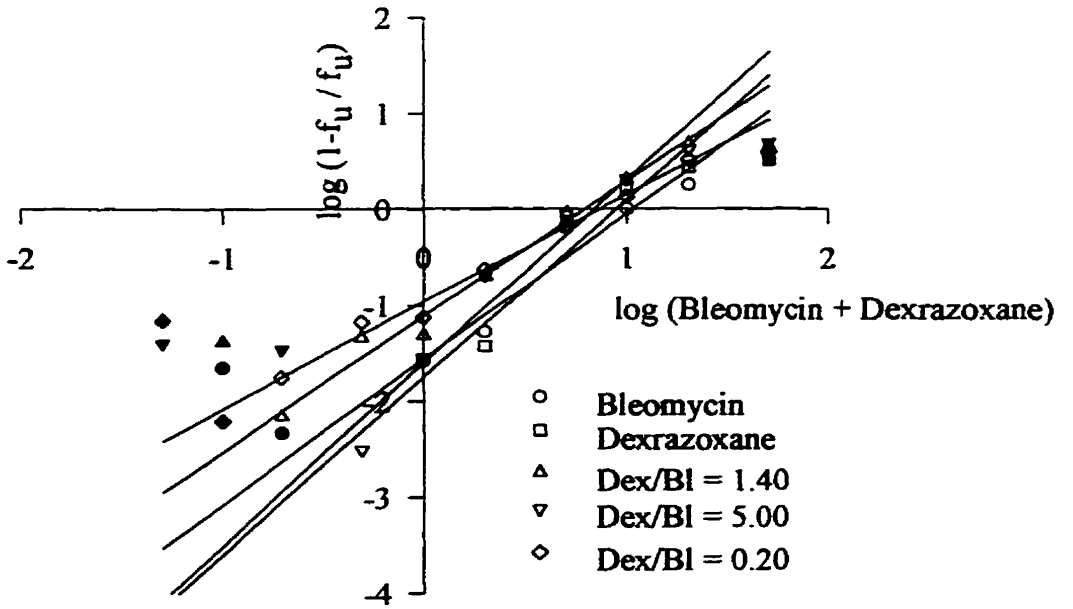

Fig. 5.7. Median effect plot for the dexrazoxane-bleomycin combination index experiment presented in Fig. 5.6. Data in solid symbols were not used to determine the linear parameters of the median effect plots.

The combination index was calculated using equations for mutually exclusive (Fig. 5.8, $\alpha = 0$) and mutually non-exclusive drugs (Fig. 5.9, $\alpha = 1$) for the 0.2-0.6 range of fraction affected (the range of experimental data defining the median effect plot).

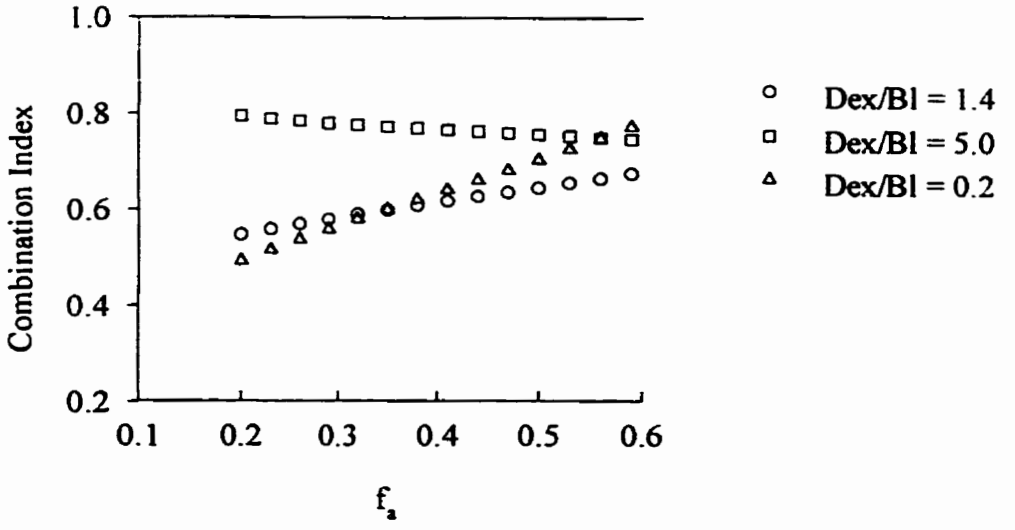

Fig. 5.8. Plot of combination index against fraction affected for three combinations of dexrazoxane and bleomycin with 18 h preincubation of dexrazoxane. Combination index was calculated for $\alpha = 0$.

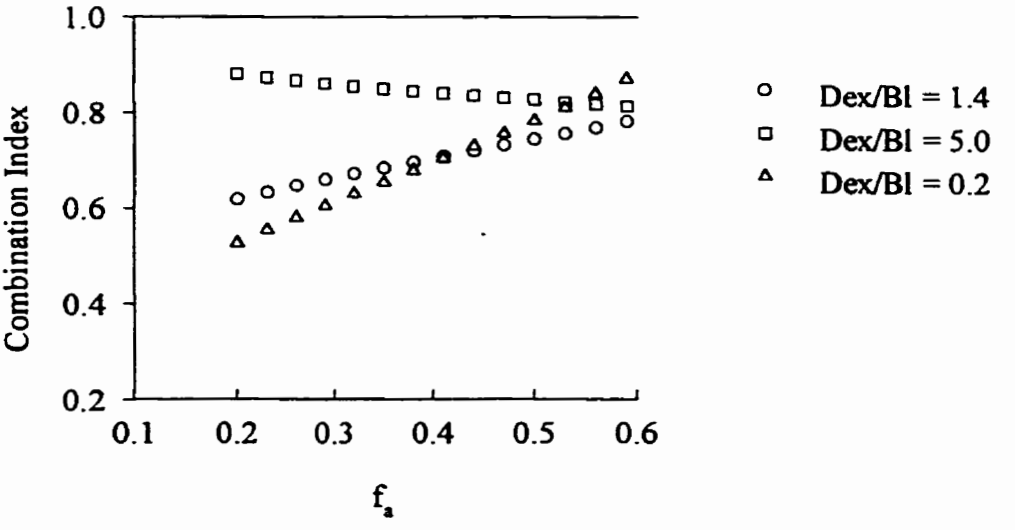

Fig. 5.9. Plot of combination index against fraction affected for three combinations of dexrazoxane and bleomycin with 18 h preincubation of dexrazoxane. Combination index was calculated for $\alpha = 1$.

The combination index calculated for $\alpha = 0$ and $\alpha = 1$ was less than one for all three ratios, over the considered range of fraction affected (0.2-0.6). These combination index values indicate that 18 h preincubation of the cells with dexrazoxane before the addition of bleomycin, caused a synergistic cytotoxic effect toward Chinese hamster ovary cells. The ranges of combination index values with corresponding f_a are given in Table 5.1.

Table 5.1. Values of combination index (*CI*) and corresponding ranges of fraction affected (f_a) for two bleomycin-dexrazoxane combination index experiments[a].

α	0						1					
Ratio	1.4		5.0		0.2		1.4		5.0		0.2	
Effect	Ant[b]	Syn[b]	Ant	Syn	Ant	Syn	Ant	Syn	Ant	Syn	Ant	Syn
CI_1[c]	**1.43-1.0**	**1.0-0.75**	**1.40-1.0**	**1.0-0.88**	**2.42-1.0**	**1.0-0.62**	**1.90-1.0**	**1.0-0.87**	**1.84-1.0**	**1.0-0.96**	**2.83-1.0**	**1.0-0.69**
f_a[e]	0.20-0.33	0.33-0.54	0.20-0.40	0.40-0.54	0.20-0.40	0.40-0.54	0.20-0.45	0.45-0.54	0.20-0.50	0.50-0.54	0.20-0.42	0.42-0.54
CI_2[d]		**0.55-0.68**		**0.79-0.75**		**0.49-0.78**		**0.62-0.79**		**0.88-0.81**		**0.53-0.88**
f_a		0.20-0.60		0.20-0.60		0.20-0.60		0.20-0.60		0.20-0.60		0.20-0.60

[a] The combination index was calculated with two equations for α = 0 and α = 1 for three ratios of dexrazoxane to bleomycin 1.4, 5.0 and 0.2. The value of *CI* = 1.0 is a crossing point between synergy and antagonism; thus it is not recognised as additivity effect

[b] Ant and Syn mean antagonism and synergy, respectively

[c] Combination indexes calculated for experiment with drug added simultaneously

[d] Combination indexes calculated for experiment with 18 h time gap between dexrazoxane and bleomycin

[e] Fraction affected corresponding to combination indexes above

5.3.2. Results from the envelope of additivity method for the dexrazoxane-bleomycin experiments

The envelope of additivity method was used with the experimental data presented in Fig. 5.10. Chinese hamster ovary cells were exposed to bleomycin, dexrazoxane and bleomycin with fixed doses of dexrazoxane. Dexrazoxane was preincubated with the cells for 18 h before bleomycin was added. The incubation with both drugs was continued for another 72 h.

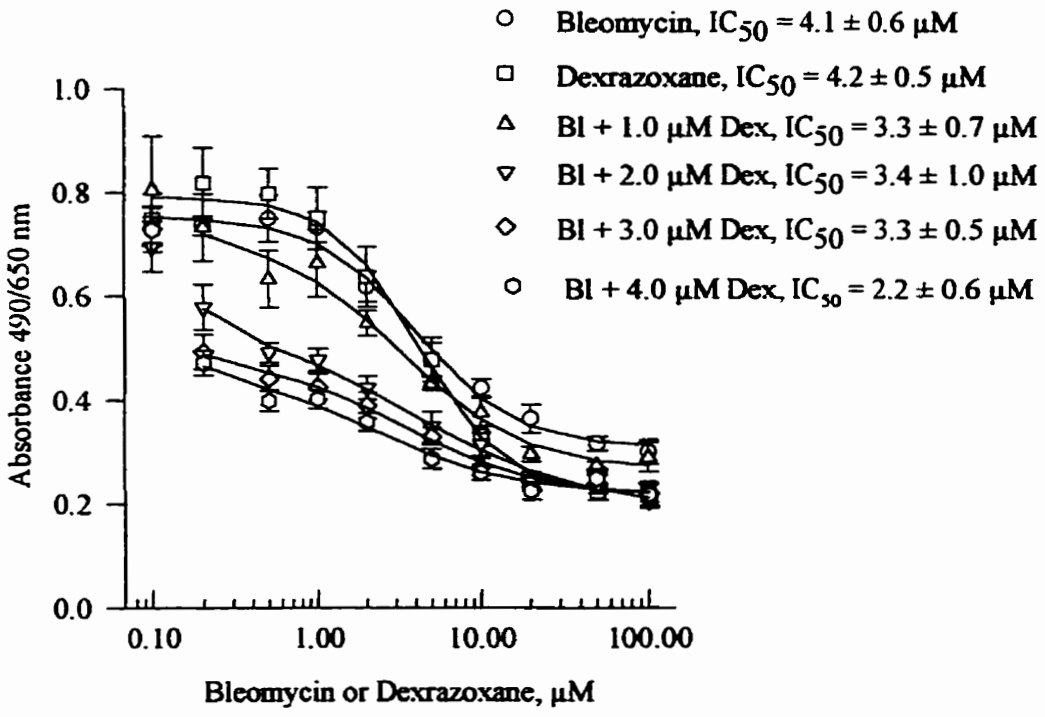

Fig. 5.10. Envelope of additivity experiment for dexrazoxane and bleomycin. Chinese hamster ovary cells were incubated with both drugs for 72 h. Dexrazoxane was added 18 h before bleomycin. The points represent absorbance means ± SD from six repetitions at each concentration. The lines represent the non-linear least squares fit of the experimental data to a four-parameter logistic equation. The lowest concentration corresponds to zero concentration of drugs plotted for convenience on a logarithmic scale with an arbitrary given value.

Based on the Experiment presented in Fig. 5.10, the envelope of additivity was constructed for 50% effect (Fig. 5.11). The obtained combination of doses are given in Table 5.2.

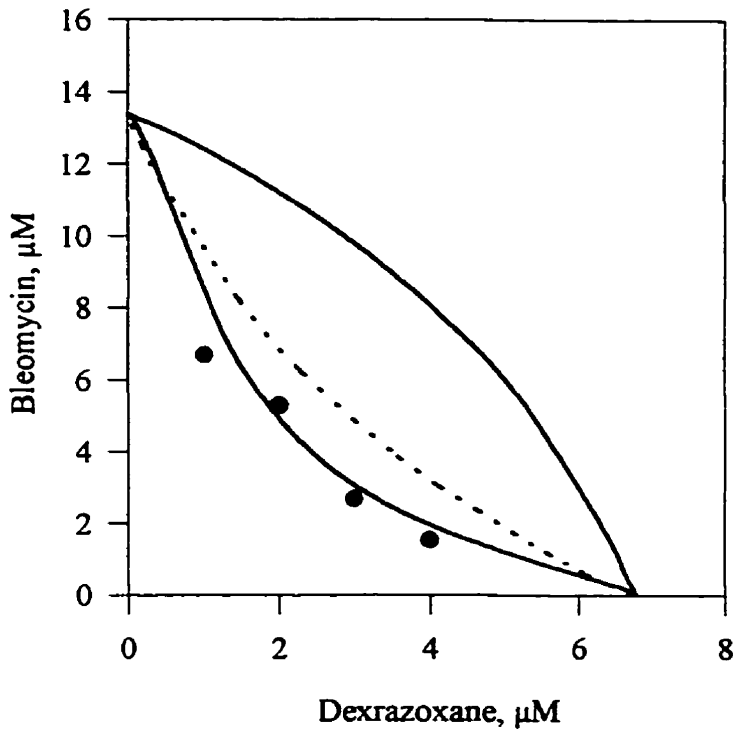

Fig. 5.11. Envelope of additivity for bleomycin and dexrazoxane constructed for 50% effect. The solid line to the left was calculated by mode I, the solid line to the right was calculated by mode IIa and the dotted line represents calculation by mode IIb. The four points (•) represent the concentrations of bleomycin and dexrazoxane that produce 50% effect when used as a mixture. The co-ordinates of the points (dexrazoxane; bleomycin) starting from the left are as follows: (1.0 μM: 6.7 μM), (2.0 μM: 5.3 μM), (3.0 μM: 2.7 μM), (4.0 μM: 1.5 μM).

Table 5.2. Calculated doses of bleomycin that in combination with dexrazoxane produce 50% effect.

Dexrazoxane μM	Bleomycin μM
1.0	6.7 Syn[a]
2.0	5.3 Syn
3.0	2.7 Ad[b]
4.0	1.5 Syn

[a] Synergy
[b] Additivity

Three dexrazoxane : bleomycin points (1.0 μM: 6.7 μM), (3.0 μM: 2.7 μM) and (4.0 μM: 1.5 μM) that produce a 50% effect, fell to the left of envelope of additivity, indicating synergy (Fig. 5.11 and Table5.2). The (2.0 μM: 5.3 μM) point is inside the envelope, indicating additivity of the effects.

5.3.3. Results from the response surface method for the dexrazoxane-bleomycin experiments

The combination index (Fig. 5.2 and 5.6) and envelope of additivity Experiments (Fig. 5.10) were also analysed by the response surface method. The equation (5.1) was used for calculations. The meaning of the variables is given in Chapter III, Section 3.2.4.3.

$$\frac{d_{Bl}}{IC_{50,Bl}\left(\frac{E-B}{E_{max}-E+B}\right)^{1/m_{Bl}}}+\frac{d_{Dex}}{IC_{50,Dex}\left(\frac{E-B}{E_{max}-E+B}\right)^{1/m_{Dex}}}+\frac{a'\cdot d_{Dex}\cdot d_{Bl}}{IC_{50,Dex}\cdot IC_{50,Bl}\left(\frac{E-B}{E_{max}-E+B}\right)^{(1/m_{Dex}+1/m_{Bl})}}=1 \qquad (5.1)$$

The best fit parameters obtained for three bleomycin-dexrazoxane Experiments are given in Table 5.3.

Table 5.3. Best fit parameter estimates ± SEM obtained from fitting the bleomycin-dexrazoxane experimental data to equation (5.1) for three different single experiments.

Experiment	α' ± SEM	$IC_{50,Bl}$ ± SEM μM	$IC_{50,Dex}$ ± SEM μM	m_{Bl} ± SEM	m_{Dex} ± SEM	E_{max} ± SEM	B ± SEM
CI-exp[a]	-0.116 ± 0.256	3.349 ± 0.678	5.210 ± 1.141	-0.809 ● 0.111	-1.276 ● 0.229	0.700 ± 0.043	0.383 ± 0.033
CI-exp[b] 18 h	3.151 ± 2.413	8.825 ± 2.291	5.603 ± 1.173	-0.803 ± 0.098	-1.405 ± 0.205	0.930 ± 0.020	0.158 ± 0.014
Env-exp[c] 18 h	0.961 ± 0.363	5.854 ● 0.697	2.934 ± 0.252	-0.882 ± 0.063	-1.615 ± 0.209	0.815 ± 0.017	0.291 ± 0.007

[a] 72 h combination index experiment where drugs were added simultaneously.
[b] 72 h combination index experiment where dexrazoxane was added 18 h before bleomycin.
[c] 72 h envelope of additivity experiment where dexrazoxane was added 18 h before bleomycin, these parameters were obtained when E_{max} was constrained to 0.82 and 50 μM data were omitted.

Based on the best fit parameters from Table 5.3, the theoretical effects were calculated as described in Chapter III, Section 3.2.4.3. The theoretical data calculated with the bisection root finder (lines in Fig. 5.12, 5.13 and 5.14), showed good agreement with measured data (symbols) for each experiment.

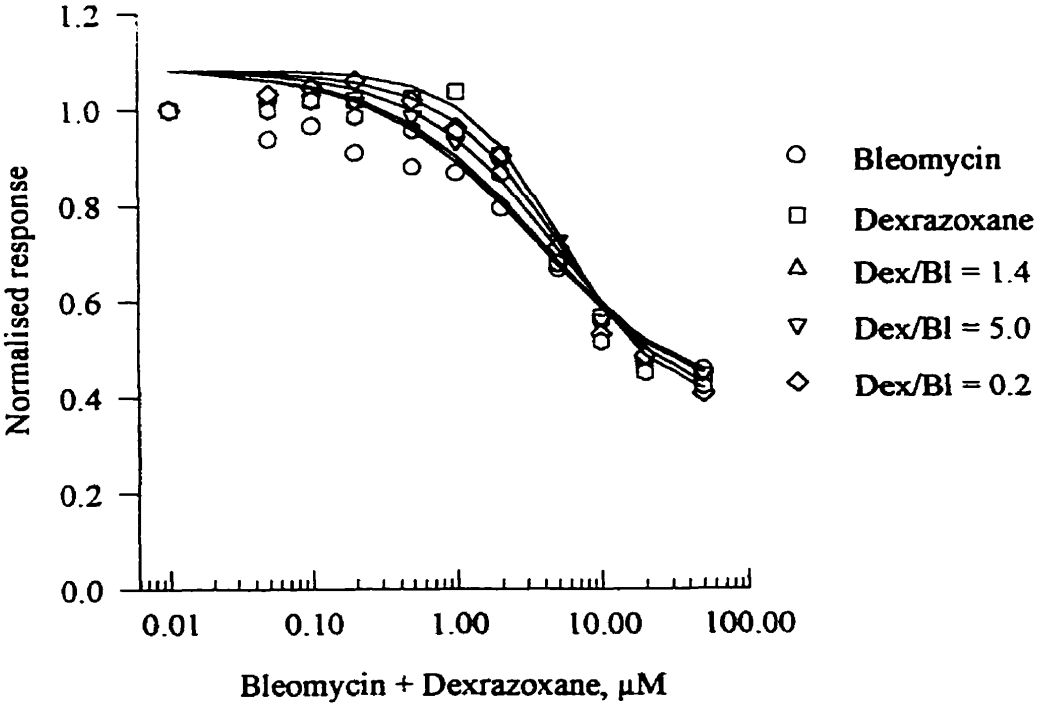

Fig. 5.12. Evaluation of the results from the response surface method used for the dexrazoxane and bleomycin combination index experiment. The normalised measured (symbols) and calculated (lines) effects are plotted. The effects were calculated based on the seven parameters given in Table 5.3. The lowest concentration values correspond to zero concentration of drugs (control values). The experimental data from the 72 h combination index experiment without preincubation with dexrazoxane are presented in Fig.5.2.

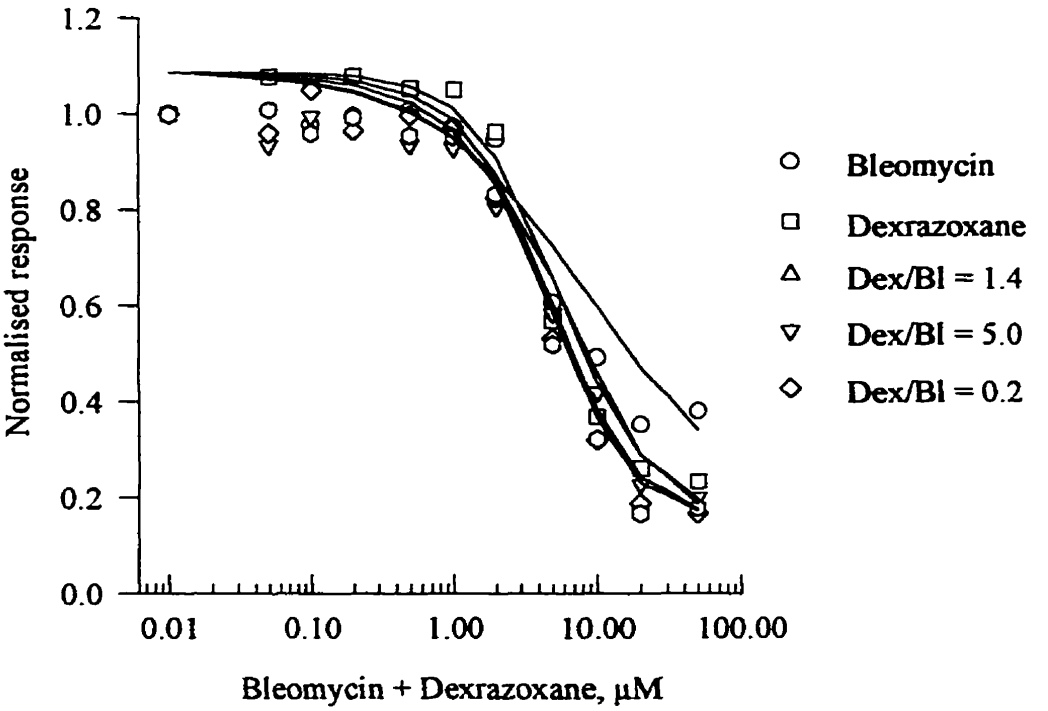

Fig. 5.13. Evaluation of the results from the response surface method used for the dexrazoxane and bleomycin combination index experiment. The normalised measured (symbols) and calculated (lines) effects are plotted. The effects were calculated based on the seven parameters given in Table 5.3. The lowest concentration values correspond to zero concentration of drugs (control values). The experimental data from the 72 h combination index experiment with 18 h preincubation of dexrazoxane are presented in Fig. 5.6.

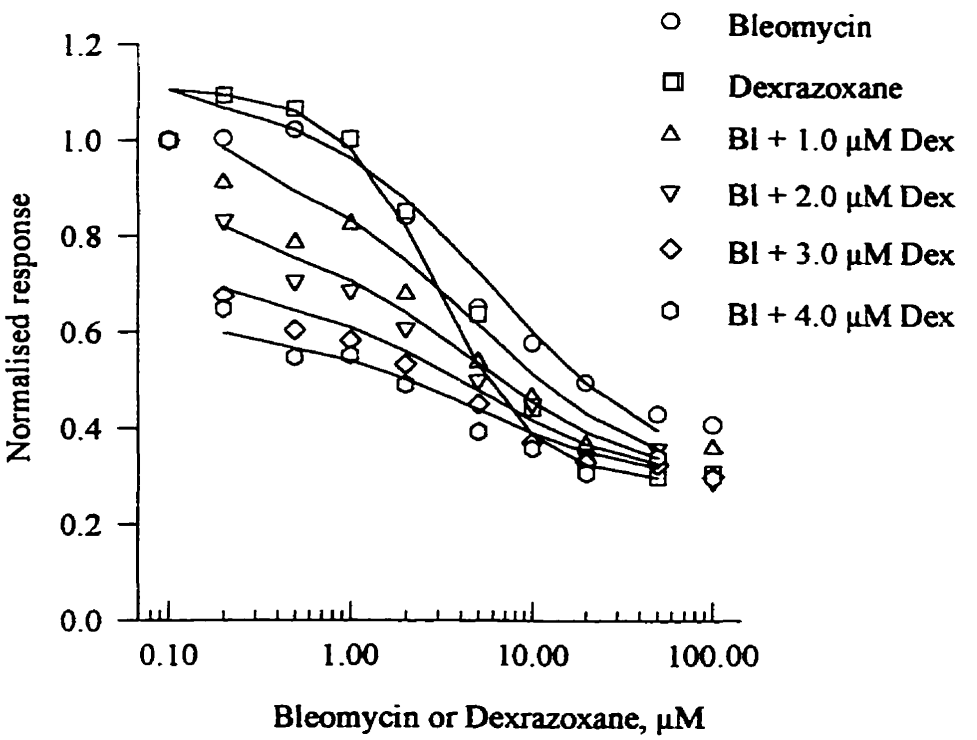

Fig. 5.14. Evaluation of the results from the response surface method used for the dexrazoxane and bleomycin envelope of additivity experiment. The normalised measured (symbols) and calculated (lines) effects are plotted. The effects were calculated based on the seven parameters given in Table 5.3. The best fit parameters were obtained when the 100 μM data were omitted and E_{max} was constrained below 0.82. The lowest concentration values correspond to zero concentration of drugs (control values). The experiment is the 72 h envelope of additivity experiment with 18 h preincubation of dexrazoxane presented in Fig. 5.10.

The interaction index, α', for the combination index Experiment without preincubation with dexrazoxane was - 0.116 ± 0.256. Due to the large value of SEM, the value of α' is not different from zero which indicates an additive effect of dexrazoxane and bleomycin when added simultaneously. The interaction index, α', for the combination index Experiment with 18 h preincubation of dexrazoxane was 3.151 ± 2.413; for the

envelope of additivity data with 18 h preincubation of dexrazoxane α' was 0.961 ● 0.363. The positive value of α' indicates that the effect of dexrazoxane and bleomycin was synergistic when cells were preincubated with dexrazoxane for 18 h before bleomycin was added.

5.3.4. Results from the slope comparison method for the dexrazoxane-bleomycin experiments

The Experiment for evaluation using the slope comparison method was designed to obtain 48 h dose-response curves for dexrazoxane and dexrazoxane with fixed doses of bleomycin. The 48 h median inhibitory concentration of bleomycin was $IC_{50,Bl}$ = 226.8 ± 27.0 μM (three-parameter fit). Dexrazoxane was added 1 h before bleomycin. The results of the Experiment are presented in Fig. 5.15. A log-log scale was used to obtain linear dose-response curves.

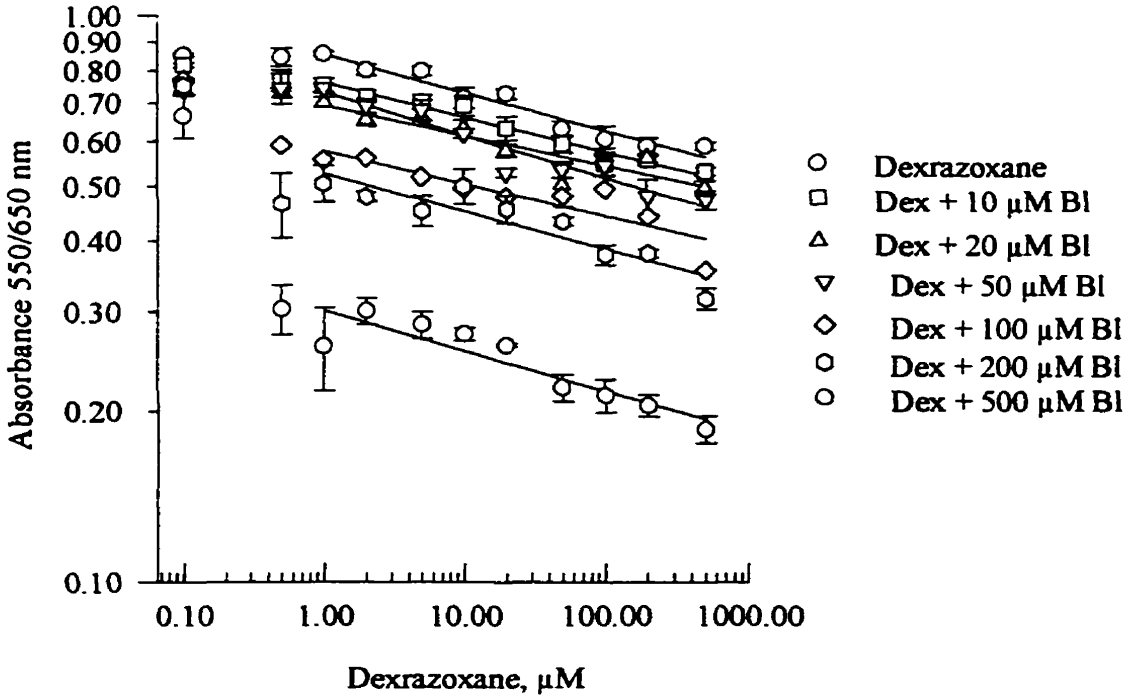

Fig. 5.15. Slope comparison experiment for dexrazoxane and bleomycin. The 48 h inhibitory effect of dexrazoxane and dexrazoxane with fixed doses of bleomycin on Chinese hamster ovary cells is presented in log-log scale. The symbols represent the means of absorbance ± SD from three repetitions. Dexrazoxane with 100 μM bleomycin was not repeated. The lowest concentrations correspond to control values with zero concentration of drugs. The second control value is the effect of bleomycin alone (this control is for dexrazoxane with fixed doses of bleomycin).

The slope of the linear dexrazoxane dose-response curve was compared with those of dexrazoxane with fixed doses of bleomycin. The regression parameters and results of the Student *t*-test are presented in Table 5.4. The slopes were considered different when $P < 0.05$. A list of the variables used in the *t*-test is given in Chapter III, Section 3.3.4.

Table 5.4. Slope comparison of dexrazoxane and dexrazoxane with fixed doses of bleomycin linear dose-response curves presented in Fig. 5.15[a].

Parameters	Doses of Bleomycin, μM						
	0	10	20	50	100	200	500
a ● SEM	-0.068 ± 0.010	-0.1172 ± 0.008	-0.158 ± 0.014	-0.135 ± 0.013	-0.238 ± 0.019	-0.279 ± 0.019	-0.520 ± 0.020
b ● SEM	-0.067 ± 0.006	-0.061 ± 0.005	-0.0528 ± 0.009	-0.075 ± 0.008	-0.057 ± 0.012	-0.066 ± 0.012	-0.072 ± 0.012
Tb		-0.757	-1.282	0.796	-0.729	-0.044	0.338
Vb		14	14	14	14	14	14

[a] All slopes of dexrazoxane with fixed doses of bleomycin were not significantly different from the dexrazoxane alone

The slope values as a function of bleomycin concentrations are presented in Fig. 5.16.

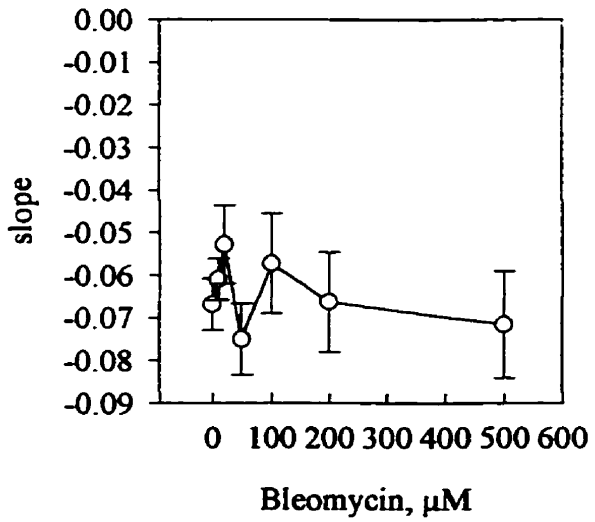

Fig. 5.16. Slopes obtained from the dexrazoxane-bleomycin slope method experiment. The slopes of linear dose-response curves are plotted against concentrations of bleomycin. The slope of dexrazoxane alone was not different from the dexrazoxane with fixed doses of bleomycin. The error bars represent SEM.

None of the slopes of dexrazoxane with fixed doses of bleomycin differed from dexrazoxane alone. All the linear dose-response curves were parallel to the dexrazoxane dose-response curve. The 48 h effect of dexrazoxane and bleomycin was additive when cells were preincubated with dexrazoxane for 1 h prior to the addition of bleomycin.

5.3.5. Results from the cytotoxicity experiment for the combination of ADR-925 with bleomycin

The effects of 72 h exposure of bleomycin alone and bleomycin with fixed doses of ADR-925 were studied on Chinese hamster ovary cells (Fig. 5.17). The cells were preincubated with ADR-925 for 18 h before bleomycin was added. In Fig. 5.18, the cytotoxicity effect of ADR-925 on Chinese hamster ovary cells is presented. In Fig 5.19,

the median inhibitory concentrations of bleomycin and bleomycin with fixed doses of ADR-925 obtained from the Experiment presented in Fig. 5.17 are plotted against the ADR-925 doses.

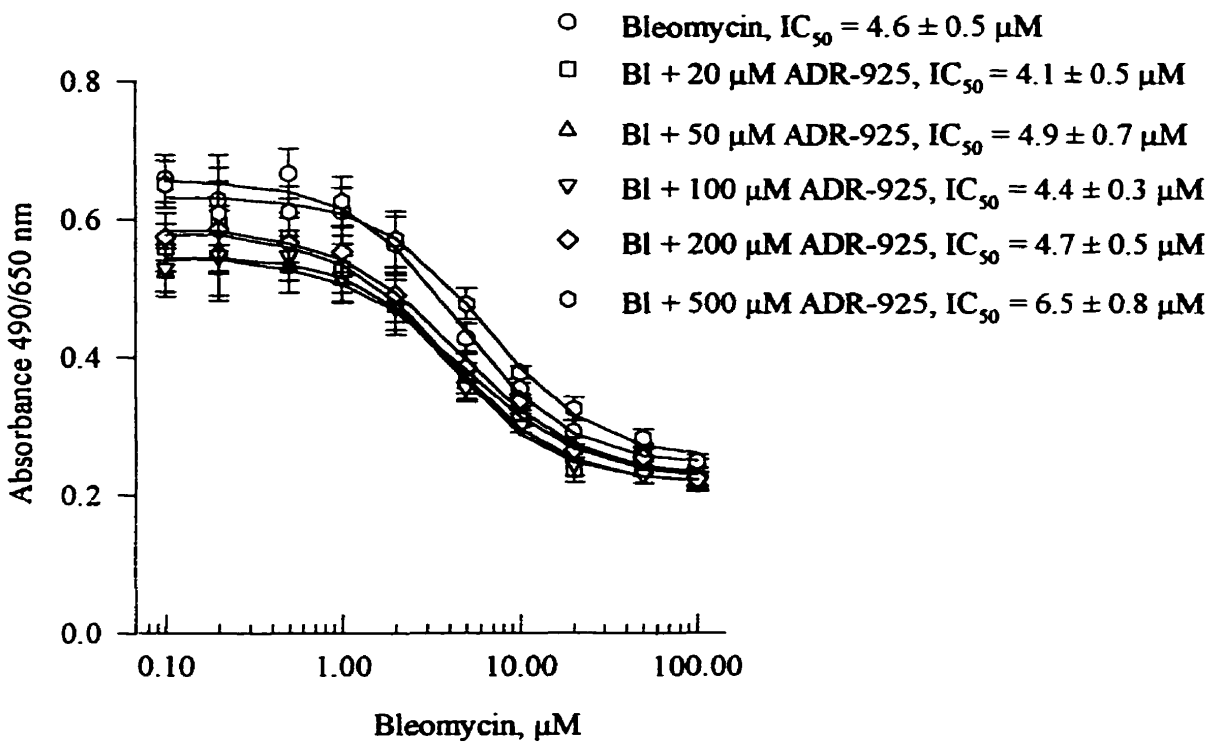

Fig. 5.17. Effect of ADR-925 on 72 h cytotoxicity of bleomycin toward Chinese hamster ovary cells. The symbols represent means of absorbance ● SD from six repetitions of each concentration. The cells were preincubated for 18 h with ADR-925 before bleomycin was added. The lines represent the non-linear best fit of experimental data to a four-parameter logistic equation. The IC_{50} values ● SEM were obtained as parameters of the logistic fit. The lowest concentrations correspond to zero concentration of the drugs. The second values of the dose-response curves for bleomycin with ADR-925 correspond to concentration of ADR-925 without bleomycin.

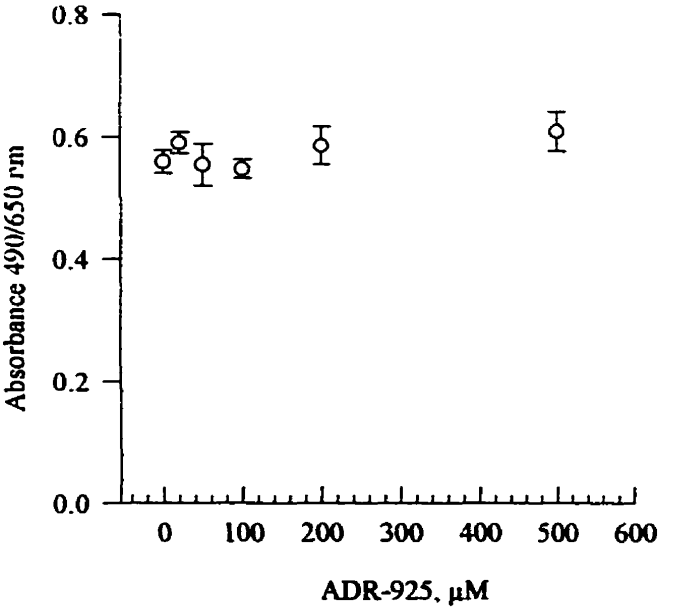

Fig. 5.18. Effect of 72 h exposure of Chinese hamster ovary cells to ADR-925. The error bars represent SEM.

The median inhibitory concentration for bleomycin alone was 4.6 ± 0.5 μM. The median inhibitory concentrations for bleomycin combined with the fixed doses of ADR-925 were as follows: 20 μM ADR-925: 4.1 ± 0.5 μM, 50 μM ADR-925: 4.9 ± 0.7 μM, 100 μM ADR-925: 4.4 ± 0.3 μM, 200 μM ADR-925: 4.7 ± 0.5 μM and 500 μM ADR-925: 6.5 ± 0.8. As shown in Fig. 5.18, ADR-925 does not have cytotoxic effect toward Chinese hamster ovary cells even at a concentration of 500 μM. The regression line of IC_{50} plotted against concentrations of ADR-925 in Fig. 5.19 has a positive slope of 0.004 ● 0.001. Considering the slight increase of the slope and the magnitude of the $IC_{50,BI}$ standard errors, ADR-925 does not have an effect on bleomycin cytotoxicity.

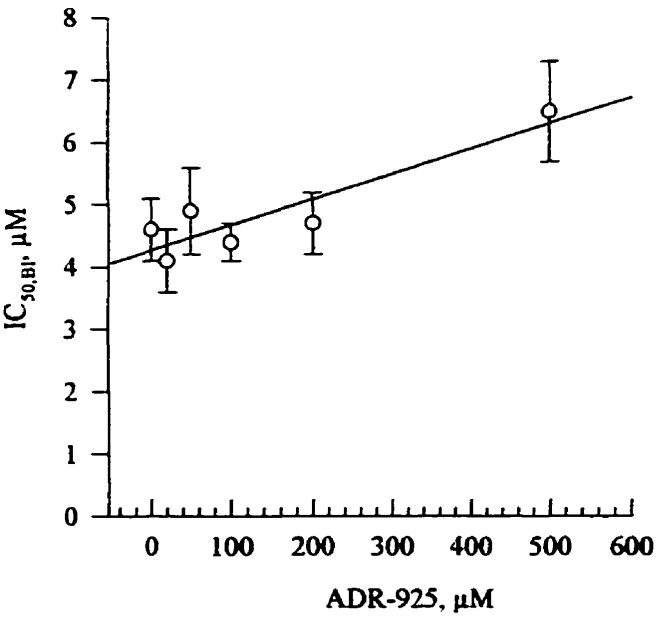

Fig. 5.19. Effect of ADR-925 on the median inhibitory concentration of bleomycin. The $IC_{50,BI}$ plotted against concentration of ADR-925 data were fitted into linear equation: $A_{490/650} = a + b\ D_{ADR\text{-}925}$, where a = 4.3 ± 0.2, b = 0.004 ± 0.001 μM, $A_{490/650}$ is an absorbance at 490-650 nm and $D_{ADR\text{-}925}$ is a concentration of ADR-925. The error bars are SEM.

5.3.6. Combined results from the combination index, envelope of additivity, response surface and slope comparison methods for the dexrazoxane-bleomycin experiments

The results obtained from all evaluating methods for dexrazoxane combined with bleomycin are presented in Table 5.5.

Table 5.5. Effect of combination of dexrazoxane with bleomycin evaluated with different methods.

	Dexrazoxane with Bleomycin												
	Combination Index[a]						Envelope[b] for 50% effect				Res. Surface[c]		Slope[d]
	α = 0			α = 1									
	Dex/Bl 1.4	Dex/Bl 5.0	Dex/Bl 0.2	Dex/Bl 1.4	Dex/Bl 5.0	Dex/Bl 0.2	Dex 1.0 μM	Dex 2.0 μM	Dex 3.0 μM	Dex 4.0 μM	CI	Env.	
Exp.1[e]	Ant (0.33)[g] Syn	Ant (0.40) Syn	Ant (0.40) Syn	Ant (0.45) Syn	Ant (0.50) Syn	Ant (0.42) Syn					Ad		
Exp.2[f]	Syn	Syn	Syn	Syn	Syn	Syn	Syn	Syn	Ad	Syn	Syn	Syn	Ad

[a] The combination index method was used to evaluate the results of 72 h exposure of the cells to dexrazoxane and bleomycin in three concentration ratios Dex/Bl = 1.4, 5.0 and 0.2; the equations with α = 0 and 1 were used

[b] The envelope of additivity was used to evaluate the results of 72 h cell exposure to the drugs with 20 min preincubation to four different concentrations of dexrazoxane (Dex)

[c] The response surface method was used with combination index (CI) and envelope of additivity (Env.) experimental data

[d] The slope method was used for 48 h exposure of cells to the drugs with 1 h preincubation with dexrazoxane

[e] Experiment where drugs were added simultaneously

[f] Experiments where dexrazoxane was added 18 or 1 h (slope) before bleomycin

[g] Value of fraction affected from the range 0.20-0.54, where $CI \approx 1.0$ (the crossing point between antagonism and synergy)

5.4. Conclusions

Synergy, antagonism and additivity were observed between dexrazoxane and bleomycin depending on experimental design (Table 5.5). Antagonism was demonstrated when the drugs were supplied simultaneously and the combination index was used to determine the effect. The drugs showed antagonism for lower and synergy for higher ranges of fraction affected (Figs. 5.4, 5.5, Tables 5.1 and 5.6) for all three ratios and both equations (α = 0 or 1). When the cells were preincubated with dexrazoxane for 18 h before bleomycin was added, the combination index was less than one for all ratios and both combination index equations (Figs.5.8, 5.9, Tables 5.1 and 5.6); thus, synergy was indicated. The envelope of additivity Experiment involving an 18 h preincubation of dexrazoxane also showed synergy (Fig. 5.11, Tables 5.2 and 5.6). When Greco's method was used, additivity was seen for the Experiment without preincubation, and synergy for the Experiments with preincubation of dexrazoxane (Tables 5.3 and 5.6). No interaction between dexrazoxane and bleomycin was observed in the 48 h Experiment with 1 h preincubation of dexrazoxane evaluated by the slope comparison method. The dexrazoxane linear dose-response curve was parallel to that of dexrazoxane with fixed doses of bleomycin. The effect of the drugs was additive (Tables 5.5, 5.6 and Fig. 5.16).

When dexrazoxane was preincubated with the cells for 18 h before bleomycin was delivered, all methods indicated that the interaction was synergistic. When both drugs were added simultaneously, or when preincubation with dexrazoxane was short (20 min or 1 h), both the response surface and slope comparison methods showed the effects of 72 and 48 h exposure to the drugs to be additive. When the combination index method was

used to evaluate the effects of dexrazoxane and bleomycin added simultaneously, the calculated results of drug interaction were antagonism or synergy, depending on the concentration of the combination.

ADR-925 did not have cytotoxic effect on Chinese hamster ovary cells (Fig. 5.18). When ADR-925 was used in combination with bleomycin, it showed no effect on bleomycin cytotoxicity (Figs. 5.17 and 5.19).

Iron is considered to be a cofactor of bleomycin antitumor activity [1]. Although some studies show that iron chelators are able to inhibit bleomycin activity [11, 13], Lyman found that iron chelators had no effect on bleomycin cytotoxicity [9]. Dexrazoxane is able to remove iron from bleomycin-iron complexes [4]. The results of synergy and additivity obtained in this study suggest that dexrazoxane does not trap all available iron for bleomycin. Other factors which determine bleomycin cytotoxicity, such as permeability of the plasma membrane or cell cycle sensitivity [5], may also be altered by the presence of dexrazoxane and bleomycin.

References

1. Hecht SM, Bleomycin-group antitumor agents. In: *Cancer Chemotherapeutic Agents.* (Ed. Foye WO), pp. 369-388. American Chemical Society, Washington, DC, 1995.

2. Bower M, Brock C, Gulliford T, O'Reilly SM, Smith DB and Newlands ES, A weekly alternating chemotherapy regimen with low toxicity for treatment of aggressive lymphoma. *Cancer Chemother Pharmacol* **38:** 106-109, 1996.

3. *Compendium of Pharmaceuticals and Specialties. 32nd ed.* Canadian Pharmaceutical Association, Ottawa, Ontario, Canada, 1997:190-191; 1032 p.

4. Herman EH, Hasinoff BB, Zhang J, Raley LG, Zhang T-M, Fukada Y and Ferrans VJ, Morphologic and morphometric evaluation of the effect of ICRF-187 on bleomycin-induced pulmonary toxicity. *Toxicol* **98:** 163-175, 1995.

5. Mir LM, Tounekti O and Orlowski S, Bleomycin: revival of old drug. *Gen Pharmac* **27:** 745-748, 1996.

6. Dawson KM, Studies on the stability and cellular distribution of dioxopiperazines in cultured BHK-21S cells. *Biochem Pharmacol* **24:** 2249-2253, 1975.

7. Hasinoff BB, Pharmacodynamics of the hydrolysis-activation of the cardioprotective agent (+)-1,2-bis(3,5-dioxopiperazinyl-1-yl)propane. *J Pharm Sci* **83:** 64-67, 1994.

8. Hasinoff BB, Kuschak TI, Creighton AM, Fattman CL, Allan WP, Thampatty P and Yalowich JC, Characterization of a Chinese hamster ovary cell line with acquired resistance to the bisdioxopiperazine dexrazoxane (ICRF-187) catalytic inhibitor of topoisomerase II. *Biochem Pharmacol* **53:** 1843-1853, 1997.

9. Lyman S, Taylor P, Lornitzo F, Wier A, Stone D, Antholine WE and Petering DH, Activity of bleomycin in iron- and copper-deficient cells. *Biochem Pharmacol* **38:** 4273-4282, 1989.

10. Karam H, Hurbain-Kosmath I and Housset B, Direct toxic effect of bleomycin on alveolar type 2 cells. *Toxicol Lett* **76:** 155-163, 1995.

11. Takahashi K, Takita T and Umezawa H, Effect of *o*-phenanthroline, 2,2'-dipyridyl and neocuproine on the activities of bleomycin to inhibit DNA synthesis and growth of cultured cells. *J Antibiotics* **10:** 1473-1478, 1986.

12. Larramendy ML, Lopez-Larraza D, Vidal-Rioja L and Bianchi NO, Effect of the metal chelating agent o-phenanthroline on the DNA and chromosome damage inuced by bleomycin in Chinese hamster ovary cells. *Cancer Res* **49:** 6583-6586, 1989.

13. Moore CW, Potentiation of belomycin cytotoxicity in Saccharomyces cerevisiae. *Antimicrob Agents Chemother* **38:** 1615-1619, 1994.

14. *Drug Information for the Health Care Professional. 9th ed.* The United States Pharmacopeial Convention, Inc., Harrisonburg, Virginia, USA, 1989.

6. Evaluation of the methods for drug interaction studies

The combination index, envelope of additivity, response surface and slope comparison methods were used in this thesis work to test interaction of dexrazoxane with some anticancer drugs. The following are some comments about these methods.

The median effect plot is a part of the combination index method. Not all experimental data could be used to create the plot. Data with higher effect than the control and those which did not fit the linear median effect plot could not be used. Practically, only a few points defined the plots thus the calculations of the combination index were dependent on accuracy of these few data. The combination index is different for mutually exclusive and mutually not exclusive drugs. The exclusivity of dexrazoxane with mafosfamide, 5-fluorouracil or bleomycin could not be defined. This resulted in two sets of combination indexes for each drug ratios. The combination index could be calculated for the effects in the range of the effect of the drug with lower efficacy *e.g.* dexrazoxane when combined with mafosfamide. The combination index method tests the wide range of drug concentrations and is independent of the shape of dose-response curves.

The envelope of additivity method tests interaction of combined drugs where one is in a fixed dose and the other is in wide concentration range. The fixed doses of one drug are limited to these producing the effects falling in the range of the second drug effect. They also cannot produce the effect higher than effect for planned envelope. This method is easier to interpret than the combination index method but it tests only a few doses.

The response surface method is limited to the logistic dose-response curves. Fortunately, logistic model fits all experimental data in this thesis work. When the method

was used there were some difficulties obtaining a good fitting results for two drugs with different efficacy and it was not possible for drugs with very low kill. The interaction parameter calculated in this method defined synergy, antagonism or additivity for the whole set of tested data. The response surface method defined only one effect of interaction for two drugs thus it does not recognise different effect of drug interactions for different concentration ratios.

The slope method was developed in our laboratory by Dr. Brian Hasinoff for testing dexrazoxane with anticancer drugs in 48 h cytotoxicity experiment. The method requires that the effect-concentration data for one of the drugs fit a linear equation. In this method a few doses of a drug with a non-linear dose-response curve are tested for interaction with the second drug used over a wide range of concentrations. The results of the method are simple to interpret based on the changes in the value of the slopes.

IMAGE EVALUATION TEST TARGET (QA-3)

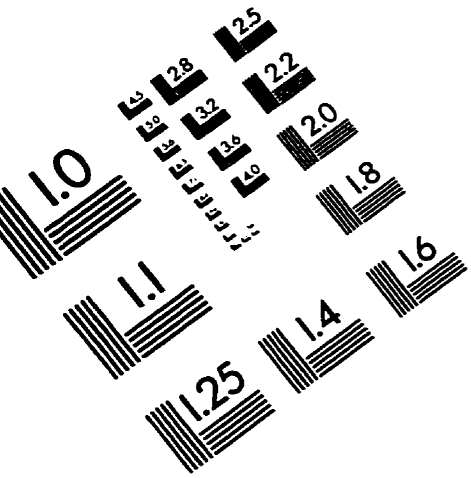

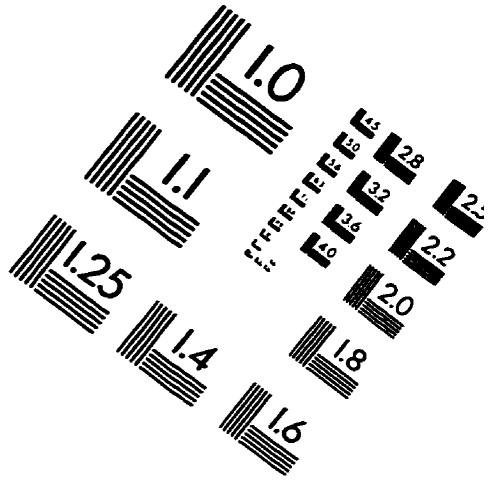

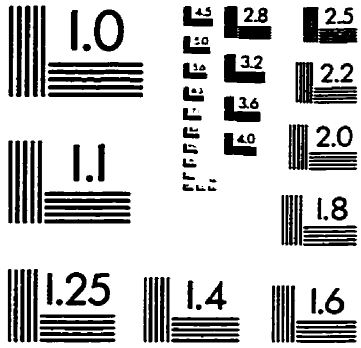

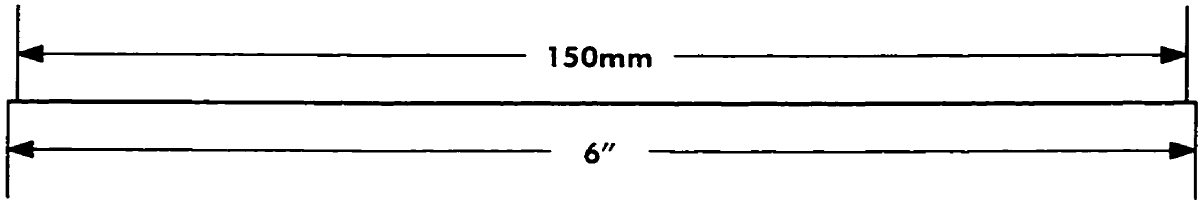

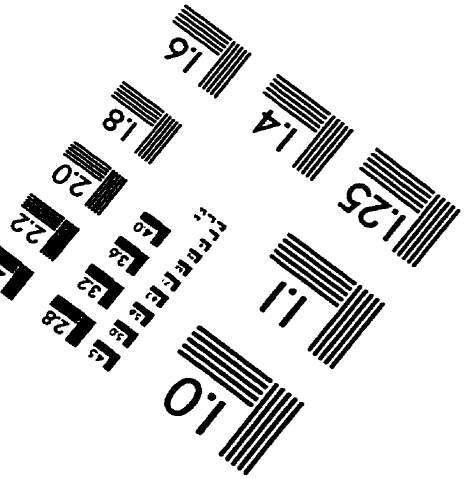

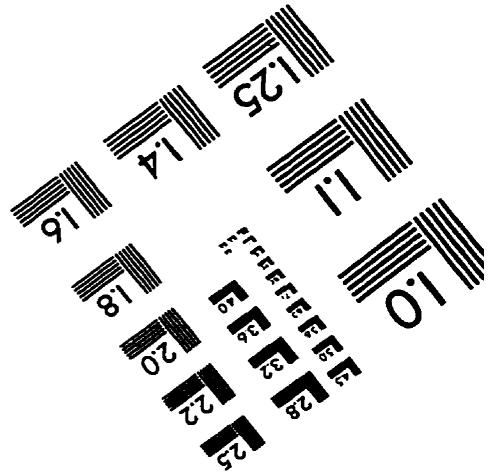

APPLIED IMAGE, Inc
1653 East Main Street
Rochester, NY 14609 USA
Phone: 716/482-0300
Fax: 716/288-5989

© 1993, Applied Image, Inc., All Rights Reserved